ASSOCIATIONS OF PLASMA AND LIPOPROTEIN LIPIDOMES WITH CORONARY ARTERY DISEASE AND EFFECTS OF APOLIPOPROTEIN M AND PARAOXONASE 1 ON PHOSPHOLIPID METABOLISM

Dissertation

zur

Erlangung der naturwissenschaftlichen Doktorwürde
(Dr. sc. nat.)

vorgelegt der

Mathematisch-naturwissenschaftlichen Fakultät

der

Universität Zürich

von

Iryna Sutter

aus

der Ukraine

Promotionskomitee

Prof. Dr. Arnold von Eckardstein (Vorsitz, Leitung der Dissertation)

P.D. Dr. Thorsten Hornemann

Prof. Dr. Katharina M. Rentsch

Prof. Dr. Olivier Devuyst

Prof. Dr. Ulf Landmesser

Zürich, 2015

TABLE OF CONTENTS

ABSTRACT

Coronary artery disease (CAD) continues to be the leading cause of death worldwide. CAD is thought to originate from the imbalance of lipids. Besides cholesterol, glycerophospholipids and sphingolipids are also emerging as important players in the pathogenesis of CAD. Among these, sphingosine-1-phosphate (S1P) is of particular interest, due to its role in the anti-inflammatory and cytoprotective functions of high-density lipoproteins (HDL).

The first part of this work included the development and validation of two analytical methods based on a liquid chromatography-mass spectrometry technique. These methods enabled us to carry out the quantification of individual molecular species of glycerophospholipids and sphingolipids, as well as S1P. Subsequently, these methods were applied in the following studies.

In a case-control study, we investigated whether plasma concentrations of glycerophospholipids and sphingolipids, as well as S1P and the sphingoid bases of sphingolipids, differ between healthy subjects and CAD or acute coronary syndrome (ACS) patients. In addition, we analysed the glycerophospholipid and sphingolipid distribution among the plasma lipoproteins of healthy individuals. We found that plasma concentrations of PC33:1, PC33:2, PC33:3 and PC35:3, that very likely represent PC plasmalogens, were the most significantly altered in CAD or ACS patients. Similar to the even-chain PC species, PC33:1, PC33:2, PC33:3 and PC35:3 were mostly associated with HDL, but also present in low-density lipoproteins (LDL). As the consequence, they exhibited a strong positive correlation with HDL-cholesterol levels. Besides 18:1-S1P, commonly known as S1P, we also identified other S1P species, which vary in the length and unsaturation degree of the sphingoid base. The most abundant S1P is 18:1-S1P. Compared to healthy subjects, it was reduced in plasma of ACS patients, while 16:1-S1P was found to be lower in plasma of both CAD and ACS patients.

Research over the last decade has revealed that HDL display anti-atherogenic effects on the cardiovascular system, which are attenuated in CAD patients. We therefore investigated the triangular relationship between HDL-associated phospholipids, the anti-apoptotic activity of HDL and the presence of CAD or ACS. The anti-apoptotic activity of HDL was tested by measuring the apoptosis of endothelial cells (ECs) in the presence of HDL. Among the 52 phospholipid species identified in HDL, PC33:3, PC35:2 and PC34:2 showed the most consistent relationships with CAD and ACS, as well as with the anti-

apoptotic activity of HDL. In addition, the HDL content of 18:1-S1P and 18:2-S1P significantly correlated with the anti-apoptotic activity of HDL, but did not associate with CAD or ACS.

In the circulatory system, HDL particles carry more than half of the plasma 18:1-S1P, termed S1P hereafter. This is explained by the presence of a specific binding protein, called apolipoprotein M (apoM). Experimental studies based on mouse models showed a limiting effect of apoM on plasma concentrations and HDL content of S1P. We investigated the effect of apoM on two potential pathways of S1P metabolism, namely HDL-mediated S1P efflux from erythrocytes and the urinary excretion of S1P. We showed that S1P efflux was enhanced in the presence of HDL from *Apom*^{tg} mice, but not diminished in the presence of HDL from *Apom*$^{-/-}$ mice when compared to HDL from wild type mice. This indicates that HDL facilitate S1P efflux from erythrocytes by both apoM-dependent and apoM-independent mechanisms. Analysis of S1P and apoM in plasma and urine samples from *Apom*$^{-/-}$ mice and from mice with defective tubular endocytosis showed that apoM facilitates the tubular reabsorption of S1P from urine, but has no impact on the plasma content of S1P.

Age-related macular degeneration (AMD) is a complex disease that can potentially lead to irreversible blindness in the elderly population. Genetic polymorphisms of paraoxonase1 (PON1), an enzyme which mediates some of the atheroprotective functions of HDL, was found to be associated with AMD. Since PON1 is thought to prevent lipid peroxidation, we used *Pon1*$^{-/-}$ mice to investigate the impact of PON1 on the phospholipid composition of the retina/eyecup tissue. The eyes of the *Pon1*$^{-/-}$ mice did not show an AMD-like phenotype. The retina/eyecup samples of young *Pon1*$^{-/-}$ mice contained less total lysophosphatidylcholines (LPCs) and LPC22:6 compared to wild type mice, reflecting a decreased activity of phospholipase A2 in these mice. Furthermore, one year old wild type mice displayed a decrease in the content of total LPCs and LPC22:6 by 63% and 75%, respectively, which could be a result of an age-related decrease in the expression of *Pon1* gene in the eyes.

In summary, we showed that reduced plasma and HDL levels of odd-chain PCs, probably corresponding to PC plasmalogens, are most consistently associated with CAD and ACS. We also showed that HDL-associated P33:3, PC35:2 and PC34:2 correlate significantly with the anti-apoptotic activity of HDL. We demonstrated that apoM has an effect on S1P metabolism: first, HDL induce S1P efflux from erythrocytes by apoM-dependent and apoM-independent mechanisms; second, apoM facilitates the reabsorption of S1P in the proximal renal tubules. Finally, we showed that retina/eyecup of *Pon1*$^{-/-}$ mice have a diminished content

of total LPCs and LPC22:6, which may reflect a decreased phospholipase A2-like activity in the eyes.

ZUSAMMENFASSUNG

Die Koronare Herzkrankheit (KHK) ist weiterhin weltweit die häufigste Todesursache. Es wird angenommen, dass KHK durch ein Ungleichgewicht der Lipide entsteht. Neben Cholesterin zeichnen sich auch Glycerophospholipide und Sphingolipide als wichtige Akteure bei der Pathogenese der KHK ab. Unter diesen ist das Sphingosin-1-Phosphat (S1P) wegen seiner Rolle bei den entzündungshemmenden und zellschützenden Funktionen der Lipoproteine mit hoher Dichte (HDL) von besonderem Interesse.

Der erste Teil dieser Arbeit umfasste die Entwicklung und Validation von zwei Analysemethoden, welche auf einer gekoppelten Flüssigkeitschromatographie-Massenspektrometrie Technik basieren. Diese Methoden ermöglichten uns eine Quantifizierung individueller Moleküle von Glycerophospholipiden und Sphingolipiden, wie auch S1P. Anschließend wurden diese Methoden in den folgenden Studien verwendet.

In einer Fall-Kontroll-Studie untersuchten wir, ob die Plasmaspiegel von Glycerophospholipiden und Sphingolipiden sowie S1P sich zwischen gesunden Probanden und KHK-Patienten oder Patienten mit akutem Koronarsyndrom (AKS) unterscheiden. Zusätzlich analysierten wir die Glycerophospholipid- und Sphingolipid-Verteilung unter den Plasma-Lipoproteinen von gesunden Personen. Wir fanden, dass die Plasmakonzentrationen von PC33:1, PC33:2, PC33:3 und PC35:3, die sehr wahrscheinlich PC-Plasmalogene darstellen, am stärksten bei Patienten mit KHK oder AKS veränderten sind. Ähnlich wie die meisten geradkettigen PC-Arten wurden PC33:1, PC33:2, PC33:3 und PC35:3 vor allem in HDL aber auch in Lipoproteinen geringer Dichte (LDL) gefunden. Als Folge hiervon korrelierten sie stark mit den HDL-Cholesterinspiegeln. Neben 18:1-S1P, allgemein bekannt als S1P, haben wir auch andere S1P-Arten identifiziert, die in der Länge und dem Grad der Nichtsättigung der Sphingoidbasis variieren. Das häufigste S1P ist 18:1-S1P. Im Vergleich zu gesunden Probanden war dessen Konzentration im Plasma von KHK-Patienten vermindert, während 16:1-S1P im Plasma sowohl der KHK als auch der AKS-Patienten in erniedrigter Konzentration gefunden wurde.

Die Forschung im letzten Jahrzehnt hat gezeigt, dass HDL anti-atherogene Auswirkungen auf das Herz-Kreislauf-System haben, die bei KHK-Patienten abgeschwächt sind. Wir untersuchten deswegen die Dreiecks-Beziehung zwischen HDL-assoziierten Phospholipiden, der anti-apoptotischen Aktivität von HDL und dem Vorhandensein von KHK oder AKS. Die anti-apoptotische Aktivität von HDL wurde durch Messung der Apoptose von Endothelzellen (ECs) in der Gegenwart von HDL getestet. Unter den 52 identifizierten

Phospholipid-Arten von HDL zeigten PC33:3, PC35:2 und PC34:2 die beständigsten Beziehungen zu KHK und AKS, so wie auch mit der anti-apoptotischen Aktivität von HDL. Darüber hinaus korrelierten die HDL-Spiegel von 18:1-S1P und 18:2-S1P signifikant mit der anti-apoptotischen Aktivität von HDL, waren aber nicht mit KHK oder AKS assoziiert.

Im Kreislaufsystem transportieren die HDL-Partikel mehr als die Hälfte des Plasma 18: 1-S1P, im Folgenden als S1P bezeichnet. Dies wird durch das Vorhandensein eines spezifischen Bindungsproteins namens Apolipoprotein M (apoM) erklärt. Experimentelle Studien in genetisch veränderten Mäusen zeigten eine einschränkende Wirkung von apoM auf Plasmakonzentrationen und den HDL-Gehalt von S1P. Wir untersuchten die Wirkung von apoM auf zwei mögliche Pfade des S1P-Metabolismus, nämlich den HDL-vermittelten S1P-Efflux auf Erythrozyten und die Urinausscheidung von S1P. Wir zeigten, dass der S1P-Efflux bei Anwesenheit von HDL von *Apom*^{tg} Mäusen, im Vergleich zu HDL von Wildtyp-Mäusen erhöht ist, und dass der S1P-Efflux bei Anwesenheit von HDL von *Apom*$^{-/-}$ Mäusen, im Vergleich zu HDL von Wildtyp Mäusen nicht verringert ist. Dies zeigt, dass HDL den S1P-Efflux aus Erythrozyten sowohl durch apoM-abhängige wie auch durch apoM-unabhängige Mechanismen erleichtert. Die Analyse von S1P und apoM in Plasma- und Urinproben von *Apom*$^{-/-}$ Mäusen und von Mäusen mit defekter Tubular-Endozytose zeigte, dass ApoM die tubuläre Reabsorption von S1P aus Urin erleichtert, aber keinen Einfluss auf den Plasmagehalt von S1P hat.

Die altersbedingte Makuladegeneration (AMD) ist eine komplexe Erkrankung, die möglicherweise zu einer irreversiblen Erblindung in der älteren Bevölkerung führen kann. Einige genetische Polymorphismen von Paraoxonase1 (PON1), einem Enzym, das einige der atheroprotektiven Funktionen von HDL vermittelt, sind mit AMD assoziiert. Da PON1 die Lipidperoxidation verhindert, haben wir *Pon1*$^{-/-}$ Mäuse, bezüglich der Phospholipid-Zusammensetzung der Retina und des Augenhintergrunds-Gewebes, untersucht. Die Augen der *Pon1*$^{-/-}$ Mäuse zeigten keinen AMD-ähnlichen Phänotyp. Die Netzhaut/Augenhintergrunds-Proben von jungen *Pon1*$^{-/-}$ Mäusen enthielt weniger Lysophosphatidylcholine (LPC) und LPC22:6 im Vergleich zu Wildtyp-Mäusen, was eine verminderte Aktivität der Phospholipase A2 bei diesen Mäusen widerspiegeln kann. Weiterhin zeigten ein Jahr alte Wildtyp-Mäuse eine Abnahme des Gehalts an LPCs und LPC22:6 um 63% und 75%, wobei dies ein Ergebnis einer altersbedingten Abnahme der Expression von *Pon1* Genen in den Augen sein könnte.

Zusammenfassend haben wir gezeigt, dass Plasma- und HDL-Spiegel ungeradkettiger PCs, wahrscheinlich PC-Plasmalogene, robust mit KHK und AKS assoziiert sind. Wir zeigten

auch, dass HDL-assoziierte P33:3, PC35:2 und PC34:2 signifikant mit der anti-apoptotischen Aktivität von HDL korrelieren. Wir zeigten, dass HDL den S1P-Efflux von Erythrozyten durch apoM-abhängige und apoM-unabhängige Mechanismen verstärkt und dass apoM die Resorption von S1P in den Nieren-Tubuli erleichtert. Schließlich zeigten wir, dass die Netzhaut/Augenhintergrunds-Gewebe der *Pon1*$^{-/-}$ Mäuse einen verringerten Gehalt an LPC und LPC22:6 haben, was eine verringerte Phospholipase A2-ähnliche Aktivität wiederspiegeln kann.

1. INTRODUCTION

1.1. Lipids

1.1.1. Lipidomics: Definition and application

Biological systems comprise thousands of chemically distinct lipids. The structural diversity of lipids explains the broad spectrum of lipid functionality. For most lipids, their functions depend on molecular structure and can be very different for the different lipid categories, classes as well as for different lipid species within the same lipid class [1]. Lipidomics is a relatively young field of science [2], which aims to identify and quantify all individual lipid species and their functions within a biological system. In the past decade, progress in the lipidomics research has been driven by the development of electrospray ionization (ESI) mass spectrometry technologies [3]. This advance in mass spectrometry enables the structural characterisation and quantification of individual lipid species within different lipid classes.

Lipidomics studies are often aimed at the identification of lipid biomarkers which can be used for the diagnostics of onset, progression or severity of disease. Lipidomics can also provide information on biochemical mechanisms and pathways leading to disease. Thereby, lipidomics can be used in the discovery and clinical validation of novel biomarkers [4, 5]. Furthermore, Laurila and colleagues showed that integration of lipidomics into genomic and transcriptomic studies can provide a new layer of information on biological pathways [6].

1.1.2. Classification and structure of lipids

Lipids are a diverse group of hydrophobic or amphipathic small molecules that originate entirely or in part by carbanion-based condensations of ketoacyl subunits (fatty acids, glycerolipids, glycerophospholipids, sphingolipids, saccharolipids and polyketides) and/or by carbocation-based condensations of isoprene subunits (sterol and prenol lipids) [7, 8]. According to a classification proposed by the members of the LIPID MAPS consortium [7, 8], all lipids are divided into eight primary categories based on their chemical structure and biochemical characteristics. These categories are fatty acids, glycerolipids, glycerophospholipids, sphingolipids, sterol lipids, prenol lipids, saccharolipids and polyketides (Fig. 1) [7, 8]. Each of these categories is subsequently subdivided into distinct classes and subclasses. The structural diversity of all identified lipids is addressed by several websites, for example LIPID MAPS (http://www.lipidmaps.org/).

Lipids exert a wide range of functions essential for living systems. Their primary functions include the formation of lipid bilayer barriers in cells and organelles, and the service as an energy source by β-oxidation. Lipids also play important roles in cell biology as signalling or regulatory molecules.

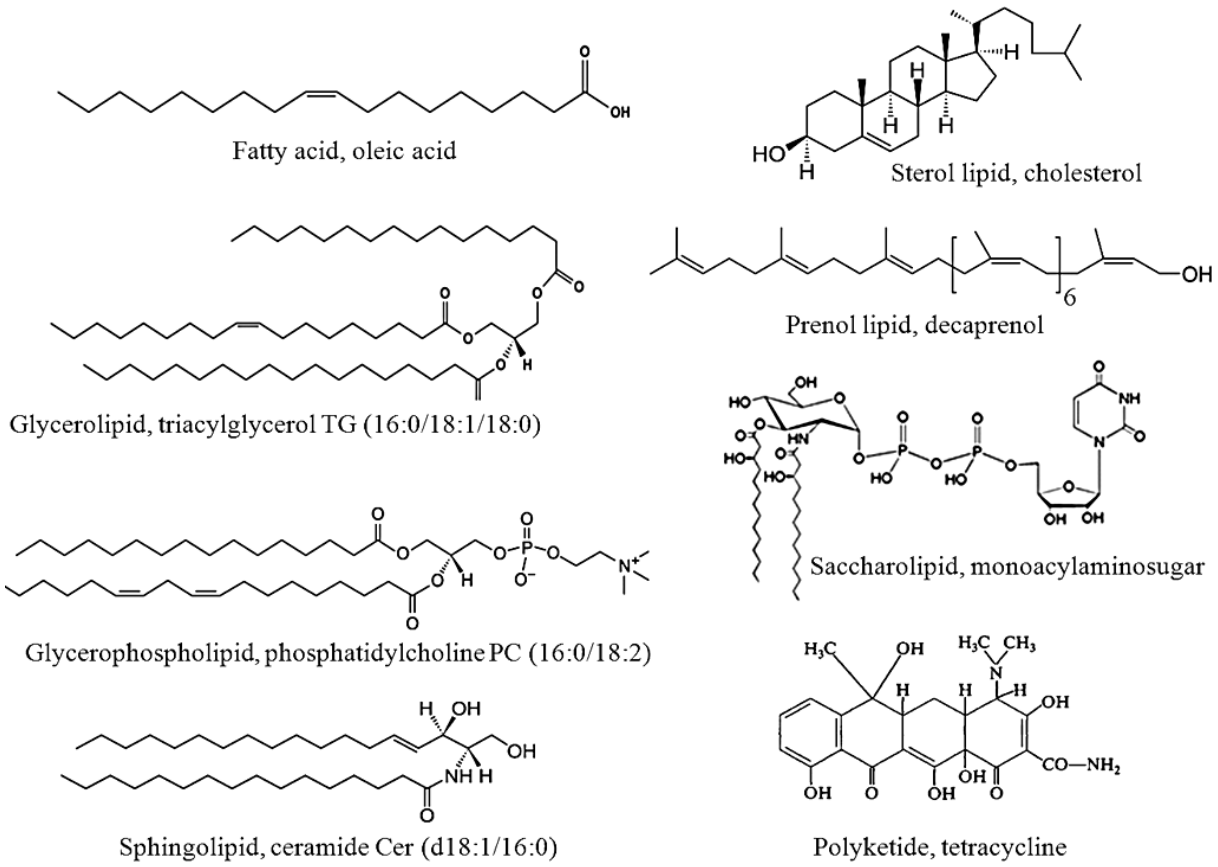

Figure 1. Representative structures for each lipid category.

1.1.2.1. Glycerophospholipids

Glycerophospholipids are amphipathic lipids that derive from glycerol-3-phosphate esterified at the *sn-1* and *sn-2* positions of the glycerol backbone with two long-chain fatty acids. Glycerophospholipids esterified with one fatty acid at either position are called lysoglycerophospholipids. Simple glycerophospholipids contain a free phosphoryl group and are known as phosphatidic acids (PAs). Complex glycerophospholipids are formed when a phosphoryl group is attached to another hydrophilic molecule like choline, ethanolamine, serine, inositol or glycerol [9]. The structure of the head group defines the class of glycerophospholipids, while variation in the numbers of carbons and double bonds in acyl chains defines lipid species (Fig. 2). Glycerophospholipids with vinyl ether double bond (-CH_2-O-CH=CH-) at the *sn-1* position and an ester bond at the *sn-2* position of the glycerol backbone represent plasmalogens. The plasmalogens mainly occur as species of

phosphatidylethanolamines (PEs) or phosphatidylcholines (PCs) and, to a lesser extent, as species of phosphatidylserines (PSs) [10].

PAs are the metabolic precursors of almost all glycerophospholipids. In eukaryotic cells, PAs can be metabolised in two ways: either PAs are hydrolysed to diacylglycerols or transformed into cytidine diphosphate diacylglycerols. In the first case, phosphate groups can be attached to diacylglycerols and form PCs or PEs. In the second case, the phosphate group of cytidine diphosphate diacylglycerols can be replaced, giving rise to phosphatidylinositols (PIs), phosphatidylglycerols (PGs) or diphosphatidylglycerols (also known as cardiolipins).

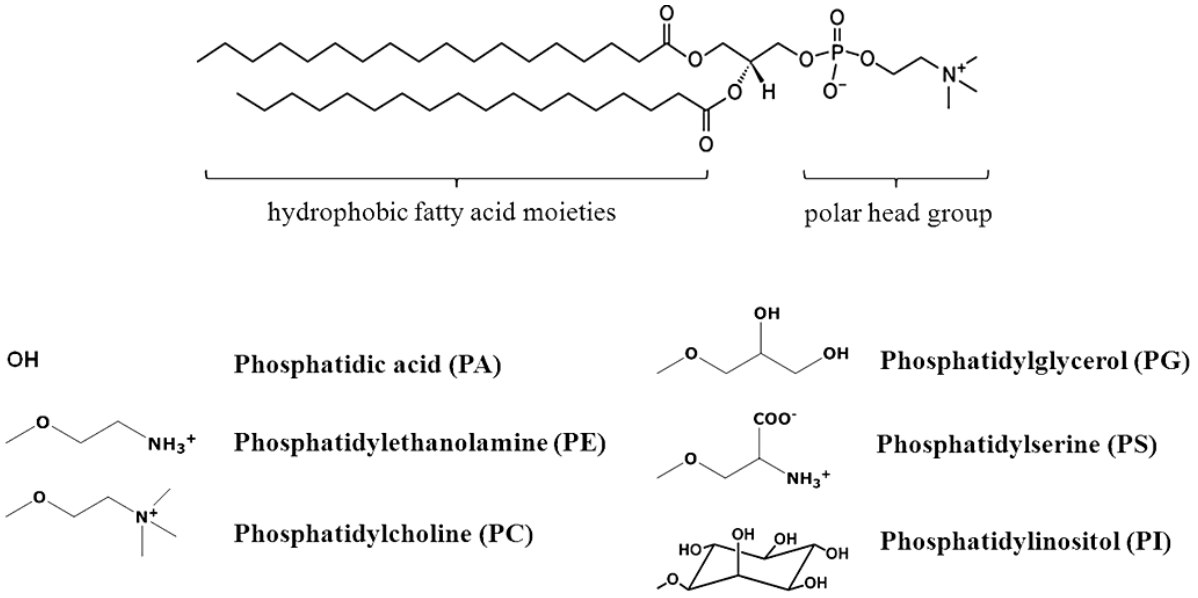

Figure 2. Structures of glycerophospholipids and head group variation. The complete molecular structure shown is phosphatidylcholine PC(16:0/16:0) (1,2-distearoyl-sn-glycerol-3-phosphocholine). Substitution of choline with the head groups listed below results in the other glycerophospholipid structures [9].

1.1.2.2. Sphingolipids

Sphingolipids are amphipathic lipids that share a common structural feature, a sphingoid backbone, which is also called sphingosine. In humans, the most common sphingoid backbone is an 18-carbon-atom-long amino alcohol with one double bond. It is synthesised *de novo* from the condensation of serine and palmitoyl (C16:0)-CoA, catalysed by enzyme serine:palmitoyltransferase (SPT) [11]. However, besides C16:0-CoA, human SPT can metabolise other acyl-CoAs, resulting in the formation of quantitatively minor sphingoid bases with different numbers of carbon atoms in the alkyl chain [12]. The sphingoid base can be linked with a fatty acid through an amide bond and/or with a head group at the primary hydroxyl position. The head group ranges from a simple hydrogen of free sphingosine or ceramides (Cers) to a more complex head group, such as phosphocholine of sphingomyelins

(SMs), a one-sugar residue of neutral glycosphingolipids, or several charged sugar residues of gangliosides [13]. According to a classification of the LIPID MAPS consortium, sphingolipids can be subdivided into several major classes: the sphingoid bases with their simple derivatives, Cers, and more complex sphingolipids, such as phosphosphingolipids [7]. The variation in the number of carbon atoms and double bounds in the sphingoid backbone and, if present, in N-linked fatty acid, determines the structural diversity of sphingolipid species.

1.1.2.3. Nomenclature of glycerophospholipids and sphingolipids

Lipids are named according to a nomenclature recommended by the LIPID MAPS consortium [7, 8], which is largely based on the nomenclature defined by the International Union of Pure and Applied Chemists and the International Union of Biochemistry and Molecular Biology (IUPAC-IUBMB) Commission on Biochemical Nomenclature (http://www.chem.qmul.ac.uk/iupac/). Glycerophospholipid species are annotated by using "head group(sn1/sn2)" format (e.g. PC(16:0/18:1)). The head group is annotated by using two-letter abbreviations (PC/PE/PA/PG/PS, etc.), which is by default assumed to be at the *sn-3* position of the glycerol backbone. The structure of the side chains is indicated within parentheses; the number before the colon denotes the number of carbon atoms and the number after the colon denotes the number of double bonds in the fatty acid moieties of the given lipid molecule. The lysoglycerophospholipid species with only one fatty acid residue are specified with a letter "L" in the abbreviation. For example, PC(16:0/18:2) refers to 1-palmitoyl-2-oleoyl-sn-glycero-3-phosphocholine, while LPC(16:0/0:0) refers to 1-palmitoyl-2-hydroxy-sn-glycero-3-phosphocholine [8].

In the sphingolipid classification, the sphingoid base sphingosine is abbreviated as d18:1 by using a shorthand form with d for the two hydroxyl groups of sphingosine, followed by the chain length (typically 18 carbons) and number of double bonds (0, 1 or 2). The shorthand notation for complex sphingolipids is presented in order of sphingoid base and N-acylated fatty acid. For example, SM(d18:1/24:1) refers to N-nervonoyl-D-erythro-sphingosylphosphorylcholine [7, 13].

Lipids can be annotated by the "molecular composition" that describes the structure of the attached fatty acid moieties (e.g. PC(16:0/18:2), LPC(16:0/0:0) and SM(d18:1/24:1)) or by the "sum composition" that indicates total numbers of carbons and double bonds for all acyl and/or alkyl chains (e.g. PC34:2, LPC16:0 and SM42:2). The abbreviation of the glycerophospholipids and sphingolipids depends on the analytical capabilities of mass

spectrometry methods applied, as described elsewhere [14]. As glycerophospholipids and SMs contain a phosphate group, they are often summarized as phospholipids.

1.1.3. Functions of glycerophospholipids and sphingolipids

Glycerophospholipids and sphingolipids function as structural components of cell membranes and lipoproteins. A biological cell membrane is a lipid bilayer that provides a barrier between the interior of the cell and surroundings. The formation of lipid bilayers can be explained by the self-association of amphipathic lipids, containing hydrophobic and hydrophilic domains, in an aqueous environment. The driving force for the formation of a lipid bilayer is the minimised interaction between hydrophobic domains and water, resulting in an entropy-driven relaxation of water. Hydrophilic domains of glycerophospholipids and sphingolipids interact with water through hydrogen bonding or ionic interaction and, therefore, are stable [9]. Biological membranes are not static; they are characterised by fluidity which is determined by the proportions of saturated and unsaturated fatty acid residues in glycerophospholipids and by the proportions of SMs and free cholesterol within the membrane. Furthermore, SMs tend to associate with each other as well as with cholesterol and form lipid rafts within the membrane [13]. Lipid rafts are relatively small subdomains of biomembranes that provide platforms for proteins needed for cell function [13].

In addition to being a component of cell membranes, some of glycerophospholipids and sphingolipids, like LPAs, LPCs, Cers and sphingosine-1-phosphate (S1P), are widely recognised as important intracellular and extracellular signalling molecules and mediators of cell-to-cell recognition and interaction [13, 15]. These lipids have rather simple molecular structures and possess significant water solubility that enables them to move from the site of synthesis to targets inside or outside the cell.

1.1.4. Glycerophospholipids and sphingolipids in human plasma

The plasma lipidome consist of more than 500 lipid species distributed among six distinct categories of lipids, including fatty acids, glycerolipids, glycerophospholipids, sphingolipids, sterol lipids and prenol lipids [16]. The number of identified species is largely limited by the sensitivity of available mass spectrometry technologies and probably will grow in the near future. Glycerophospholipids represent the second major component of the plasma lipidome, amounting to about one third of plasma lipids (Fig. 3A). Plasma glycerophospholipids comprise 160 individual molecular species with the PCs and PEs being

the most predominant lipids (Fig. 3B). In addition, plasma contains considerable amounts of LPCs, LPEs and PIs as well as minor amounts of PC-derived and PE-derived plasmalogens [16].

Plasma sphingolipids comprise more than 200 molecular species and account for ~4% of total lipids in the plasma (Fig. 3A). SMs are the major sphingolipids, representing ~95% of total sphingolipids, followed by Cers (~3.5%) and monohexosyl ceramides (<1%) (Fig. 3C) [16, 17].

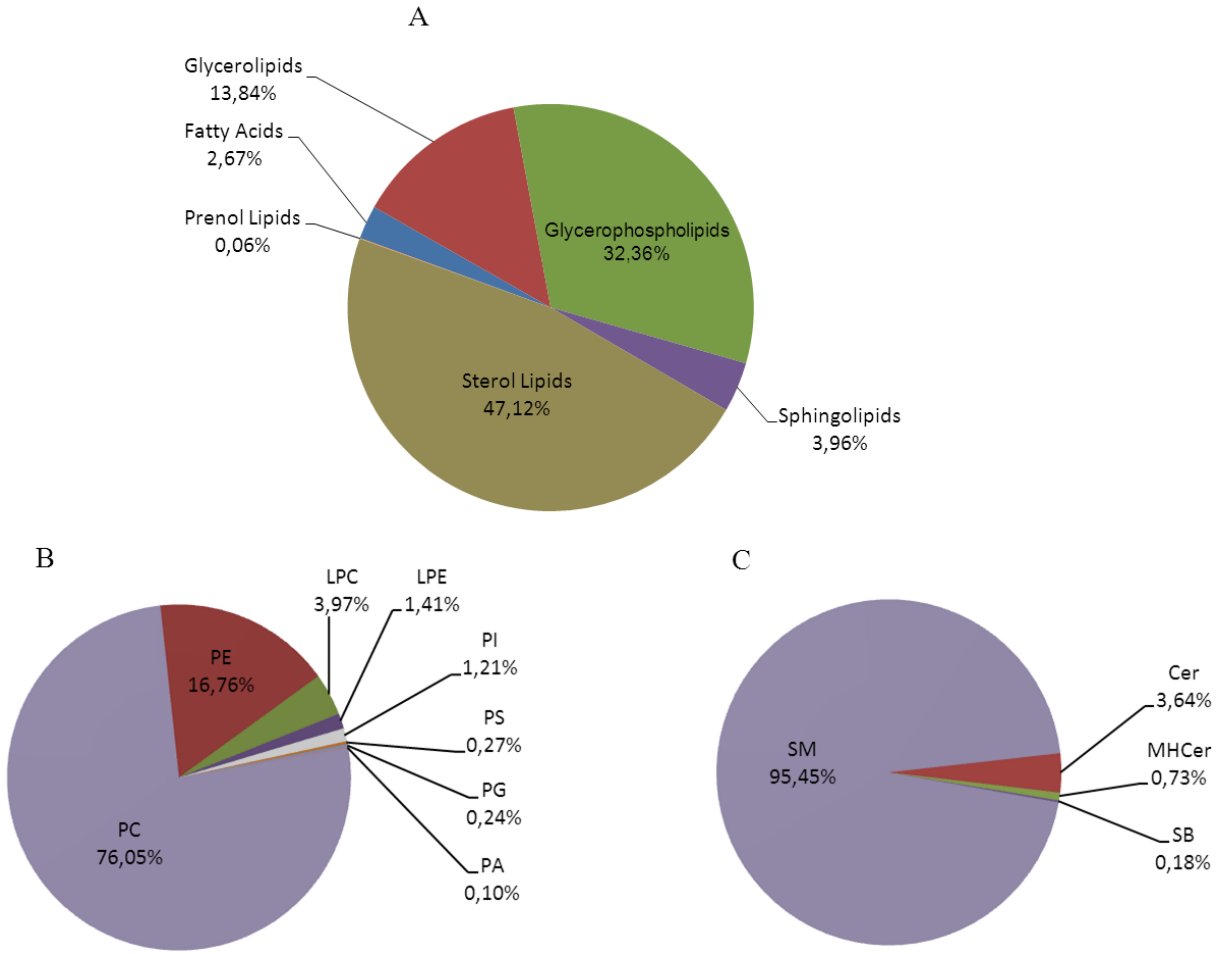

Figure 3. Distribution of plasma lipids (Figure 3A), glycerophospholipids (Figure 3B) and sphingolipids (Figure 3C). The figure is reproduced from the data reported by Quehenberger and colleagues [16]. Cer stands for ceramide; MHCer, monohexosyl ceramide; LPC, lysophosphatidylcholine; LPE, lysophosphatidylethanolamine; PA, phosphatidic acid; PC, phosphatidylcholine; PE, phosphatidylethanolamine; PG, phosphatidylglycerol; PI, phosphatidylinositol; PS, phosphatidylserine; SB, sphingoid base; SM, sphingomyelin.

Plasma glycerophospholipids and sphingolipids are associated with lipoproteins. They form the surface lipid monolayer around the hydrophobic core made of cholesteryl esters and triacylglycerols [18-20]. Glycerophospholipids and sphingolipids are unequally distributed across plasma lipoproteins. Specifically, high-density lipoproteins (HDL) are major carriers of PC, PE and PE-based plasmalogens [18, 20]. Conversely, low-density lipoproteins (LDL) represent

major carriers of SMs, Cers and monohexosyl ceramides [18, 19]. S1P is a minor biologically active lysosphingolipid. Differently to other sphingolipids, ~60% of plasma S1P is associated with HDL, ~30% of S1P is present in albumin, while the other 10% of S1P is distributed among very-low-density lipoprotein (VLDL) and LDL particles [21-23].

1.2. The pathophysiology of coronary artery disease and lipoprotein metabolism

According to the World Health Organisation statistics for 2012, ischemic heart disease, which is mainly caused by coronary artery disease (CAD), is the leading cause of death worldwide [24]. CAD most often results from atherosclerosis in the coronary arteries. Atherosclerosis is a chronic inflammatory disease which leads to narrowing of the arteries and decreasing blood flow and oxygen supply. Generally, atherosclerosis is an asymptomatic process, making the artery narrow and less flexible. Clinical manifestations of CAD commonly result from the disruption or erosion of an atherosclerotic plaque and a subsequent thrombus of one of the coronary arteries. This causes acute coronary syndromes (ACS) which encompass myocardial infarction (defined by the finding of biomarkers of myocardial necrosis in the plasma) and unstable angina (defined by chest pain without biomarkers of myocardial necrosis in the plasma). The major risk factors that significantly increase the chance of developing CAD are advanced age, male gender, smoking, physical inactivity, hypertension, dyslipidemias, obesity and diabetes [25, 26].

Several clinical studies showed a strong association between an altered plasma lipid profile, specifically elevated total cholesterol and LDL-cholesterol (LDL-C) levels, and the risk of CAD [27]. A number of epidemiological studies and studies on individuals with familial hypercholesterolemia have shown a direct correlation of high total cholesterol and LDL-C levels with the risk of incidence of CAD [27]. Furthermore, clinical trials of LDL-C lowering drugs have shown reduction in CAD events [28], indicating the central role of cholesterol metabolism in the pathogenesis of CAD.

In the circulatory system, cholesterol is transported by lipoproteins, mostly in the form of water-insoluble cholesteryl esters. The widely accepted concept of atherosclerosis suggests that accumulation of LDL-derived cholesterol within the artery wall is central in the formation of the atherosclerotic plaques. This process is initiated when the endothelial cell monolayer lining the lumen of the arteries undergoes inflammatory activation and excretes various chemokines. This directs monocytes into the intima layer of the artery where they transform into macrophages. In parallel, LDL enter the endothelial cell monolayer and are retained in the artery wall. After enzymatic and oxidative modification of the trapped LDL particles, they

are taken up by macrophages through receptors that are not regulated by the cholesterol content of the cells. The result is a massive intracellular accumulation of cholesterol, which transforms macrophages into lipid-loaded foam cells. This promotes the development of atherosclerotic lesions by stimulating inflammatory response, smooth muscle cell proliferation and migration, as well as synthesis of matrix macromolecules [29, 30].

In addition to LDL, HDL also play an important role in cholesterol metabolism, as HDL transport cholesterol from peripheral tissue, notably cholesterol-loaded macrophages, to the liver [30]. Moreover, low levels of HDL-cholesterol (HDL-C) correlate inversely with risk of CAD events [31]. In recent years, several vascular effects of HDL have been identified. *In vitro* and *in vivo* studies have shown that HDL particles from healthy subjects exert anti-inflammatory, anti-apoptotic and anti-thrombotic effects and stimulate endothelial NO production and endothelial repair. However, potentially atheroprotective effects of HDL were found to be markedly attenuated in HDL from CAD patients when compared to HDL from healthy subjects [32, 33]. The loss of atheroprotective functions of HDL was largely attributed to the alterations in protein composition and oxidative modification of the protein components of HDL particles [34-36]. This indicates that not only the quantity, reflected by HDL-C levels, but also the quality of HDL, reflected by molecular composition, plays an important role in the pathogenesis of CAD.

1.2.1. Glycerophospholipids and sphingolipids in pathogenesis of coronary artery disease

Glycerophospholipids and sphingolipids are abundant components of the vascular plaques and plasma lipoproteins. Today it is becoming clear that not only cholesterol, but other lipids, like glycerophospholipids and sphingolipids, are involved in the formation of the atherosclerotic plaques and development of CAD. Several studies have been carried out on the total plasma lipidome in relation to CAD [37, 38], as well as obesity [39] and hypertension [40].

Glycerophospholipids and SMs were identified in significant amounts in atherosclerotic plaques at different stages of lesion development [41]. Comparative analysis of stable and unstable regions within the same atherosclerotic lesion found major differences in the composition of PCs, LPCs and SMs [42]. Differences in the plasma lipidome were identified between stable CAD and unstable CAD as well as between stable CAD and healthy subjects. Specifically, reduced plasma levels of specific PCs, LPCs, PC plasmalogens and PE plasmalogens as well as increased plasma levels of PIs with 20:4 fatty acid moiety were associated with stable CAD, relative to healthy controls. In addition, diminished plasma content of specific LPCs, PE-plasmalogens and most of PIs, as well as elevated plasma

content of PEs and LPEs displayed significant association with unstable CAD when compared to stable CAD patients [37]. The large population-based Bruneck study with 10 years of follow-up identified significant associations between increased plasma concentrations of triacylglycerols (TAGs), cholesteryl esters (CEs), PEs, PCs and SMs and the incidence of cardiovascular disease. In this study, TAG54:2, CE16:1 and PE 36:5 were identified as the strongest predictive risk factors for cardiovascular disease [38]. Analyses of SMs in plasma of CAD patients yielded inconsistent results. Although few studies showed that plasma SM levels were elevated in CAD patients [43, 44], another more recent study showed no association of SM lipids with increased risk of CAD [45]. Reduced serum levels of PC-based and PE-based plasmalogens, which are known to possess anti-oxidant properties, as well as elevated serum levels of LPCs were shown to be associated with acquired obesity [39]. Furthermore, total PC plasmalogens and PE plasmalogens, as well as plasmalogens containing C20:4 and C22:5 fatty acid moieties were found at reduced plasma levels in hypertensive individuals [40].

Furthermore, the severity of CAD has been closely linked to low plasma levels of HDL-associated phospholipids [46, 47]. A NMR-based study showed lower contents of SM and PC lipids in HDL of CAD patients than in HDL of healthy controls [48]. In addition, Pruzanski and colleagues reported that acute-phase HDL are depleted of PEs, PE-based plasmalogens, polyunsaturated PCs, and SMs, specifically SM 33:1 and SM 38:1 species, and enriched with LPCs and saturated PCs [49]. HDL of patients with low HDL-C contain less PC- and/or PE-plasmalogens than HDL of patients with high HDL-C levels [6, 50].

1.2.2. Functional relevance of the lipoprotein lipidome

The composition of glycerophospholipids and sphingolipids can influence functions of plasma lipoproteins, such as LDL and HDL. A high ratio of SMs to PCs makes LDL particles more susceptible to lipolysis by SMase (secretory sphingomyelinase) [51]. As a consequence, elevated levels of Cers lead to the aggregation of LDL in the arterial walls and facilitate atherosclerosis [52]. The glycerophospholipids and sphingolipids in HDL, particularly PC and SM lipids, can influence the structure and dynamic properties of the surface monolayer of HDL. Changes in the fluidity of the lipid monolayer can have a subsequent effect on SR-B1 mediated cholesterol efflux and on over all reverse cholesterol transport [53]. It has been shown that variations in the acyl chains of PC lipids in reconstituted HDL (rHDL) influence the conformation of apoA1 [53] as well as the ability to activate lecithin:cholesterol acyltransferase (LCAT) [54], to suppress the synthesis of endothelial cell adhesion molecules [55], and to accept phospholipid hydro-peroxides from LDL [56]. Experimental studies with rHDL showed that

SMs inhibit cholesterol esterification by LCAT, which is important for the maturation of HDL particles [57]. Moreover, mice with deficient SPTLC2 (serine:palmitoyltransferase long chain base subunit 2) or SM synthase present with elevated activity of LCAT, which is caused by reduced levels of plasma SMs [58]. These facts suggest that plasma glycerophospholipids and sphingolipids are involved in lipoprotein metabolism and may be related to the pathogenesis of CAD.

1.2.3. Sphingosine-1-phosphate

S1P is a minor bioactive lysosphingolipid that plays important roles in immunity, inflammation and vascular function. S1P acts as the ligand for at least five different G protein-coupled S1P receptors (GPCRs) present on endothelial and smooth muscle cells. Through interaction with the GPCRs, S1P, for example, can regulate cell apoptosis, motility, proliferation, wound healing and immune response [59-61]. S1P is synthesised via phosphorylation of sphingosine, catalysed by sphingosine kinases 1 and 2. S1P can be irreversibly degraded by S1P-lyase to PE and fatty acid aldehyde. Because of absent S1P-lyase, erythrocytes and platelets represent the primary sources of S1P in the plasma [61, 62]. Most of S1P in the circulatory system is transported by HDL (~60%) [21-23]. Several *in vitro* and animal studies indicate that HDL-bound S1P mediates potentially atheroprotective functions of HDL, including promotion of endothelial cell growth and survival, tube formation, vasodilation as well as inhibition of the migration of vascular smooth muscle cells and apoptosis [60, 63]. Importantly, plasma and HDL levels of S1P were found to be lower in patients with stable CAD [64]. Moreover, the content of S1P and dihydro-S1P in the HDL-containing but apoB depleted serum was inversely correlated with the occurrence of ischemic heart disease [65]. In addition, the content of S1P was lower in both total plasma and the HDL-containing fraction of plasma of patients with HDL-C lowering monogenic disorders, involving mutations in *APOA1*, *LCAT* or *ABCA1* genes, when compared to unaffected family members [21]. Considering these facts, S1P appears to be associated with the atheroprotective effects of HDL and the pathogenesis of CAD.

Enrichment of HDL particles with S1P is explained by the presence of a specific S1P-binding protein, called apolipoprotein M (apoM). Christoffersen and colleagues [22] provided convincing evidence on the important role of apoM in binding and function of S1P in HDL. Furthermore, it has been shown that S1P is reduced in plasma and lacking in HDL of $Apom^{-/-}$ mice [21, 22]. In contrast, S1P was elevated in plasma and HDL of $Apom^{tg}$ mice [21, 22]. This indicates that apoM is involved in the regulation of S1P levels in both plasma and HDL.

However, a clinical study of humans with monogenic disorders of HDL metabolism did not show any significant correlation between S1P and apoM levels, neither in plasma nor in HDL-containing fractions [21]. These facts indicate complex and yet unknown interactions between HDL, apoM and S1P.

1.2.4. Paraoxonase 1 and age-related macular degeneration

Paraoxonase 1 (PON1) is a Ca^{2+} dependent, HDL-associated anti-oxidant enzyme. PON1 is a glycoprotein of 354 amino acids and approximate molecular mass of 43 kDa [66]. An X-ray crystallography study has indicated the structure of PON1 to be a six-bladed beta-propeller with two Ca^{2+} ions in the inner channel of the protein [67]. PON1 is the first discovered member of the PON multi-gene family which comprises three members, PON1, PON2 and PON3, the genes for which are located next to each other on the long arm of chromosome 7 [68]. Together with PON2 and PON3, PON1 forms a family of lactonases with anti-oxidant properties, which differ in the sites of synthesis and mechanisms of actions [69]. In the circulatory system, PON1 is almost exclusively present in HDL where it is anchored to lipids via its hydrophobic N-terminal region [67]. PON1 is considered to be a major factor in the anti-oxidant function of HDL particles [70]. *In vitro* experiments showed that PON1 inhibits lipid oxidation of LDL [71] and attenuates the oxidation of HDL and cell membranes [72, 73]. The mechanism by which PON1 inhibits LDL oxidation is unproven, but it probably involves hydrolysis of oxidised phospholipids [70]. Additionally, PON1 reduces macrophage oxidative stress and the ability of macrophages to oxidise LDL, inhibits cholesterol synthesis, and promotes cholesterol efflux [74, 75]. Consequently, PON1 plays a protective role in the early stages of atherosclerosis. This is supported by a recent study showing a reduction in atherosclerotic lesion size in mice overexpressing human PON1 [76]. Furthermore, several studies have shown prospectively that low PON1 activity is a risk factor for development of CAD [75, 77, 78]. Diminished serum arylesterase and paraoxonase activities were found to be associated with increased risk for major adverse cardiac events [79]. However, the findings are not unequivocal [80].

PON1 serum concentration and activity are highly variable in human populations [70]. This variability is largely determined by the genetic polymorphisms in the *PON1* gene. Two coding region polymorphisms - PON1 Q192R and PON1 L55M - affect substrate specificity, enzyme activity as well as the ability of HDL to protect LDL from oxidative modifications [81-83]. In addition, several polymorphisms in the promoter region of the *PON1* gene are associated with different serum concentrations of the protein [84].

Numerous studies have investigated several PON1 polymorphisms as risk factors for CAD with positive associations being identified in some, but not all studies. Two meta-analyses have shown the association of the PON1 Q192R variant with a small increase in the relative risk for CAD [85, 86]. Large genome-wide association study revealed that PON1 polymorphisms, which are highly significantly associated with serum paraoxonase or arylesterase activity, are not associated with risk of incident cardiac event or prevalent CAD [79].

Several genetic studies have found significant associations of polymorphisms within coding and upstream regulatory regions of the *PON1* gene and age-related macular degeneration (AMD) [87, 88]. Furthermore, a clinical study has reported reduced serum paraoxonase activity of PON1 in patients with AMD [89]. These data suggests that PON1 may be an important factor in the aetiology of AMD.

AMD is a complex disease that leads to the degeneration of the retina and retinal pigment epithelium (RPE) in individuals older than 60 years of age. If not treated, AMD causes gradual deterioration and loss of central vision in the elderly [90]. AMD and CAD share similar risk factors, such as advanced age, oxidative stress, smoking and inflammatory components [91, 25]. Furthermore, the severity of CAD is significantly associated with appearance of early clinical signs of AMD [92]. One of the earliest clinical hallmarks of AMD are drusen, which are formed between the retinal pigment epithelium (RPE) and Bruch`s membrane [93]. That formation of the drusen has a negative effect on functions of RPE and photoreceptors [94]. Similar to atherosclerotic plaques, the major constituents of drusen include aggregates of lipoproteins and cholesterol [91, 94]. Taken together, the data suggest a role of PON1 in the development of AMD. However, neither the functions of PON1 in the retina, in general, nor its specific role in the pathogenesis have been directly studied yet.

1.3. Mass spectrometry analysis of lipids

1.3.1. Overview of targeted lipidomics

Today, most lipidomics approaches are based on mass spectrometry (MS), which can be combined with direct-sample infusion systems or high-performance liquid chromatography (HPLC). Due to the diverse structure and chemical properties of lipids, the complete characterisation of the lipidome requires not one but several analytical methods specific to certain categories of lipids [95].

The targeted approach aims for the identification and quantification of specific lipids, or numerous individual lipids species within a lipid class. Typically it is achieved by

employing MS monitoring methods such as precursor ion scanning, neutral loss scanning or multiple reaction monitoring (MRM). Most lipids display characteristic fragmentation patterns. Precursor ion and neutral loss MS methods allow lipid-class-specific scans due to the structural similarities of the lipids within a lipid class. For example, after fragmentation, all PC and SM lipids in positive mode give rise to the phosphocholine fragment at *m/z* 184.1. Thus, only PC and SM species can be detected by precursor ion scanning at *m/z* 184.1, even though present in a complex lipid extract. This methodology was widely applied for MS-based analysis of different glycerophospholipid classes [96]. In addition, MS analysis with MRM enables the detection of specific lipid species, such as S1P, based on their unique parent/fragment ion transitions. This MS method provides highly selective and very sensitive determination of individual lipid species in the complex lipid mixture, however it requires prior knowledge about the fragmentation patterns of lipids analysed.

Targeted lipidomics is commonly used in combination with a shotgun approach or with HPLC. Targeted shotgun lipidomics refers to intra-source separation and ionization of lipids injected directly into the MS without on-line separation. Intra-source separation is usually achieved by varying the conditions of ion formation, aiming to enhance the ionization of analysed lipids and inhibit the ionization of all the matrix components. Shotgun lipidomics has been applied to the analysis of lipid species of different glycerophospholipid classes [97, 98]. However, the high ion density in the ion source reduces the ionization efficacy of the low-abundance lipids and leads to signal suppression. Moreover, a potential isotopic overlap of lipids with close molecular weight or isobaric lipids presents other important limitations of the shotgun methodology. Targeted liquid chromatography-mass spectrometry lipidomics is a reasonable solution for these problems. HPLC, combined with the MS technique, allows the separation of lipid classes or species prior to MS analysis and reduces, but does not eliminate, the isotopic overlap and co-elution of isobaric lipids. Furthermore, the HPLC system can be adjusted for the optimal retention of the lipids, while the sample matrix will be removed, ensuring maximal ionization in the ion source. Normal-phase HPLC (based on the retention of the polar head group in the column) is usually applied for the separation of lipid classes, while reversed-phase HPLC (based on the retention of the carbon chain in the column) is commonly used for the separation of individual lipid species [96]. The targeted liquid chromatography-mass spectrometry approach has been widely employed for quantitative analysis of different glycerophospholipids and sphingolipids [96, 99, 100].

1.3.2. Data processing and interpretation in lipidomics research

Data processing is an important part of the workflow where recorded MS data are transformed into the knowledge about biological processes being studied [95]. Briefly, processing of spectral data consists of several steps including peak detection, lipid identification, isotope correction and data normalization. Today, all MS instruments are supplied with built-in software that facilitates the processing of multidimensional spectral data. In addition, important steps in data processing, like lipid identification and isotope correction, can be done by lipid focused software, such as open-source software LIMSA [101] or LipidXplorer [102]. Data normalization is usually achieved by comparisons of endogenous lipids with internal standards and results in quantitative information on identified lipids. Internal standards are often added to the samples before lipid extraction to compensate for losses during extraction and ionization efficiency, and to perform semi-quantitative analysis of identified lipid species. Stable-isotope labelled lipids present ideal internal standards, as they are chemically identical to non-labelled analogues. However, since not all lipids have commercially available stable-isotope labelled standards, a suitable alternative is the use of non-natural lipids belonging to the same lipid class. In addition, when lipidomics analysis includes screening of a large number of lipids, it is difficult to match every lipid species with internal standards, therefore only one or two internal standards from the same lipid class are used [5].

The interpretation of quantitative lipidomics data largely depends on the experimental design and study objectives. Univariate and multivariate statistical analyses are routinely used for comparative analysis of study groups to extract relevant information from lipidomics data. Univariate analyses identify the lipid species with a significant difference between average content, analysing one lipid species at a time. Depending on the sample population, parametric (Student t-test) or nonparametric (Mann-Whitney U) statistical tests are used [95]. Since univariate analyses of lipidomics data include testing for large numbers of different lipids, it may increase the probability of false positive results. Thus, *p* values should be corrected to account for multiple comparisons by using Bonferroni or Benjamini and Hochberg procedures [103]. In contrast to the Bonferroni procedure, which strictly controls for even single false positive result, the Benjamini and Hochberg method tolerates a certain number of tests being incorrectly discovered, keeping the false discovery rate at 5% of all discoveries. Less conservative Benjamini and Hochberg procedure is commonly used in metabolomics and lipidomics studies.

Multivariate statistical analysis takes into account all lipid variables and their interrelationships simultaneously. Principal component analysis (PCA) is a key method in unsupervised analysis of multiple data. In practice, PCA reduces dimensionality of the data to the few uncorrelated variables (principal components) that explain the largest proportion of the variance within the data set. A score plot of the resulting model represents the distribution of individual samples, while a variable importance of the projection (VIP) coefficient plot provides a measure of the contribution of each lipid variable to the model. Supervised analysis of multivariate data can be performed by an orthogonal partial least square-discriminant analysis (OPLS-DA). This method is based on the concept of PCA, but also includes the information on the class membership. The acquired OPLS-DA model summarises data into predictive and orthogonal components that describe the between-group and the within-group variations, respectively [95, 104, 105]. Previously, our group applied the OPLS-DA to evaluate association of deoxysphingolipids with diabetes and the metabolic syndrome [105].

1.4. Aim of the study

We applied lipidomics to address the following research questions:

1. Do plasma concentrations of glycerophospholipids, sphingolipids and S1P differ between healthy controls and patients with either stable or acute CAD, and what is the distribution of glycerophospholipids and sphingolipids among plasma lipoproteins?
2. Are stable CAD or ACS associated with differences in the composition of glycerophospholipids, sphingolipids and S1P in HDL, and do differences in the lipidome affect the functionality of HDL?
3. Does apoM affect the ability of HDL to elicit S1P efflux from erythrocytes and the renal excretion of S1P?
4. Does the presence of PON1 affect the composition of glycerophospholipids and sphingolipids in the mouse retina, and thereby modulate the pathogenesis of AMD?

References

1. Stahlman M, Boren L., Ekross K. High-throughput molecular lipidomics. In: Ekross K. (ed), *Lipidomics*: Wiley-VCH Verlag GmbH & Co. KGaA.; 2012:35-51.
2. Han X, Gross RW. Global analyses of cellular lipidomes directly from crude extracts of biological samples by ESI mass spectrometry: a bridge to lipidomics. *Journal of lipid research* 2003;44:1071-1079.
3. Postle AD. Lipidomics. *Curr Opin Clin Nutr* 2012;15:127-133.
4. Wenk MR. The emerging field of lipidomics. *Nature reviews Drug discovery* 2005;4:594-610.
5. Meikle P. BC, Weir J. Lipidomics and lipid biomarker discovery. *Australian Biochemist* 2009;40:12-16.
6. Laurila PP, Surakka I, Sarin AP, et al. Genomic, transcriptomic, and lipidomic profiling highlights the role of inflammation in individuals with low high-density lipoprotein cholesterol. *Arteriosclerosis, thrombosis, and vascular biology* 2013;33:847-857.
7. Fahy E, Subramaniam S, Brown HA, et al. A comprehensive classification system for lipids. *Journal of lipid research* 2005;46:839-861.
8. Fahy E, Subramaniam S, Murphy RC, et al. Update of the LIPID MAPS comprehensive classification system for lipids. *Journal of lipid research* 2009;50 Suppl:S9-14.
9. Dowhan W, Bogdanov M., Mileykovskaya E., Functional roles of lipids in membranes. In: Vance D.E., Vance, J.E. (ed), *Biochemistry of lipids, lipoproteins and membranes*: Elsevier B.V.; 2008:2-36.
10. Wallner S, Schmitz G. Plasmalogens the neglected regulatory and scavenging lipid species. *Chemistry and physics of lipids* 2011;164:573-589.
11. Weiss B, Stoffel W. Human and murine serine-palmitoyl-CoA transferase--cloning, expression and characterization of the key enzyme in sphingolipid synthesis. *European journal of biochemistry / FEBS* 1997;249:239-247.
12. Penno A, von Eckardstein A, Hornemann T. SPTLC3 subunit of serine palmitoyltransferase is responsible for the generation of short chain sphingoid bases. *Chemistry and physics of lipids* 2008;154:S40-S41.
13. Merrill AH. Sphingolipids. In: Vance DE, Vance, J.E. (ed), *Biochemistry of lipids, lipoproteins and membranes*: Elsevier B.V.; 2008:364-396.
14. Ekroos K. Lipidomics perspective: from molecular lipidomics to validated diagnostics. In: Ekroos K (ed), *Lipidomics*: Wiley-VCH Verlag GmbH & KGaA.; 2012:1-19.

15. Grzelczyk A, Gendaszewska-Darmach E. Novel bioactive glycerol-based lysophospholipids: new data -- new insight into their function. *Biochimie* 2013;95:667-679.
16. Quehenberger O, Armando AM, Brown AH, et al. Lipidomics reveals a remarkable diversity of lipids in human plasma. *Journal of lipid research* 2010;51:3299-3305.
17. Hammad SM, Pierce JS, Soodavar F, et al. Blood sphingolipidomics in healthy humans: impact of sample collection methodology. *Journal of lipid research* 2010;51:3074-3087.
18. Wiesner P, Leidl K, Boettcher A, Schmitz G, Liebisch G. Lipid profiling of FPLC-separated lipoprotein fractions by electrospray ionization tandem mass spectrometry. *Journal of lipid research* 2009;50:574-585.
19. Scherer M, Bottcher A, Schmitz G, Liebisch G. Sphingolipid profiling of human plasma and FPLC-separated lipoprotein fractions by hydrophilic interaction chromatography tandem mass spectrometry. *Biochimica et biophysica acta* 2011;1811:68-75.
20. Dashti M, Kulik W, Hoek F, Veerman EC, Peppelenbosch MP, Rezaee F. A phospholipidomic analysis of all defined human plasma lipoproteins. *Scientific reports* 2011;1:139.
21. Karuna R, Park R, Othman A, et al. Plasma levels of sphingosine-1-phosphate and apolipoprotein M in patients with monogenic disorders of HDL metabolism. *Atherosclerosis* 2011;219:855-863.
22. Christoffersen C, Obinata H, Kumaraswamy SB, et al. Endothelium-protective sphingosine-1-phosphate provided by HDL-associated apolipoprotein M. *Proceedings of the National Academy of Sciences of the United States of America* 2011;108:9613-9618.
23. Rodriguez C, Gonzalez-Diez M, Badimon L, Martinez-Gonzalez J. Sphingosine-1-phosphate: A bioactive lipid that confers high-density lipoprotein with vasculoprotection mediated by nitric oxide and prostacyclin. *Thrombosis and haemostasis* 2009;101:665-673.
24. World Health Organization. "The top 10 causes of death". 2012.
25. Anderson JL, Adams CD, Antman EM, et al. ACC/AHA 2007 guidelines for the management of patients with unstable angina/non ST-elevation myocardial infarction: a report of the American College of Cardiology/American Heart Association Task Force on Practice Guidelines (Writing Committee to Revise the 2002 Guidelines for the Management of Patients With Unstable Angina/Non ST-Elevation Myocardial Infarction): developed in collaboration with the American College of Emergency Physicians, the Society for Cardiovascular Angiography and Interventions, and the Society of Thoracic Surgeons:

endorsed by the American Association of Cardiovascular and Pulmonary Rehabilitation and the Society for Academic Emergency Medicine. *Circulation* 2007;116:e148-304.

26. Antman EM, Anbe DT, Armstrong PW, et al. ACC/AHA guidelines for the management of patients with ST-elevation myocardial infarction--executive summary: a report of the American College of Cardiology/American Heart Association Task Force on Practice Guidelines (Writing Committee to Revise the 1999 Guidelines for the Management of Patients With Acute Myocardial Infarction). *Circulation* 2004;110:588-636.

27. Prospective Studies C, Lewington S, Whitlock G, et al. Blood cholesterol and vascular mortality by age, sex, and blood pressure: a meta-analysis of individual data from 61 prospective studies with 55,000 vascular deaths. *Lancet* 2007;370:1829-1839.

28. Cholesterol Treatment Trialists C, Baigent C, Blackwell L, et al. Efficacy and safety of more intensive lowering of LDL cholesterol: a meta-analysis of data from 170,000 participants in 26 randomised trials. *Lancet* 2010;376:1670-1681.

29. Lusis AJ. Atherosclerosis. *Nature* 2000;407:233-241.

30. Libby P, Ridker PM, Hansson GK. Progress and challenges in translating the biology of atherosclerosis. *Nature* 2011;473:317-325.

31. Emerging Risk Factors C, Di Angelantonio E, Gao P, et al. Lipid-related markers and cardiovascular disease prediction. *JAMA : the journal of the American Medical Association* 2012;307:2499-2506.

32. Luscher TF, Landmesser U, von Eckardstein A, Fogelman AM. High-density lipoprotein: vascular protective effects, dysfunction, and potential as therapeutic target. *Circulation research* 2014;114:171-182.

33. Riwanto M, Landmesser U. High density lipoproteins and endothelial functions: mechanistic insights and alterations in cardiovascular disease. *Journal of lipid research* 2013;54:3227-3243.

34. Riwanto M, Rohrer L, Roschitzki B, et al. Altered activation of endothelial anti- and proapoptotic pathways by high-density lipoprotein from patients with coronary artery disease: role of high-density lipoprotein-proteome remodeling. *Circulation* 2013;127:891-904.

35. Alwaili K, Bailey D, Awan Z, et al. The HDL proteome in acute coronary syndromes shifts to an inflammatory profile. *Biochimica et biophysica acta* 2012;1821:405-415.

36. Vaisar T, Mayer P, Nilsson E, Zhao XQ, Knopp R, Prazen BJ. HDL in humans with cardiovascular disease exhibits a proteomic signature. *Clinica chimica acta; international journal of clinical chemistry* 2010;411:972-979.

37. Meikle PJ, Wong G, Tsorotes D, et al. Plasma lipidomic analysis of stable and unstable coronary artery disease. *Arteriosclerosis, thrombosis, and vascular biology* 2011;31:2723-2732.

38. Stegemann C, Pechlaner R, Willeit P, et al. Lipidomics profiling and risk of cardiovascular disease in the prospective population-based Bruneck study. *Circulation* 2014;129:1821-1831.

39. Pietilainen KH, Sysi-Aho M, Rissanen A, et al. Acquired obesity is associated with changes in the serum lipidomic profile independent of genetic effects--a monozygotic twin study. *PloS one* 2007;2:e218.

40. Graessler J, Schwudke D, Schwarz PE, Herzog R, Shevchenko A, Bornstein SR. Top-down lipidomics reveals ether lipid deficiency in blood plasma of hypertensive patients. *PloS one* 2009;4:e6261.

41. Ravandi A, Babaei S, Leung R, et al. Phospholipids and oxophospholipids in atherosclerotic plaques at different stages of plaque development. *Lipids* 2004;39:97-109.

42. Stegemann C, Drozdov I, Shalhoub J, et al. Comparative lipidomics profiling of human atherosclerotic plaques. *Circulation Cardiovascular genetics* 2011;4:232-242.

43. Jiang XC, Paultre F, Pearson TA, et al. Plasma sphingomyelin level as a risk factor for coronary artery disease. *Arteriosclerosis, thrombosis, and vascular biology* 2000;20:2614-2618.

44. Nelson JC, Jiang XC, Tabas I, Tall A, Shea S. Plasma sphingomyelin and subclinical atherosclerosis: findings from the multi-ethnic study of atherosclerosis. *American journal of epidemiology* 2006;163:903-912.

45. Yeboah J, McNamara C, Jiang XC, et al. Association of plasma sphingomyelin levels and incident coronary heart disease events in an adult population: Multi-Ethnic Study of Atherosclerosis. *Arteriosclerosis, thrombosis, and vascular biology* 2010;30:628-633.

46. Piperi C, Kalofoutis C, Papaevaggeliou D, Papapanagiotou A, Lekakis J, Kalofoutis A. The significance of serum HDL phospholipid levels in angiographically defined coronary artery disease. *Clin Biochem* 2004;37:377-381.

47. Hsia SL, Duncan R, Schob AH, et al. Serum levels of high-density lipoprotein phospholipids correlate inversely with severity of angiographically defined coronary artery disease. *Atherosclerosis* 2000;152:469-473.

48. Kostara CE, Papathanasiou A, Psychogios N, et al. NMR-based lipidomic analysis of blood lipoproteins differentiates the progression of coronary heart disease. *Journal of proteome research* 2014;13:2585-2598.

49. Pruzanski W, Stefanski E, de Beer FC, de Beer MC, Ravandi A, Kuksis A. Comparative analysis of lipid composition of normal and acute-phase high density lipoproteins. *Journal of lipid research* 2000;41:1035-1047.

50. Yetukuri L, Soderlund S, Koivuniemi A, et al. Composition and lipid spatial distribution of HDL particles in subjects with low and high HDL-cholesterol. *Journal of lipid research* 2010;51:2341-2351.

51. Schissel SL, Jiang X, Tweedie-Hardman J, et al. Secretory sphingomyelinase, a product of the acid sphingomyelinase gene, can hydrolyze atherogenic lipoproteins at neutral pH. Implications for atherosclerotic lesion development. *The Journal of biological chemistry* 1998;273:2738-2746.

52. Devlin CM, Leventhal AR, Kuriakose G, Schuchman EH, Williams KJ, Tabas I. Acid sphingomyelinase promotes lipoprotein retention within early atheromata and accelerates lesion progression. *Arteriosclerosis, thrombosis, and vascular biology* 2008;28:1723-1730.

53. Davidson WS, Gillotte KL, Lundkatz S, Johnson WJ, Rothblat GH, Phillips MC. The Effect of High-Density-Lipoprotein Phospholipid Acyl-Chain Composition on the Efflux of Cellular Free-Cholesterol. *Journal of Biological Chemistry* 1995;270:5882-5890.

54. Parks JS, Huggins KW, Gebre AK, Burleson ER. Phosphatidylcholine fluidity and structure affect lecithin:cholesterol acyltransferase activity. *Journal of lipid research* 2000;41:546-553.

55. Baker PW, Rye KA, Gamble JR, Vadas MA, Barter PJ. Phospholipid composition of reconstituted high density lipoproteins influences their ability to inhibit endothelial cell adhesion molecule expression. *Journal of lipid research* 2000;41:1261-1267.

56. Zerrad-Saadi A, Therond P, Chantepie S, et al. HDL3-mediated inactivation of LDL-associated phospholipid hydroperoxides is determined by the redox status of apolipoprotein A-I and HDL particle surface lipid rigidity: relevance to inflammation and atherogenesis. *Arteriosclerosis, thrombosis, and vascular biology* 2009;29:2169-2175.

57. Rye KA, Hime NJ, Barter PJ. The influence of sphingomyelin on the structure and function of reconstituted high density lipoproteins. *The Journal of biological chemistry* 1996;271:4243-4250.

58. Subbaiah PV, Jiang XC, Belikova NA, Aizezi B, Huang ZH, Reardon CA. Regulation of plasma cholesterol esterification by sphingomyelin: effect of physiological variations of plasma sphingomyelin on lecithin-cholesterol acyltransferase activity. *Biochimica et biophysica acta* 2012;1821:908-913.

59. Lucke S, Levkau B. Endothelial functions of sphingosine-1-phosphate. *Cellular physiology and biochemistry : international journal of experimental cellular physiology, biochemistry, and pharmacology* 2010;26:87-96.

60. Sattler K, Levkau B. Sphingosine-1-phosphate as a mediator of high-density lipoprotein effects in cardiovascular protection. *Cardiovascular research* 2009;82:201-211.

61. Kim RH, Takabe K, Milstien S, Spiegel S. Export and functions of sphingosine-1-phosphate. *Biochimica et biophysica acta* 2009;1791:692-696.

62. Kumar A, Saba JD. Lyase to live by: sphingosine phosphate lyase as a therapeutic target. *Expert opinion on therapeutic targets* 2009;13:1013-1025.

63. Nofer JR, Assmann G. Atheroprotective effects of high-density lipoprotein-associated lysosphingolipids. *Trends in cardiovascular medicine* 2005;15:265-271.

64. Sattler KJ, Elbasan S, Keul P, et al. Sphingosine 1-phosphate levels in plasma and HDL are altered in coronary artery disease. *Basic research in cardiology* 2010;105:821-832.

65. Argraves KM, Sethi AA, Gazzolo PJ, et al. S1P, dihydro-S1P and C24:1-ceramide levels in the HDL-containing fraction of serum inversely correlate with occurrence of ischemic heart disease. *Lipids in health and disease* 2011;10:70.

66. Mackness B, Durrington PN, Mackness MI. Human serum paraoxonase. *Gen Pharmacol.* 1998;31:329-336.

67. Harel M, Aharoni A, Gaidukov L, et al. Structure and evolution of the serum paraoxonase family of detoxifying and anti-atherosclerotic enzymes. *Nat Struct Mol Biol.* 2004;11:412-419.

68. Primo-Parmo SL, Sorenson RC, Teiber J, La Du BN. The human serum paraoxonase/arylesterase gene (PON1) is one member of a multigene family. *Genomics.* 1996;33:498-507.

69. Draganov DI, La Du BN. Pharmacogenetics of paraoxonases: a brief review. *Naunyn Schmiedebergs Arch Pharmacol.* 2004;369:78-88.

70. Deakin SP, James RW. Genetic and environmental factors modulating serum concentrations and activities of the antioxidant enzyme paraoxonase-1. *Clin Sci (Lond).* 2004;107:435-447.

71. Mackness MI, Arrol S, Abbott C, Durrington PN. Protection of low-density lipoprotein against oxidative modification by high-density lipoprotein associated paraoxonase. *Atherosclerosis.* 1993;104:129-135.

72. Aviram M, Rosenblat M, Bisgaier CL, Newton RS, Primo-Parmo SL, La Du BN. Paraoxonase inhibits high-density lipoprotein oxidation and preserves its functions - A

possible peroxidative role for paraoxonase. *Journal of Clinical Investigation.* 1998;101:1581-1590.

73. Deakin SP, Bioletto S, Bochaton-Piallat ML, James RW. HDL-associated paraoxonase-1 can redistribute to cell membranes and influence sensitivity to oxidative stress. *Free Radic Biol Med.* 2011;50:102-109.

74. Aviram M, Rosenblat M. Paraoxonases 1, 2, and 3, oxidative stress, and macrophage foam cell formation during atherosclerosis development. *Free Radic Biol Med.* 2004;37:1304-1316.

75. Mackness M, Mackness B. Targeting paraoxonase-1 in atherosclerosis. *Expert Opin Ther Targets.* 2013;17:829-837.

76. Tward A, Xia YR, Wang XP, Shi YS, Park C, Castellani LW, Lusis AJ, Shih DM. Decreased atherosclerotic lesion formation in human serum paraoxonase transgenic mice. *Circulation.* 2002;106:484-490.

77. Mackness B, Durrington P, McElduff P, Yarnell J, Azam N, Watt M, Mackness M. Low paraoxonase activity predicts coronary events in the Caerphilly Prospective Study. *Circulation.* 2003;107:2775-2779.

78. Bhattacharyya T, Nicholls SJ, Topol EJ, et al. Relationship of paraoxonase 1 (PON1) gene polymorphisms and functional activity with systemic oxidative stress and cardiovascular risk. *JAMA.* 2008;299:1265-1276.

79. Tang WH, Hartiala J, Fan Y, et al. Clinical and genetic association of serum paraoxonase and arylesterase activities with cardiovascular risk. *Arterioscler Thromb Vasc Biol.* 2012;32:2803-2812.

80. Birjmohun RS, Vergeer M, Stroes ES, et al. Both paraoxonase-1 genotype and activity do not predict the risk of future coronary artery disease; the EPIC-Norfolk Prospective Population Study. *PLoS One.* 2009;4:e6809.

81. Garin MC, James RW, Dussoix P, Blanche H, Passa P, Froguel P, Ruiz J. Paraoxonase polymorphism Met-Leu54 is associated with modified serum concentrations of the enzyme. A possible link between the paraoxonase gene and increased risk of cardiovascular disease in diabetes. *J Clin Invest.* 1997;99:62-66.

82. Humbert R, Adler DA, Disteche CM, Hassett C, Omiecinski CJ, Furlong CE. The molecular basis of the human serum paraoxonase activity polymorphism. *Nat Genet.* 1993;3:73-76.

83. Mackness B, Mackness MI, Arrol S, et al. Serum paraoxonase (PON1) 55 and 192 polymorphism and paraoxonase activity and concentration in non-insulin dependent diabetes mellitus. *Atherosclerosis.* 1998;139:341-349.

84. Leviev I, James RW. Promoter polymorphisms of human paraoxonase PON1 gene and serum paraoxonase activities and concentrations. *Arterioscler Thromb Vasc Biol.* 2000;20:516-521.

85. Wheeler JG, Keavney BD, Watkins H, Collins R, Danesh J. Four paraoxonase gene polymorphisms in 11212 cases of coronary heart disease and 12786 controls: meta-analysis of 43 studies. *Lancet.* 2004;363:689-695.

86. Wang M, Lang X, Zou L, Huang S, Xu Z. Four genetic polymorphisms of paraoxonase gene and risk of coronary heart disease: a meta-analysis based on 88 case-control studies. *Atherosclerosis.* 2011;214:377-385.

87. Ikeda T, Obayashi H, Hasegawa G, et al. Paraoxonase gene polymorphisms and plasma oxidized low-density lipoprotein level as possible risk factors for exudative age-related macular degeneration. *Am J Ophthalmol.* 2001;132:191-195.

88. Oczos J, Grimm C, Barthelmes D, et al. Regulatory regions of the paraoxonase 1 (PON1) gene are associated with neovascular age-related macular degeneration (AMD). *Age (Dordr).* 2013;35:1651-1662.

89. Baskol G, Karakucuk S, Oner AO, et al. Serum paraoxonase 1 activity and lipid peroxidation levels in patients with age-related macular degeneration. *Ophthalmologica.* 2006;220:12-16.

90. Gehrs KM, Anderson DH, Johnson LV, Hageman GS. Age-related macular degeneration--emerging pathogenetic and therapeutic concepts. *Ann Med.* 2006;38:450-471.

91. Smith W, Assink J, Klein R, et al. Risk factors for age-related macular degeneration: Pooled findings from three continents. *Ophthalmology.* 2001;108:697-704.

92. Wang SB, Mitchell P, Chiha J, et al. Severity of coronary artery disease is independently associated with the frequency of early age-related macular degeneration. *Br J Ophthalmol.* 2014.

93. Pauleikhoff D, Harper CA, Marshall J, Bird AC. Aging changes in Bruch's membrane. A histochemical and morphologic study. *Ophthalmology.* 1990;97:171-178.

94. Curcio CA, Johnson M, Huang JD, Rudolf M. Apolipoprotein B-containing lipoproteins in retinal aging and age-related macular degeneration. *J Lipid Res.* 2010;51:451-467.

95. Ejsing EC, Husen, P., Tarasov, K. Lipid informatics: from a mass spectrum to interactomics. In: Ekross k, ed. *Lipidomics*: Wiley-VCH Verlag GmbH & KGaA.; 2012:147-174.

96. Pulfer M, Murphy RC. Electrospray mass spectrometry of phospholipids. *Mass Spectrom Rev.* 2003;22:332-364.

97. Ejsing CS, Duchoslav E, Sampaio J, et al. Automated identification and quantification of glycerophospholipid molecular species by multiple precursor ion scanning. *Anal Chem.* 2006;78:6202-6214.

98. Yang K, Zhao Z, Gross RW, Han X. Systematic analysis of choline-containing phospholipids using multi-dimensional mass spectrometry-based shotgun lipidomics. *J Chromatogr B Analyt Technol Biomed Life Sci.* 2009;877:2924-2936.

99. Houjou T, Yamatani K, Imagawa M, Shimizu T, Taguchi R. A shotgun tandem mass spectrometric analysis of phospholipids with normal-phase and/or reverse-phase liquid chromatography/electrospray ionization mass spectrometry. *Rapid Commun Mass Spectrom.* 2005;19:654-666.

100. Sullards MC, Allegood JC, Kelly S, et al. Structure-specific, quantitative methods for analysis of sphingolipids by liquid chromatography-tandem mass spectrometry: "inside-out" sphingolipidomics. *Methods Enzymol.* 2007;432:83-115.

101. Haimi P, Chaithanya K, Kainu V, Hermansson M, Somerharju P. Instrument-independent software tools for the analysis of MS-MS and LC-MS lipidomics data. *Methods Mol Biol.* 2009;580:285-294.

102. Herzog R, Schwudke D, Schuhmann K, et al. A novel informatics concept for high-throughput shotgun lipidomics based on the molecular fragmentation query language. *Genome Biol.* 2011;12:R8.

103. Hochberg Y, Benjamini Y. More powerful procedures for multiple significance testing. *Stat Med.* 1990;9:811-818.

104. Saccenti E, Hoefsloot HCJ, Smilde AK, Westerhuis JA, Hendriks MMWB. Reflections on univariate and multivariate analysis of metabolomics data. *Metabolomics.* 2014;10:361-374.

105. Othman A, Rutti MF, Ernst D, et al. Plasma deoxysphingolipids: a novel class of biomarkers for the metabolic syndrome? *Diabetologia.* 2012;55:421-431.

2. Association with Coronary Artery Disease and Lipoprotein Distribution of Plasma Glycerophospholipids and Sphingolipids

Iryna Sutter[1,2], Alaa Othman[1,3], Lucia Rohrer[1], Roland Klingenberg[4], Arnold von Eckardstein[1,2,3] and Thorsten Hornemann[1,2]

1. Institute of Clinical Chemistry, University and University Hospital of Zurich, Zurich, Switzerland
2. Competence Center for Integrated Human Physiology, University of Zurich, Zurich, Switzerland
3. Competence Center for System Physiology and Metabolic Diseases, ETH Zurich and University of Zurich, Zurich, Switzerland
4. Department of Cardiology, University Hospital Zurich, Zurich, Switzerland

[in preparation]

Abstract

Background: Coronary artery disease (CAD) is a chronic disease resulting from the formation of atherosclerotic lesions within the arterial wall. Glycerophospholipids and sphingolipids play an important role in lipoprotein metabolism, plaque formation and therefore in the development of atherosclerosis.

Objectives and Methods: Here, we show the association of plasma levels of glycerophospholipids and sphingolipids as well as sphingosine-1-phosphate (S1P) species and sphingoid bases of sphingolipids with CAD and acute coronary syndrome (ACS). In this study, we included comparison of statin-treated and untreated CAD patients. Furthermore, we described the distribution of phosphatidylcholines (PCs) and sphingomyelins (SMs) among plasma lipoproteins. Plasma lipids were measured using three different liquid chromatography-mass spectrometry methods.

Results: The glycerophospholipid and sphingolipid profile was altered in plasma of CAD and ACS patients. Specifically, 45 out of 65 quantified glycerophospholipid and sphingolipid species, 16:1-S1P as well as four sphingoid bases were lower in plasma of CAD patients as compared to healthy controls. Similarly, plasma levels of 42 glycerophospholipids and sphingolipids, 16:1-S1P, 18:1-S1P as well as six sphingoid bases were lower in ACS patients, relative to healthy subjects. The statin therapy did not have any significant effect on the plasma concentrations of glycerophospholipids and sphingolipids. The odd-chain PCs, PC33:1, PC33:2, PC33:3 and PC35:3, which are PC plasmalogens, were the most significantly and consistently altered species in plasma of both CAD and ACS patients. The PC and SM species were abundant exclusively in lipoprotein particles, whereas LPCs were mainly present in the lipoprotein-free fraction.

Conclusion: Both CAD and ACS are associated with alterations in the plasma concentrations of glycerophospholipids and sphingolipids, among them four PC plasmalogens were the most significantly altered lipids. Since the vast majority of glycerophospholipids and sphingolipids are present in lipoproteins, our observations are likely to be related to the changes in composition, number and/or oxidative state of lipoproteins.

2.1. Introduction

Coronary artery disease (CAD) remains the leading cause of death worldwide [1]. The primary cause of CAD is atherosclerosis, which results from plaque formation within the arterial wall [2]. CAD can take several years before it becomes symptomatic, for example, before manifestation of an acute coronary syndrome (ACS). Imbalanced lipid metabolism plays a central role in the pathogenesis of CAD. Indeed, elevated levels of total cholesterol and low-density lipoprotein cholesterol (LDL-C) as well as reduced levels of high-density lipoprotein cholesterol (HDL-C) have been widely recognised as independent risk factors for CAD [3,4]. Today, it is becoming clear that beyond cholesterol other lipids, including glycerophospholipids and sphingolipids, contribute to the development of atherosclerosis [5, 6].

In the circulatory system, plasma glycerophospholipids and sphingolipids are mainly associated with lipoprotein particles [7, 8]. They form a lipid monolayer around the hydrophobic core made of triglycerides and cholesteryl esters. Hundreds of different glycerophospholipid and sphingolipid species were identified in plasma lipoproteins and vascular plaques [9-11]. The lipid composition of lipoprotein particles was found to be altered in different pathologies related to CAD. Specifically, the acute-phase high-density lipoproteins (HDL) were found depleted of sphingomyelins (SMs), polyunsaturated phosphatidylcholines (PCs), phosphatidylethanolamines (PEs) and phosphatidylinositols (PIs), and enriched with lysophosphatidylcholines (LPCs) and saturated PCs when compared to normal HDL [12]. The PCs associated with very-low-density lipoproteins (VLDL) and low-density lipoproteins (LDL) had increased levels of C16:1 and C20:3 fatty acid residues in patients with dyslipidaemic type 2 diabetes [13]. Furthermore, alterations in the plasma or serum content of specific glycerophospholipids and sphingolipids have been described for hypertensive and obese individuals as well as for patients with stable and unstable CAD [14-16]. The prospective population-based Bruneck study has identified triacylglycerol TAG54:2, cholesteryl ester CE16:1 and PE36:5 lipids as strong predictive risk factors of cardiovascular disease [17]. A few studies in humans have shown that the plasma content of SMs is significantly elevated in CAD patients [18, 19], and that plasma SMs represent an independent predictor of myocardial infarction in ACS patients [20]. However, a more recent clinical study did not find any significant association of high plasma SM levels with increased risk of CAD [21]. In addition, sphingosine-1-phosphate (S1P), which exerts several atheroprotective effects of HDL [22, 23], was found at lower levels in the plasma and HDL of CAD patients [24, 25]. Furthermore, S1P in the HDL-containing fraction of serum, has been inversely correlated with the occurrence of ischemic heart disease [26]. Recently, in human plasma, Quehenberger and colleagues have

identified different S1P species which vary in length and disaturation degree of sphingoid base [27]. However, until now the association of these S1P species with CAD has not been studied. In addition, our group previously showed altered profiles of sphingoid bases in plasma of patients with metabolic syndrome [28] or type 2 diabetes mellitus [29], which are major risk factors for cardiovascular disease [30].

In this study, we used three different liquid chromatography - mass spectrometry (LC-MS) methods to identify and quantify glycerophospholipids and sphingolipids, including phosphatidic acids (PAs), phosphatidylglycerols (PGs), PCs, PEs, SMs, ceramides/hexosylceramides (Cers/HexCers) as well as different S1P species and 11 sphingoid bases of sphingolipids. First, we explored differences in the composition of glycerophospholipids and sphingolipids in plasma of CAD and ACS patients relative to healthy subjects. Then, we assessed the relationships between plasma lipidome and traditional risk factors for CAD. Finally, we characterised the distribution of glycerophospholipids and sphingolipids among the lipoprotein fractions of healthy subjects.

2.2. Materials and methods

2.2.1. Patients

Patients with stable CAD (n=18) or ACS (n=17) were selected from the SPUM cohort (Special Program University Medicine) [31] and compared to healthy subjects (n=14). In addition, ten patients with CAD but not on statin treatment were selected to explore the influence of cholesterol-lowering therapy (statins) on glycerophospholipid and sphingolipid levels. The age of the patients ranged between 43 and 77 years.

2.2.2. Clinical chemistry

Plasma concentrations or activities of total cholesterol, triglycerides, LDL-C and HDL-C, glucose, creatine kinase, CK-MB, and troponin levels were determined by photometric tests or immunoassay by using the Cobas 8000 autoanalyser from Roche diagnostics (Rotkreuz, Switzerland).

2.2.3. Isolation of lipoproteins

Human lipoprotein fractions and the lipoprotein-free fraction (LFF) were isolated from 2 ml of plasma of three healthy blood donors by stepwise ultracentrifugation, as described previously [32] using solid potassium bromide for density adjustment and a tube slicer for collection of the lipoprotein fractions.

2.2.4. Analysis of plasma glycerophospholipids and sphingolipids

In the present study, we analysed six lipid classes of glycerophospholipids or sphingolipids. Lipids were compared to 200 ng of the internal standards PG(17:0/17:0), LPG(17:1/0:0), PA(14:0/14:0), LPA(17:0/0:0), PE(14:0/14:0), LPE(17:1/0:0), PC(14:0/14:0), PC(24:0/24:0), LPC(17:0/0:0), SM (d18:1/12:0) and Cer(d18:1/17:0) (Avanti Polar Lipids, Alabaster, AL, USA). A sample volume of 20 µl was extracted with 375 µl of methanol/chloroform (2:1 v/v). After vortexing, 100 µl water and 125 µl chloroform were added. The mixture was shaken for 15 minutes and centrifuged at 16,100×g for 5 minutes at 25°C. The lower phase was collected and an additional 250 µl chloroform was added. The mixture was shaken for 15 minutes and centrifuged at 16,100×g for 5 minutes at 25°C. All lower phases were combined and evaporated to dryness under a stream of nitrogen. Dried material was reconstituted in 200 µl of a mixture of mobile phases A (80%) and B (20%). Then, 10 µl were injected into the LC-MS system.

The total lipid extract was analysed by LC-MS which comprised a Rheos 2200 pump and a TSQ Quantum Access triple quadrupole mass analyser. The lipid extract was separated on a diol silica-based column (QS Uptisphere 6 OH, 150 x 2.1 mm, 5 µm). The mobile phase A was a mixture of hexane/isopropanol/water (70:30:2 v/v) containing 15 mM NH_4COOH and mobile phase B was a mixture of isopropanol/water (50:2 v/v) containing 15 mM NH_4COOH. The solvent gradient was 0-7 min A/B (%) 80/20; 8-10 min A/B (%) 60/40, 11-23 min A/B (%) 40/60 and 25-30 min A/B (%) 80/20 at a flow rate of 0.35 ml/min. Molecular masses provided by a neutral loss and precursor scans were used to detect specific glycerophospholipids and sphingolipids. A neutral loss scan of *m/z* 115 and 189 from $[M+NH_4]^+$ ions were used for the analysis of PA and PG lipids, respectively. A precursor ion scan of *m/z* 184, which is specific for phosphocholine-containing lipids, was used for PC, SM and LPC lipids. A neutral loss scan of *m/z* 141 was used for PEs and a precursor scanning of *m/z* 264 was applied for screening of Cers and HexCers with d18:1 sphingoid base. Data obtained were analyzed using Xcalibur software (version 2.0.6) from Thermo Scientific. Identification of molecular species was performed by lipid mass spectrum analysis software (LIMSA) [33].

The assignment of glycerophospholipids includes total numbers of carbons and double bonds in two acyl chains. The SM assignment comprises total numbers of carbons and double bonds in the sphingoid base and N-linked fatty acid. Hexosylceramide species include isomeric glucosyl- and galactosylceramides. For identified Cers and HexCers, molecular structures are reported. Quantification was done in relation to the added internal standards.

2.2.5. Quantification of sphingosine-1-phosphate species

Determination of the sphingosine-1-phosphates (S1Ps) in plasma samples was performed by LC-MS as described previously [25]. Concentrations of S1P species were measured in 25 µl of plasma supplemented with 10 pmol internal standard 18:1-D7S1P (Avanti Polar Lipids, Alabaster, AL, USA). Samples were extracted with ethyl acetate/iso-propanol (6:1 v/v). The lipid extracts obtained were evaporated to dryness under a stream of nitrogen, and derivatised by adding 50 µl of acetic anhydride and 100 µl of pyridine. Acetylated S1P species were separated on a C_{18} column (Nucleosil 125 x 2 mm, 100 Å, 5 m) and analysed on a TSQ Quantum Access triple quadrupole mass analyser. The lower level of quantification amounted to 1 pmol extracted S1P corresponding to 0.04 µM in plasma. Analysis of S1P species included the quantification of 16:1-S1P, 17:1-S1P, 18:1-S1P and 18:0-S1P lipids.

2.2.6. Quantification of sphingoid bases

The LC-MS method was applied to quantify 11 sphingoid bases in 100 µl of human plasma supplemented with 200 pmol of the internal standards d7-sphingosine (D7SO) and d7-sphinganine (D7SA) (Avanti Polar Lipids, Alabaster, AL, USA), as described earlier [28]. After acid-base hydrolysis of the plasma samples, the sphingoid bases were separated on a C18 column (Uptispere 120 Å, 5 µm, 125 × 2 mm) and analysed on a TSQ Quantum Ultra mass spectrometer.

2.2.7. Statistical analysis

Statistical analysis was performed using SPSS, version 19 (IBM Corporation, Somers NY, USA). Normality of the data was determined by using the Kolmogorov-Smirnov test**.** Because values of variables did not follow a Gaussian frequency distribution, the univariate statistics were performed by applying the Kruskal-Wallis and the Mann-Whitney U tests. Categorical variables were compared using the Chi-square test. Spearman rank tests were used to describe the correlations of plasma glycerophospholipids and sphingolipids with total cholesterol, LDL-C and HDL-C levels. To maintain the rate of false-positive results, *p* values were adjusted for multiple comparisons by applying the Benjamini-Hochberg procedure [34]. The adjusted (adj.) *p* values of < 0.05 were considered as statistically significant.

2.3. Results

2.3.1. Clinical characteristics of the CAD and ACS patients

In the present study, we compared the plasma lipid profile of healthy subjects with the lipid profile of stable CAD or ACS patients. On average, healthy subjects (56.4 ± 7.5 years) and CAD patients (61.3 ± 8.3 years) were ten and five years younger than ACS patients (66.8 ± 10.0 years), respectively. In addition, the prevalence of smoking was significantly higher in the CAD and ACS patients than in healthy subjects. Average BMI was higher in the CAD patients when compared with healthy subjects. Furthermore, all CAD and ACS patients in the cohort were treated with statins, which resulted in significantly lower LDL-C and total cholesterol levels compared to healthy subjects. The ACS patients showed several features of acute myocardial infarction, including elevated plasma levels of NT-proBNP, creatine kinase, CK-MB and troponin (Table 1).

2.3.2. CAD effect on plasma lipidome

We compared plasma levels of 65 lipid species of glycerophospholipids and sphingolipids between healthy subjects, CAD and ACS patients. To exclude the possibility that the observed differences are caused by cholesterol lowering drugs, we also compared the lipid profiles of CAD patients with and without statin treatment. However, no differences were observed between CAD patients that were treated with statins and those who were not (Table 2). This agrees with earlier results from Meikle et al. [16] who showed that only few of plasma glycerophospholipids and sphingolipids associate with statin use.

Univariate statistical analysis revealed significantly different lipid profiles of plasmas from CAD and ACS patients compared to healthy individuals (Table 3). The total content of PC, LPC, PE, SM and Cer/HexCer lipids was significantly lower in the CAD and ACS patients compared to healthy subjects (Table 3). However, only total Cer/HexCer was present at lower plasma concentration in ACS patients when compared with CAD subjects. Comparison of the individual lipid species in the plasmas of CAD patients with healthy controls revealed differences in concentrations of 45 molecular species including 19 PCs, 4 LPCs, 5 PEs, 12 SMs and 5 Cers/HexCers. Furthermore, in patients with ACS, plasma levels of 42 lipid species, including 15 PCs, 2 LPCs, 9 PEs, 11 SMs and 5 Cers/HexCers, were decreased relative to healthy subjects (Table 3).

Analysis of plasma samples revealed the presence of typical 18:1-S1P as well as other S1P species including: 16:1-S1P, 17:1-S1P and 18:0-S1P. Abbreviations of S1P species indicate total numbers of carbons and double bonds in sphingoid base. In plasma of healthy

subjects, 17:1-S1P was found at very low concentration below or close to lower level of quantification, which corresponds to 0.04 µmol per liter plasma. In plasma of CAD and ACS patients, 17:1-S1P was below the detection limit. Furthermore, the plasma content of 18:1-S1P was lower in ACS patients than in healthy individuals (Table 3). The plasma levels of 16:1-S1P were lower in both CAD and ACS patients when compared with healthy controls (Table 3).

All plasma sphingolipid species share a common structural feature, a sphingoid base, which can be amide-linked with fatty acid and conjugated to different head groups giving rise to a number of different sphingolipids. To analyse the composition of the sphingoid bases, all sphingolipids extracted from plasma samples were hydrolysed to remove the N-acyl chains and head groups. Hence, sphingoid base concentrations reported here refer to the total content of sphingoid bases, present in different sphingolipid species.

Plasma levels of C17SO, C18SO, C18SA and C18SAdiene were found to be lower in both CAD and ACS patients compared to healthy subjects but did not differ between CAD and ACS patients (Table 3). Moreover, the plasma content of C16SO and C16SA was significantly lower in ACS patients relative to healthy controls (Table 3). Plasma concentrations of doxSO and doxSA sphingoid bases were not significantly different between healthy individuals and CAD or ACS patients.

Data representation with volcano plots helped to identify the most significantly changed parameters with the magnitude of change and significance of change displayed on the *x* and *y* axes, respectively. All data on plasma samples were divided into four groups: group of glycerophospholipids includes even-chain PCs, PEs, LPCs and PGs; group of odd-chain PCs includes all PCs with odd number of carbons in two acyl chains; group of sphingolipids includes SMs, Cers/HexCers, S1P species and sphingoid bases; clinical measures include patient`s data and data on clinical chemistry. The volcano plots in Fig. 1 compare the relative abundance of the analysed lipids and clinical measures of healthy subjects vs. CAD patients (Fig. 1A), healthy subjects vs. ACS patients (Fig. 1B), CAD vs. ACS patients (Fig. 1C). Four species of odd-chain PCs, including PC33:1, PC33:2, PC33:3 and PC35:3, differed most significantly between CAD patients and healthy subjects (Fig. 1A). ACS patients differed from healthy subjects more prominently by troponin level, but also by PC33:1, PC33:2, PC33:3 and PC35:3 levels (Fig. 1B). The CAD and ACS patients differed most prominently by routine clinical measures, including troponin, creatine kinase and CK-MB (Fig. 1C).

Table 1. Clinical characteristics of the study population.

Characteristics	Healthy subjects (n=14)	CAD (n=18)	ACS (n=17)	Kruskal-Wallis, adj. *p* values	Mann-Whitney U, adj. *p* values		
	Mean ± SD	Mean ± SD	Mean ± SD		H vs CAD	H vs ACS	CAD vs ACS
Age (years)	56.4±7.5	61.3±8.3	66.8±10.0	**0.005**	0.164	**0.004**	0.084
Gender, female (%)	36	22	18	0.488	0.492	0.347	0.784
Smoking (%)	0	75	56	**0.001**	**<0.001**	**0.04**	0.352
Statin treatment (%)	0	100	100	**<0.001**	**<0.001**	**<0.001**	0.649
BMI (kg/m2)	24.5±3.48	27.85±3.52	26.45±3.15	**0.03**	**0.035**	0.084	0.22
Systolic blood pressure (mmHg)	119.36±13.99	129.89±16.52	128.59±19.11	0.248	0.163	0.232	0.92
Diastolic blood pressure (mmHg)	71.36±9.79	76.50±10.76	76.06±11.27	0.267	0.22	0.215	0.981
Glucose (mmol/l)	5.18±0.44	5.43±0.56	6.32±0.98	**0.005**	0.362	**0.006**	**0.018**
Total cholesterol (mmol/l)	5.78±0.97	4.05±0.89	3.84±1.00	**<0.001**	**<0.001**	**<0.001**	0.448
LDL-C (mmol/l)	3.53±0.83	2.39±0.76	2.28±0.92	**0.001**	**0.004**	**0.004**	0.609
HDL-C (mmol/l)	1.83±0.42	1.18±0.32	1.22±0.28	**<0.001**	**<0.001**	**0.001**	0.618
Triglycerides (mmol/l)	0.98±0.43	1.07±0.46	0.75±0.53	0.099	0.738	0.132	0.081
NT- proBNP (ng/L)	41.21±35.36	140.22±108.47	817.88±1013.81	**<0.001**	**0.006**	**<0.001**	**0.026**
Creatine kinase (µg/l)	136.18±76.96	119.65±42.47	1304.76±828.56	**<0.001**	0.981	**<0.001**	**<0.001**
CK-MB (µg/l)*	11.60±3.47	10.86±5.41	141.49±103.43	**<0.001**	0.558	**<0.001**	**<0.001**
Troponin T (ug/l)*	0.01±0	0.03±0.03	2.65±1.89	**<0.001**	**0.013**	**<0.001**	**<0.001**

Values are expressed as means ± SD or percentages for scale or categorical variables, respectively. Statistical significance was determined by the Kruskal-Wallis test used for multiple group comparisons, and by the Mann-Whitney U test applied for two group comparisons. The *p* values for the categorical variables were calculated by using Chi-square test. The *p* values were adjusted for multiple testing by using the Benjamini-Hochberg procedure. Statistically significant results are indicated in bold font. Values marked by asterisk * were measured in the patient samples before hospital discharge. Abbreviations: ACS, acute coronary syndrome; CAD, coronary artery disease; CK-MB, creatine kinase MB; BMI, body mass index; H, healthy subjects; HDL-C, high-density lipoprotein cholesterol; LDL-C, low-density lipoprotein cholesterol; NT- proBNP, amino terminal prohormone B-type natriuretic peptide.

Table 2. Plasma glycerophospholipids and sphingolipids don`t differ between statin-treated and untreated CAD patients.

Lipids, µmol/l	CAD statin-treated (n=10)	CAD statin-untreated (n=10)	Mann-Whitney U, adj. *p* values
	Median(Min; Max)	Median(Min; Max)	CAD statin-treated vs CAD statin-untreated
Total PC	795.3(614.8;895.6)	823.6(692.2;1195.8)	0.649
PC32:0	5.6(3.1;7.8)	6.8(4.6;9.5)	0.406
PC32:1	8.5(3;15.5)	11.6(3.6;15.4)	0.649
PC33:1	5.3(2.4;9)	6.7(4.3;9.3)	0.402
PC33:2	5.4(3.3;12.3)	7(3.7;10.5)	0.402
PC33:3	2.8(1.4;5.9)	3.5(2.5;7.8)	0.48
PC34:0	7.5(4.4;11.7)	9.1(5;11.6)	0.553
PC34:1	87.4(50;126.5)	112.9(77.4;152.8)	0.402
PC34:2	152.2(88;222.1)	174.5(115.6;297.4)	0.649
PC34:3	6.3(4.3;9)	7.3(3.9;10.6)	0.498
PC35:1	2.7(1;3.5)	3.8(1.9;5.5)	0.402
PC35:2	5.8(3.5;6.3)	6.9(4.7;11.2)	0.465
PC35:3	4.4(2.3;8)	5.6(3.9;9.7)	0.429
PC35:4	11.6(8.9;17.9)	14.9(8.6;19.3)	0.48
PC35:5	7.8(4.8;15.3)	9.3(6.8;12.9)	0.649
PC36:0	4(2.8;5.7)	3.9(1.8;6.6)	0.837
PC36:1	22.6(16.8;31.2)	31.1(18.9;42.7)	0.402
PC36:2	81.8(56.3;115.2)	86.4(67.2;144.3)	0.702
PC36:3	53(41.6;68.1)	54.9(38;77.5)	0.869
PC36:4	81.8(47.4;103.9)	74.5(53.9;120.8)	0.869
PC36:5	8.6(2;19.8)	9.9(6.2;15.6)	0.759
PC37:4	10.3(7.2;15.9)	11.6(7.3;14.2)	0.649
PC37:5	12.5(7.8;16.4)	15.2(9.3;21.6)	0.465
PC37:6	5.3(4.1;9)	6.7(4.6;9.9)	0.406
PC38:3	27.7(18.9;37.1)	24.1(20.4;43.3)	0.9
PC38:4	65.1(28.3;75.7)	55.8(37.7;101.3)	0.735
PC38:5	23.3(12.3;30)	21.8(17.3;27)	0.735
PC38:6	24.9(10.4;34.5)	24(15.5;31.5)	0.9
PC40:5	6.1(4.3;7.4)	6.1(4.5;9.6)	0.848
PC40:6	10.6(5;14.1)	10.3(5.7;15.7)	0.869
Total LPC	123.6(80.5;154.7)	129.3(88.7;179.2)	0.735
LPC16:0	67.4(44.8;77.5)	75.2(53;96.7)	0.48
LPC18:0	21.3(14.8;27.7)	25.8(12;34)	0.649
LPC18:1	14.7(8.8;20.4)	14(9;26.2)	0.702
LPC18:2	20.6(8.8;37.9)	15.1(9.1;32.3)	0.649
Total PE	14.2(6.3;40.2)	16.3(8.2;70)	0.759
PE34:2	0.9(0.2;3.3)	1.6(0.3;5.5)	0.649
PE35:2	0.1(0.03;0.3)	0.3(0.1;0.6)	0.402
PE36:4	1.3(0.8;3.4)	1.7(0.5;6.2)	0.837
PE36:3	0.8(0.1;1.7)	0.9(0.2;4.5)	0.759
PE36:2	2.8(0.7;8.7)	3.5(0.6;20.6)	0.759
PE36:1	0.6(0.1;2.5)	0.8(0.1;5.3)	0.56
PE37:5	0.4(0.03;0.5)	0.8(0.2;1.3)	0.402
PE37:4	0.2(0.1;0.6)	0.2(0.1;0.5)	0.848
PE38:6	2(0.5;7.3)	2.2(0.9;7.4)	0.702
PE38:5	1(0.6;2.5)	1.3(0.5;3.2)	0.804
PE38:4	3.9(1.9;10.4)	4.4(2.1;15.6)	0.804
Total PG	0.4(0.2;0.7)	0.4(0.2;1.7)	0.94
Total PA	n.d.	n.d.	-

(Continued)

Lipids, µmol/l	CAD statin-treated (n=10) Median(Min; Max)	CAD statin-untreated (n=10) Median(Min; Max)	Mann-Whitney U, adj. *p* values CAD statin-treated vs CAD statin-untreated
Total SM	502.6(283.2;628)	560.4(428.8;702)	0.465
SM32:1	11.1(5.5;18)	14.6(12;17.7)	0.402
SM34:0	4(1.1;5)	4.4(1.5;6.1)	0.694
SM34:1	100.3(62.1;136)	115.8(86.2;161.1)	0.402
SM34:2	14.6(8.5;22.8)	16.2(12.5;28.3)	0.498
SM36:1	29.9(15.6;42)	26.3(22.9;46.6)	0.94
SM36:2	10.3(7.1;14.3)	11.4(8.1;16.8)	0.735
SM38:1	26.7(15;32.1)	29.4(21.5;36.6)	0.465
SM39:1	9.9(5.2;16.7)	10.9(6.9;15)	0.702
SM39:2	1.3(0.8;2.3)	1.5(0.7;1.9)	0.694
SM40:1	53.7(28.3;66)	67.5(42.8;95)	0.406
SM40:2	31.9(19;39.5)	38.9(24.7;49.5)	0.402
SM41:1	26.2(11.1;38)	34.7(23.7;42.7)	0.406
SM41:2	17.1(8.8;25.6)	21.9(14.3;31.2)	0.618
SM42:1	43(20.7;52.3)	48.7(33.7;75.6)	0.649
SM42:2	74.3(53.1;113.7)	88.1(68.1;123.5)	0.56
SM42:3	28.9(21.3;39.5)	34(19.9;48.5)	0.702
Total Cer/HexCer	7.6(4.6;13.4)	9.4(6.5;21.5)	0.465
Cer(d18:1/24:0)	2.3(1.5;3.5)	2.6(1.4;5.4)	0.837
HexCer(d18:1/22:0)	1.4(0.8;2.1)	1.3(0.5;5.3)	0.848
HexCer(d18:1/23:0)	0.6(0.1;1.5)	1.4(0.6;2.4)	0.402
HexCer(d18:1/24:0)	2(1.1;3.7)	2.8(1.4;6.5)	0.429
HexCer(d18:1/24:1)	1.2(0.6;2.6)	1.7(0.7;2.9)	0.649
S1P species			
16:1-S1P	0.1(0.07;0.15)	0.11(0.07;0.13)	0.649
17:1-S1P	n.d.	n.d.	-
18:1-S1P	0.45(0.39;0.64)	0.55(0.51;0.78)	0.402
18:0-S1P	0.08(0.04;0.15)	0.06(0.03;0.1)	0.649
Sphingoid bases of sphingolipids			
C16SO	21.96(10.47;29.5)	23.45(13.69;27.98)	0.735
C16SA	0.56(0.25;0.99)	0.55(0.27;0.8)	0.9
C17SO	9.09(4.43;10.95)	10.31(6.92;14.97)	0.406
C18SO	89.08(57.3;122.08)	112.52(79.23;140.89)	0.498
C18SA	3.29(1.4;5.36)	3.35(1.85;6.49)	0.848
C18SAdiene	34.81(24.08;46.54)	41.76(25.29;51.8)	0.402
C19SO	3.56(1.71;6.75)	3.34(1.73;4.68)	0.869
C20SO	0.23(0.2;0.37)	0.22(0.18;0.34)	0.735
C20SA	0.04(0.02;0.06)	0.04(0.02;0.06)	0.848
doxSO	0.18(0.09;0.39)	0.18(0.04;0.4)	0.735
doxSA	0.09(0.04;0.18)	0.09(0.02;0.17)	0.735

Values are expressed as medians with ranges. Statistical significance was determined by the Mann-Whitney U test. Statistically significant results are indicated in bold font. The *p* values were adjusted for multiple testing by using the Benjamini-Hochberg procedure. Total lipids are presented for phosphatidylcholines (PCs), lysophosphatidylcholines (LPCs), phosphatidylethanolamines (PEs), phosphatidylglycerols (PGs), sphingomyelins (SMs), ceramide/hexosylceramides (Cers/HexCers). Glycerophospholipids are named according to the summarized numbers of carbons and double bounds in two acyl chains. Names of SM species reflect summarized numbers of carbons and double bounds in sphingoid base and N-linked fatty acid. An assignment of sphingosine-1-phosphate (S1P) species includes numbers of carbons and double bounds in sphingoid base. HexCer species include isomeric glucosyl- and galactosylceramides. For Cer/HexCer species molecular structures are reported. n.d. stands for not detected.

Table 3. Plasma glycerophospholipids and sphingolipids differ significantly between healthy subjects, CAD and ACS patients.

Lipids, μmol/l	Healthy subjects (n=14)	CAD (n=18)	ACS (n=17)	Kruskal-Wallis,	Mann-Whitney U, adj. *p* values		
	Median(Min; Max)	Median(Min; Max)	Median(Min; Max)	adj. *p* values	H vs CAD	H vs ACS	CAD vs ACS
Total PC	829.3(692.3;974.1)	725.6(522.7;793.4)	670.4(595.9;868.8)	**<0.001**	**0.002**	**0.001**	0.38
PC32:0	6.8(5;9.3)	5(3.3;6.8)	5.6(3.5;7.9)	**0.002**	**0.002**	**0.02**	0.314
PC32:1	9(4.9;18.4)	6.2(3.2;12)	7.3(4.2;16.6)	0.094	0.05	0.2	0.697
PC33:1	7.7(7;11.7)	5.5(2.5;6.7)	5.8(3.9;7.9)	**<0.001**	**<0.001**	**0.001**	0.584
PC33:2	10.1(6.7;16)	5.9(2.6;7.3)	6.4(4.3;8.8)	**<0.001**	**<0.001**	**0.001**	0.314
PC33:3	5.6(3.6;10.7)	2.8(1.7;4.2)	3.2(1.6;4.7)	**<0.001**	**<0.001**	**<0.001**	0.584
PC34:0	9.3(6.3;12.7)	7.1(4.3;10.5)	7.4(5.4;9.2)	**0.004**	**0.015**	**0.002**	0.877
PC34:1	92.6(74.9;122.2)	76.2(42;101.3)	81.7(51.7;101.2)	**0.043**	**0.026**	0.108	0.681
PC34:2	187.8(156.6;226.7)	135.9(72.2;181.7)	129.5(98;150.1)	**<0.001**	**<0.001**	**<0.001**	0.471
PC34:3	8.7(5.1;9.7)	5.5(3.6;8.1)	4.5(3.2;6.8)	**<0.001**	**0.002**	**0.001**	0.391
PC35:1	10.3(8;20.6)	7.4(3.5;13.1)	7.5(5.8;12.3)	**0.004**	**0.006**	**0.006**	0.863
PC35:2	8.1(7;11.4)	6.3(2.9;8.8)	5.9(4.2;9.3)	**<0.001**	**0.001**	**0.002**	0.681
PC35:3	7.5(6;11)	5.1(2.3;7.4)	5.1(2.7;6.9)	**<0.001**	**<0.001**	**<0.001**	0.932
PC35:4	15.4(8.7;22.6)	13(7.4;15.8)	13.1(7.6;20.7)	**0.031**	**0.015**	0.116	0.644
PC35:5	11.9(6.1;21)	8.4(4.4;11.2)	9.2(4.7;17.6)	**0.041**	**0.024**	0.148	0.482
PC36:0	5.3(3.8;7.7)	4(2.6;5.4)	4(2.4;6.7)	**0.005**	**0.003**	**0.022**	0.877
PC36:1	32.7(23.9;38.3)	22.7(13.4;30.5)	22.7(17.1;33.3)	**<0.001**	**<0.001**	**0.002**	0.681
PC36:2	106.7(77.7;124.3)	78.6(51.9;112.1)	72.1(52.8;87.3)	**<0.001**	**0.001**	**<0.001**	0.509
PC36:3	48.7(44;68.8)	44.7(29.7;57.6)	40.7(29.8;47.2)	**0.001**	0.09	**0.001**	0.175
PC36:4	70(39.4;84.3)	73.7(44;102)	74.4(47.4;89.1)	0.682	0.506	0.595	0.932
PC36:5	8.8(5.8;21.7)	8.8(1.3;14.9)	9.2(2;22.7)	0.725	0.491	0.877	0.768
PC37:4	12.7(8.3;17)	11.4(6;14.1)	10.8(7.3;15.3)	0.226	0.235	0.159	0.863
PC37:5	17.3(11;23.1)	13.5(7.7;18.6)	14.5(9;22.5)	**0.026**	**0.018**	0.085	0.509
PC37:6	8.6(5.9;14.9)	6.2(3.4;8)	7(3.3;11.6)	**0.003**	**0.002**	**0.028**	0.286
PC38:3	21.6(11.2;31.9)	23.5(14.4;38.5)	19.8(10.9;28.6)	0.157	0.506	0.386	0.091
PC38:4	49.5(28.9;70.1)	60.7(41.5;77.5)	60.6(38.4;72.8)	0.091	**0.047**	0.29	0.482
PC38:5	19.3(11.8;26.7)	18.3(8.2;28.1)	18.9(12.2;27.7)	0.979	0.95	0.877	0.863
PC38:6	17(12.7;34.3)	20.7(9.3;32.4)	18.7(11.1;34.6)	0.259	0.148	0.815	0.38
PC40:5	5.3(3.3;7.1)	5.9(3.5;8.8)	5(2.8;9.2)	0.387	0.34	0.904	0.343
PC40:6	7.7(5.1;14.1)	10(5.5;14.2)	8.5(5.7;16.1)	0.201	0.104	0.506	0.482
Total LPC	179.2(156.8;245.2)	136.3(105.3;181.5)	136.6(110.5;199.9)	**<0.001**	**0.001**	**0.004**	0.623
LPC16:0	90.8(77.4;121.1)	72.5(52.3;95.9)	64.1(49.6;104.2)	**<0.001**	**0.001**	**0.001**	0.235
LPC18:0	30.7(26.4;46.7)	25.6(20;34.1)	22(15.7;33.3)	**0.001**	**0.006**	**0.002**	0.098
LPC18:1	21.3(15.4;28.5)	15.6(10.6;21.8)	21.2(9.1;27.6)	**0.004**	**0.004**	0.572	**0.022**
LPC18:2	32.5(25.6;50.6)	19.5(9.6;50)	32.1(11.6;71.6)	**0.005**	**0.005**	0.67	**0.024**
Total PE	16.3(9.9;26)	11.2(3.4;23.4)	9.4(5;17.6)	**0.003**	**0.028**	**0.003**	0.26
PE34:2	1.7(0.9;3.2)	0.7(0.1;2.3)	0.6(0.3;1.8)	**0.001**	**0.003**	**0.001**	0.697
PE35:2	0.3(0.1;0.5)	0.1(0.03;0.3)	0.1(0.01;0.2)	**<0.001**	**0.002**	**0.001**	0.768
PE36:4	1.4(0.8;2.7)	1(0.3;2.3)	0.9(0.4;2)	0.07	0.11	**0.049**	0.721
PE36:3	1.1(0.5;3.1)	0.6(0.02;1.3)	0.5(0.2;0.8)	**0.001**	**0.006**	**0.002**	0.605
PE36:2	4(2.1;8.5)	1.9(0.4;5.1)	1.6(0.5;3.4)	**<0.001**	**0.005**	**0.001**	0.248
PE36:1	0.7(0.2;2)	0.5(0.05;1.1)	0.4(0.1;1)	**0.041**	0.065	**0.049**	0.391
PE37:5	0.7(0.4;1.1)	0.4(0.1;0.7)	0.4(0.2;1)	**0.004**	**0.003**	**0.015**	0.79
PE37:4	0.4(0.2;0.8)	0.3(0.02;0.6)	0.2(0.1;0.4)	**0.014**	0.069	**0.006**	0.623
PE38:6	1.6(0.5;3.7)	1.6(0.4;4)	1.1(0.5;2.9)	0.401	0.857	0.276	0.449
PE38:5	1.1(0.4;2.6)	0.8(0.3;2)	0.8(0.4;1.8)	0.068	0.069	0.065	0.932
PE38:4	2.9(1.9;6.3)	2.9(1;5.5)	2.3(1.3;4.9)	0.055	0.811	**0.049**	0.079
Total PG	0.3(0.1;0.8)	0.3(0.1;0.7)	0.2(0.1;0.6)	0.099	0.543	0.108	0.117
Total PA	n.d.	n.d.	n.d.	-	-	-	-

(Continued)

Lipids, μmol/l	Healthy subjects (n=14)	CAD (n=18)	ACS (n=17)	Kruskal-Wallis, adj. *p* values	Mann-Whitney U, adj. *p* values		
	Median(Min; Max)	Median(Min; Max)	Median(Min; Max)		H vs CAD	H vs ACS	CAD vs ACS
Total SM	462.9(359.6;600.4)	385.4(262.7;547.9)	355.4(275.6;475.7)	**0.002**	**0.007**	**0.002**	0.523
SM32:1	16.1(12.2;22.6)	10.7(5.3;17.8)	10.7(5.3;16.4)	**0.001**	**0.006**	**0.001**	0.972
SM34:0	4.8(3.1;6.1)	2.9(0.3;4.5)	2.7(1.1;4.2)	**0.001**	**0.003**	**0.002**	0.863
SM34:1	123.6(88.3;169.2)	99.3(63;131)	90.6(63.8;127.6)	**<0.001**	**0.002**	**0.001**	0.41
SM34:2	17.8(13;23.5)	14.6(7.8;27.8)	13.2(10.8;20.1)	**0.017**	**0.043**	**0.012**	0.823
SM36:1	23.4(16.4;33.5)	22(14.8;32.3)	19.6(11.9;26.4)	0.345	0.523	0.185	0.623
SM36:2	9.6(7.4;14.7)	8.8(6.4;18.8)	8.5(4.9;13.1)	0.361	0.652	0.231	0.482
SM38:1	23.2(15.8;28.2)	17.9(12.3;26.5)	16.9(12.2;21.7)	**0.006**	**0.04**	**0.006**	0.286
SM39:1	9.2(5.9;11.7)	6.8(4.3;11.3)	5.6(4.3;10.6)	**0.005**	**0.028**	**0.004**	0.499
SM39:2	1.2(0.5;2.2)	1(0.3;2.2)	0.9(0.3;1.8)	0.371	0.435	0.29	0.566
SM40:1	42.6(31.7;59.8)	33.7(25.9;47.4)	32(22.2;44.8)	**0.004**	**0.015**	**0.004**	0.697
SM40:2	28(18.6;35.8)	23.1(16.4;36.1)	21(16.9;37.2)	**0.017**	**0.026**	**0.022**	0.681
SM41:1	22.2(17;32.9)	19.3(9.7;28.3)	15.4(13.3;21.9)	**0.001**	**0.016**	**0.001**	0.314
SM41:2	14(11.6;23.1)	12(7.3;17.3)	11.8(8;20.6)	**0.049**	**0.043**	0.065	0.823
SM42:1	39.6(25.8;53.1)	29.8(19;42.5)	25.8(19.1;40.2)	**0.005**	**0.03**	**0.005**	0.327
SM42:2	66.4(51.6;82.8)	53.6(40.9;77.6)	55.3(38.4;79.6)	**0.016**	**0.018**	**0.026**	0.823
SM42:3	22.8(16.7;33.4)	21.4(15.3;30.9)	21.5(13.6;36.8)	0.38	0.324	0.326	0.811
Total Cer/HexCer	12.2(4.9;20.2)	8.5(2.8;11.7)	5.4(3.1;7.4)	**<0.001**	**0.013**	**0.001**	**0.026**
Cer(d18:1/24:0)	2.2(1.4;4.9)	1.7(1;2.6)	1.6(0.7;2.7)	**0.041**	**0.04**	**0.049**	0.932
HexCer(d18:1/22:0)	2.8(0.9;5)	1.9(0.3;3)	1.1(0.3;1.7)	**<0.001**	**0.033**	**0.001**	**0.01**
HexCer(d18:1/23:0)	1.5(0.5;2.9)	0.8(0.2;1.7)	0.6(0.2;1.1)	**0.001**	**0.016**	**0.001**	0.117
HexCer(d18:1/24:0)	3.5(1.6;5.7)	2.2(0.3;3.8)	1.3(0.7;2.3)	**<0.001**	**0.012**	**<0.001**	**0.022**
HexCer(d18:1/24:1)	2.2(0.5;2.9)	1.3(0.5;2.5)	0.9(0.3;1.7)	**0.004**	**0.04**	**0.004**	0.185
S1P species							
16:1-S1P	0.12(0.09;0.15)	0.1(0.05;0.17)	0.1(0.07;0.13)	**0.006**	**0.014**	**0.009**	0.952
17:1-S1P	0.03(0.02;0.05)	n.d.	n.d.	-	-	-	-
18:1-S1P	0.55(0.5;0.81)	0.5(0.38;0.82)	0.44(0.29;0.79)	**0.011**	0.096	**0.013**	0.11
18:0-S1P	0.05(0.03;0.07)	0.04(0.03;0.09)	0.03(0.02;0.14)	0.198	0.248	0.159	0.523
Sphingoid bases of sphingolipids							
C16SO	31.91(14.84;46.01)	24.97(13.24;58.88)	21.05(9.48;48.36)	**0.011**	0.06	**0.004**	0.78
C16SA	0.73(0.3;1.38)	0.63(0.21;1.26)	0.46(0.24;1.13)	**0.011**	0.263	**0.006**	0.139
C17SO	13.49(8.45;22.2)	9.65(3.43;17.94)	9(4.75;23.95)	**0.003**	**0.016**	**0.003**	0.485
C18SO	145.13(104.41;203.95)	110.45(64.43;177.81)	105.05(67.5;160.82)	**<0.001**	**0.002**	**0.001**	0.475
C18SA	4.5(3.11;6.77)	3.2(1.28;10.65)	3.02(1.68;9.48)	**0.001**	**0.012**	**0.001**	0.544
C18SAdiene	52.44(30.66;78.94)	37.15(24.66;74.43)	35.66(23.3;48.22)	**0.005**	**0.043**	**0.003**	0.501
C19SO	3.79(1.66;7.28)	4.09(1.33;8.66)	3.12(1.2;6.81)	0.378	0.932	0.269	0.386
C20SO	0.24(0.14;0.35)	0.23(0.12;0.55)	0.21(0.09;0.36)	0.648	0.628	0.433	0.904
C20SA	0.02(0.01;0.04)	0.02(0.01;0.03)	0.02(0.01;0.04)	0.747	0.911	0.805	0.509
doxSO	0.2(0.15;0.7)	0.17(0.08;0.44)	0.19(0.07;0.78)	0.353	0.248	0.39	0.697
doxSA	0.1(0.07;0.24)	0.09(0.03;0.24)	0.07(0.03;0.33)	0.238	0.208	0.211	0.762

Values are expressed as medians with ranges. Statistical significance was determined by the Kruskal-Wallis test used for multiple group comparisons, and by the Mann-Whitney U test applied for two group comparisons. Statistically significant results are indicated in bold font. The *p* values were adjusted for multiple testing by using the Benjamini-Hochberg procedure. ACS stands for acute coronary syndrome; CAD, coronary artery disease; n.d., not detected.

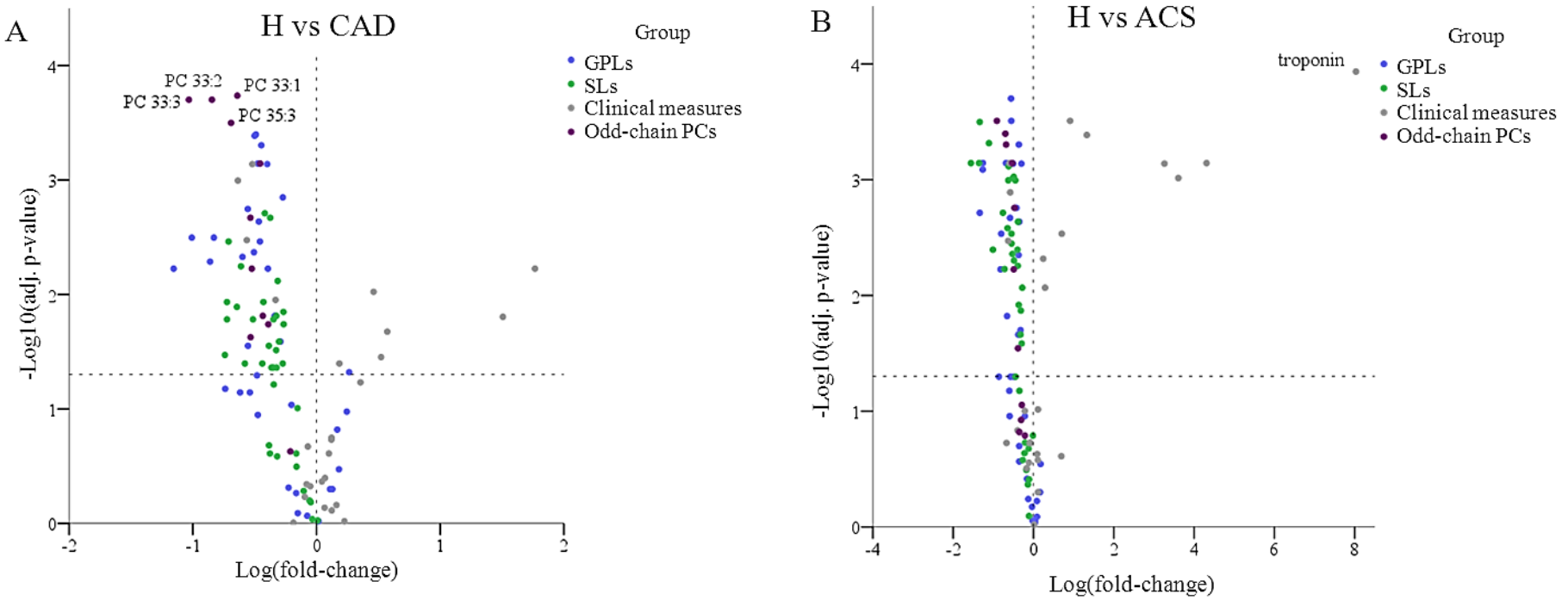

Figure 1. Volcano plots illustrating differences in the clinical measures and plasma lipidome of healthy subjects, CAD and ACS patients. The *x* axis shows the magnitude of change (displayed as Log(fold-change)), while the *y* axis shows the significance of change (displayed as -Log 10(adj. *p* value), *p* values were calculated by the Mann-Whitney U test). Volcano plots were used for the comparisons of healthy subjects (H) with CAD or ACS patients: H vs. CAD patients (Figure 1A), H vs. ACS (Figure 1B); as well as for the comparison of CAD vs. ACS patients (Figure 1C). Colour of each dot represents group of the data (blue, GPLs; green, SLs including SMs, Cers/HexCers, S1Ps and sphingoid bases of SLs; grey, clinical measures; crimson, odd-chain PCs). The dashed horizontal line denotes the cut-off thresholds (adj. $p < 0.05$) to define the significantly altered parameters. The *p* values were adjusted for multiple comparisons according to the Benjamini-Hochberg procedure. The most significant parameters present those that are distributed much above the dash line. Abbreviations: ACS, acute coronary syndrome; CAD, coronary artery disease; PC, phosphatidylcholine; GPL, glycerophospholipids; SL, sphingolipid.

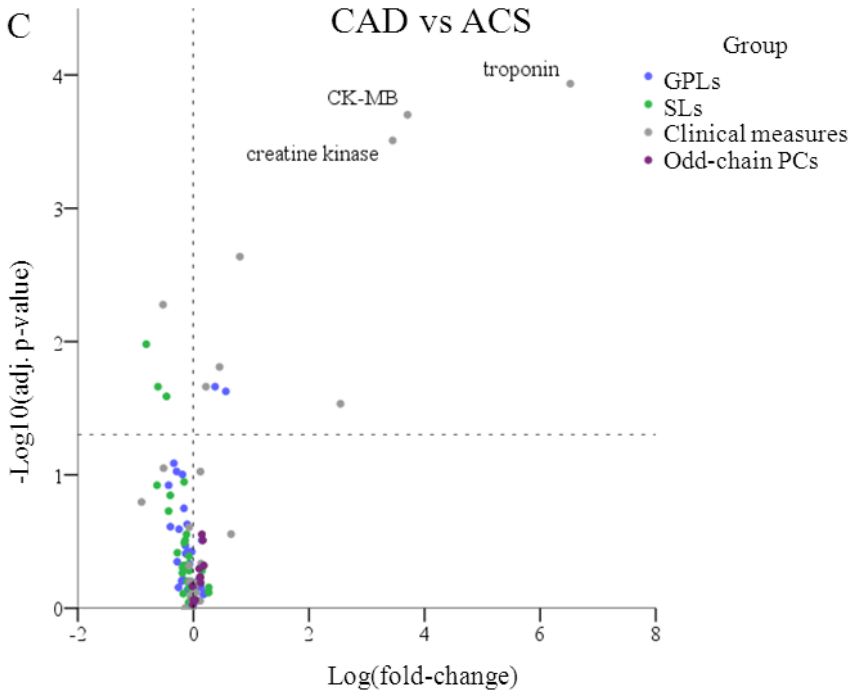

Figure 1. (Continued)

2.3.3. Structural analysis of odd-chain phosphatidylcholines

Odd-chain PC species – PC33:1, PC33:2, PC33:3 and PC35:3 – which showed the greatest difference between the healthy individuals and CAD patients, can be either PCs with an odd number of carbon atoms in one of the acyl chains, or PC plasmalogens with a vinyl-ether bond at the *sn-1* position of the glycerol backbone. Structural analysis of PC35:3 using collision-induced dissociation of $[M\text{-}CH_3]^-$ showed a fragmentation pattern like a commercially-available plasmalogen PC(P-18:0/18:1), indicating that this species represents plasmalogen PC(P-18:0/18:2) (Fig. 2A and 2B). In contrast to fragmentation pattern of even-chain PCs, for example PC(16:0/18:1) (Fig. 2C), fragmentation of plasmalogens shows only one carboxylate ion that corresponds to the *sn-2* substituent, whereas cleavage of the vinyl-ether or the ether-linked substituent from the *sn-1* position of the glycerol backbone is unfavourable. A similar fragmentation pattern for PC lipids and PC-based plasmalogens was previously described by Berdeaux et al. [35]. After detailed structural analysis of PC33:1, PC33:2, PC33:3 and PC35:3, these species were identified as PC plasmalogens PC(P-18:0/16:0), PC(P-16:0/18:1), PC(P-16:0/18:2) and PC(P-18:0/18:2), respectively. Even though the structural identity of some odd-chain PCs was established, the molecular structure of other odd-chain PC species remains unknown. Thus, in the volcano plots, odd-chain PCs and identified PC plasmalogens were grouped together and named "odd-chain PCs" (Fig. 1).

2.3.4. Correlations of the plasma glycerophospholipids and sphingolipids with cholesterol levels

Plasma concentrations of several glycerophospholipids and sphingolipids showed significant positive correlations with total cholesterol, HDL-C and LDL-C (Fig. 3). Among all glycerophospholipid and sphingolipid species, PC33:1, PC33:2, PC33:3 and PC35:3 exhibited the strongest positive correlation with HDL-C levels (Spearman correlation coefficient $r = 0.81$, $r = 0.71$, $r = 0.75$ and $r = 0.68$, respectively). We also noted a similar correlation pattern for total cholesterol and LDL-C. Both total cholesterol and LDL-C correlated very strongly with sphingoid bases C18SO ($r = 0.93$ and $r = 0.86$, respectively) and C17SO ($r = 0.85$ and $r = 0.81$, respectively). Furthermore, total cholesterol as well as LDL-C correlated more strongly than HDL-C with saturated LPC species, i.e. LPC16:0 ($r = 0.81$, $r = 0.74$ and $r = 0.53$, respectively) and LPC18:0 ($r = 0.73$, $r = 0.71$ and $r = 0.32$, respectively).

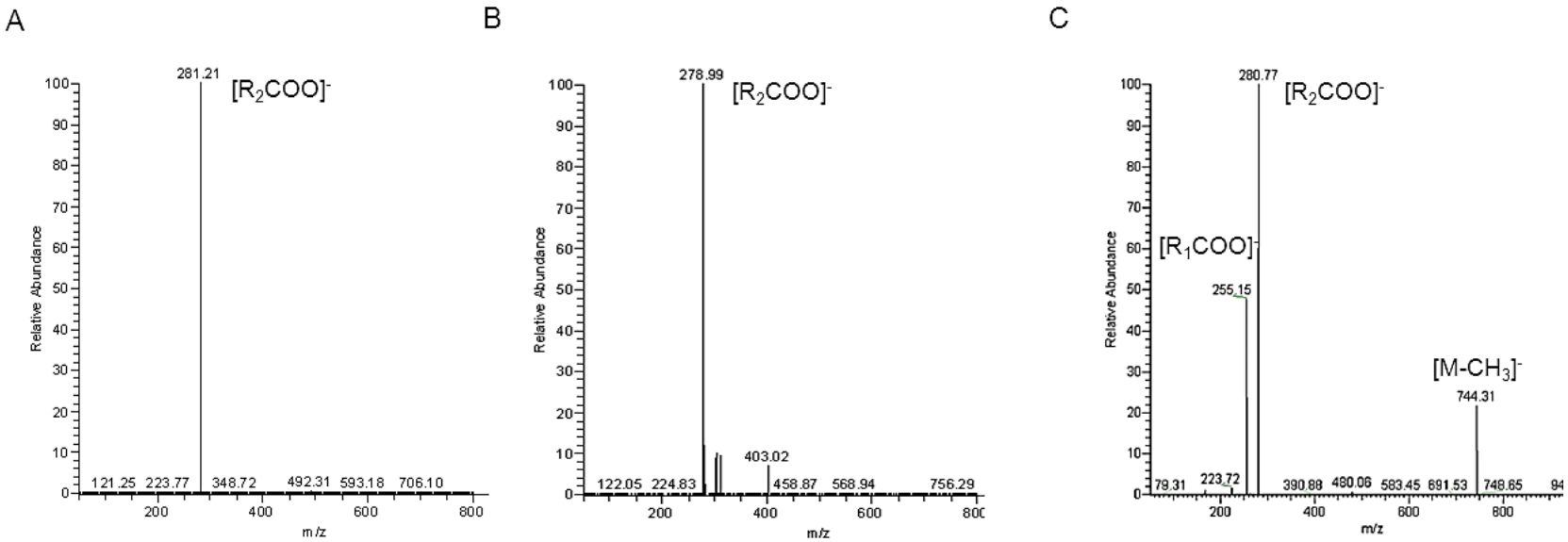

Figure 2. Product ion spectrum of negative ions of plasmalogen PC(P-18:0/18:1), plasma phosphatidylcholine PC35:3 and PC(16:0/18:1) (collision energy 35V).

Product ion spectrum of the selected molecular ion $[M\text{-}CH_3]^-$ of PC(P-18:0/18:1) at *m/z* 756,4 shows the carboxylate anion at *m/z* 281.2 which correspond to the fatty acid C18:1 at the *sn-2* position of the glycerol backbone (Figure 2A). Product ion spectrum of the selected molecular anion $[M\text{-}CH_3]^-$ of plasma PC35:3 at *m/z* 754,8 shows one prominent ion at *m/z* 278.99 which correspond to the fatty acid C18:2 at the *sn-2* position of the glycerol backbone indicating that PC35:3 is PC-derived plasmalogen, PC(P-18:0/18:2) (Figure 2B). Product ion spectrum of the selected molecular anion $[M\text{-}CH_3]^-$ of PC(16:0/18:1) at *m/z* 744,3 shows two carboxylate anions first at *m/z* 255,15 and second at *m/z* 280,77 which correspond to the fatty acids C16:0 and C18:1 at the *sn-1* and *sn-2* position of the glycerol backbone, respectively (Figure 2C).

Lipids	Total cholesterol	HDL-C	LDL-C
Total PC	0.81	0.66	0.68
PC32:0	0.58	0.65	0.45
PC32:1	0.49	0.51	0.42
PC33:1	0.72	0.8	0.57
PC33:2	0.63	0.71	0.5
PC33:3	0.57	0.75	0.43
PC34:0	0.64	0.59	0.52
PC34:1	0.57	0.64	0.44
PC34:2	0.68	0.5	0.6
PC34:3	0.64	0.61	0.54
PC35:1	0.72	0.57	0.66
PC35:2	0.66	0.61	0.56
PC35:3	0.66	0.68	0.52
PC35:4	0.44	0.45	0.36
PC35:5	0.48	0.54	0.39
PC36:0	0.55	0.42	0.46
PC36:1	0.73	0.53	0.68
PC36:2	0.55	0.33	0.49
PC36:3	0.72	0.43	0.62
PC36:4	0.13	0.1	0.12
PC36:5	0.27	0.48	0.17
PC37:4	0.48	0.38	0.43
PC37:5	0.44	0.56	0.3
PC37:6	0.53	0.61	0.43
PC38:3	0.42	-0.18	0.44
PC38:4	0.08	-0.16	0.1
PC38:5	0.33	0.35	0.24
PC38:6	0.1	0.01	0.07
PC40:5	0.29	0.11	0.25
PC40:6	0.06	-0.18	0.07
Total LPC	0.62	0.47	0.59
LPC16:0	0.81	0.53	0.74
LPC18:0	0.73	0.32	0.71
LPC18:1	0.28	0.46	0.26
LPC18:2	0.01	0.12	0.04
Total PE	0.54	0.2	0.48
PE34:2	0.56	0.26	0.5
PE36:4	0.45	0.2	0.38
PE36:3	0.54	0.29	0.49
PE36:2	0.6	0.2	0.54
PE36:1	0.47	0.06	0.45
PE37:5	0.51	0.53	0.36
PE37:4	0.38	0.36	0.32
PE38:6	0.29	0.1	0.23
PE38:5	0.4	0.26	0.34
PE38:4	0.4	0.07	0.37

Lipids	Total cholesterol	HDL-C	LDL-C
Total SM	0.77	0.59	0.7
SM32:1	0.73	0.65	0.65
SM34:0	0.59	0.54	0.5
SM34:1	0.8	0.63	0.71
SM34:2	0.69	0.6	0.63
SM36:1	0.56	0.33	0.54
SM36:2	0.51	0.32	0.5
SM38:1	0.63	0.47	0.55
SM39:1	0.66	0.42	0.66
SM40:1	0.62	0.34	0.59
SM40:2	0.64	0.53	0.6
SM41:1	0.81	0.46	0.75
SM41:2	0.59	0.57	0.56
SM42:1	0.65	0.33	0.63
SM42:2	0.6	0.57	0.52
SM42:3	0.41	0.41	0.37
Total Cer/HexCer	0.78	0.35	0.75
Cer(d18:1/24:0)	0.46	0.09	0.45
HexCer(d18:1/22:0)	0.76	0.27	0.75
HexCer(d18:1/23:0)	0.72	0.4	0.67
HexCer(d18:1/24:0)	0.76	0.34	0.75
HexCer(d18:1/24:1)	0.65	0.36	0.58
S1P species			
16:1-S1P	0.6	0.54	0.55
18:1-S1P	0.44	0.2	0.41
18:0-S1P	0.28	0.06	0.29
Sphingoid bases of sphingolipids			
C16SO	0.77	0.47	0.75
C16SA	0.8	0.26	0.8
C17SO	0.85	0.51	0.81
C18SO	0.93	0.6	0.86
C18SA	0.82	0.47	0.77
C18SAdiene	0.78	0.55	0.73
C19SO	0.63	0.08	0.7
C20SO	0.57	0.21	0.59
C20SA	0.47	-0.06	0.55
doxSO	0.35	0.14	0.31
doxSA	0.44	0.03	0.43

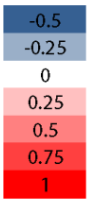

Figure 3. Spearman correlation matrix of glycerophospholipids and sphingolipids with cholesterol levels of the entire cohort (N=49), presented as a heat map.

Red color indicates positive correlation, blue - negative. Intensive color indicates stronger correlations.

2.3.5. Glycerophospholipid and sphingolipid levels in the lipoprotein fractions

Because of very strong correlations between cholesterol levels and the plasma content of glycerophospholipids and sphingolipids, we decided to characterise the distribution of these lipids across various lipoproteins. We analysed the lipoprotein fractions of the plasma samples isolated from three healthy volunteers. We calculated the lipid composition of the four major lipoprotein fractions: the chylomicron/very-low-density lipoprotein (CM/VLDL), the LDL, the HDL fractions and the lipoprotein-free fraction (LFF). Species of PC, SM and LPC were recovered in all plasma lipoprotein fractions. LC-MS analysis showed the presence of PE and Cer/HexCer species in the lipoprotein fractions, but at very low levels that could not be quantified by our LC-MS method. Furthermore, neither PG nor PA lipids were identified in the plasma lipoprotein and LFF fractions.

Figures 4A, 4B and 4C show the percentage of total PC, SM and LPC lipids in the lipoprotein fractions of normal plasma. Figures 4D, 4E and 4F indicate the percentages of the individual PC, SM and LPC species relative to the total concentration of a given species in all lipoprotein fractions. In agreement with previous publications, the largest amount of total PCs were found in HDL (Fig. 4A) [7]. Specifically, 55% of total PCs were found in the HDL, approximately 34% were found in the LDL, 9% were found in the LFF and 2% of PCs were found in the combined CM/VLDL fractions. The distribution of the odd-chain PC species was found to be similar to the distribution of even-chain PCs, with HDL being the major carrier of these lipids in the circulatory system (Fig. 4D). As shown in Fig. 4B, 56% of total circulating SMs were found in LDL, 36% were found in HDL, 5% were found in LFF and 2% were found in CM/VLDL. These findings agree with the literature that the largest part of sphingolipids in circulation is carried by LDL [7]. Although not very pronounced, all SM species showed heterogeneous distribution across lipoprotein fractions (Fig. 4E). 80% of the total LPC molecular species were found in the LFF, indicating that a substantial amount of plasma LPCs is bonded by albumin (Fig. 4C). Furthermore, rather small amounts of total LPCs were found associated with LDL (11%) and HDL (7%). A remarkable difference in the lipoprotein distribution was noted for LPC18:0, when compared to other LPC species (Fig. 4F). The proportion of LPC18:0 was decreased by 20% in the LFF and increased by 11% in the LDL fraction relative to the proportion of LPC16:0 in the same fractions.

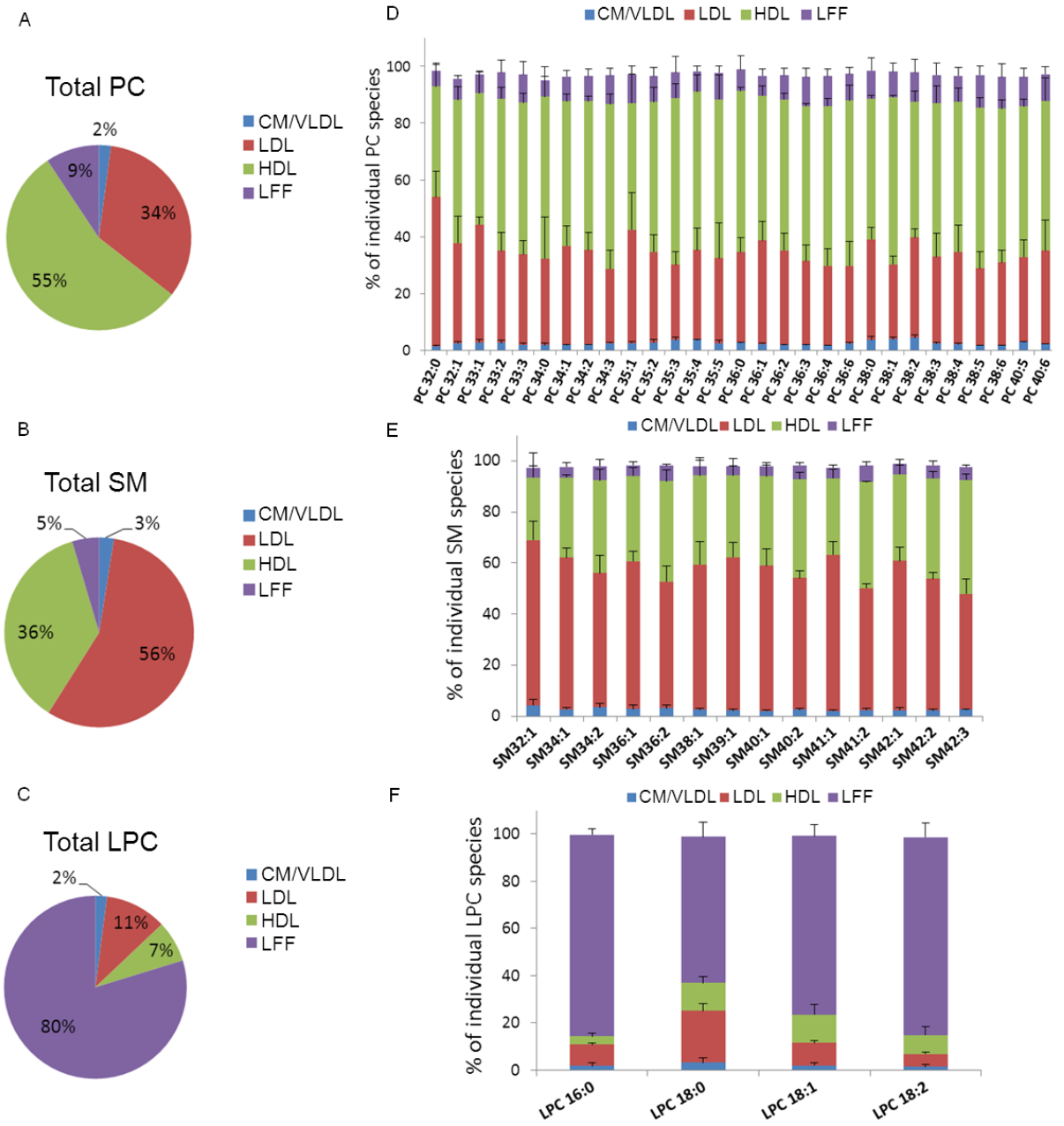

Figure 4. Distribution of the total phosphatidylcholines, lysophosphatidylcholines and sphingomyelins (pie charts) and individual species (bar diagram) in different lipoprotein fractions isolated from plasma of healthy volunteers.

Displayed are the percentages of total phosphatidylcholines (PCs), lysophosphatidylcholines (LPCs) and sphingomyelins (SMs) and their species relative to the summarized content of a representative lipid class or species found in all lipoprotein fractions, respectively. Values are expressed as mean for total lipids (Figures 4A, 4B and 4C) and as mean ± SD for molecular species (Figures 4D, 4E and 4F) of three healthy blood donors. Figures 4A and 4D display total PCs and PC species, respectively (upper row). Figures 4B and 4E display total SMs and SM species (middle row). Figures 4C and 4F display total LPCs and LPC species (lower row). Abbreviations: CM/VLDL, chylomicron/very-low-density lipoprotein, HDL, high-density lipoprotein; LDL, low-density lipoprotein; LFF, lipoprotein-free fraction.

2.4. Discussion

In the present study, we aimed to assess differences in the composition of glycerophospholipids and sphingolipids in the plasma of CAD and ACS patients relative to healthy subjects. Univariate statistical analysis revealed the association of chronic and acute CAD with distinct alterations in the plasma lipidome independent of statin therapy. Overall, in comparison with healthy individuals, 45 molecular species of glycerophospholipids and sphingolipids, 16:1-S1P as well as C17SO, C18SO, C18SA and C18Adiene sphingoid bases were significantly lowered in the plasma of CAD subjects. Moreover, 42 molecular species of glycerophospholipids and sphingolipids, 16:1-S1P, 18:1-S1P as well as C16SO, C16SA, C17SO, C18SO, C18SA and C18SAdiene sphingoid bases were found at significantly reduced plasma levels in patients with ACS when compared to healthy subjects. These associations are likely related to CAD rather than to ACS, as only a few lipids differed by plasma levels between CAD and ACS patients. Furthermore, our analysis of the lipid distribution among the plasma lipoprotein fractions indicated that the vast majority of PCs and SMs are associated with lipoprotein particles, whereas only LPCs are substantially recovered in the lipoprotein-free fraction (LFF). Similar results were previously reported by others suggesting that lipoprotein particles are the main carriers of major plasma glycerophospholipids and sphingolipids [7, 8]. Thus, the alterations in plasma lipidome of CAD and ACS patients may be related to the variations in particle numbers and/or composition of these lipoproteins.

Four odd-chain PC species – PC33:1, PC33:2, PC33:3 and PC35:3 – assumed to be PC plasmalogens, were significantly altered in plasma of both CAD and ACS patients. Diminished plasma levels of plasmalogens have previously been shown in hypertensive and obese patients [14, 15]. Furthermore, these findings support previously described significant associations of reduced plasma levels of PC plasmalogens with stable CAD [16]. In addition, decreased levels of HDL-associated PE plasmalogens have been found in patients with low HDL-C levels and in acute-phase HDL [12, 36]. Our analysis of lipoprotein fractions showed that PC33:1, PC33:2, PC33:3 and PC35:3 (= PC plasmalogens) are largely associated with HDL. This is reflected in strong positive correlations of these lipids with HDL-C found both by our and other studies [37].

Although the physiological functions of plasmalogens are very poorly understood, the decreased levels of PC plasmalogens noted in CAD and ACS patients indicate that they play a role in the pathogenesis of atherosclerotic CAD. It is known that plasmalogens possess antioxidant properties due to their ability to scavenge oxygen radicals [38]. Evidence from *in*

vitro studies indicates that plasmalogens are capable of reducing the oxidation of cell membrane cholesterol, polyunsaturated fatty acids and LDL [39-41]. Thus, low levels of PC plasmalogens observed in the plasmas of CAD and ACS patients may relate to increased oxidative stress causing oxidative degradation of plasmalogens in the lipoprotein particles. This can also explain why PC plasmalogens, but not polyunsaturated PCs, were significantly lower in CAD and ACS patients. Considering this and that oxidative modification of the lipid component of LDL is thought to promote the formation of vascular plaques, it is plausible that a deficiency of PC plasmalogens in LDL particles may contribute to the initial steps of CAD pathogenesis. It is also possible that diminished contents of PC plasmalogens in plasmas of CAD and ACS patients can be directly or indirectly linked to low plasma levels of HDL-C, which is an independent risk factor for CAD [4].

The LC-MS analysis of plasma samples revealed the presence of various S1P species, including typical 18:1-S1P and atypical 16:1-S1P, 17:1-S1P and 18:0-S1P. Different S1P species have been previously identified in plasma samples of healthy subjects [27], however, 17:1-S1P is reported for the first time in the present study. Variations in the structure of S1Ps result from the promiscuous substrate use by serine:palmitoyltransferase (SPT), the enzyme responsible for the first step in the *de novo* synthesis of sphingolipids. Besides the canonical substrates L-serine and C16:0-CoA, SPT can metabolize other acyl-CoAs in the range of C12 to C18 which results in the number of sphingoid bases with variable carbon chain length [42]. The 18:1-S1P represents the most abundant S1P species and was found to be lower in the plasma of ACS patients. In addition, 16:1-S1P was diminished in the plasma of CAD and ACS patients compared to healthy subjects. Other studies reported reduced S1P levels in the plasma and HDL samples of CAD patients [24, 25] and a significant inverse relationship between 18:1-S1P and 18:0-S1P levels in the HDL-containing fraction of serum and the occurrence of ischemic heart disease [26]. However, in contrary to Argraves and colleagues, we did not find any association between plasma levels of 18:0-S1P and CAD or ACS.

Several lipids exhibit biological activity through interaction with various G protein-coupled receptors. Among them 18:1-S1P is an important regulator of vascular function, immune and inflammation responses. HDL is the major carrier of 18:1-S1P in the circulatory system. 18:1-S1P in HDL mediates several atheroprotective properties of these lipoproteins [26], which are attenuated in HDL of CAD patients [43]. Thus, differences in the plasma composition of S1Ps in CAD and ACS patients may contribute to the loss of atheroprotective functions of HDL.

Our analysis of the sphingoid bases of plasma sphingolipids revealed a reduced content of four and six out of eleven identified sphingoid bases in CAD and ACS patients, respectively, when compared to healthy subjects. This agrees with the significantly reduced plasma levels of SM species in CAD and ACS patients relative to healthy individuals, described above. Although sphingoid bases strongly correlate with the total cholesterol and LDL-C levels, statin therapy did not show any significant association with the composition of sphingoid bases. In agreement with previous studies [7, 44], we showed that LDL are the main carriers of plasma sphingolipids. This resulted in strong positive correlations between sphingoid bases and total cholesterol and LDL-C levels, observed in the present study. However, plasma levels of the sphingoid bases doxSA and doxSO, which were found elevated in patients with metabolic syndrome and in patients with type 2 diabetes mellitus [28, 29], did not differ between healthy controls and CAD or ACS patients.

One limitation of the present study is the relatively small study size (n = 69). Another limitation is that the CAD and ACS patients were receiving statins, which may influence glycerophospholipid and sphingolipid composition and metabolism, although we did not see any statistically significant differences between statin-treated and untreated patients. The main strength of this study is the analysis of a wide range of the lipid species. However, larger studies are needed to confirm our findings. Prospective studies are needed to unravel any prognostic clinical relevance.

In conclusion, we show that the levels of various glycerophospholipid and sphingolipid species are diminished in plasma of CAD and ACS patients relative to healthy controls. Among them, PC33:1, PC33:2, PC33:3 and PC35:3 – indirectly identified as PC plasmalogens – are the most significantly altered species in plasmas of CAD patients. Correlation analysis provides interesting insights into the relationship between odd-chain PCs and HDL-C levels. We also report that PC and SM lipids are preferentially localised in HDL and LDL particles, while LPCs are mostly present in the LFF. The results of this study should be further verified in larger case-control and prospective studies.

Acknowledgments

This research was undertaken at the University Hospital Zurich and was supported by a grant from the Zurich Center of Integrated Human Physiology, University of Zurich (ZIHP). The authors wish to thank Silvia Radosavljevic for the isolation of the lipoprotein fractions and all volunteers for participation.

References

1. World Health Organization. "The top 10 causes of death". 2012.
2. Lusis AJ. Atherosclerosis. *Nature* 2000;407:233-241.
3. Lewington S, Whitlock G, Clarke R, et al. Blood cholesterol and vascular mortality by age, sex, and blood pressure: a meta-analysis of individual data from 61 prospective studies with 55,000 vascular deaths. *Lancet* 2007;370:1829-1839.
4. Di Angelantonio E, Sarwar N, Perry P, et al. Major lipids, apolipoproteins, and risk of vascular disease. *JAMA* 2009;302:1993-2000.
5. Wenk MR. The emerging field of lipidomics. *Nature reviews Drug discovery* 2005;4:594-610.
6. Ekroos K, Janis M, Tarasov K, Hurme R, Laaksonen R. Lipidomics: a tool for studies of atherosclerosis. *Curr Atheroscler Rep* 2010;12:273-281.
7. Wiesner P, Leidl K, Boettcher A, Schmitz G, Liebisch G. Lipid profiling of FPLC-separated lipoprotein fractions by electrospray ionization tandem mass spectrometry. *Journal of lipid research* 2009;50:574-585.
8. Dashti M, Kulik W, Hoek F, Veerman EC, Peppelenbosch MP, Rezaee F. A phospholipidomic analysis of all defined human plasma lipoproteins. *Scientific reports* 2011;1:139.
9. Kontush A, Chapman MJ. Lipidomics as a tool for the study of lipoprotein metabolism. *Curr Atheroscler Rep* 2010;12:194-201.
10. Stegemann C, Drozdov I, Shalhoub J, et al. Comparative lipidomics profiling of human atherosclerotic plaques. *Circ Cardiovasc Genet* 2011;4:232-242.
11. Hornemann T, Worgall TS. Sphingolipids and atherosclerosis. *Atherosclerosis* 2013;226:16-28.
12. Pruzanski W, Stefanski E, de Beer FC, de Beer MC, Ravandi A, Kuksis A. Comparative analysis of lipid composition of normal and acute-phase high density lipoproteins. *Journal of lipid research* 2000;41:1035-1047.
13. Stahlman M, Pham HT, Adiels M, et al. Clinical dyslipidaemia is associated with changes in the lipid composition and inflammatory properties of apolipoprotein-B-containing lipoproteins from women with type 2 diabetes. *Diabetologia* 2012;55:1156-1166.
14. Graessler J, Schwudke D, Schwarz PE, Herzog R, Shevchenko A, Bornstein SR. Top-down lipidomics reveals ether lipid deficiency in blood plasma of hypertensive patients. *PloS one* 2009;4:e6261.

15. Pietilainen KH, Sysi-Aho M, Rissanen A, et al. Acquired obesity is associated with changes in the serum lipidomic profile independent of genetic effects--a monozygotic twin study. *PloS one* 2007;2:e218.

16. Meikle PJ, Wong G, Tsorotes D, et al. Plasma lipidomic analysis of stable and unstable coronary artery disease. *Arteriosclerosis, thrombosis, and vascular biology* 2011;31:2723-2732.

17. Stegemann C, Pechlaner R, Willeit P, et al. Lipidomics Profiling and Risk of Cardiovascular Disease in the Prospective Population-Based Bruneck Study. *Circulation* 2014.

18. Jiang XC, Paultre F, Pearson TA, et al. Plasma sphingomyelin level as a risk factor for coronary artery disease. *Arterioscler Thromb Vasc Biol* 2000;20:2614-2618.

19. Nelson JC, Jiang XC, Tabas I, Tall A, Shea S. Plasma sphingomyelin and subclinical atherosclerosis: findings from the multi-ethnic study of atherosclerosis. *American journal of epidemiology* 2006;163:903-912.

20. Schlitt A, Blankenberg S, Yan D, et al. Further evaluation of plasma sphingomyelin levels as a risk factor for coronary artery disease. *Nutr Metab (Lond)* 2006;3:5.

21. Yeboah J, McNamara C, Jiang XC, et al. Association of plasma sphingomyelin levels and incident coronary heart disease events in an adult population: Multi-Ethnic Study of Atherosclerosis. *Arterioscler Thromb Vasc Biol* 2010;30:628-633.

22. Argraves KM, Argraves WS. HDL serves as a S1P signaling platform mediating a multitude of cardiovascular effects. *J Lipid Res* 2007;48:2325-2333.

23. Sattler K, Levkau B. Sphingosine-1-phosphate as a mediator of high-density lipoprotein effects in cardiovascular protection. *Cardiovascular research* 2009;82:201-211.

24. Sattler KJ, Elbasan S, Keul P, et al. Sphingosine 1-phosphate levels in plasma and HDL are altered in coronary artery disease. *Basic research in cardiology* 2010;105:821-832.

25. Sutter I, Park R, Othman A, et al. Apolipoprotein M modulates erythrocyte efflux and tubular reabsorption of sphingosine-1-phosphate. *Journal of lipid research* 2014;55:1730-1737.

26. Argraves KM, Sethi AA, Gazzolo PJ, et al. S1P, dihydro-S1P and C24:1-ceramide levels in the HDL-containing fraction of serum inversely correlate with occurrence of ischemic heart disease. *Lipids in health and disease* 2011;10:70.

27. Quehenberger O, Armando AM, Brown AH, et al. Lipidomics reveals a remarkable diversity of lipids in human plasma. *Journal of lipid research* 2010;51:3299-3305.

28. Othman A, Rutti MF, Ernst D, et al. Plasma deoxysphingolipids: a novel class of biomarkers for the metabolic syndrome? *Diabetologia* 2012;55:421-431.

29. Bertea M, Rutti MF, Othman A, et al. Deoxysphingoid bases as plasma markers in diabetes mellitus. *Lipids Health Dis* 2010;9:84.

30. Diabetes mellitus: a major risk factor for cardiovascular disease. A joint editorial statement by the American Diabetes Association; The National Heart, Lung, and Blood Institute; The Juvenile Diabetes Foundation International; The National Institute of Diabetes and Digestive and Kidney Diseases; and The American Heart Association. *Circulation* 1999;100:1132-1133.

31. Carballo D, Auer R, Carballo S, et al. [A Swiss multicentric project to improve the prevention of cardiovascular event recurrence after acute coronary syndromes]. *Rev Med Suisse* 2010;6:518, 520-512, 524.

32. Cavelier C, Rohrer L, von Eckardstein A. ATP-Binding cassette transporter A1 modulates apolipoprotein A-I transcytosis through aortic endothelial cells. *Circ Res* 2006;99:1060-1066.

33. Haimi P, Uphoff A, Hermansson M, Somerharju P. Software tools for analysis of mass spectrometric lipidome data. *Anal Chem* 2006;78:8324-8331.

34. Yekutieli D, Benjamini Y. Resampling-based false discovery rate controlling multiple test procedures for correlated test statistics. *J Stat Plan Infer* 1999;82:171-196.

35. Berdeaux O, Juaneda P, Martine L, Cabaret S, Bretillon L, Acar N. Identification and quantification of phosphatidylcholines containing very-long-chain polyunsaturated fatty acid in bovine and human retina using liquid chromatography/tandem mass spectrometry. *J Chromatogr A* 2010;1217:7738-7748.

36. Laurila PP, Surakka I, Sarin AP, et al. Genomic, transcriptomic, and lipidomic profiling highlights the role of inflammation in individuals with low high-density lipoprotein cholesterol. *Arteriosclerosis, thrombosis, and vascular biology* 2013;33:847-857.

37. Maeba R, Maeda T, Kinoshita M, et al. Plasmalogens in human serum positively correlate with high- density lipoprotein and decrease with aging. *Journal of atherosclerosis and thrombosis* 2007;14:12-18.

38. Wallner S, Schmitz G. Plasmalogens the neglected regulatory and scavenging lipid species. *Chemistry and physics of lipids* 2011;164:573-589.

39. Reiss D, Beyer K, Engelmann B. Delayed oxidative degradation of polyunsaturated diacyl phospholipids in the presence of plasmalogen phospholipids in vitro. *The Biochemical journal* 1997;323 (Pt 3):807-814.

40. Jurgens G, Fell A, Ledinski G, Chen Q, Paltauf F. Delay of copper-catalyzed oxidation of low density lipoprotein by in vitro enrichment with choline or ethanolamine plasmalogens. *Chemistry and physics of lipids* 1995;77:25-31.

41. Maeba R, Ueta N. Ethanolamine plasmalogens prevent the oxidation of cholesterol by reducing the oxidizability of cholesterol in phospholipid bilayers. *Journal of lipid research* 2003;44:164-171.

42. Hornemann T, Penno A, Rutti MF, et al. The SPTLC3 subunit of serine palmitoyltransferase generates short chain sphingoid bases. *The Journal of biological chemistry* 2009;284:26322-26330.

43. Luscher TF, Landmesser U, von Eckardstein A, Fogelman AM. High-density lipoprotein: vascular protective effects, dysfunction, and potential as therapeutic target. *Circulation research* 2014;114:171-182.

44. Hammad SM, Pierce JS, Soodavar F, et al. Blood sphingolipidomics in healthy humans: impact of sample collection methodology. *J Lipid Res* 2010;51:3074-3087.

3. PLASMALOGENS OF HIGH-DENSITY LIPOPROTEINS (HDL) ARE ASSOCIATED WITH CORONARY ARTERY DISEASE AND ANTI-APOPTOTIC ACTIVITY OF HDL

Iryna Sutter[1,2], Alaa Othman[1,3], Meliana Riwanto[4], Jasmin Manz[5,6] , Lucia Rohrer[1,2], Katharina Rentsch[1,2,7], Thorsten Hornemann[1,2], Ulf Landmesser[2,5,6,8], and Arnold von Eckardstein[1,2,3]

1. Institute of Clinical Chemistry, University and University Hospital of Zurich, Zurich, Switzerland
2. Competence Center for Integrated Human Physiology, University of Zurich, Zurich, Switzerland
3. Competence Center for Systems Physiology and Metabolic Diseases, ETH Zurich and University of Zurich, Zurich, Switzerland
4. Division of Nephrology, Institute of Physiology, University of Zurich, Zurich, Switzerland
5. Cardiology, Cardiovascular Center, University Hospital Zurich, Zurich, Switzerland
6. Cardiovascular Research, Institute of Physiology, University of Zurich, Zurich, Switzerland
7. present address: Laboratory Medicine, University Hospital Basel, Basel, Switzerland
8. present address: Cardiology, University medicine Charité, Berlin, Germany

[Atherosclerosis, submitted]

Abstract

Objective*:* Low high-density lipoprotein (HDL) cholesterol and loss of atheroprotective functions of HDL are associated with coronary artery disease (CAD). Here, we investigated the associations of HDL phospholipids with acute and stable CAD as well as with the anti-apoptotic activity of HDL.

Methods: 49 species of phosphatidylcholines (PCs), lysophosphatidylcholines and sphingomyelins (SMs) as well as three species of sphingosine-1-phosphate (S1P) were quantified by liquid chromatography - mass spectrometry in HDL isolated from 22 healthy subjects as well as 23 and 22 patients with stable CAD and acute coronary syndrome (ACS), respectively. HDL was tested for its capacity to inhibit apoptosis of endothelial cells (ECs) induced by serum deprivation.

Results: HDL of CAD or ACS patients differed from HDL of healthy controls by the content in nine of the 52 quantified phospholipid species as well as reduced anti-apoptotic activity. EC apoptosis in the presence of HDL exhibited significant inverse correlations with five of eleven odd-chain PC's (= plasmalogens), two S1P's, SM42:2, PC34:2, and PC32:0. An orthogonal partial least square - discriminant analysis revealed independent associations of stable CAD with HDL-associated PC34:2, PC33:3 and PC35:2 as well as anti-apoptotic activity of HDL and of ACS with HDL-associated PC33:3, PC35:2, SM42:1, PC34:2 and PC36:2.

Conclusions: Two *apriori* undefined plasmalogens – PC33:3 and PC35:2 – as well as PC34:2 – showed the most consistent relationships with the presence of both stable and acute CAD as well as the capacity of HDL to inhibit EC apoptosis.

3.1. Introduction

High-density lipoprotein (HDL) particles are believed to play an important role in the pathogenesis of coronary artery disease (CAD). Indeed, a low plasma level of HDL cholesterol (HDL-C) represents a strong independent risk factor for CAD [1]. Moreover, HDLs isolated from healthy blood donors exert multiple atheroprotective functions that are attenuated or lost in HDLs of CAD patients [2, 3]. Recent proteomic studies related the loss of atheroprotective functions to alterations in the protein composition of HDL [4, 5] as well as to structural modifications of HDL proteins [6]. However, not only proteins but also lipids contribute to the structural and functional heterogeneity of HDL.

The HDL lipidome is complex and contains more than 200 different molecular lipid species. Among them phospholipids comprise the major part of the HDL lipidome, followed by cholesteryl esters, triglycerides and free cholesterol [7]. Phosphatidylcholines (PCs), sphingomyelins (SMs), and free cholesterol are key structural molecules of the surface monolayer of HDL particles [7]. The length and desaturation degree of acyl chains of PC species as well as the content of SMs and free cholesterol define the fluidity of the lipid monolayer [8, 9]. Through modulation of the fluidity, the surface PCs directly affect HDL's ability to accept cholesterol from peripheral tissues [8] as well as phospholipid hydroperoxides from low-density lipoproteins (LDLs) [10]. Moreover, the fatty acid composition of PCs defines the capacity of artificially reconstituted HDL (rHDL) to inhibit the expression of inflammatory markers in activated endothelial cells (ECs) [11]. HDL phospholipids also have impact on HDL-associated proteins and enzymes. Indeed, a reduced abundance of phospholipids on the surface of HDL facilitates CETP-mediated dissociation of lipid-free apoA-I from HDL particles [12]. Furthermore, changes in the molecular composition of PCs in rHDL lead to conformational changes of apoA-I and changes in the activity of lecithin:cholesterol acyltransferase (LCAT) [13]. In contrary, enrichment of HDL with SMs inhibits the unfolding of apoA-I and cholesterol esterification catalyzed by LCAT [9, 14]. In previous studies, total content of PCs and SMs in HDL was found to correlate with the severity of coronary atherosclerosis [15, 16].

In addition to PCs and SMs, of which 10 to 100 molecules are present on each HDL particle, HDLs contain low abundant lipids at concentrations which are below particle concentration [2]. For example, plasmalogens constitute a subclass of PCs and phosphatidylethanolamines (PEs) [17] which scavenge oxygen radicals and thereby inhibit the oxidation of cholesterol and polyunsaturated fatty acids in plasma membranes and LDL [18-20]. Other low abundant lipids exert biological activities through direct interaction with G-protein

coupled receptors. Among them sphingosine-1-phosphate (S1P) is the best characterised lipid agonist carried by HDL. HDL-associated S1P mediates several atheroprotective functions of HDL via interaction with at least five different S1P receptors [21, 22]. Specifically, S1P modulates the capacity of HDL to stimulate nitric oxide production, promote EC growth and survival, inhibit EC apoptosis and migration of smooth muscle cells [21-23]. However, S1P is not a distinct molecule but in contrast to the general notion differs by the length and desaturation degree of its sphingoid base [24,25]. The heterogeneity in length results from the substrate promiscuity of serine:palmitoyltransferase [26], the rate limiting enzyme in sphingolipid biosynthesis. However, the functional importance of S1P's structural heterogeneity is as yet unknown.

In this cross-sectional study we used both hypothesis-free and hypothesis driven approaches to identify phospholipids which are associated with both CAD and correlate with the capacity of HDL to inhibit the apoptosis of ECs. 49 phospholipid species of unknown relevance were measured by liquid chromatography – tandem mass spectrometry (LC-MS/MS). Three species of S1P which is a known mediator of HDL's anti-apoptotic activity and has been previously associated with CAD were quantified by a targeted LC-MS/MS method.

3.2. Materials and methods

3.2.1. Subjects and blood samples

Patients with coronary artery disease (CAD) or acute coronary syndrome (ACS; ST elevation myocardial infarction (STEMI) or non-ST elevation myocardial infarction (NSTEMI)) were recruited at the University Hospital of Zurich as described previously [27]. The diagnosis of stable CAD or an ACS was made according to the guidelines of the American College of Cardiology/American Association task force [28, 29]. Patients with ACS (STEMI or NSTEMI) were recruited into the study within the first 12 h after the onset of the symptoms. The following exclusion criteria were considered for both CAD and ACS patients: evidence for accompanying infectious, inflammatory or autoimmune disorders, diabetes, advanced kidney or liver failure, neoplastic disorders and a history about major surgery or trauma within the previous month. Advanced kidney failure was defined as < 60 ml/min of glomerular filtration rate (GFR). Age- and sex-matched healthy control individuals were enrolled by the Blood Donation Service Zurich and had no cardiovascular risk factors (according to history, clinical examination and laboratory tests) or accompanying disorders. All subjects gave written informed consent prior to inclusion in the study. This study was

approved by the local ethics committee (Kantonale Ethik – Kommission, Zurich, Switzerland).

Venous blood was collected from the antecubital vein into sterile evacuated tubes (BD Vacutainer) in the absence of anticoagulants (to obtain serum) or in the presence of EDTA (to obtain EDTA-plasma). After blood collection, EDTA plasma was immediately separated by centrifugation at 4°C (20 min at 2000 rcf) and aliquoted by 1 ml into cryotubes and stored at -20°C. Blood in the absence of anticoagulants was kept at room temperature for 30-60 min and then centrifuged at 4°C (20 min at 4000 rcf). Serum was then isolated, aliquoted (~1 ml in each cryotube) and stored at -20°C.

3.2.2. Isolation of HDL

HDL was isolated from EDTA-plasma by sequential ultracentrifugation (*d*=1,063-1,21 kg/l) using solid potassium bromide (Merck KGaA, Germany) for density adjustment as described previously [30]. For phospholipid analysis, HDL samples were supplemented with antioxidant butylhydroxytoluene (BHT) to the final concentration 50 µg/mg of HDL and stored at -80°C. HDL for functional studies were isolated from serum samples. These HDL samples were stored at 4°C.

3.2.3. Clinical laboratory measurements

Routine blood testing was performed at the clinical laboratories of the University Hospital Zurich. Plasma concentrations or activities of total cholesterol, triglycerides, and HDL- cholesterol, glucose, creatinine, creatinine kinase and troponin levels were determined by photometric tests or immunoassay by using the Cobas 8000 autoanalyser from Roche diagnostics (Rotkreuz, Switzerland). Automated differential blood counts were performed on the ADVIA 2120 Hematology System. Cholesterol concentrations in isolated HDL were measured by using the Amplex®Red Cholesterol Assay Kit (Roche, Switzerland) according to the manufacturer's instructions.

3.2.4. Endothelial cell culture

Human aortic endothelial cells (ECs) were cultured as described previously [4]. Briefly, ECs were obtained from (LONZA) and cultured in (EBM-2, Lonza) supplemented with endothelial growth medium–SingleQuots as indicated by the manufacturer (37°C, 95% air / 5% CO2). SingleQuots contain human epidermal growth factor (hEGF), hydrocortisone, gentamicin and amphotericin-B, fetal bovine serum, vascular endothelial growth factor

(VEGF), human fibroblast growth factor-basic (hFGF-B), insulin-like growth factor (R3-IGF-1), and ascorbic acid. ECs were grown to sub-confluency and rendered quiescent before experiments by incubation in medium containing 0.5% FCS. Serum and growth factor deprivation was induced by changing the medium to serum-free RPMI. ECs (7500 cells/well in 96 well plates) were exposed to serum and growth factor deprivation in the absence or presence of 100 µg/ml of HDL (10 µg HDL in 100 µl RPMI medium) for 24 h.

3.2.5. Measurement of endothelial cell apoptosis

ECs were lysed and apoptotic cell death was measured by the Cell Death Detection ELISA^{PLUS} (Roche, Switzerland) according to the supplier's instructions. This quantitative sandwich-enzyme-immunoassay records the amount of mono- and oligonucleosomes generated by apoptotic cells. EC apoptosis is expressed as fold increase over the basal level of apoptosis without the cell death inducing treatment.

3.2.6. Quantification of phospholipids and S1P

Phosphatidylcholines (PCs), lysophosphatidylcholines (LPCs) and sphingomyelins (SMs) in 12.5 µg of HDL (by protein mass) were quantified by LC-MS essentially as described previously [31]. Briefly, HDL samples were fortified with the internal standards (ISs), including phosphatidylglycerol PG(17:0/17:0), lysophosphatidylglycerol LPG(17:1/0:0), phosphatidic acid PA(14:0/14:0), lysophosphatidic acid LPA(17:0/0:0), PE(14:0/14:0), lysophosphatidylethanolamine LPE(17:1/0:0), PC(14:0/14:0), PC(24:0/24:0), LPC(17:0/0:0), SM (d18:1/12:0) and ceramide Cer(d18:1/17:0) obtained from Avanti Polar Lipids (Alabaster, AL, USA), and extracted with chloroform/methanol/water (2:2:1, v/v) solvent system. After evaporation and reconstitution in 200 µl of mobile phase, samples were injected on the Rheos 2200/TSQ Access LC-MS system and eluted from a diol silica, 150 x 2.1 mm, 5 µm particle size column with solvent system containing hexane/isopropanol/water (70:30:2, v/v) with 15 mM NH_4COOH and isopropanol/water (50:2, v/v) with 15 mM NH_4COOH. Phospholipid species were detected by using precursor ion and neutral loss scans. A neutral loss scan of *m/z* 115 (collision energy, 27 eV) and 189 (17 eV) were used for analysis of PA and PG lipids, respectively. A precursor ion scan of *m/z* 184 (30 eV) was used for screening of PC, SM and LPC lipids. A neutral loss scan of *m/z* 141 (25 eV) was used for PE and a precursor ion scan of *m/z* 264 (30 eV) was applied for screening of Cer and HexCer. The data were collected and processed using the Xcalibur and LIMSA software systems.

Quantitative analysis was based on calibration curves for seven lipid standards including PC(16:0/18:2), SM(d18:1/16:0), LPC(16:0), PE(18:0/18:0), Cer(d18:1/14:0), PG(16:0/16:0) and PA(14:0/14:0). The calibration curves were constructed by plotting the lipid standard/IS peak area ratios against the nominal concentrations of the standards. The concentrations for the identified lipid species were calculated from linear regressions of the calibration curves. To estimate the total serum content of HDL-associated lipids, the protein normalized amount of lipid species were divided by the protein-normalized amount of cholesterol measured in isolated HDL and multiplied with the HDL-C concentration measured in serum by the homogenous clinical assay.

S1P species were quantified in 50 µg of HDL proteins supplemented with 10 pmol of 18:1-D7S1P which was used as IS. Extracted and derivatized S1P lipids were subjected to LC-MS/MS analysis using a previously described method [32] with minor modifications. Beyond the canonical 18:1-S1P derived from the d18:1 sphingoid base formed by the condensation of serine with palmitoyl (C16:0)-CoA catalyzed by serine:palmitoyltransferase, we also measured the non-canonical 16:1-S1P and 18:2-S1P species derived from d16:1 and d18:2 sphingoid bases. Previously, in the human plasma, d18:2 and d16:1 sphingosines were identified as the second and third most abundant sphingoid bases next to the predominant d18:1 sphingosine [24, 33, 34]. S1Ps were analysed on a Rheos 2200/TSQ Access LC-MS system, operating in a Selective Reaction Monitoring (SRM) positive ionization mode. The SRM transitions monitored were as follows: 18:1-S1P$(Ac)_2$ m/z 446.2/264.2 (30 eV); 16:1-S1P$(Ac)_2$ m/z 418.2/236.2 (30 eV); 18:2-S1P$(Ac)_2$ m/z 444.2/262.2 (30 eV) and 18:1-D7S1P$(Ac)_2$ (IS) m/z 453.2/271.2 (27 eV). The tube lens voltage for all SRM transitions was set to 130.1 V. Quantitative analysis of 18:1-S1P, 16:1-S1P and 18:2-S1P was based on the 18:1-S1P calibration curve. This calibration curve was constructed by adding increasing amounts of 18:1-S1P to 10 pmol of IS, followed by extraction with ethyl acetate/2-propanol (6:1, v/v) and derivatization with acetic anhydride. Linearity of calibration curve and correlation coefficient were obtained by linear regression analysis.

3.2.7. Statistical analysis

Statistical analyses were performed using SPSS version 19 (IBM Corporation, Somers NY, USA), Graph-Pad Prism (GraphPad Software, San Diego, CA, USA) and SIMCA-P +12.0.1.0 (Umetrics, Ume, Sweden). Normality of the data was determined by using the Kolmogorov-Smirnov test**.** Because many variables did not follow a Gaussian frequency distribution, even after log-transformation, the univariate statistics were performed by

applying Kruskal-Wallis and Mann-Whitney U tests. Categorical variables were compared using the Chi-square test. Spearman rank tests were used to analyze and describe the correlation between HDL-associated phospholipids and EC apoptosis. To maintain the rate of false-positive results, *p* values were adjusted for multiple comparisons by applying the Benjamini-Hochberg procedure [35]. The adjusted (adj.) *p* values of <0.05 were considered as statistically significant.

A multiple regression analysis was used to identify independent variables capable of predicting the EC apoptosis.

Multivariate analyses were performed by using an orthogonal partial least square-discriminant analysis (OPLS-DA) to identify most discriminating parameters among two groups of samples. Data on HDL-associated phospholipids and EC apoptosis were exported to SIMCA-P +12.0.1.0. The three groups (Healthy, CAD, ACS) were assigned as classes. Models were used to compare only two groups at the time: Healthy vs CAD; Healthy vs ACS; CAD vs ACS. The OPLS-DA models were fitted to the classes in order to get the highest Q^2Y (goodness of prediction) and R^2Y (percent of the model fitting the data) values. The data set was normalized to unit variance (UV) and centered on the mean. Model evaluation was performed by cross-validation with seven groups as a default. The quality of the model was represented by cross-validated Q^2Y and R^2Y values. Furthermore, CV-ANOVA was calculated to identify significance of the predicted Y-variation. The Hotelling`s T^2 and distance to model, DmodX, were used to identify outliers.

3.3. Results

3.3.1. Characteristics of the study population

HDL samples were isolated from 23 and 22 patients with stable coronary artery disease (CAD) and acute coronary syndrome (ACS), respectively, as well as from 22 healthy subjects. Their clinical and biochemical characteristics are shown in Table 1. All CAD patients but only 86% of the healthy controls and the ACS patients were male. Furthermore, 91% of CAD patients but only 41% of ACS patients and no healthy subject received statin medication. Patients with CAD were older (adj. p = 0.049; adj. p = 0.019) and had higher systolic BP (adj. p = 0.008; adj. p = 0.004) than healthy subjects and ACS patients, respectively. Both CAD and ACS patients had higher glucose levels (adj. p =0.022 and adj. p = 0.017, respectively) than healthy subjects. The ACS patients had lower HDL-C (adj. p <0.001; adj. p = 0.027) than both healthy subjects and CAD patients. Probably as the consequence of more prevalent statin treatment, the ACS patients had lower levels of total cholesterol (adj. p = 0.022), while CAD patients had lower levels of both total cholesterol (adj. p = 0.002) and LDL-C (adj. p = 0.002) as compared to healthy subjects. As expected, troponin T levels (adj. p <0.001) and leukocyte counts (adj. p <0.001) were higher in blood samples of ACS patients as compared to healthy individuals or CAD patients.

3.3.2. Characteristics of the HDL lipidome

The LC-MS/MS analysis of HDL-associated phospholipids resulted in the quantification of 29 PC species, 4 LPC species and 16 SM species (Table 2). Several PE and Cer species were also recovered in HDL, however at levels below the limit of quantification. PG and PA lipids were below the level of detection.

HDL-associated PC lipids comprise species with even or odd numbers of carbon atoms in the acyl chains. Structural analysis of the plasma odd-chain PC35:3 using collision-induced dissociation of $[M\text{-}CH_3]^-$ ions showed similar fragmentation patterns as a commercially available plasmalogen standard PC(P-18:0/18:1) (= PC35:2). The structural analysis of plasma PC35:3 revealed that this odd-chain PC lipid represents PC-derived plasmalogen, PC(P-18:0/18:2). See Chapter 1 for more information on fragmentation pattern of PC-derived plasmalogens and even-chain PC species. Thus, HDL-associated odd-chain PCs most likely are PC plasmalogens.

Our second LC-MS/MS method identified three S1P species in HDL which differ by length or desaturation of the sphingoid base: 18:1-S1P, corresponding to the canonical S1P, 16:1-S1P and 18:2-S1P.

Table 1. Characteristics of the study population.

Characteristics	Healthy subjects (n=22)	CAD (n=23)	ACS (n=22)	Kruskal-Wallis Test, adj. *p* values	Mann-Whitney Test, adj. *p* values		
					H vs CAD	H vs ACS	CAD vs ACS
Age (years)	56.5(42;73)	63,0(45;70)	56.5(39;69)	**0.023**	**0.049**	0.842	**0.019**
Sex (Male) (%)	86	100	86	0.188*			
History of smoking (%)	0	13	41	**0.001***			
BP systolic (mmHg)	122(103;135)	136(104;156)	117(96;158)	**0.002**	**0.008**	0.304	**0.004**
BP diastolic (mmHg)	84(64;97)	81(58;90)	75(48;100)	0.051	0.304	**0.026**	0.196
Puls	60(48;76)	60(48;73)	76(55;95)	**<0.001**	0.497	**<0.001**	**0.001**
BMI (kg/m2)	25.3(20;32.5)	28.05(19.4;40.2)	26.9(21.5;35.35)	0.18	0.109	0.329	0.409
Glucose (mmol/l)	5(4.4;6.6)	5.6(4.5;14.5)	6.75(5.2;14.7)	**<0.001**	**0.022**	**<0.001**	**0.017**
Cholesterol (mmol/l)	5.5(3.4;7.7)	4.35(2.3;6.7)	4.65(3.1;6.6)	**0.002**	**0.002**	**0.022**	0.304
HDL-C (mmol/l)	1.39(1.05;2.96)	1.32(0.65;2.59)	1(0.65;1.72)	**<0.001**	0.109	**<0.001**	**0.027**
LDL-C (mmol/l)	3.55(1.9;5.2)	2.3(1.1;4.4)	2.9(1.3;5.2)	**0.003**	**0.002**	0.159	0.062
Triglyceride (mmol/l)	0.88(0.59;2.11)	1.25(0.39;6.8)	1.52(0.36;7.61)	0.314	0.159	0.408	0.842
Troponin T (ug/l)	0.01(0.01;0.02)	0.01(0.01;0.02)	0.08(0.01;7.31)	**<0.001**	0.332	**<0.001**	**<0.001**
Creatine kinase (µg/l)	141(51;346)	87(47;177)	147.5(38;3043)	**0.023**	0.078	0.295	**0.019**
Leukocytes (103/µl)	5.29(0.59;6.97)	5.68(2.66;10.25)	8.97(5.4;15.83)	**<0.001**	0.199	**<0.001**	**<0.001**
Medication, %							
Statins	0	91	41	**<0.001**			
β-Bloker	0	61	18	**<0.001**			
Diuretics	0	22	5	**0.036***			
ACE-I	0	26	18	0.053*			
Calcium blocker	0	13	5	0.188*			
Aspirin	0	91	32	**<0.001**			
Clopidogrel	0	4	27	**0.01***			

Data are expressed as medians (with ranges) and percentages for scale and categorical variables, respectively. Statistical significance of the categorical variables was evaluated by Chi-square test. The *p* values marked by asterisk indicate that results of Chi-square test may be invalid, because more than 20% of the expected frequencies have a value less than 5. Since some of the continuous variables were not normally distributed, statistical significance was determined by the Kruskal-Wallis test applied for multiple group comparisons and by the Mann-Whitney U test applied for two group comparisons. The *p* values were adjusted for multiple testing by using the Benjamini-Hochberg procedure. Significant *p* values are marked in bold font. ACE-I indicates angiotensin-converting enzyme inhibitor; ACS, acute coronary syndrome; BMI, body mass index; CAD, coronary artery disease; H, healthy subjects; HDL-C, high-density lipoprotein cholesterol; LDL-C, low-density lipoprotein cholesterol.

3.3.3. Associations of HDL phospholipids with CAD

We compared the protein normalized content of phospholipid species in HDL isolated from healthy subjects with those in HDL isolated from CAD or ACS patients. The entire data set is shown in the Table 2. After adjustment for multiple testing, levels of HDL-associated PC34:2 (adj. $p = 0.022$), PC34:3 (adj. $p = 0.033$), PC33:3 (adj. $p = 0.033$) and PC35:2 (adj. $p = 0.033$) were found significantly lower in CAD patients as compared to healthy subjects. In contrary, PC38:4 (adj. $p = 0.018$) was more abundant in HDL of CAD patients than in HDL of healthy controls. The levels of HDL-associated PC33:3 (adj. $p = 0.008$), PC35:2 (adj. $p = 0.018$), PC35:3 (adj. $p = 0.04$), PC35:5 (adj. $p = 0.018$) and SM42:1 (adj. $p = 0.018$) were significantly lower in ACS patients than in healthy individuals. However, their HDL content did not differ between CAD and ACS patients (Table 2). Cholesterol per protein levels were lower in HDL of ACS patient than in HDL of healthy subjects (adj. $p = 0.033$). We did not find any statistically significant differences in the HDL content of individual S1P species or total S1P although by trend, the 18:1-S1P and 16:1-S1P content in HDL of CAD and ACS patients was lower than in HDL of healthy controls (Table 2).

To estimate the serum levels of HDL-associated lipids, the protein-normalized amount of lipid species were divided by the protein-normalized amount of cholesterol measured in isolated HDL and multiplied with the HDL-C concentration measured in serum by the homogenous clinical assay. Only serum levels of HDL-associated PC33:3 (adj. $p = 0.013$) were significantly lower in ACS patients compared to healthy controls (Table 3).

Table 2. Phospholipid composition of HDL from healthy subjects, CAD and ACS patients.

Lipids, nmol/mg of HDL	Healthy subjects (n=22)	CAD (n=23)	ACS (n=22)	Kruskal-Wallis Test, adj. *p* values	Mann-Whitney Test, adj. *p* values		
					H vs CAD	H vs ACS	CAD vs ACS
PC32:0	1.74(0.82;4.02)	1.98(0.86;4.97)	1.58(0.64;2.86)	0.294	0.981	0.282	0.319
PC32:1	3.4(1.4;9.22)	3.04(1.25;6.65)	3.36(1.4;16.31)	0.801	0.684	0.981	0.712
PC33:1	1.75(0.93;3.19)	1.32(0.61;3.17)	1.39(0.62;2.06)	0.18	0.165	0.319	0.684
PC33:2	2.03(0.73;3.67)	1.24(0.61;4.2)	1.47(0.64;2.34)	0.09	0.165	0.077	0.981
PC33:3	1.13(0.39;1.82)	0.58(0.12;1.67)	0.52(0.1;1.21)	**0.006**	**0.034**	**0.006**	0.727
PC34:0	1.9(0.71;5.27)	1.63(0.76;3.17)	1.65(0.52;2.76)	0.224	0.588	0.191	0.478
PC34:1	41.31(25.94;68.86)	42.27(31.18;54.57)	40.38(28.98;77.09)	0.925	0.899	0.988	0.782
PC34:2	89.72(63.08;125.35)	67.85(41.41;118.33)	72.72(51.35;103.41)	**0.017**	**0.02**	0.055	0.584
PC34:3	3.88(1.79;6.97)	2.96(1.31;4.86)	3.1(1.4;6.87)	0.065	**0.034**	0.225	0.646
PC35:1	0.94(0.35;2.86)	0.98(0.17;2.24)	0.91(0.16;1.94)	0.925	0.889	0.864	0.839
PC35:2	3.27(1.13;4.91)	1.95(0.8;4.72)	2(0.94;3.22)	**0.017**	**0.034**	**0.018**	0.94
PC35:3	1.6(0.72;3.83)	1.36(0.26;3.89)	1.12(0.55;2.41)	0.08	0.287	**0.041**	0.531
PC35:4	3.86(1.94;6.05)	3.63(1.78;5.95)	2.79(1.8;5.69)	0.117	0.773	0.098	0.225
PC35:5	2.28(1.11;4.27)	1.93(0.85;3.9)	1.29(0.6;2.92)	**0.017**	0.588	**0.018**	0.082
PC36:0	0.88(0.01;2.89)	0.92(0.3;1.86)	0.74(0.1;2.19)	0.602	0.932	0.655	0.452
PC36:1	9.7(4.82;14.36)	9.65(6.57;13.37)	9.1(5.08;14.71)	0.85	0.973	0.891	0.632
PC36:2	50.04(32.26;61.68)	39.02(27.79;68.61)	39.06(26.51;59.23)	0.05	0.069	0.069	0.839
PC36:3	29.43(21.28;41)	26.97(21.85;35.76)	25.53(11.36;38.17)	0.08	0.398	0.055	0.277
PC 36:4	37.34(26.62;48.68)	39.54(26.68;62.18)	34.57(23.75;63.54)	0.117	0.225	0.588	0.104
PC36:5	5.27(2.32;8.19)	4.05(2.18;7.56)	4.09(2.28;7.74)	0.237	0.187	0.389	1,000
PC37:4	3.13(1.05;5.35)	2.99(1.34;5.1)	2.46(1.63;3.62)	0.161	0.973	0.165	0.225
PC37:5	4.53(2.75;6.06)	4.17(2.26;7.5)	3.53(1.77;5.73)	0.097	0.741	0.077	0.225
PC37:6	1.76(0.88;3.43)	1.43(0.48;3.07)	1.24(0.52;2.06)	0.08	0.135	0.077	0.756
PC38:3	9.38(6.1;11.56)	9.16(5.21;13.46)	9.01(3.25;15.84)	0.734	0.981	0.632	0.632
PC38:4	19.81(15.07;28.34)	27.63(18.22;45.91)	22.17(16.37;34.65)	**0.017**	**0.018**	0.513	0.077
PC38:5	12.73(7.96;16.28)	12.04(8.34;17.89)	10.88(7.77;16.68)	0.216	0.891	0.243	0.225
PC38:6	13.2(8.41;18.6)	11.65(8.01;21.29)	9.9(6.88;26.09)	0.148	0.839	0.135	0.225
PC40:5	2.27(1;3.92)	2.56(1.56;4.95)	2.12(1.13;3.44)	0.161	0.225	0.769	0.17
PC40:6	4.47(2.33;7.14)	5.16(2.56;9.32)	3.95(1.82;8.92)	0.08	0.225	0.398	0.074
Total PC	363.76(263.24;449.86)	345.86(264.94;479)	308.13(261.08;463.72)	0.09	0.398	0.077	0.225
LPC16:0	2.99(1.83;4.08)	3(1.2;6.04)	2.81(1.44;6.67)	0.976	0.988	0.889	0.973
LPC18:0	2.76(1.87;3.61)	2.51(1.34;4.84)	2.5(1.31;4.38)	0.215	0.398	0.191	0.531

(Continued)

LPC18:1	2.39(1.05;3.6)	2.23(1.1;4.06)	1.75(0.95;4.84)	0.571	0.805	0.531	0.484
LPC18:2	2.51(1.29;3.79)	2.28(1.03;3.97)	1.73(0.93;5.96)	0.25	0.389	0.227	0.655
Total LPC	10.45(6.72;14.33)	10.41(4.78;17.89)	8.46(5.24;21.85)	0.602	0.773	0.465	0.698
SM32:1	1.15(0.66;2.04)	1.04(0.67;1.81)	1.1(0.68;1.37)	0.589	0.52	0.52	0.889
SM34:0	1.24(0.63;1.85)	0.98(0.71;2.14)	1.1(0.7;1.46)	0.09	0.077	0.165	0.769
SM34:1	11.66(7.48;24.87)	10.5(3.83;25.03)	8.88(2.86;16.96)	0.098	0.329	0.069	0.601
SM34:2	1.37(0.38;2.08)	1.24(0.61;2.63)	1.09(0.78;1.94)	0.381	0.82	0.269	0.531
SM36:1	2.69(1.8;4.8)	2.56(1.26;5.92)	3.21(1.31;6.71)	0.602	0.797	0.632	0.517
SM36:2	1.24(0.75;1.86)	1.12(0.62;1.85)	1.15(0.86;2.27)	0.425	0.345	0.822	0.509
SM38:1	3.31(1.35;5.87)	2.72(1.33;4.78)	2.64(0.97;4.92)	0.301	0.269	0.355	0.94
SM39:1	1.28(0.59;2.28)	0.96(0.66;2.11)	1.04(0.73;1.53)	0.161	0.186	0.345	0.398
SM39:2	0.57(0.36;0.92)	0.75(0.35;0.96)	0.79(0.38;1.02)	0.237	0.496	0.165	0.839
SM40:1	6.09(4.18;8.69)	5.25(2.21;9.36)	5.02(2.55;8.13)	0.161	0.269	0.118	0.887
SM40:2	4.86(2.03;7.51)	4.35(1.79;7.13)	3.79(1.87;6.58)	0.25	0.52	0.225	0.571
SM41:1	2.58(1.29;4.85)	2(0.87;3.99)	1.94(0.65;4.06)	0.134	0.287	0.077	0.839
SM41:2	2.11(0.99;4.04)	1.76(1.04;3.65)	1.89(0.99;4.28)	0.216	0.181	0.382	0.782
SM42:1	4.16(1.76;5.74)	3.16(1.36;8.21)	2.77(1.45;4.78)	**0.017**	0.098	**0.018**	0.464
SM42:2	10.88(6.42;16.46)	9.4(3.91;18.8)	9.46(4.84;16.72)	0.224	0.225	0.269	0.972
SM42:3	4.87(2.49;7.2)	4.37(1.63;8.15)	3.89(2.27;8.12)	0.625	0.899	0.57	0.562
Total SM	57.54(38.5;95.38)	52.17(26.25;100.43)	50.58(26.13;85.67)	0.148	0.282	0.098	0.805
Chol. in HDL	414,99(198,44;780,65)	343,2(129,74;745,55)	288,97(140,45;574,62)	0.064	0.225	**0.034**	0.415

Lipids, pmol/mg of HDL	**Healthy subjects (n=22)**	**CAD (n=23)**	**ACS (n=22)**	**Kruskal-Wallis Test, adj. *p* values**	**Mann-Whitney Test, adj. *p* values**		
					H vs CAD	**H vs ACS**	**CAD vs ACS**
16:1-S1P	26.7(10.83;54.26)	19.84(8.69;42.62)	17.65(9.78;32.86)	0.09	0.222	0.077	0.632
18:1-S1P	86.04(47.43;146.69)	71.07(41.87;173.85)	76.1(40.61;124.02)	0.184	0.187	0.243	0.891
18:2-S1P	17.65(8.75;55.65)	13.94(8.98;34.97)	16.14(8.81;29.35)	0.436	0.345	0.524	0.839
Total S1P	123.5(67.3;256.5)	100.1(60.1;238.9)	116.8(60.5;171.1)	0.161	0.175	0.225	0.981

Data are medians (and ranges). Of note, all PC lipids identified as odd-chain PC species probably represent PC plasmalogens. Statistical significance was determined by using the Kruskal-Wallis test for multiple group comparisons and the Mann-Whitney U test for two group comparisons. The *p* values were adjusted for multiple testing by using the Benjamini-Hochberg procedure. Significant *p* values are marked in bold font. PC and LPC species are named according to the summarized numbers of carbons and double bounds in acyl chains. Names of SM species reflect summarized numbers of carbons and double bounds in sphingoid base and N-linked fatty acid. ACS stands for acute coronary syndrome; CAD, coronary artery disease; Chol. in HDL, cholesterol in isolated HDL; H, healthy subjects; LPC, lysophosphatidylcholine; PC, phosphatidylcholine; SM, sphingomyelin; 16:1-S1P, sphingosine-1-phosphate with 16:1 sphingoid base; 18:1-S1P, sphingosine-1-phosphate with 18:1 sphingoid base; 18:2-S1P, sphingosine-1-phosphate with 18:2 sphingoid base.

Table 3. Estimated serum concentrations of HDL-associated phospholipids in healthy subjects, CAD and ACS patients.

Lipids, nmol/mg of HDL	Healthy subjects (n=22)	CAD (n=23)	ACS (n=22)	Kruskal-Wallis Test, adj. *p* values	Mann-Whitney Test, adj. *p* values		
					H vs CAD	H vs ACS	CAD vs ACS
PC32:0	1.74(0.82;4.02)	1.98(0.86;4.97)	1.58(0.64;2.86)	0.294	0.981	0.282	0.319
PC32:1	3.4(1.4;9.22)	3.04(1.25;6.65)	3.36(1.4;16.31)	0.801	0.684	0.981	0.712
PC33:1	1.75(0.93;3.19)	1.32(0.61;3.17)	1.39(0.62;2.06)	0.18	0.165	0.319	0.684
PC33:2	2.03(0.73;3.67)	1.24(0.61;4.2)	1.47(0.64;2.34)	0.09	0.165	0.077	0.981
PC33:3	1.13(0.39;1.82)	0.58(0.12;1.67)	0.52(0.1;1.21)	**0.006**	**0.034**	**0.006**	0.727
PC34:0	1.9(0.71;5.27)	1.63(0.76;3.17)	1.65(0.52;2.76)	0.224	0.588	0.191	0.478
PC34:1	41.31(25.94;68.86)	42.27(31.18;54.57)	40.38(28.98;77.09)	0.925	0.899	0.988	0.782
PC34:2	89.72(63.08;125.35)	67.85(41.41;118.33)	72.72(51.35;103.41)	**0.017**	**0.02**	0.055	0.584
PC34:3	3.88(1.79;6.97)	2.96(1.31;4.86)	3.1(1.4;6.87)	0.065	**0.034**	0.225	0.646
PC35:1	0.94(0.35;2.86)	0.98(0.17;2.24)	0.91(0.16;1.94)	0.925	0.889	0.864	0.839
PC35:2	3.27(1.13;4.91)	1.95(0.8;4.72)	2(0.94;3.22)	**0.017**	**0.034**	**0.018**	0.94
PC35:3	1.6(0.72;3.83)	1.36(0.26;3.89)	1.12(0.55;2.41)	0.08	0.287	**0.041**	0.531
PC35:4	3.86(1.94;6.05)	3.63(1.78;5.95)	2.79(1.8;5.69)	0.117	0.773	0.098	0.225
PC35:5	2.28(1.11;4.27)	1.93(0.85;3.9)	1.29(0.6;2.92)	**0.017**	0.588	**0.018**	0.082
PC36:0	0.88(0.01;2.89)	0.92(0.3;1.86)	0.74(0.1;2.19)	0.602	0.932	0.655	0.452
PC36:1	9.7(4.82;14.36)	9.65(6.57;13.37)	9.1(5.08;14.71)	0.85	0.973	0.891	0.632
PC36:2	50.04(32.26;61.68)	39.02(27.79;68.61)	39.06(26.51;59.23)	0.05	0.069	0.069	0.839
PC36:3	29.43(21.28;41)	26.97(21.85;35.76)	25.53(11.36;38.17)	0.08	0.398	0.055	0.277
PC 36:4	37.34(26.62;48.68)	39.54(26.68;62.18)	34.57(23.75;63.54)	0.117	0.225	0.588	0.104
PC36:5	5.27(2.32;8.19)	4.05(2.18;7.56)	4.09(2.28;7.74)	0.237	0.187	0.389	1,000
PC37:4	3.13(1.05;5.35)	2.99(1.34;5.1)	2.46(1.63;3.62)	0.161	0.973	0.165	0.225
PC37:5	4.53(2.75;6.06)	4.17(2.26;7.5)	3.53(1.77;5.73)	0.097	0.741	0.077	0.225
PC37:6	1.76(0.88;3.43)	1.43(0.48;3.07)	1.24(0.52;2.06)	0.08	0.135	0.077	0.756
PC38:3	9.38(6.1;11.56)	9.16(5.21;13.46)	9.01(3.25;15.84)	0.734	0.981	0.632	0.632
PC38:4	19.81(15.07;28.34)	27.63(18.22;45.91)	22.17(16.37;34.65)	**0.017**	**0.018**	0.513	0.077
PC38:5	12.73(7.96;16.28)	12.04(8.34;17.89)	10.88(7.77;16.68)	0.216	0.891	0.243	0.225
PC38:6	13.2(8.41;18.6)	11.65(8.01;21.29)	9.9(6.88;26.09)	0.148	0.839	0.135	0.225
PC40:5	2.27(1;3.92)	2.56(1.56;4.95)	2.12(1.13;3.44)	0.161	0.225	0.769	0.17
PC40:6	4.47(2.33;7.14)	5.16(2.56;9.32)	3.95(1.82;8.92)	0.08	0.225	0.398	0.074
Total PC	363.76(263.24;449.86)	345.86(264.94;479)	308.13(261.08;463.72)	0.09	0.398	0.077	0.225
LPC16:0	2.99(1.83;4.08)	3(1.2;6.04)	2.81(1.44;6.67)	0.976	0.988	0.889	0.973
LPC18:0	2.76(1.87;3.61)	2.51(1.34;4.84)	2.5(1.31;4.38)	0.215	0.398	0.191	0.531

(Continued)

LPC18:1	2.39(1.05;3.6)	2.23(1.1;4.06)	1.75(0.95;4.84)	0.571	0.805	0.531	0.484
LPC18:2	2.51(1.29;3.79)	2.28(1.03;3.97)	1.73(0.93;5.96)	0.25	0.389	0.227	0.655
Total LPC	10.45(6.72;14.33)	10.41(4.78;17.89)	8.46(5.24;21.85)	0.602	0.773	0.465	0.698
SM32:1	1.15(0.66;2.04)	1.04(0.67;1.81)	1.1(0.68;1.37)	0.589	0.52	0.52	0.889
SM34:0	1.24(0.63;1.85)	0.98(0.71;2.14)	1.1(0.7;1.46)	0.09	0.077	0.165	0.769
SM34:1	11.66(7.48;24.87)	10.5(3.83;25.03)	8.88(2.86;16.96)	0.098	0.329	0.069	0.601
SM34:2	1.37(0.38;2.08)	1.24(0.61;2.63)	1.09(0.78;1.94)	0.381	0.82	0.269	0.531
SM36:1	2.69(1.8;4.8)	2.56(1.26;5.92)	3.21(1.31;6.71)	0.602	0.797	0.632	0.517
SM36:2	1.24(0.75;1.86)	1.12(0.62;1.85)	1.15(0.86;2.27)	0.425	0.345	0.822	0.509
SM38:1	3.31(1.35;5.87)	2.72(1.33;4.78)	2.64(0.97;4.92)	0.301	0.269	0.355	0.94
SM39:1	1.28(0.59;2.28)	0.96(0.66;2.11)	1.04(0.73;1.53)	0.161	0.186	0.345	0.398
SM39:2	0.57(0.36;0.92)	0.75(0.35;0.96)	0.79(0.38;1.02)	0.237	0.496	0.165	0.839
SM40:1	6.09(4.18;8.69)	5.25(2.21;9.36)	5.02(2.55;8.13)	0.161	0.269	0.118	0.887
SM40:2	4.86(2.03;7.51)	4.35(1.79;7.13)	3.79(1.87;6.58)	0.25	0.52	0.225	0.571
SM41:1	2.58(1.29;4.85)	2(0.87;3.99)	1.94(0.65;4.06)	0.134	0.287	0.077	0.839
SM41:2	2.11(0.99;4.04)	1.76(1.04;3.65)	1.89(0.99;4.28)	0.216	0.181	0.382	0.782
SM42:1	4.16(1.76;5.74)	3.16(1.36;8.21)	2.77(1.45;4.78)	**0.017**	0.098	**0.018**	0.464
SM42:2	10.88(6.42;16.46)	9.4(3.91;18.8)	9.46(4.84;16.72)	0.224	0.225	0.269	0.972
SM42:3	4.87(2.49;7.2)	4.37(1.63;8.15)	3.89(2.27;8.12)	0.625	0.899	0.57	0.562
Total SM	57.54(38.5;95.38)	52.17(26.25;100.43)	50.58(26.13;85.67)	0.148	0.282	0.098	0.805
Chol. in HDL	414,99(198,44;780,65)	343,2(129,74;745,55)	288,97(140,45;574,62)	0.064	0.225	**0.034**	0.415

Lipids, pmol/mg of HDL	**Healthy subjects (n=22)**	**CAD (n=23)**	**ACS (n=22)**	**Kruskal-Wallis Test, adj. *p* values**	**Mann-Whitney Test, adj. *p* values**		
					H vs CAD	**H vs ACS**	**CAD vs ACS**
16:1-S1P	26.7(10.83;54.26)	19.84(8.69;42.62)	17.65(9.78;32.86)	0.09	0.222	0.077	0.632
18:1-S1P	86.04(47.43;146.69)	71.07(41.87;173.85)	76.1(40.61;124.02)	0.184	0.187	0.243	0.891
18:2-S1P	17.65(8.75;55.65)	13.94(8.98;34.97)	16.14(8.81;29.35)	0.436	0.345	0.524	0.839
Total S1P	123.5(67.3;256.5)	100.1(60.1;238.9)	116.8(60.5;171.1)	0.161	0.175	0.225	0.981

Data represent medians (with ranges). To estimate the serum levels of HDL-associated lipids, the protein-normalized amount of lipid species were divided by the protein-normalized amount of cholesterol measured in isolated HDL and multiplied with the HDL-C concentration measured in serum by the homogenous clinical assay. Of note, all PC lipids identified as odd-chain PC species probably represent PC plasmalogens. Statistical significance was determined by using the Kruskal-Wallis test for multiple group comparisons and the Mann-Whitney U test for two group comparisons. The *p* values were adjusted for multiple testing by using the Benjamini-Hochberg procedure. Significant *p* values are marked in bold font. ACS stands for acute coronary syndrome; CAD, coronary artery disease; H, healthy subjects; LPC, lysophosphatidylcholine; PC, phosphatidylcholine; SM, sphingomyelin; 16:1-S1P, sphingosine-1-phosphate with 16:1 sphingoid base; 18:1-S1P, sphingosine-1-phosphate with 18:1 sphingoid base; 18:2-S1P, sphingosine-1-phosphate with 18:2 sphingoid base.

3.3.4. Associations of anti-apoptotic activity of HDL with CAD and HDL lipids

The anti-apoptotic activity of HDL was evaluated by measuring the apoptosis of ECs in the presence of HDL, while cell death was induced by serum and growth factor deprivation. Consistent with previous data [4], HDL from CAD patients was less effective in inhibiting EC apoptosis (p = 0.0005) as compared to HDL from healthy subjects (Fig. 1). However, HDL from ACS patients and healthy individuals did not differ by their anti-apoptotic activities (Fig. 1).

We revealed negative correlations of EC apoptosis in the presence of HDL with several lipid components of HDL: SM42:2 (Spearman coefficient r = -0.49, adj. p = 0.019), PC33:3 (r = -0.45; adj. p = 0.029), 18:1-S1P (r = -0.43; adj. p = 0.035), and PC34:2 (r = -0.42; adj. p = 0.035), PC33:1 (r = -0.397; adj. p = 0.036), PC35:1 (r = -0.39; adj. p = 0.036), PC35:2 (r = -0.39; adj. p = 0.036), PC37:6 (r = -0.39; adj. p = 0.036) as well as PC32:0 (r = -0.38; adj. p = 0.036) and 18:2-S1P (r = -0.38; adj. p = 0.036) (Table 4). Upon multiple regression analysis entering into the model seven lipids with the strongest association with EC apoptosis, i.e. SM42:2, PC33:3, 18:1-S1P, PC34:2, PC33:1, PC35:1 and PC35:2, none of them evolved as an independent determinant of HDL's anti-apoptotic activity (adjusted R square = 0.22; F = 2.97; p = 0.013). The contribution of each lipid species to the model is shown in the Table 5.

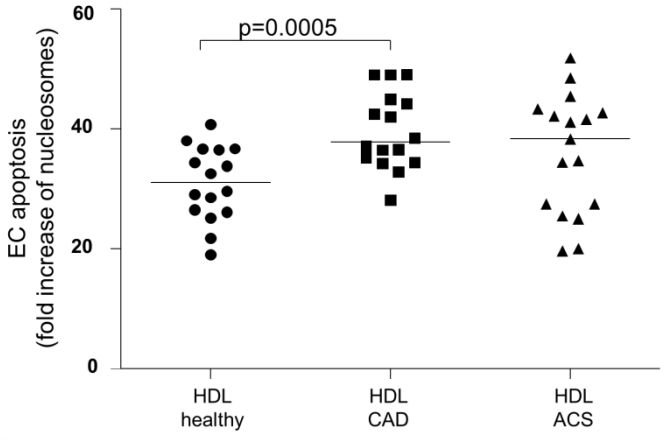

Figure 1. Association of CAD status with endothelial cell apoptosis in the presence of HDL.

Data show the impact of 100 µg/ml HDL from 16 healthy subjects, 16 CAD patients and 17 ACS patients on endothelial cell (EC) apoptosis. EC apoptosis was induced by serum and growth factor deprivation and determined by measuring nucleosomes in the lysate of ECs. Presented are fold increases over the basal level of apoptosis without cell death induction. Solid lines indicate median values. Since data were not normally distributed, p values were calculated by using the Mann-Whitney U test. ACS indicates acute coronary syndrome; CAD, coronary artery disease.

Table 4. Spearman correlations of endothelial cell apoptosis in the presence of HDL with HDL-associated phospholipids.

Lipids	EC apoptosis (fold increase of nucleosomes)	
	Spearman r	adj. *p* values
PC32:0	**-0.38**	**0.036**
PC32:1	-0.21	0.285
PC33:1	**-0.4**	**0.036**
PC33:2	-0.36	0.051
PC33:3	**-0.45**	**0.029**
PC34:0	-0.22	0.285
PC34:1	-0.31	0.101
PC34:2	**-0.42**	**0.035**
PC34:3	-0.34	0.062
PC35:1	**-0.39**	**0.036**
PC35:2	**-0.39**	**0.036**
PC35:3	-0.15	0.439
PC35:4	-0.14	0.446
PC35:5	0.02	0.888
PC36:0	-0.06	0.803
PC36:1	-0.23	0.28
PC36:2	-0.35	0.057
PC36:3	-0.15	0.439
PC36:4	-0.05	0.839
PC36:5	0.04	0.849
PC37:4	-0.26	0.189
PC37:5	-0.22	0.28
PC37:6	**-0.39**	**0.036**
PC38:3	0.11	0.531
PC38:4	0.12	0.518
PC38:5	-0.04	0.849
PC38:6	-0.18	0.357
PC40:5	0.04	0.849
PC40:6	0.03	0.849

Lipids	EC apoptosis (fold increase of nucleosomes)	
	Spearman r	adj. *p* values
LPC16:0	-0.18	0.347
LPC18:0	-0.16	0.437
LPC18:1	-0.2	0.302
LPC18:2	-0.14	0.445
SM32:1	-0.12	0.525
SM34:0	-0.36	0.051
SM34:1	-0.3	0.102
SM34:2	0.19	0.347
SM36:1	-0.28	0.135
SM36:2	-0.21	0.285
SM38:1	-0.19	0.347
SM39:1	-0.33	0.075
SM39:2	-0.03	0.849
SM40:1	-0.05	0.831
SM40:2	-0.14	0.445
SM41:1	-0.32	0.088
SM41:2	-0.21	0.285
SM42:1	-0.26	0.189
SM42:2	**-0.49**	**0.019**
SM42:3	-0.15	0.439
16:1-S1P	-0.16	0.416
18:1-S1P	**-0.43**	**0.035**
18:2-S1P	**-0.38**	**0.036**

Adj. *p* values display Benjamini-Hochberg corrected *p* values. Bold font indicates $p < 0.05$. 16:1-S1P represents sphingosine-1-phosphate with 16:1 sphingoid base; 18:1-S1P, sphingosine-1-phosphate with 18:1 sphingoid base; 18:2-S1P, sphingosine-1-phosphate with 18:2 sphingoid base, LPC, lysophosphatidylcholine; PC, phosphatidylcholine; SM, sphingomyelin.

Table 5. Multiple regression analysis of HDL-associated phospholipids and endothelial cell apoptosis in the presence of HDL.

Determinant variables	Dependent variable, EC apoptosis	
	Standardized coefficients, Beta	*p* values
PC33:3	-0.223	0.291
PC34:2	0.051	0.813
SM42:2	-0.207	0.265
PC33:1	-0.255	0.193
PC35:1	-0.246	0.125
PC35:2	0.175	0.395
18:1-S1P	-0.013	0.955

Seven phospholipids showing the strongest correlation with EC apoptosis in the presence of HDL (see Table 4) were entered into the model.

3.3.5. An orthogonal partial least square - discriminant analysis (OPLS-DA)

Due to the highly correlative nature of lipid data, an orthogonal partial least square - discriminant analysis (OPLS-DA) was applied to identify parameters that associate with stable or acute CAD. The data matrix contained values of 53 individual lipid species of HDL including HDL cholesterol as well as EC apoptosis in the presence of HDL. Fig. 2 shows the results of the OPLS-DA. After reducing the dimensions of the data to the principle components, OPLS-DA models Healthy vs CAD and Healthy vs ACS showed good fit (R2Y) and predictive power (Q2Y) (Table 6). In contrary, the OPLS-DA analysis of the CAD vs ACS samples led to an insignificant model (Table 6).

The score plot of the Healthy vs CAD model (Fig. 2A) showed complete separation of the healthy and CAD samples localized in the right and left part of the ellipse, respectively. The variable importance for the projection (VIP) plot shows the contribution of each variable to the model. Only variables with coefficient value VIP and confidence intervals not crossing 1 are considered as significant contributors to the model. According to the VIP plot of the Healthy vs CAD model (Fig. 2B), EC apoptosis, PC34:2, PC33:3 and PC35:2 contribute significantly to the CAD state model.

The score plot of the Healthy vs ACD model (Fig. 2C) revealed clustering into separate groups of the healthy and ACS samples with a minor overlap at the middle of ellipse. The VIP plot (Fig. 2E) showed that PC33:3, PC35:2, SM42:1, PC34:2 and PC36:2 made significant contributions to the ACS state model.

In summary, the OPLS-DA analysis highlighted that some HDL phospholipid species as well as the anti-apoptotic activity of HDL associate with stable CAD and/or ACS

independently of other lipid parameters. PC33:3, PC34:2 and PC35:2 were the only variables which discriminated HDL of healthy subjects from both patients with stable CAD and patients with ACS.

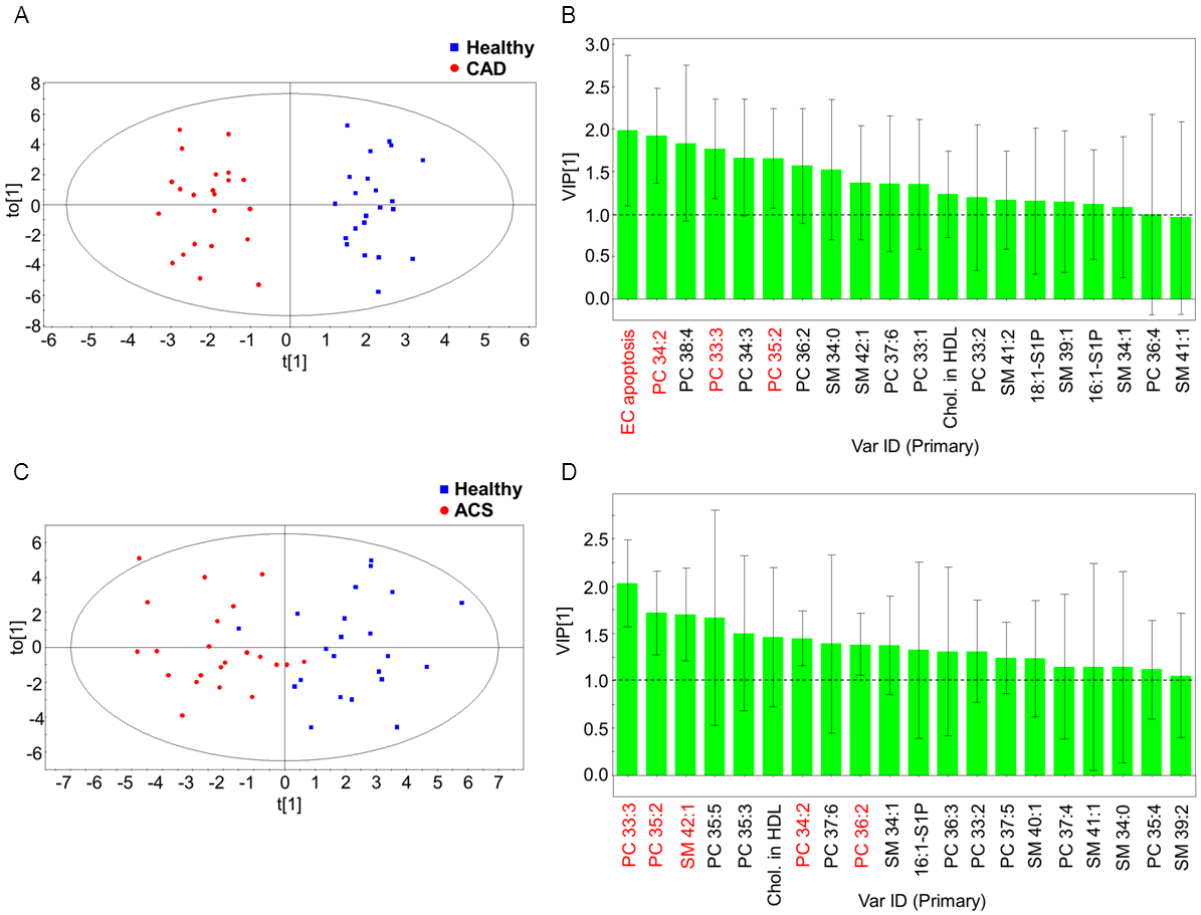

Figure 2. An orthogonal partial least square-discriminant analysis on HDL lipids and the anti-apoptotic capacity of HDL from healthy subjects, CAD and ACS patients.
Figures 2A and 2C display **s**core plots of Healthy vs CAD and Healthy vs ACS models, respectively. Individual observations are shown as: blue squares, healthy subjects; red dots, CAD or ACS patients. The data matrix contained values of 53 individual lipid species of HDL, total cholesterol in HDL and EC apoptosis in the presence of HDL. Variations on the x-axis reflect between-group separation, while variations on the y-axis reflect within-group variation. Figures 2B and 2D show variable importance of the projection (VIP) plots of Healthy vs CAD and Healthy vs ACS models, respectively. VIP plot indicates which variables are important in explaining both the X- and Y-data. Error bars show 95% confidence intervals (CIs) for the calculated VIP coefficients. Variables with VIP values exceeding 1.0 are important contributors to the model, whereas contribution of the variables with their 95% CI exceeding 1.0 should be interpreted with caution. Variable cut off is shown as dash line in the VIP plot. Only first twenty variables are shown in the VIP plot. Important discriminative variables are depicted in red. ACS indicates acute coronary syndrome; CAD, coronary artery disease; S1P, sphingosine-1-phosphate; EC apoptosis, endothelial cell apoptosis in the presence of HDL; Chol. in HDL, cholesterol determined in isolated HDL; LPC, lysophosphatidylcholine; PC, phosphatidylcholine; SM, sphingomyelin.

Table 6. Evaluation of the orthogonal partial least square-discriminate analysis (OPLS-DA) models.

Model	R2X	R2Y	Q2Y	CV-ANOVA F values	CV-ANOVA *p* values
Healthy vs CAD	0.59	0.916	0.62	5.2	0.0001
Healthy vs ACS	0.4	0.683	0.417	6.9	0.0002
CAD vs ACS	0.45	0.653	0.178	1.29	0.2857

OPLS-DA models were fitted for the classes to get the highest R^2Y and Q^2Y values. R^2X, R^2Y and Q^2Y represent amount of explained X-variation, Y-variation and predicted Y-variation. Cross validation is evaluated using CV-ANOVA *p* value, which represents significance of the predicted Y-variation for the given F value. ACS indicates acute coronary syndrome; CAD, coronary artery disease.

3.4. Discussion

Despite the inverse association of HDL-C levels and cardiovascular risk and despite many anti-atherogenic functions of HDL, it has been proven difficult to successfully reduce risk of CAD with drugs increasing HDL-C such as fibrates, niacin, or inhibitors of cholesteryl ester transfer protein. Because of these controversial data, the pathogenic role and, thus, suitability of HDL as a therapeutic target has been increasingly questioned. However, HDLs form a very heterogeneous class of lipoproteins which differ by protein and lipid composition and, hence, functionality which is not recovered by the measurement of the routine clinical parameter "HDL-cholesterol" (= HDL-C) [2]. In fact, HDL isolated from plasmas of patients with CAD and other inflammatory diseases were found to have diminished atheroprotective properties in several bioassays. As yet, the search for the underlying disturbed structure-function-relationships was focused on compositional and structural modifications of HDL-associated proteins. The contribution of alterations in the lipidome of HDL to physiological function and pathological dysfunction of HDL as well as disease association has only started to be explored. In this cross-sectional case-control study we used a combination of a hypothesis-free lipidomics approach and a hypothesis-driven candidate approach to investigate the triangular relationship of HDL-associated phospholipids, anti-apoptotic capacity of HDL (i.e. EC apoptosis in the presence of HDL) and presence of acute or stable CAD. Two *apriori* undefined plasmalogens – PC33:3 and PC35:2 – as well as PC34:2 – showed the most consistent relationships with both CAD and the capacity of HDL to inhibit apoptosis of ECs. Furthermore, two SMs – SM42:1 and SM42:2 – showed significant associations with ACS and EC apoptosis, respectively. By contrast, S1P which was pre-

defined as a candidate because of its well established anti-apoptotic activity, did not show any association with CAD phenotype although it correlated with the anti-apoptotic activity of HDL as much as the plasmalogens and SM42:2.

PC33:3 and PC35:2 were equally decreased by 50% and 30%, respectively, in HDL of patients with either acute ACS or chronic CAD and remained significantly associated with ACS and CAD upon multivariate OPLS-DA analysis. The statistical significance and independence, the more strongly decreased concentrations of plasmalogens relative to total PC, and the lack of difference between HDL of acute and stable CAD patients indicate that the deprivation of HDL in plasmalogens is a specific feature of HDL from CAD patients. Our observation is in line with those of other researchers: two studies found that HDL of patients with low HDL-C contain significantly less PC- and/or PE-derived plasmalogens when compared to HDL of patients with high HDL-C [37, 38]. The content of PE plasmalogens was also found to be lower in acute-phase HDL than in non-inflammatory HDL [39]. Furthermore, different species of PE- or PC-plasmalogens were found at reduced serum or plasma concentrations in hypertensive [40], obese [41], stable and unstable CAD patients [42].

Interestingly both PC33:3 and PC35:2 also showed significant positive correlations with the ability of HDL to prevent apoptosis of ECs. As yet a direct anti-apoptotic effect of extracellular plasmalogens has only been demonstrated for the neuronal cell line Neuro-2A [43]. Moreover, disturbed formation of plasmalogens in cells with peroxisomal dysfunction was found to be associated with increased apoptosis [44]. Thus, the significant correlations between specific plasmalogens and the anti-apoptotic activity of HDL may point to a direct causal relationship. For example, plasmalogens are known to scavenge oxygen radicals with their vinyl-ether bound of alkenyl chain [17] and to reduce the oxidation of cholesterol by free radicals [18] and to delay the oxidative degradation of polyunsaturated fatty acids [20] and LDL [19]. If exerted on plasma membranes, HDL-associated plasmalogens may exhibit direct cytoprotective effects. If happening within HDL, plasmalogens may prevent the formation of pro-apoptotic agonists or help to maintain the anti-apoptotic properties of other HDL-associated anti-apoptotic agonists. The demonstration of any direct anti-apoptotic or other anti-atherogenic activities of plasmalogens will raise the question of whether also the inverse association between plasmalogen content of HDL and CAD reflects a causal relationship. However, low plasmalogen levels may also be the result of enhanced oxidative degradation caused by reactive oxygen species and increased oxidative stress in CAD and ACS patients. Of note myeloperoxidase which is present in plasma and atheroma of CAD patients at increased concentration and generates dysfunctional HDL by multiple protein modifications

[45, 46] was previously demonstrated to generate α-chlorofatty aldehydes from plasmalogens [47]. Thus, the decreased concentration of plasmalogens in HDL of CAD patients may reflect enhanced plasmalogen degradation by myeloperoxidase or other oxidative processes. This process may generate pro-apoptotic derivatives of plasmalogens such as α-chlorofatty aldehydes or acids which counteract the anti-apoptotic activity of HDL. Alternatively the myeloperoxidase mediated modification of plasmalogens is only an innocent bystander and reporter of other causative protein and lipid modifications exerted by myeloperoxidase in HDL.

Like two plasmalogens and unlike all other even-chain PC species or total PC, PC34:2 showed significant and independent associations with both CAD and ACS. Furthermore, PC34:2 significantly correlated with the anti-apoptotic activity of HDL . With a proportion of about 25% PC34:2 constitutes the majority of HDL-associated PC's as compared to only 1% constituted by PC33:3 and PC35:2. Also other studies found PC34:2 to be the quantitatively predominant PC species of lipoproteins including HDL[48]. Yetukuri and colleagues showed that HDL-associated PC34:2 comprises only one molecular species, namely PC(16:0/18:2) [38]. Interestingly, PC(16:0/18:2) but not other PCs present in HDL was found to mimic the inhibitory effect of HDL on the Th1 function of mature dendritic cells [49]. Artificially reconstituted HDL (rHDL) containing apoA-I and PC(16:0/18:2) were found more effective than rHDL containing saturated or mono-unsaturated PCs in inhibiting endothelial expression of VCAM1 or inhibiting NADPH oxidase activation in neutrophils [11, 50, 51]. Moreover, in the presence of cholesteryl ester transfer protein (CETP), rHDL containing PC(16:0/18:2) but not rHDL containing PC(16:0/18:1) released prebeta1-HDL, an important stimulator of cholesterol efflux [52]. A recent lipidomic analysis of HDL by NMR spectroscopy revealed low contents of total PC in HDL as independently associated with CAD in a case-control study [53]. As discussed for plasmalogens before, the associations of PC34:2 with CAD as well as the correlation with EC apoptosis do not allow any conclusion on causality: the reduced HDL content in CAD patients in combination with the significant correlation with the anti-apoptotic activity of HDL may directly reflect anti-atherogenic effects of PC34:2. However, it may also be an indirect reporter of oxidative and enzymatic activities which affect the functionality of HDL beyond the modification of the specific PCs and may even exert pro-atherogenic effects independently of HDL [10, 54].

The SM42:1 showed a strong and independent association with ACS. Its average concentration in HDL was 35% lower in ACS patients than in healthy controls. Of note, neither total SM nor any other SM species showed any association with CAD. As yet only

data on associations of CAD with total SM levels in HDL have been reported. Two cross-sectional studies quantified total SM in HDL by the use of either NMR spectroscopy or an enzymatic test found inverse associations between HDL content of SM and the presence and extent of CAD [53, 55]. Since only the association of SM42:1 with ACS was statistically significant and independent and because SM42:1 did not show any significant correlation with the anti-apoptotic activity of HDL, the decreased SM42:1 levels may be the result rather than the cause of CAD. In fact, Pruzanski and colleagues previously reported that acute phase depletes HDL of some SM species, specifically SM33:1 and SM38:1 [39]. Although less prominent, also SM42:1 was present at reduced concentrations in acute-phase HDL [39].

Several cytoprotective functions of HDL including inhibition of EC apoptosis have been assigned to S1P which signals to a variety of cells upon interaction with at least five different G-protein coupled S1P receptors [21, 22]. At least one half of S1P in plasma is transported by HDL [22, 56, 57]. We therefore complemented the general phospholipid profiling approach by targeted quantification of S1P to test whether the anti-apoptotic activity of HDL-associated S1P is reflected by significant correlations and associations with the anti-apoptotic activity of HDL and the presence of CAD, respectively. Rather than total S1P we quantified S1P species which differ by the chain length and desaturation of the sphingoid bases [24]. As yet little appreciated structural variety of the S1P chain length (and sphingolipids in general) results from the promiscuous substrate use of serine:palmitoyltransferase (SPT) [26]. This enzyme catalyses the first step in sphingolipid synthesis and uses acyl-CoAs beyond its canonical substrate palmitoyl (C16:0)-CoA. In fact, in our hands only 70% of HDL associated S1P corresponds to 18:1-S1P, which is the canonical metabolite. About 20% and 10% of HDL-associated S1P are the non-canonical 16:1-S1P and 18:2-S1P, respectively. Whereas 16:1-S1P is formed on a sphingoid base that results from the SPT-mediated condensation of serine with myristoyl (C14:0)-CoA[26], 18:2-S1P is probably formed on a sphingadiene (d18:2) backbone with a second double bond at presumably delta position [58, 59]. Interestingly, only 18:1-S1P and 18:2-S1P but not 16:1-S1P correlated significantly with the anti-apoptotic activity of HDL indicating that the carbon chain length affects the biological activity of S1P species. By contrast to the plasmalogens, this correlation is not translated into significant association of S1P species with the presence of stable CAD or ACS. At first sight this lack of association is in contrast to the findings of two previous studies which reported that S1P levels of HDL are associated with the presence, extent, or incidence of CAD [60-62]. However, Sattler and colleagues recovered S1P of plasma from healthy individuals almost completely in HDL [61, 62] which is in sharp contrast to the observations of several other labs which found

about 30% and 10% of plasma S1P associated with albumin and apoB containing lipoproteins, respectively [22, 56, 57]. Furthermore, measurements of S1P in these studies were performed by HPLC coupled with fluorescence detection which does not discriminate the different S1P species. In addition, the nested case-control study of Argraves and colleagues measured S1P after precipitation of apoB containing lipoproteins and hence did not separate HDL- and albumin-associated S1P [60]. These differences in magnitude of concentration and methodology interfere with any interpretation of reasons for the different findings in our and the other studies.

In conclusion, our cross-sectional case-control study unravelled significant associations and correlations of specific phospholipid species with the presence of acute or stable CAD and the capacity of HDL to inhibit apoptosis. The plasmalogens PC33:3 and PC35:2 as well as PC34:2 showed consistent associations and correlations with clinical presentation of CAD as well as anti-apoptotic activity of HDL. This makes them interesting candidates for both clinical validation in larger studies and functional characterization *in vitro*, to assess their importance as biomarkers for CAD risk prediction and determinants of HDL functionality, respectively.

Acknowledgments and sources of funding

We gratefully acknowledge the patient care of Maja Müller. This work was financed by grants from Zurich Center of Integrated Human Physiology, University of Zurich (ZIHP) and the 7th Framework Program of the European Commission ("RESOLVE", Project number 305707). Arnold von Eckardstein and Ulf Landmesser are members of the COST action "HDLnet" (BM904).

References

1. Di Angelantonio E, Sarwar N, Perry P, et al. Major lipids, apolipoproteins, and risk of vascular disease. *JAMA* 2009;302:1993-2000.

2. Annema W, von Eckardstein A. High-density lipoproteins. Multifunctional but vulnerable protections from atherosclerosis. *Circulation journal : official journal of the Japanese Circulation Society* 2013;77:2432-2448.

3. Luscher TF, Landmesser U, von Eckardstein A, Fogelman AM. High-density lipoprotein: vascular protective effects, dysfunction, and potential as therapeutic target. *Circulation research* 2014;114:171-182.

4. Riwanto M, Rohrer L, Roschitzki B, et al. Altered activation of endothelial anti- and proapoptotic pathways by high-density lipoprotein from patients with coronary artery disease: role of high-density lipoprotein-proteome remodeling. *Circulation* 2013;127:891-904.

5. Alwaili K, Bailey D, Awan Z, et al. The HDL proteome in acute coronary syndromes shifts to an inflammatory profile. *Biochimica et biophysica acta* 2012;1821:405-415.

6. Vaisar T, Mayer P, Nilsson E, Zhao XQ, Knopp R, Prazen BJ. HDL in humans with cardiovascular disease exhibits a proteomic signature. *Clinica chimica acta; international journal of clinical chemistry* 2010;411:972-979.

7. Kontush A, Lhomme M, Chapman MJ. Unraveling the complexities of the HDL lipidome. *Journal of lipid research* 2013;54:2950-2963.

8. Davidson WS, Gillotte KL, Lund-Katz S, Johnson WJ, Rothblat GH, Phillips MC. The effect of high density lipoprotein phospholipid acyl chain composition on the efflux of cellular free cholesterol. *The Journal of biological chemistry* 1995;270:5882-5890.

9. Rye KA, Hime NJ, Barter PJ. The influence of sphingomyelin on the structure and function of reconstituted high density lipoproteins. *The Journal of biological chemistry* 1996;271:4243-4250.

10. Zerrad-Saadi A, Therond P, Chantepie S, et al. HDL3-mediated inactivation of LDL-associated phospholipid hydroperoxides is determined by the redox status of apolipoprotein A-I and HDL particle surface lipid rigidity: relevance to inflammation and atherogenesis. *Arteriosclerosis, thrombosis, and vascular biology* 2009;29:2169-2175.

11. Baker PW, Rye KA, Gamble JR, Vadas MA, Barter PJ. Phospholipid composition of reconstituted high density lipoproteins influences their ability to inhibit endothelial cell adhesion molecule expression. *Journal of lipid research* 2000;41:1261-1267.

12. Ibdah JA, Lund-Katz S, Phillips MC. Molecular packing of high-density and low-density lipoprotein surface lipids and apolipoprotein A-I binding. *Biochemistry* 1989;28:1126-1133.

13. Parks JS, Huggins KW, Gebre AK, Burleson ER. Phosphatidylcholine fluidity and structure affect lecithin:cholesterol acyltransferase activity. *Journal of lipid research* 2000;41:546-553.

14. Subbaiah PV, Liu M. Role of sphingomyelin in the regulation of cholesterol esterification in the plasma lipoproteins. Inhibition of lecithin-cholesterol acyltransferase reaction. *The Journal of biological chemistry* 1993;268:20156-20163.

15. Piperi C, Kalofoutis C, Papaevaggeliou D, Papapanagiotou A, Lekakis J, Kalofoutis A. The significance of serum HDL phospholipid levels in angiographically defined coronary artery disease. *Clinical biochemistry* 2004;37:377-381.

16. Hsia SL, Duncan R, Schob AH, et al. Serum levels of high-density lipoprotein phospholipids correlate inversely with severity of angiographically defined coronary artery disease. *Atherosclerosis* 2000;152:469-473.

17. Wallner S, Schmitz G. Plasmalogens the neglected regulatory and scavenging lipid species. *Chemistry and physics of lipids* 2011;164:573-589.

18. Maeba R, Ueta N. Ethanolamine plasmalogens prevent the oxidation of cholesterol by reducing the oxidizability of cholesterol in phospholipid bilayers. *Journal of lipid research* 2003;44:164-171.

19. Jurgens G, Fell A, Ledinski G, Chen Q, Paltauf F. Delay of copper-catalyzed oxidation of low density lipoprotein by in vitro enrichment with choline or ethanolamine plasmalogens. *Chemistry and physics of lipids* 1995;77:25-31.

20. Reiss D, Beyer K, Engelmann B. Delayed oxidative degradation of polyunsaturated diacyl phospholipids in the presence of plasmalogen phospholipids in vitro. *The Biochemical journal* 1997;323 (Pt 3):807-814.

21. Poti F, Simoni M, Nofer JR. Atheroprotective role of high-density lipoprotein (HDL)-associated sphingosine-1-phosphate (S1P). *Cardiovascular research* 2014;103:395-404.

22. Rodriguez C, Gonzalez-Diez M, Badimon L, Martinez-Gonzalez J. Sphingosine-1-phosphate: A bioactive lipid that confers high-density lipoprotein with vasculoprotection mediated by nitric oxide and prostacyclin. *Thrombosis and haemostasis* 2009;101:665-673.

23. Levkau B. Cardiovascular effects of sphingosine-1-phosphate (S1P). *Handbook of experimental pharmacology* 2013;147-170.

24. Quehenberger O, Armando AM, Brown AH, et al. Lipidomics reveals a remarkable diversity of lipids in human plasma. *Journal of lipid research* 2010;51:3299-3305.
25. Narayanaswamy P, Shinde S, Sulc R, et al. Lipidomic "deep profiling": an enhanced workflow to reveal new molecular species of signaling lipids. *Anal Chem* 2014;86:3043-3047.
26. Hornemann T, Penno A, Rutti MF, et al. The SPTLC3 subunit of serine palmitoyltransferase generates short chain sphingoid bases. *The Journal of biological chemistry* 2009;284:26322-26330.
27. Besler C, Heinrich K, Rohrer L, et al. Mechanisms underlying adverse effects of HDL on eNOS-activating pathways in patients with coronary artery disease. *J Clin Invest* 2011;121:2693-2708.
28. Antman EM, Anbe DT, Armstrong PW, et al. ACC/AHA guidelines for the management of patients with ST-elevation myocardial infarction--executive summary: a report of the American College of Cardiology/American Heart Association Task Force on Practice Guidelines (Writing Committee to Revise the 1999 Guidelines for the Management of Patients With Acute Myocardial Infarction). *Circulation* 2004;110:588-636.
29. Anderson JL, Adams CD, Antman EM, et al. ACC/AHA 2007 guidelines for the management of patients with unstable angina/non ST-elevation myocardial infarction: a report of the American College of Cardiology/American Heart Association Task Force on Practice Guidelines (Writing Committee to Revise the 2002 Guidelines for the Management of Patients With Unstable Angina/Non ST-Elevation Myocardial Infarction): developed in collaboration with the American College of Emergency Physicians, the Society for Cardiovascular Angiography and Interventions, and the Society of Thoracic Surgeons: endorsed by the American Association of Cardiovascular and Pulmonary Rehabilitation and the Society for Academic Emergency Medicine. *Circulation* 2007;116:e148-304.
30. Sorrentino SA, Besler C, Rohrer L, et al. Endothelial-vasoprotective effects of high-density lipoprotein are impaired in patients with type 2 diabetes mellitus but are improved after extended-release niacin therapy. *Circulation* 2010;121:110-122.
31. Oczos J, Sutter, I., Kloeckener-Gruissem, B., Berger, W., Riwanto, M., Rentsch, K., Hornemann, T., von Eckardstein, A., Grimm, C. . Lack of paraoxonase-1 alters phospholipid composition but nhot morphology and function of the mouse retina. . *Invest Ophthalmol Vis Sci* 2014; in press
32. Sutter I, Park R, Othman A, et al. Apolipoprotein M modulates erythrocyte efflux and tubular reabsorption of sphingosine-1-phosphate. *Journal of lipid research* 2014;55:1730-1737.

33. Scherer M, Bottcher A, Schmitz G, Liebisch G. Sphingolipid profiling of human plasma and FPLC-separated lipoprotein fractions by hydrophilic interaction chromatography tandem mass spectrometry. *Biochimica et biophysica acta* 2011;1811:68-75.

34. Othman A, Rutti MF, Ernst D, et al. Plasma deoxysphingolipids: a novel class of biomarkers for the metabolic syndrome? *Diabetologia* 2012;55:421-431.

35. Yekutieli D, Benjamini Y. Resampling-based false discovery rate controlling multiple test procedures for correlated test statistics. *J Stat Plan Infer* 1999;82:171-196.

37. Laurila PP, Surakka I, Sarin AP, et al. Genomic, transcriptomic, and lipidomic profiling highlights the role of inflammation in individuals with low high-density lipoprotein cholesterol. *Arteriosclerosis, thrombosis, and vascular biology* 2013;33:847-857.

38. Yetukuri L, Soderlund S, Koivuniemi A, et al. Composition and lipid spatial distribution of HDL particles in subjects with low and high HDL-cholesterol. *Journal of lipid research* 2010;51:2341-2351.

39. Pruzanski W, Stefanski E, de Beer FC, de Beer MC, Ravandi A, Kuksis A. Comparative analysis of lipid composition of normal and acute-phase high density lipoproteins. *Journal of lipid research* 2000;41:1035-1047.

40. Graessler J, Schwudke D, Schwarz PE, Herzog R, Shevchenko A, Bornstein SR. Top-down lipidomics reveals ether lipid deficiency in blood plasma of hypertensive patients. *PloS one* 2009;4:e6261.

41. Pietilainen KH, Sysi-Aho M, Rissanen A, et al. Acquired obesity is associated with changes in the serum lipidomic profile independent of genetic effects--a monozygotic twin study. *PloS one* 2007;2:e218.

42. Meikle PJ, Wong G, Tsorotes D, et al. Plasma lipidomic analysis of stable and unstable coronary artery disease. *Arteriosclerosis, thrombosis, and vascular biology* 2011;31:2723-2732.

43. Hossain MS, Ifuku M, Take S, Kawamura J, Miake K, Katafuchi T. Plasmalogens rescue neuronal cell death through an activation of AKT and ERK survival signaling. *PloS one* 2013;8:e83508.

44. Brites P, Mooyer PA, El Mrabet L, Waterham HR, Wanders RJ. Plasmalogens participate in very-long-chain fatty acid-induced pathology. *Brain : a journal of neurology* 2009;132:482-492.

45. Huang Y, DiDonato JA, Levison BS, et al. An abundant dysfunctional apolipoprotein A1 in human atheroma. *Nature medicine* 2014;20:193-203.

46. Fisher EA, Feig JE, Hewing B, Hazen SL, Smith JD. High-density lipoprotein function, dysfunction, and reverse cholesterol transport. *Arteriosclerosis, thrombosis, and vascular biology* 2012;32:2813-2820.

47. Wang WY, Albert CJ, Ford DA. Alpha-chlorofatty acid accumulates in activated monocytes and causes apoptosis through reactive oxygen species production and endoplasmic reticulum stress. *Arteriosclerosis, thrombosis, and vascular biology* 2014;34:526-532.

48. Wiesner P, Leidl K, Boettcher A, Schmitz G, Liebisch G. Lipid profiling of FPLC-separated lipoprotein fractions by electrospray ionization tandem mass spectrometry. *Journal of lipid research* 2009;50:574-585.

49. Perrin-Cocon L, Diaz O, Carreras M, et al. High-density lipoprotein phospholipids interfere with dendritic cell Th1 functional maturation. *Immunobiology* 2012;217:91-99.

50. Zhang WJ, Stocker R, McCall MR, Forte TM, Frei B. Lack of inhibitory effect of HDL on TNFalpha-induced adhesion molecule expression in human aortic endothelial cells. *Atherosclerosis* 2002;165:241-249.

51. Peshavariya H, Dusting GJ, Di Bartolo B, Rye KA, Barter PJ, Jiang F. Reconstituted high-density lipoprotein suppresses leukocyte NADPH oxidase activation by disrupting lipid rafts. *Free radical research* 2009;43:772-782.

52. Rye KA, Duong M, Psaltis MK, et al. Evidence that phospholipids play a key role in pre-beta apoA-I formation and high-density lipoprotein remodeling. *Biochemistry* 2002;41:12538-12545.

53. Kostara CE, Papathanasiou A, Psychogios N, et al. NMR-Based Lipidomic Analysis of Blood Lipoproteins Differentiates the Progression of Coronary Heart Disease. *Journal of proteome research* 2014.

54. Duong M, Psaltis M, Rader DJ, Marchadier D, Barter PJ, Rye KA. Evidence that hepatic lipase and endothelial lipase have different substrate specificities for high-density lipoprotein phospholipids. *Biochemistry* 2003;42:13778-13785.

55. Horter MJ, Sondermann S, Reinecke H, et al. Associations of HDL phospholipids and paraoxonase activity with coronary heart disease in postmenopausal women. *Acta physiologica Scandinavica* 2002;176:123-130.

56. Karuna R, Park R, Othman A, et al. Plasma levels of sphingosine-1-phosphate and apolipoprotein M in patients with monogenic disorders of HDL metabolism. *Atherosclerosis* 2011;219:855-863.

57. Christoffersen C, Obinata H, Kumaraswamy SB, et al. Endothelium-protective sphingosine-1-phosphate provided by HDL-associated apolipoprotein M. *Proceedings of the National Academy of Sciences of the United States of America* 2011;108:9613-9618.

58. Renkonen O, Hirvisalo EL. Structure of plasma sphingadienine. *Journal of lipid research* 1969;10:687-693.

59. Panganamala RV, Geer JC, Cornwell DG. Long-chain bases in the sphingolipids of atherosclerotic human aorta. *Journal of lipid research* 1969;10:445-455.

60. Argraves KM, Sethi AA, Gazzolo PJ, et al. S1P, dihydro-S1P and C24:1-ceramide levels in the HDL-containing fraction of serum inversely correlate with occurrence of ischemic heart disease. *Lipids Health Dis* 2011;10.

61. Sattler KJ, Elbasan S, Keul P, et al. Sphingosine 1-phosphate levels in plasma and HDL are altered in coronary artery disease. *Basic research in cardiology* 2010;105:821-832.

62. Sattler K, Lehmann I, Graler M, et al. HDL-bound sphingosine 1-phosphate (S1P) predicts the severity of coronary artery atherosclerosis. *Cellular physiology and biochemistry : international journal of experimental cellular physiology, biochemistry, and pharmacology* 2014;34:172-184.

4. APOLIPOPROTEIN M MODULATES ERYTHROCYTE EFFLUX AND TUBULAR REABSORPTION OF SPHINGOSINE-1-PHOSPHATE

Iryna Sutter[1,2], Rebekka Park[3,4], Alaa Othman[1,4], Lucia Rohrer[1,2], Thorsten Hornemann[1,2], Markus Stoffel[3,4], Olivier Devuyst[2,5], and Arnold von Eckardstein[1,2,4,*]

1. Institute of Clinical Chemistry, University and University Hospital of Zurich, Zurich, Switzerland
2. Competence Center for Integrated Human Physiology, University of Zurich, Zurich, Switzerland
3. Institute of Molecular Health Sciences, ETH Zurich, Zurich, Switzerland
4. Competence Center for Systems Physiology and Metabolic Diseases, ETH Zurich and University of Zurich, Zurich, Switzerland
5. Institute of Physiology, University of Zurich, Zurich, Switzerland

[Journal of Lipid Research 2014; 55: 1730-1737]

Abstract

Sphingosine-1-phosphate (S1P) mediates several cytoprotective functions of HDL. ApoM acts as a specific S1P binding protein in HDL. Erythrocytes are the major source of S1P in plasma. After glomerular filtration, apoM is endocytosed in the proximal renal tubules. Human and murine HDL elicited time- and dose-dependent S1P efflux from erythrocytes. Compared with HDL of wild-type (wt) mice, S1P efflux was enhanced in the presence of HDL from apoM transgenic mice, but not diminished in the presence of HDL from apoM knockout (*Apom*$^{-/-}$) mice. Artificially reconstituted and apoM-free HDL also effectively induced S1P efflux from erythrocytes. S1P and apoM were not measurable in the urine of wt mice. *Apom*$^{-/-}$ mice excreted significant amounts of S1P. ApoM was detected in the urine of mice with defective tubular endocytosis because of knockout of the LDL receptor-related protein, chloride-proton exchanger ClC-5 (*Clcn5*$^{-/-}$), or the cystine transporter cystinosin. Urinary levels of S1P were significantly elevated in *Clcn5*$^{-/-}$ mice. In contrast to *Apom*$^{-/-}$ mice, these mice showed normal plasma concentrations for apoM and S1P. In conclusion**,** HDL facilitates S1P efflux from erythrocytes by both apoM-dependent and apoM-independent mechanisms. Moreover, apoM facilitates tubular reabsorption of S1P from the urine, however, with no impact on S1P plasma concentrations.

Abbreviations:

Apom$^{-/-}$	apoM knockout mice
Apom^{tg}	Mice transgenic for apoM
IS	Internal standard
LRP2	LDL receptor-related protein 2
rHDL	Reconstituted HDL
S1P	Sphingosine-1-phosphate
S1P(Ac)$_2$	Acetylated S1P
TBS-T	TBS Tween
wt	Wild-type

4.1. Introduction

Sphingosine-1-phosphate (S1P) acts both as an intracellular signaling molecule and an extracellular agonist of at least five different G protein-coupled receptors. By its dual functions, S1P regulates the survival, proliferation, and migration as well as the functionality of many cells, eventually in opposite directions [1-4]. Therefore the absolute and relative abundance of S1P in intracellular and extracellular compartments appears to be important for its biological functionality[4].

Most cells form S1P by the phosphorylation of sphingosine, a degradation product of ceramides, through sphingosine kinase and degrade S1P to phosphoethanolamine and fatty aldehyde through S1P-lyase [1-4]. By contrast, not only erythrocytes and platelets, but also other cells which have low or no lyase activity, release S1P [4-6], probably by an as yet unidentified ABC transporter [4, 7, 8]. Within the plasma compartment, the majority of S1P is transported by HDLs in which it exerts many cytoprotective and anti-inflammatory effects, for example, on endothelial cells [8-10]. The enrichment of S1P in HDL has been explained by the presence of a specific S1P binding protein, namely apoM [10]. Purified and recombinant apoM binds S1P with an IC_{50} of 0.9 µmol/l, which is in the range of physiological S1P plasma concentrations [11]. X-ray crystallography of apoM identified an S1P binding domain which was confirmed by the recombinant generation of non-S1P binding apoM mutants [11]. In agreement with these physicochemical data, S1P was copurified with apoM containing HDL, but not apoM-free HDL, from both human and murine plasma. Moreover, S1P concentrations were dramatically decreased in HDL of the apoM knockout (*Apom*$^{-/-}$), but increased in HDL of mice transgenic for apoM (*Apom*^{tg}). As an *in vitro* indication of functional relevance, the stimulatory effects of S1P on nitric oxide production by endothelial cells were mimicked by apoM-containing HDL, but not by apoM-free HDL. Finally, the physiological relevance of S1P binding by apoM was indicated by the reduced basal endothelial barrier function in lungs of *Apom*$^{-/-}$ mice [12]. Despite this very strong *in vitro* and *in vivo* evidence for the limiting effect of apoM on the transport and function of S1P in plasma and HDL, concentrations of S1P and apoM in either plasma or HDL do not correlate with each other [12, 13]. Moreover, stoichiometric calculations revealed that apoM is not saturated with S1P but present at an up to 8-f molar excess [12, 13]. We therefore investigated the impact of apoM on two other potential pathways of S1P metabolism, namely efflux from erythrocytes and urinary excretion.

Plasma concentrations of S1P were recently shown to correlate with red blood cell counts [5, 6, 14], probably because the lack of the S1P-degrading lyase makes erythrocytes the main source of S1P in plasma [4, 5]. Because HDL was previously found to induce S1P efflux

from erythrocytes [5], we compared the S1P efflux capacity of HDL from wild-type (wt), *Apom*$^{-/-}$, and *Apom*^{tg} mice [15].

After glomerular filtration, apoM is reabsorbed from the primary urine into proximal tubular epithelial cells by binding to the endocytic receptor megalin [LDL receptor-related protein 2 (LRP2)]. Accordingly, mice with a conditional renal knockout of megalin excrete apoM in urine [16]. Megalin and its coreceptor cubilin also mediate the tubular reabsorption of several small plasma proteins which carry small molecules and are filtrated through the glomeruli [17, 18]. Not only megalin and cubilin, but also endosomal and lysosomal proteins such as chloride-proton exchanger ClC-5 (mutated in Dent's disease) and the cystine transporter cystinosin (mutated in cystinosis), respectively, are key components of the machinery that rescues essential molecules such as vitamin B12 and vitamin D from inappropriate urinary loss [17, 19, 20]. To test whether this is also of relevance for the metabolism of S1P, we compared the urinary excretion of S1P and apoM in wt and *Apom*$^{-/-}$ mice [15] as well as mice with dysfunctional megalin (*Lrp2*$^{-/-}$) [21], ClC-5 (*Clcn5*$^{-/-}$) [22], or cystinosin (*Ctns*$^{-/-}$) [23].

4.2. Methods

4.2.1. Plasma and urine collection from mice

Mice with knockout of apoM (*Apom*$^{-/-}$) [34] as well as mice with defective expression of megalin (*Lrp2*$^{-/-}$) [21], ClC-5 (*Clcn5*$^{-/-}$) [22], or cystinosin (*Ctns*$^{-/-}$) [23] were previously described. Mice with transgenic overexpression of murine apoM (*Apom*^{tg}) have not been published yet, but the generation of these animals is briefly described in Fig. 1. Blood samples were obtained by cardiac puncture immediately after euthanization. Plasma was prepared by 15 min of centrifugation of blood at 2,000 g. Urine samples were collected in metabolic cages for 8 h (*Clcn5*$^{-/-}$, *Ctns*$^{-/-}$, and their littermate controls), 16 h (*Lrp2*$^{-/-}$ and their littermate controls), or 24 h (*Apom*$^{-/-}$, *Apom*^{tg}, and their littermate controls) according to standard protocols. Each drop of urine was immediately cooled down to -20°C in the collector of the metabolic cages. All plasma and urine samples were kept frozen at -80°C before further use or analysis. The age of the mice, at which samples were obtained, is reported in the Results section. All animal procedures were approved by the appropriate National Research Council Guide for the Care and Use of Laboratory Animals/Animal Ethics Committee.

4.2.2. Generation of transgenic TTR-apoM mice

The murine apoM cDNA was cloned downstream of the liver-specific transthyretin (TTR) promoter within a modified TTR expression plasmid described earlier [35] (Fig. 1).

Transgenic lines were generated following pronuclear microinjection in fertilized mouse eggs (C57B1/6). The genotype was determined by Southern blotting and PCR using the Southern probe and PCR primers indicated in Fig. 1. The Southern probe was amplified by PCR spanning exon 2 of TTR and the apoM cDNA (≈50bp each). PCR primers spanning exon 1 and 2 of apoM were used to distinguish wt litter from apoM transgenic animals.

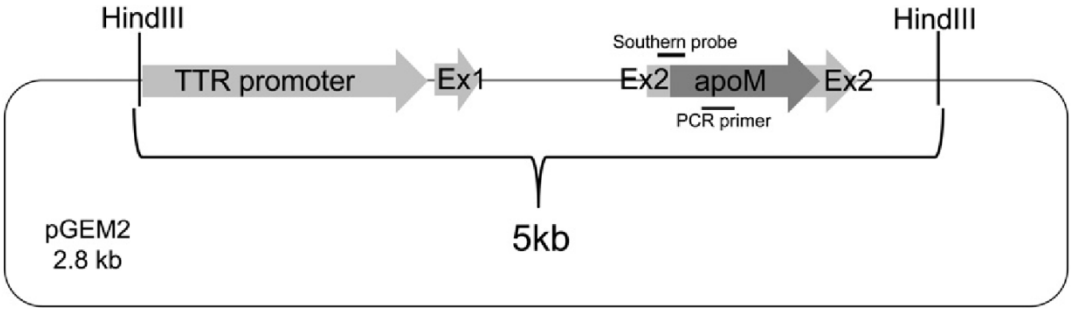

Figure 1. Schematic overview of cloning strategy used to generate *Apom^{tg}* mice.
Murine apoM cDNA was inserted into a modified transthyretin (TTR) expression plasmid described earlier [35] downstream of the TTR promoter. Position of the Southern probe and PCR primers used for genotyping transgenic animals are indicated.

4.2.3. Isolation and reconstitution of HDL

Human HDL was isolated from plasma of healthy blood donors (Kantosspital Schaffhausen, Switzerland) or mouse plasma by stepwise ultracentrifugation (d = 1.063-1.21 kg/l) at 360,000 g for 15 h at 15°C, as described previously [24], using solid potassium bromide (Sigma Aldrich, Buchs, Switzerland) for density adjustment. ApoA-I was further purified from delipidated HDL as described previously [24]. Discoidal reconstituted HDL (rHDL) particles were produced by the cholate dialysis method and contained apoA-I, POPC (Sigma), and sodium cholate (Sigma) in a molar ratio of 1/100/100 [24].

4.2.4. S1P efflux from erythrocytes

Erythrocytes were isolated from the blood of healthy adult volunteers. The blood was anticoagulated with sodium citrate and then centrifuged at 2,000 g for 5 min at 4°C. After removing the plasma, the sedimented erythrocytes were washed three times with sterile PBS and resuspended 1:1 in PBS (v/v) containing either BSA, human or murine HDL, rHDL, or lipid-free apoA-I at the concentrations indicated in the Results section and incubated at 37°C. Aliquots were removed at different time points (as indicated in the Results section) and immediately centrifuged at 2,000 g for 3 min at 4°C to sediment erythrocytes. The supernatants were carefully transferred into new tubes avoiding any contamination with

erythrocytes. For S1P measurement, 25 µl aliquots of the supernatant were taken and processed as described below.

4.2.5. Quantification of S1P in plasma, HDL, and urine

S1P was quantified by LC-MS/MS after derivatization with acetic anhydride. The S1P concentrations in plasma or erythrocyte supernatants (25µl), HDL (50 µg), and urine (500µl) were analyzed after adding 10 pmol internal standard (D_7S1P, Avanti Polar Lipids, Alabaster, AL, USA). For calibration, S1P (Avanti Polar Lipids) was dissolved in DMSO/concentrated-HCl (100:2, v/v) at a concentration of 0.28 mmol/l stock solution. Each series of measurements was calibrated with 1, 2.5, 5, 10, 15, 20, and 25 pmol of S1P supplemented with 10 pmol of D_7S1P as the internal standard (IS). Quality control samples with 7.5 and 22.5 pmol S1P were evaluated at the beginning and at the end of each sample series. Double blank and blank samples for carry-over control were prepared by adding methanol and internal standard, respectively, to 25 µl of water and processed as plasma samples.

Lipids were extracted with 1 ml of an organic solution consisting of ethyl acetate/2-propanol (6:1, v/v) and 50µl of concentrated formic acid added for phase separation [25]. The upper organic phase was separated and evaporated to dryness under a stream of nitrogen. For the derivatisation of the primary amino and the secondary alcohol groups of S1P [26], the dried lipids were dissolved in 100µl of pyridine and 50µl of acetic anhydride and incubated at 40°C for 20 min. After evaporating the acetylation reagents, the reaction products were dissolved in 100µl of methanol and transferred to glass vials prior to LC-MS/MS analysis.

Acetylated S1P [S1P $(Ac)_2$] was analyzed on an LC-MS system consisting of an HTC PAL autosampler (CTC Analytics, Zwingen, Switzerland), a Rheos 2200 HPLC pump (Flux Instruments, Reinach, Switzerland), and a TSQ Quantum Access mass spectrometer (Thermo Fisher Scientific, Waltham, MA, USA). Chromatographic conditions for reverse-phase separation of S1P$(Ac)_2$ were modified from Berdyshev et al. [26]. Separation of S1P$(Ac)_2$ was done on a Nucleosil C18 HD column (125 x 2 mm, 100 Å, 5 µm) at 40°C. Mobile phase A consisted of water/methanol/formic acid (20:80:0.5, v/v) and mobile phase B consisted of methanol/acetonitrile/formic acid (59:40:0.5, v/v), both containing 5mM ammonium formate. Elution started with 100% A for 1.0 min (0.25 ml/min) and increased to 100% B within 4.0 min and was then kept constant for 4 min. Finally the column was reequilibrated with 100% mobile phase A for 5.5 min. The injection volume was 10 µL. The injection system and syringe were washed twice with methanol/acetone/2-propanol (1:1:1, v/v), containing HCOOH 0.1% and acetone/methanol/water (2:2:1, v/v) solutions after every injection.

$S1P(Ac)_2$ and $D_7S1P(Ac)_2$ eluted at t_r ~6.3 min. Double blank and blank samples were analysed before each set of calibrators and samples to exclude carry-over.

For ionization, ESI was used and detection was performed in the positive mode, monitoring $[M\text{-}H2O]^+$ ions using selective reaction monitoring (SRM) for the transitions of m/z 446.2 → 264.2 (30V) for $S1P(Ac)_2$ and m/z 453.2 → 271.2 (27 V) for $D_7S1P(Ac)_2$ (spray voltage 5000 V, skimmer offset 10 V and ion transfer capillary temperature 300°C). Further ionization and detection parameters were optimized by tuning the system with $S1P(Ac)_2$ standard. Data analysis was performed on XCalibur 2.0.6 (Thermo Scientific).

The standard curve was constructed by plotting the $S1P/D_7S1P$ peak area ratios against the concentrations of the S1P standards. The S1P concentration in samples was determined by linear regression obtained from the standard curve. The lower level of quantification was defined as the 10% functional assay sensitivity and amounted to 1 pmol extracted S1P corresponding to 40 nmol/l plasma or 2 nmol/l urine. At amounts of 7.5 pmol and 22.5 pmol, the intra-day imprecision was 5.8% and 2.3%, respectively, and the inter-day imprecision was 4.3% and 8.1%, respectively.

4.2.6. Western blotting of apoM in plasma and urine

Proteins were separated on 14% SDS polyacrylamide gels and transferred onto nitrocellulose membrane. The membranes were blocked with 5% milk in 0.1% TBS Tween (TBS-T) buffer for 1 h at room temperature. Thereafter, the membranes were incubated overnight at 4°C with a commercially available apoM antibody (LC-C51665; LifeSpam BioSciences). The 1:1,000 dilution of antibody was made in 5% milk TBS-T. The membranes were then washed three times with TBS-T and incubated with secondary antibody anti-rabbit coupled with HRP (1:10,000). After washing three times for 10 minutes, the membrane was developed with ECL Plus Western blotting detection reagent (Pierce) according to the manufacturer's instructions.

4.2.7. Statistical analyses

Statistical analyses were performed by using Graph-Pad. Normality of the data was determined by using the Kolmogorov-Smirnov test. Normally distributed data were analyzed by the two-tailed unpaired Student`s *t*-test, and data that was not normally distributed were analysed by the Mann-Whitney U test. Differences in prevalences were analysed by chi-square test.

4.3. Results

4.3.1. HDL and apoM promote S1P efflux from erythrocytes

To confirm previous data that HDL induces S1P efflux from erythrocytes [5], 1 ml of washed human erythrocytes were incubated with two different concentrations of human HDL for increasing time. Figures 2A and 2B show the time-dependent accumulation of S1P in human HDL without and with correction for the endogenous S1P content, respectively. Maximal efflux, which doubled the concentration of S1P preexisting in HDL, was reached after 4 h. Half-maximal efflux was reached after 1-2 h of incubation. Albumin (500 µg/ml), which is the second most important carrier of S1P in plasma [4, 10], elicited very little S1P efflux under the same conditions.

Next we monitored the time-dependent S1P efflux from erythrocytes in the presence of 300 µg/ml HDLs which were isolated from plasma of wt, *Apom*$^{-/-}$, or *Apom*^{tg} mice in comparison with 300 µg/ml albumin. As reported previously, HDLs of these three mouse strains differ by endogenous S1P content (see also baseline data in Fig. 2C). Therefore, we present S1P efflux before and after correction for the endogenous S1P content of HDLs (Fig. 2C and 2D). During 8 h of incubation, S1P concentrations increased steadily in the HDL of all three mouse strains. S1P efflux capacity of HDL from wt mice resembled that of human HDL. The maximal net S1P efflux measured was significantly increased in the presence of HDL from *Apom*^{tg} mice, but not decreased in the presence of HDL from *Apom*$^{-/-}$ mice (Fig. 2D). Also of note, S1P efflux in the presence of HDL from both wt and *Apom*$^{-/-}$ mice reached saturation after 2-4 h, whereas S1P efflux in the presence of HDL from *Apom*^{tg} mice did not reach saturation within 8 h, the maximal time the experiment could be performed without hemolysis.

To provide further evidence that HDL can elicit S1P efflux independently of apoM, we compared the capacity of native HDL, rHDL, lipid-free apoA-I, and albumin to induce S1P efflux. Whereas lipid-free apoA-I was not capable of inducing S1P efflux, reconstituted apoM-free HDLs were even more active in stimulating S1P efflux than native HDLs at concentration of 200 µg/ml (Fig. 3).

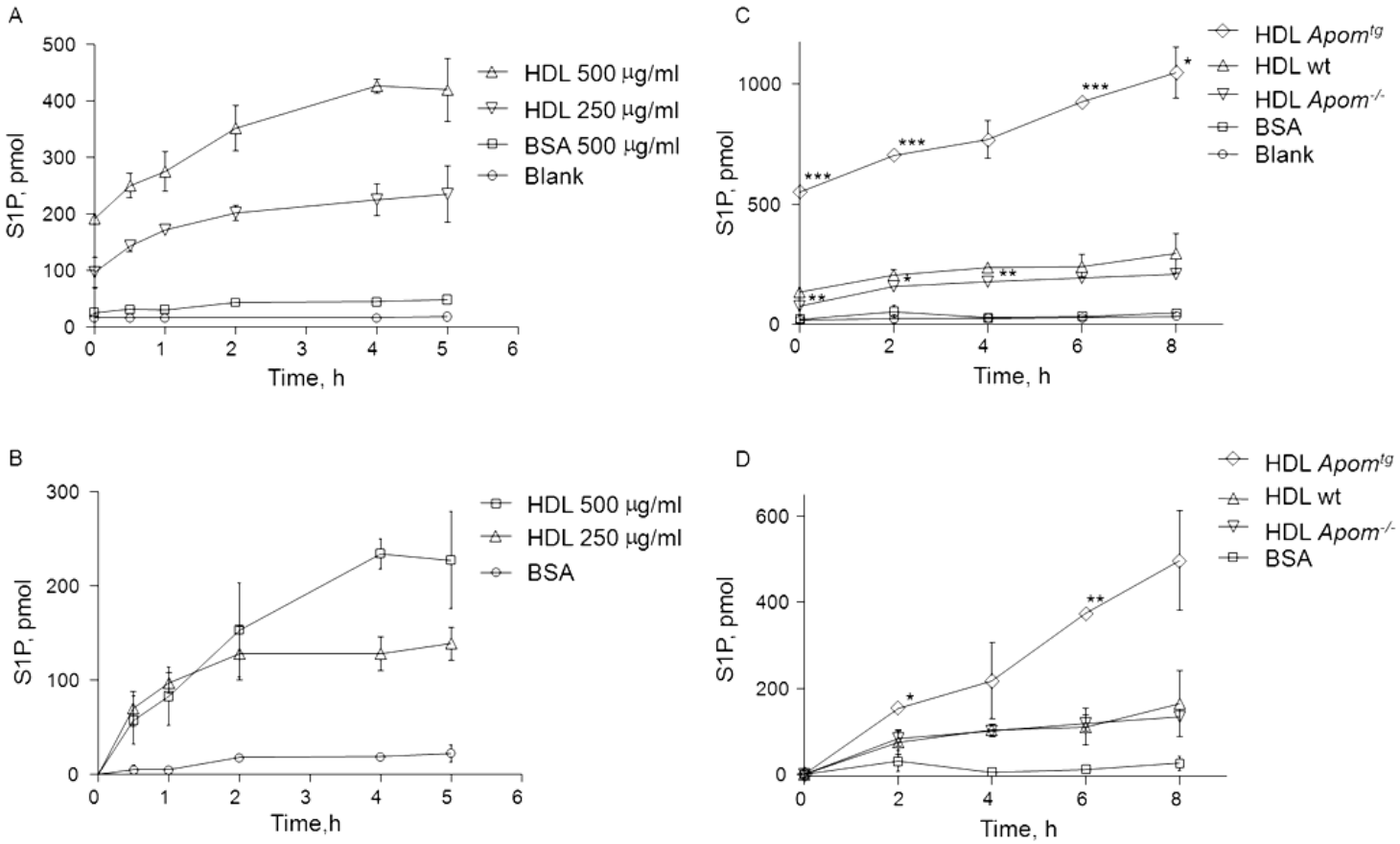

Figure 2. Time-dependent efflux of S1P from washed human erythrocytes in the presence of 500 µg/ml BSA (Figures 2A-2D), 250 or 500 µg/ml human HDL (Figures 2A, 2B), or 300 µg/ml HDL from wt, *Apom*$^{-/-}$, or *Apom*^{tg} mice (Figures 2C, 2D).

Figures 2A, 2C: Absolute S1P amounts in 1 ml of supernatant after incubation of HDL or albumin with erythrocytes for the indicated time intervals and subsequent removal of erythrocytes by centrifugation. Figures 2B, 2D: Data on net S1P efflux which were obtained by subtracting the S1P concentrations of the various HDL preparations at baseline from the S1P concentrations at the indicated time points. Values are mean ± SD. Statistically significant differences between HDL of *Apom*$^{-/-}$ and wt mice, as well as between HDL of *Apom*^{tg} and wt mice, are indicated by asterisks. (* $p \leq 0.05$, ** $p \leq 0.01$, *** $p \leq 0.001$; Student´s *t*-test).

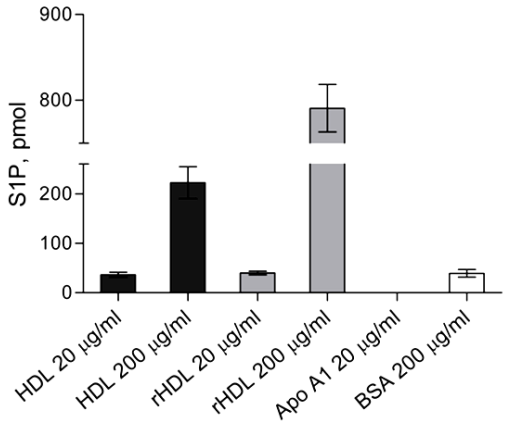

Figure 3. Net S1P efflux from washed human erythrocytes in the presence of native and rHDL, lipid-free apoA-I, or BSA.

Presented are net amounts of S1P released by erythrocytes in 1 ml of supernatant after 4 h incubation with 20 µg/ml or 200 µg/ml HDL isolated either from human plasma or artificially reconstituted by cholate dialysis of apoA-I and POPC (rHDL), 20 µg/ml lipid-free apoA-I, or 200 µg/ml BSA. Values are mean ± SD.

4.3.2. Urinary excretion of S1P is increased in *Apom*$^{-/-}$ mice, as well as in mice with dysfunctional tubular protein reabsorption

As reported previously [12, 13] and as compared to their wt littermates, S1P levels in plasma and HDL were significantly decreased by 20 and 50%, respectively, in 12-14-week-old *Apom*$^{-/-}$ mice, and were significantly increased by factors three and five, respectively, in plasma and HDL of age-matched *Apom*^{tg} mice (Fig. 4A and 4B) .

In 21 urine samples of wt mice, we measured S1P at very low concentration below or close to the lower level of quantification of our method (10% functional assay sensitivity: 1 pmol S1P corresponding to 2 nmol S1P per liter urine). In fact, only 5 of 21 samples of wt mice, but 4 of 5 samples *Apom*$^{-/-}$ mice, had S1P levels above this threshold ($p = 0.018$, chi-square test). In the direct comparison, urine concentrations of S1P were significantly higher in 6- and 16-week-old *Apom*$^{-/-}$ mice than in 6- and 16-week-old wt controls ($p < 0.05$, Fig. 4C).

Next, we investigated whether disturbances of tubular apoM reabsorption are associated with increased urinary S1P excretion. By Western blotting, we found apoM present in the urine samples of mice with nonfunctional megalin (*Lrp2*$^{-/-}$), ClC-5 (*Clcn5*$^{-/-}$), or cystinosin (*Ctns*$^{-/-}$) (Fig. 5A). ApoM was not detectable in the urine of wt littermates.

In the urine samples of 21 wt mice from three different laboratories, S1P was below or close to the level of quantification (2 nmol/l). By contrast, three of four urine samples from 11-week-old *Lrp2*$^{-/-}$ mice and six of seven samples from 12-16-week-old *Clcn5*$^{-/-}$ mice contained clearly quantifiable concentrations of S1P (Fig. 6A and 6B). Upon direct comparison of mutant mice and littermate controls, S1P excretion was significantly increased

in *Clcn5*$^{-/-}$ mice (Fig. 6B), which are known to suffer from a severe dysfunction of the proximal tubule [27]. At ages of 18 weeks, 20-24 weeks, or 30-38 weeks, neither male nor female *Ctns*$^{-/-}$ mice showed increased S1P excretion.

Western blotting did not provide any evidence for grossly altered concentrations of apoM in the plasma of *Lrp2*$^{-/-}$, *Clcn5*$^{-/-}$, or *Ctns*$^{-/-}$ mice (Fig. 5B). These three mouse models with tubular apoM proteinuria also did not show any statistically significant or consistent differences in plasma concentrations of S1P (Fig. 6D-6F).

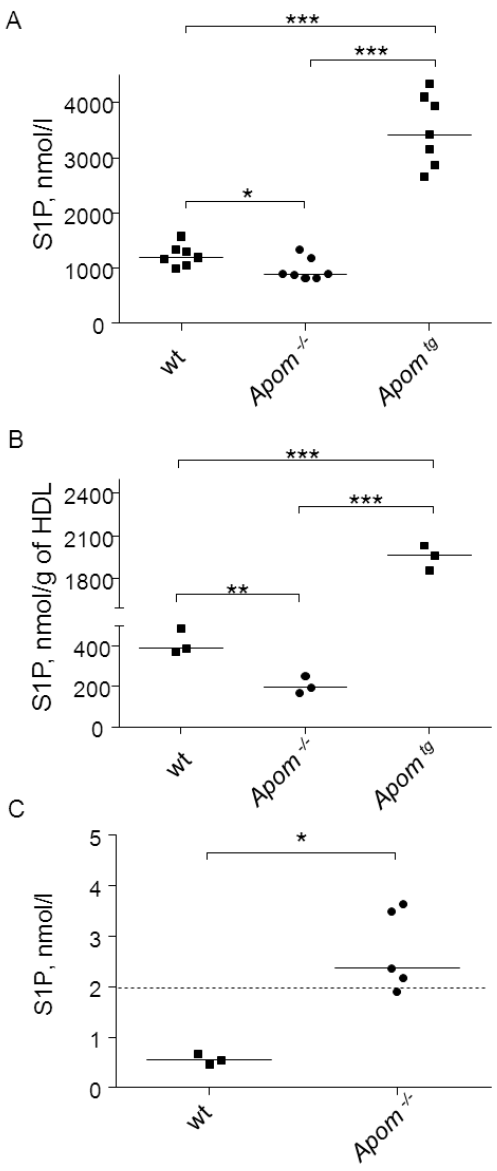

Figure 4. ApoM determines S1P concentration in plasma (Figure 4A), HDL (Figure 4B), and urine (Figure 4C) of wt, *Apom*$^{-/-}$, and *Apom*^{tg} mice.

Figures 4A, 4B: S1P levels in plasma and HDL samples from 12-14-week-old wt, *Apom*$^{-/-}$, and *Apom*^{tg} mice. Figure 4C: Urinary S1P excretion by 6- and 16-week-old *Apom*$^{-/-}$ mice and their wt littermates. Each point identifies data from individual mice. Solid lines indicate median values. The dashed line indicates the lower level of quantification of S1P by LC-MS in urine samples. (* $p \leq 0.05$, ** $p \leq 0.01$, *** $p \leq 0.001$; Mann-Whitney U test).

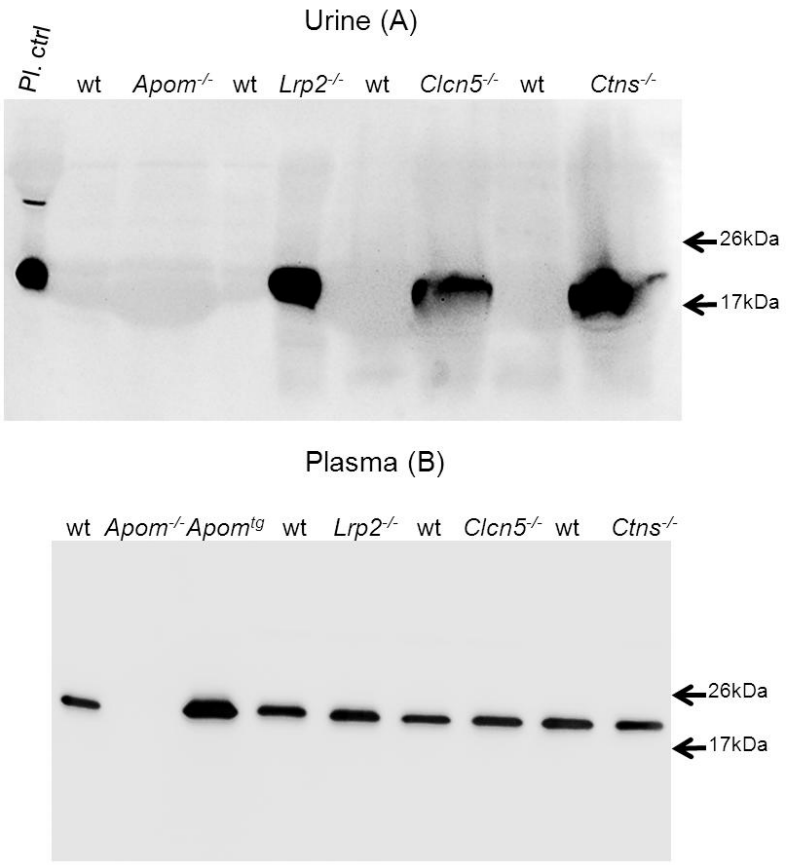

Figure 5. Western blotting of apoM in urine (Figure 5A) and plasma (Figure 5B) of *Apom*$^{-/-}$, *Apom*^{tg} mice and mice with defective megalin (*Lrp2*$^{-/-}$), ClC-5 (*Clcn5*$^{-/-}$), and cystinosin (*Ctns*$^{-/-}$) and their wt controls.

Urine (20 µl) or 11.5 µl of 1/10 diluted plasma were separated by SDS-PAGE and immunoblotted as described in the Methods section. Note the absence of apoM from urine samples of wt mice, but the presence in urine samples of mice with defective tubular transport (Figure 5A). By contrast apoM plasma levels appear indistinguishable between wt mice and the different tubular proteinuria models (Figure 5B).

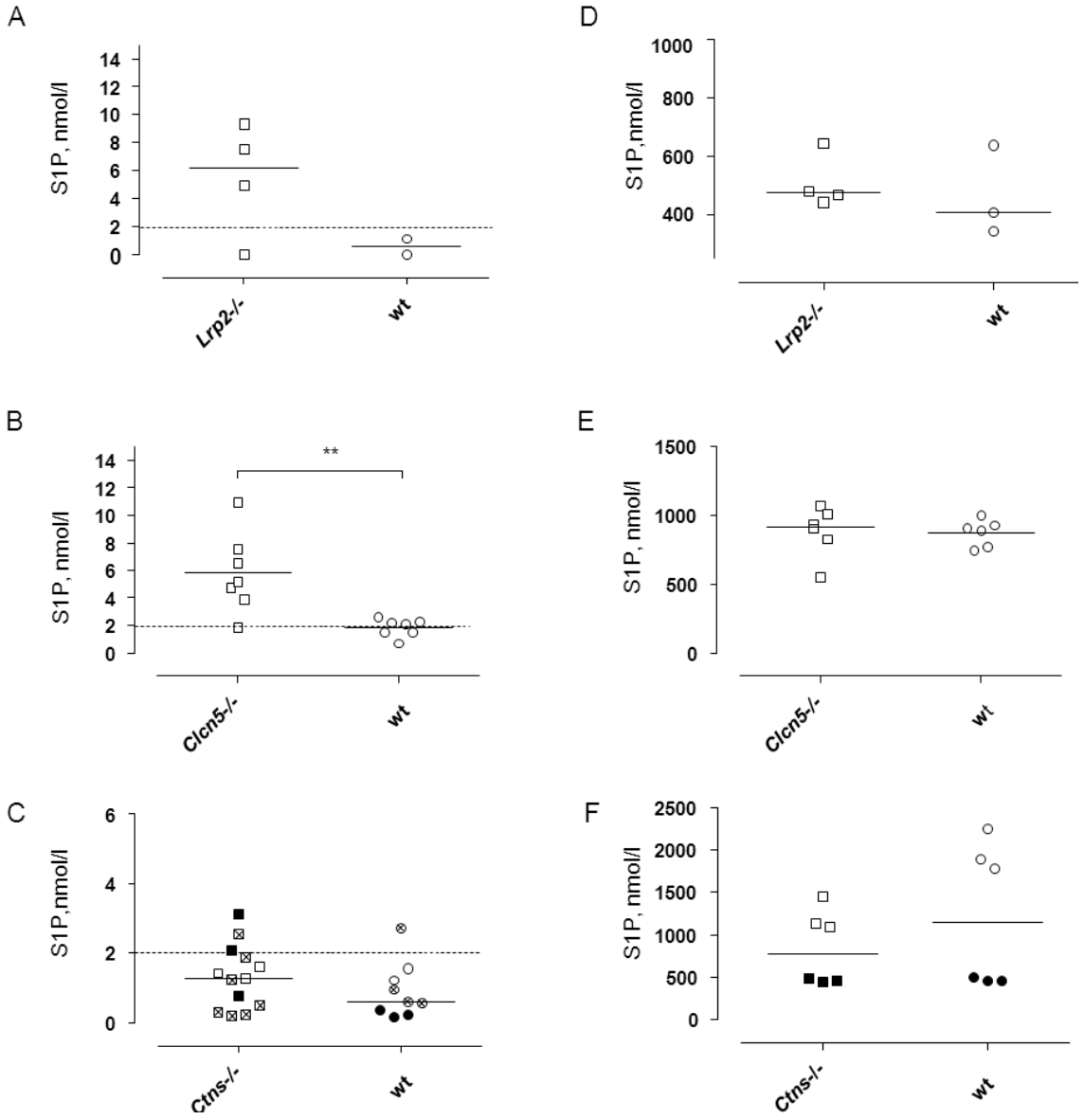

Figure 6. Concentrations of S1P in urine (Figures 6A-6C) or plasma (Figures 6D-6F) of mice with defective megalin (*Lrp2*$^{-/-}$) (Figures 6A, 6D), ClC-5 (*Clcn5*$^{-/-}$) (Figures 6B, 6E), or cystinosin (*Ctns*$^{-/-}$) (Figures 6C, 6F) as compared with their wt controls.

Each point represents data from an individual mouse sample. Figures 6A, 6D: Urine and plasma levels of S1P in 11-week-old *Lrp2*$^{-/-}$ mice (open symbols). Figures 6B, 6E: Urine and plasma levels of S1P in 12-16-week-old *Clcn5*$^{-/-}$ mice (open symbols). Figures 6C, 6F: Urine and plasma S1P levels in 18-week-old *Ctns*$^{-/-}$ mice (open symbols), in 20-24-week-old *Ctns*$^{-/-}$ mice (closed symbols), and in 30-38-week-old *Ctns*$^{-/-}$ mice (crossed symbols). Dashed lines indicate the lower level of quantification of S1P by LC-MS in urine samples. (** $p \leq 0.01$; Mann-Whitney U test). Note the higher medians of S1P excretion in mice with defective tubular protein reabsorption as compared with wt controls.

4.4. Discussion

Previous work by the laboratories of Dahlbäck and colleagues and Nielssen and colleagues [11, 12] identified apoM as a physiologically relevant binding protein of S1P in HDLs of plasma. Our lab previously confirmed the limiting effect of apoM on S1P levels in plasma, but also found indications for more complex relationships between HDL, apoM, and S1P [13]. Most notably, concentrations of apoM and S1P in total or apoB-depleted plasma did not correlate with each other [13], possibly due to the molar excess of apoM compared to its ligand S1P, which varies inter-individually between factors 1.2 and 8 and/or in the presence of alternative ligands, which compete with S1P for binding to apoM [10, 13]. However, we also observed statistically significant correlations of S1P concentrations with concentrations of HDL-cholesterol, apoA-I and other measures of HDLs [13]. This raised the questions whether HDLs can handle S1P also independently of apoM and whether apoM may influence S1P plasma levels independently of its transport function in plasma.

To answer the first question, we investigated the capacity of HDLs to induce S1P efflux from erythrocytes. HDLs of both humans and wt mice were found to induce time-dependent and saturable S1P efflux leading to maximal doubling of the endogenous S1P concentration in normal human or murine HDLs (400 pmol/l/l S1P per mg HDL protein). Assuming that 80% of HDL protein mass corresponds to apoA-I, i.e. the predominant protein of HDLs which has a molecular mass of 28 kDa, the molar concentration of S1P per apoA-I amounts to 1/72. Assuming that the HDL particles contain an average of three molecules of apoA-I [28, 29], every 24th HDL particle in our experiments contained one molecule of S1P at baseline. The doubling of S1P content by efflux indicates the saturation of S1P efflux much below the HDL particle concentration. This can be explained by the presence of a specific S1P binding site in HDLs which is not saturated in HDLs isolated from plasma, such as apoM [10-12]. At first sight and in agreement with this explanation, we found the net S1P efflux capacity of HDLs from *Apom*^{tg} mice significantly increased without reaching saturation. By contrast, HDLs from both wt and *Apom*$^{-/-}$ mice elicited time-dependent and saturable S1P efflux from erythrocytes, which did not differ from each other and that was markedly greater than in the presence of albumin. Moreover, rHDL consisting only of apoA-I and POPC induced S1P efflux from erythrocytes. The apparent 2- to 3-fold higher efficacy of rHDL, as compared with native HDL, probably reflects the higher particle concentration at identical protein mass concentrations, because rHDL contains two molecules of apoA-I, whereas native HDL contains at least three molecules of apoA-I plus other proteins. Our finding of rHDL-

induced S1P efflux does also explain the previous observation that, initially, S1P-free rHDLs exert cytoprotective effects on cardiomyocytes in a S1P receptor-dependent fashion.[30]

Taken together, our findings indicate the presence of an additional apoM-independent mechanism by which HDLs can induce efflux and/or mediate the binding of S1P. Because of the saturation much below the concentration of HDL particles or phospholipids, it is unlikely that this apoM-independent fraction of HDL-induced S1P efflux is unspecific, for example, as the result of association with phospholipids. The nonsaturation of S1P efflux in the presence of HDLs from *Apom*^{tg} mice indicates that apoM, rather than phosphatidylcholine, acts as the slow determinant of S1P binding capacity. The saturable S1P efflux in the presence of HDLs from *Apom*$^{-/-}$ mice points to the presence of an as yet unknown relatively fast inducer of S1P efflux. Because rHDL contains only apoA-I in addition to phospholipids, apoA-I is the prime candidate for this activity. In this respect, it is noteworthy that ABCA1 and ABCG1, and scavenger receptor B1, which are important cellular interaction partners for apoA-I or HDL-induced efflux of cholesterol or phosphatidylcholine, have been suspected to promote or modulate cellular S1P efflux as well [4, 8]. In fact, glyburide, a pharmacological inhibitor of ABC transporters including ABCA1, was previously found to inhibit S1P efflux from red blood cells. However, although present in erythrocytes, functional experiments excluded ABCA1 and ABCA7 as the mediators of S1P efflux from these cells [7]. In agreement with the lack of involvement of ABCA1, we did not find any S1P efflux induced by lipid-free apoA-I, which, as the primary interaction partner of ABCA1, stimulates efflux of cholesterol and phosphatidylcholine from many cells. The roles of ABCG1 and scavenger receptor BI, which typically interact with both native and artificially lipidated HDL [29], for S1P efflux, are as yet unknown.

To address the second question, whether apoM may regulate S1P plasma concentrations beyond transport in plasma, we compared the urinary excretion of S1P of wt and *Apom*$^{-/-}$ mice. Not unexpectedly, the urine of wt mice did not contain much S1P. However, quantifiable amounts of S1P were excreted with the urine by *Apom*$^{-/-}$ mice. These data indicated that apoM plays some role for preventing urinary S1P excretion, but does not indicate whether the excreted S1P is of plasmatic or renal origin. On the one hand and next to hepatocytes, the epithelial cells lining the proximal tubules of the kidney are the only cells which express apoM [31]. Hence, kidney-derived apoM may play an important role in handling S1P, for example for the interaction with S1P receptors. In fact, S1P and S1P receptors were reported to convey protection of the proximal tubule epithelium against oxidative stress induced by ischemia/ reperfusion injury [32]. On the other hand, the plasma-derived 22 kDa

large murine apoM or 26 kDa large human apoM is ultrafiltrated through glomeruli and reabsorbed from the primary urine by the endocytic receptor megalin into the proximal tubule epithelial cells [16], so that the lack of apoM could interfere with the tubular recovery of S1P. To discriminate between these two explanations, we investigated the urinary excretion of apoM and S1P by mice which lack megalin, the chloride-proton exchanger ClC-5, or the lysosomal cystine transporter cystinosin, which all play important roles for the tubular reabsorption of carrier proteins and their cargo from the primary urine [17, 19, 20]. We confirmed the previously observed urinary apoM excretion by megalin knockout mice [16]. In addition, mice without ClC-5 or cystinosin showed a urinary loss of apoM. Like *Apom*$^{-/-}$ mice, *Lrp2*$^{-/-}$ and *Clcn5*$^{-/-}$ mice showed clearly increased urinary S1P excretion. This difference in urinary S1P excretion was much less prominent, if not absent, in *Ctns*$^{-/-}$ mice. This may reflect the fact that the cystinosis model develops tubular dysfunction later in life [33]. In our hands, even at the age of 30-38 weeks when tubular dysfunction is manifested, we did not see any increase in S1P excretion, although apoM was excreted with the urine. Nevertheless, the unusual urinary excretion of S1P in the urine of *Apom*$^{-/-}$, *Lrp2*$^{-/-}$, and *Clcn5*$^{-/-}$ mice suggests that tubular reabsorption of apoM interferes with the urinary loss of S1P. However, in *Lrp2*$^{-/-}$ and *Clcn5*$^{-/-}$ mice, the urinary loss of apoM and S1P appears to be too low to substantially decrease the plasma concentrations of apoM and S1P. Therefore, it is also unlikely that the urinary loss contributes to the lower plasma and HDL-S1P levels observed in *Apom*$^{-/-}$ mice [12, 13]. However, cubilin deficiency was previously reported to increase the turnover and decrease plasma albumin and apoA-I concentrations slightly, but significantly [18]. Quantitative studies in larger numbers of mice may hence unravel subtle differences.

In conclusion, our studies of mice differing by the expression of apoM or the activity of proteins involved in the tubular endocytosis of apoM indicate that binding of S1P by apoM plays at least two further roles in S1P metabolism beyond mediating S1P transport in HDL. First, HDL facilitates S1P efflux from erythrocytes by both apoM-dependent and apoM-independent mechanisms. Second, apoM facilitates the reabsorption of S1P from the primary urine into tubular epithelial cells, however, with no impact on S1P plasma concentration. By the two newly identified activities, apoM may modulate the paracrine and autocrine interactions of S1P with vascular endothelial and renal tubular epithelial cells, respectively. In addition, we provide evidence for an additional HDL-associated factor which contributes to S1P efflux and transport by HDLs.

Acknowledgements

The authors gratefully acknowledge the support by Dr. Thomas Willnow (Max Delbrück Centrum, Berlin-Buch, Germany), who provided plasma and urine samples of *Lrp2*$^{-/-}$ mice. Furthermore, the authors wish to thank Yvette Cnops for providing them with urine samples of Ctns$^{-/-}$ mice**.**

References

1. Fyrst H, Saba JD. An update on sphingosine-1-phosphate and other sphingolipid mediators. *Nature chemical biology* 2010;6:489-497.

2. Hla T, Dannenberg AJ. Sphingolipid signaling in metabolic disorders. *Cell metabolism* 2012;16:420-434.

3. Hornemann T, Worgall TS. Sphingolipids and atherosclerosis. *Atherosclerosis* 2013;226:16-28.

4. Nishi T, Kobayashi N, Hisano Y, Kawahara A, Yamaguchi A. Molecular and physiological functions of sphingosine 1-phosphate transporters. *Biochimica et biophysica acta* 2014;1841:759-765.

5. Bode C, Sensken SC, Peest U, et al. Erythrocytes serve as a reservoir for cellular and extracellular sphingosine 1-phosphate. *Journal of cellular biochemistry* 2010;109:1232-1243.

6. Ono Y, Kurano M, Ohkawa R, et al. Sphingosine 1-phosphate release from platelets during clot formation: close correlation between platelet count and serum sphingosine 1-phosphate concentration. *Lipids in health and disease* 2013;12:20.

7. Kobayashi N, Kobayashi N, Yamaguchi A, Nishi T. Characterization of the ATP-dependent sphingosine 1-phosphate transporter in rat erythrocytes. *The Journal of biological chemistry* 2009;284:21192-21200.

8. Liu X, Xiong SL, Yi GH. ABCA1, ABCG1, and SR-BI: Transit of HDL-associated sphingosine-1-phosphate. *Clinica chimica acta; international journal of clinical chemistry* 2012;413:384-390.

9. Sattler K, Levkau B. Sphingosine-1-phosphate as a mediator of high-density lipoprotein effects in cardiovascular protection. *Cardiovascular research* 2009;82:201-211.

10. Christoffersen C, Nielsen LB. Apolipoprotein M: bridging HDL and endothelial function. *Current opinion in lipidology* 2013;24:295-300.

11. Sevvana M, Ahnstrom J, Egerer-Sieber C, Lange HA, Dahlback B, Muller YA. Serendipitous fatty acid binding reveals the structural determinants for ligand recognition in apolipoprotein M. *Journal of molecular biology* 2009;393:920-936.

12. Christoffersen C, Obinata H, Kumaraswamy SB, et al. Endothelium-protective sphingosine-1-phosphate provided by HDL-associated apolipoprotein M. *Proceedings of the National Academy of Sciences of the United States of America* 2011;108:9613-9618.

13. Karuna R, Park R, Othman A, et al. Plasma levels of sphingosine-1-phosphate and apolipoprotein M in patients with monogenic disorders of HDL metabolism. *Atherosclerosis* 2011;219:855-863.

14. Ohkawa R, Nakamura K, Okubo S, et al. Plasma sphingosine-1-phosphate measurement in healthy subjects: close correlation with red blood cell parameters. *Annals of clinical biochemistry* 2008;45:356-363.

15. Wolfrum C, Poy MN, Stoffel M. Apolipoprotein M is required for prebeta-HDL formation and cholesterol efflux to HDL and protects against atherosclerosis. *Nature medicine* 2005;11:418-422.

16. Faber K, Hvidberg V, Moestrup SK, Dahlback B, Nielsen LB. Megalin is a receptor for apolipoprotein M, and kidney-specific megalin-deficiency confers urinary excretion of apolipoprotein M. *Molecular endocrinology* 2006;20:212-218.

17. Christensen EI, Birn H, Storm T, Weyer K, Nielsen R. Endocytic receptors in the renal proximal tubule. *Physiology* 2012;27:223-236.

18. Aseem O, Smith BT, Cooley MA, et al. Cubilin Maintains Blood Levels of HDL and Albumin. *Journal of the American Society of Nephrology : JASN* 2013.

19. Wilmer MJ, Emma F, Levtchenko EN. The pathogenesis of cystinosis: mechanisms beyond cystine accumulation. *American journal of physiology Renal physiology* 2010;299:F905-916.

20. Devuyst O, Thakker RV. Dent's disease. *Orphanet journal of rare diseases* 2010;5:28.

21. Nykjaer A, Dragun D, Walther D, et al. An endocytic pathway essential for renal uptake and activation of the steroid 25-(OH) vitamin D3. *Cell* 1999;96:507-515.

22. Christensen EI, Devuyst O, Dom G, et al. Loss of chloride channel ClC-5 impairs endocytosis by defective trafficking of megalin and cubilin in kidney proximal tubules. *Proceedings of the National Academy of Sciences of the United States of America* 2003;100:8472-8477.

23. Nevo N, Chol M, Bailleux A, et al. Renal phenotype of the cystinosis mouse model is dependent upon genetic background. *Nephrology, dialysis, transplantation : official publication of the European Dialysis and Transplant Association - European Renal Association* 2010;25:1059-1066.

24. Ohnsorg PM, Rohrer L, Perisa D, et al. Carboxyl terminus of apolipoprotein A-I (ApoA-I) is necessary for the transport of lipid-free ApoA-I but not prelipidated ApoA-I particles through aortic endothelial cells. *The Journal of biological chemistry* 2011;286:7744-7754.

25. Bielawski J, Pierce JS, Snider J, Rembiesa B, Szulc ZM, Bielawska A. Comprehensive quantitative analysis of bioactive sphingolipids by high-performance liquid chromatography-tandem mass spectrometry. *Methods in molecular biology* 2009;579:443-467.

26. Berdyshev EV, Gorshkova IA, Garcia JG, Natarajan V, Hubbard WC. Quantitative analysis of sphingoid base-1-phosphates as bisacetylated derivatives by liquid chromatography-tandem mass spectrometry. *Analytical biochemistry* 2005;339:129-136.

27. Wang SS, Devuyst O, Courtoy PJ, et al. Mice lacking renal chloride channel, CLC-5, are a model for Dent's disease, a nephrolithiasis disorder associated with defective receptor-mediated endocytosis. *Human molecular genetics* 2000;9:2937-2945.

28. Segrest JP, Cheung MC, Jones MK. Volumetric determination of apolipoprotein stoichiometry of circulating HDL subspecies. *Journal of lipid research* 2013;54:2733-2744.

29. Annema W, von Eckardstein A. High-density lipoproteins. Multifunctional but vulnerable protections from atherosclerosis. *Circulation journal : official journal of the Japanese Circulation Society* 2013;77:2432-2448.

30. Frias MA, Lang U, Gerber-Wicht C, James RW. Native and reconstituted HDL protect cardiomyocytes from doxorubicin-induced apoptosis. *Cardiovascular research* 2010;85:118-126.

31. Zhang XY, Dong X, Zheng L, et al. Specific tissue expression and cellular localization of human apolipoprotein M as determined by in situ hybridization. *Acta histochemica* 2003;105:67-72.

32. Koch A, Pfeilschifter J, Huwiler A. Sphingosine 1-phosphate in renal diseases. *Cellular physiology and biochemistry : international journal of experimental cellular physiology, biochemistry, and pharmacology* 2013;31:745-760.

33. Raggi C, Luciani A, Nevo N, Antignac C, Terryn S, Devuyst O. Dedifferentiation and aberrations of the endolysosomal compartment characterize the early stage of nephropathic cystinosis. *Human molecular genetics* 2014;23:2266-2278.

34 Wolfrum C, Howell JJ, Ndungo E, Stoffel M. Foxa2 activity increases plasma high density lipoprotein levels by regulating apolipoprotein M. *The Journal of biological chemistry* 2008;283:16940-16949.

35 Costa RH, Lai E, Darnell JE, Jr. Transcriptional control of the mouse prealbumin (transthyretin) gene: both promoter sequences and a distinct enhancer are cell specific. *Molecular and cellular biology* 1986;6:4697-4708.

5. LACK OF PARAOXONASE 1 ALTERS PHOSPHOLIPID COMPOSITION, BUT NOT MORPHOLOGY AND FUNCTION OF THE MOUSE RETINA

Jadwiga Oczos[1,2,3,*], Iryna Sutter[3,4,*], Barbara Kloeckener-Gruissem[2,6], Wolfgang Berger[2,3,5], Meliana Riwanto[7,8], Katharina Rentsch[3,4,9], Thorsten Hornemann[3,4], Arnold von Eckardstein[3,4] and Christian Grimm[1,3,5]

* These authors contributed equally to the work

1 Lab for Retinal Cell Biology, Department of Ophthalmology, University of Zurich, Zurich, Switzerland

2 Institute of Medical Molecular Genetics, University of Zurich, Schlieren, Switzerland

3 Zurich Center for Integrative Human Physiology (ZIHP), University of Zurich, Zurich, Switzerland

4 Institute of Clinical Chemistry, University of Zurich, Zurich, Switzerland

5 Zurich Center of Neuroscience (ZNZ)

6 Department of Biology, ETH Zurich, Zurich, Switzerland

7 Institute of Physiology, University of Zurich, Zurich, Switzerland

8 present address:Division of Nephrology, Institute of Physiology, University of Zurich, Zurich, Switzerland

9 present address: Laboratory Medicine, University Hospital Basel, Basel, Switzerland

[Investigative ophthalmology & visual science 2014; 55: 4714-4727]

Contribution statement

I. Sutter did lipidomics analysis. J. Oczos did characterisation of morphology and function of the mouse retina.

Abstract

Purpose: Biochemical and genetic analyses established a contribution of lipid metabolism to age-related macular degeneration (AMD) pathology. Paraoxonase 1 (PON1) is an antioxidative protein involved in high density lipoprotein (HDL) function and was found to be associated with AMD. Here, we used *Pon1*$^{-/-}$ mice to study the influence of PON1 on retinal physiology and to reveal the potential impact of PON1 on AMD aetiology.

Methods: Laser capture microdissection served to isolate single retinal layers. Retinal function was assessed by ERG. Retinal and RPE morphology were monitored by fundus imaging, fluorescein angiography, light and transmission electron microscopy, and immunofluorescence microscopy. Levels of mRNA and composition of phospholipid species were determined by real-time PCR and LC-MS, respectively.

Results: Adult (8 weeks old) *Pon1*$^{-/-}$ mice displayed normal retinal function and morphology, but their retinas contained reduced amounts of lysophosphatidylcholines (LPCs) compared to controls. Aged (12 months old) *Pon1*$^{-/-}$ animals did not show any morphologic or molecular signs of photoreceptor or RPE degeneration, or of accelerated aging. Photoreceptors of *Pon1*$^{-/-}$ and control mice were similarly susceptible to light damage.

Conclusions: Results indicate that PON1 is not essential for normal development, function, ageing, and the defense against light damage of the mouse retina. Reduced levels of LPCs in eyes of *Pon1*$^{-/-}$ mice may reflect a decreased activity of phospholipase A2 or altered antioxidative activity in aged eyes.

5.1. Introduction

Age-related macular degeneration (AMD) is the leading cause of irreversible blindness and visual disability in the elderly population of industrialized countries. Various environmental risk factors, such as advanced age, cigarette smoking, diet, obesity, atherosclerosis, hypertension, inflammatory disease, as well as genetic predisposition have been implicated in this complex disease[1-3]. The epidemiological risk factors point toward various molecular mechanisms that might be involved in the aetiology of AMD. Among those, cellular and extracellular oxidative stress, along with chronic inflammation are best-known to have a role in disease development and/or progression[4-6].

Aging, the strongest risk factor for AMD, is associated with structural and functional changes in Bruch`s membrane and the retinal-pigment epithelium (RPE). Drusen, a hallmark of AMD[7], are formed between RPE and Bruch's membrane, and contain polymorphous material. Major components of this material are lipid aggregates containing numerous lipoproteins and cholesterol[8, 9]. These results established a connection between lipid metabolism and AMD aetiology, which was confirmed further by genetic studies. Genome-wide association scans identified several genes contributing to HDL metabolism to be associated with AMD, among them hepatic lipase (*LIPC*), cholesterylester transfer protein (*CETP*), lipoprotein lipase (*LPL*), and ATP-binding cassette, sub-family A1 (*ABCA1*) [10, 11]. We and others also have found an association of paraoxonase 1 (*PON1*), a gene involved in HDL function, with advanced AMD in single populations[12-14].

Together with PON2 and PON3, PON1 forms a family of lactonases with antioxidant properties, which differ in sites of synthesis and mechanisms of action[15]. The *PON1* gene is mainly expressed in liver[16] and encodes a secreted enzyme with a broad spectrum of functions that favor the involvement of PON1 in AMD pathology. In particular, PON1 present in serum HDL inhibits low-density lipoprotein (LDL) oxidation, or "neutralizes" oxidized LDL by hydrolyzing lipid peroxides[17, 18]. Additionally, PON1 acts in an anti-inflammatory manner by reducing monocyte chemotaxis and adhesion to endothelial cells[19], inhibiting monocyte-to-macrophage differentiation[20], and directly suppressing macrophage proinflammatory responses[21]. The antioxidant as well as the anti-inflammatory activities of PON1 suppress the formation of atherosclerotic plaques, pathologic lesions that share several properties with drusen[22, 23]. Whereas PON2 is an ubiquitous intracellular protein that can protect endoplasmic reticulum and mitochondria against reactive oxygen species (ROS)-mediated damage[24, 25], PON3 acts similarly to PON1, as it is transported by HDL and protects HDL from oxidation[26].

The genetic studies mentioned above, biochemical analyses reporting lower serum paraoxonase activity in patients with AMD[27], and reports showing that smoking reduces PON1 activity in serum[28, 29] are indications for a potential involvement of PON1 in the pathophysiology of AMD. Nevertheless, the role of PON1 in the eye has not been studied to our knowledge. We used *Pon1*$^{-/-}$ mice to investigate the role of PON1 in the retina / RPE to elucidate its potential contribution to retinal lesions and eye pathology.

5.2. Materials and methods

5.2.1. Mice

Animals were treated in accordance with the regulations of the Veterinary Authority of Zurich and with the statement of `The Association for Research in Vision and Ophthalmology` for the use of animals in research. Wild type (WT) 129S6/SvEvTac mice were purchased from Taconics (Eiby, Denmark). *Pon1*$^{-/-}$ mice (B6.129X1-Pon1^{tm1Lus}/J)[30] were purchased from Jackson Laboratory (Bar Harbor, ME, USA), and genotyped by PCR using the following primers: common forward primer 5`-CTT GTC CAT CCT CAG CTT GT-3`, WT reverse primer 5`-CCG ATG GTT CTT GTA AAG TGC-3`, mutant reverse primer 5`-CTT GGG TGG AGA GGC TAT TC-3`. *Pon1*$^{-/-}$ mice were backcrossed for 10 generations onto the 129S6/SvEvTac background prior to analyses. All mice were kept at the animal facility of the University Hospital Zurich in a dark-light cycle (12 h: 12 h) with 60 lux of light at cage level and a normal chow diet.

5.2.2. Light exposure

Six- to 8-week-old mice were dark adapted overnight (16 h). Pupils were dilated with 1% cyclogyl (Alcon, Cham, Switzerland) and 5% phenylephrine (Ciba Vision, Niederwangen, Switzerland) 30 minutes before exposure to 17,000 lux of white light for 2 hours. After light exposure mice were kept in darkness until the next day before being returned to cyclic light. Mice were killed at different time points after light offset (N=3 for each group) and retinas, eyecups, or whole eyeballs were removed. Mice that were dark-adapted but not exposed to light served as controls.

5.2.3. Laser capture microdissection

Eyes of 8-week-old WT and *Pon1*$^{-/-}$ mice were enucleated, immediately embedded in tissue freezing medium (Leica Microsystems Nussloch GmbH, Nussloch, Germany), and frozen in a 2-methylbutane bath cooled in liquid nitrogen. Retinal sections (20 µm) were

collected on Arcturus PEN Membrane Glass Slides (Applied Biosystems, Foster City, CA, USA), fixed (5 min acetone), air dried (5 min), and dehydrated (30 sec 100% ethanol, 5 min xylol). Retinal layers were isolated using an Arcturus XT Laser Capture Microdissection system (Bucher Biotec AG, Basel, Switzerland) and Arcturus CapSure Macro LCM Caps (Applied Biosystems). RNA was isolated using the Arcturus PicoPure RNA Isolation Kit (Applied Biosystems) according to the manufacturer's directions, including a DNase treatment to remove residual genomic DNA. cDNA was synthesized using random hexamer primers (High-Capacity cDNA Reverse Transcription Kit; Applied Biosystems), and further analyzed by real-time PCR as described in section `RNA preparation and semi-quantitative real-time PCR`.

5.2.4. Electroretinogram (ERG)

Electroretinograms were recorded from both eyes simultaneously following published protocols[31, 32]. Briefly, mice were dark-adapted overnight and anesthetized the next day with ketamine (66.7 mg/kg; Ratiopharm GmbH, Ulm, Germany) and xylazine (11.7 mg/kg; Bayer HealthCare, Monheim, Germany). Pupils were dilated with 1% cyclogyl and 5% phenylephrine 30 min before performing single flash ERG recordings under dark-adapted (scotopic) and light adapted (photopic) conditions. Light adaptation was accomplished with low background illumination starting 5 min before photopic recordings. Single white-flash stimulus intensities ranged from –3.7 to 1.9 log cd*s/m^2 under scotopic and from –0.6 to 2.9 log cd*s/m^2 under photopic conditions, divided into 12 and 8 steps, respectively. Ten responses per flash intensity were averaged with an interstimulus interval of either 4.95 sec or 16.95 sec (for 1.4, 1.9, 2.4, and 2.9 log cd*s/m^2).

5.2.5. Fundus imaging and fluorescein angiography

Pupils were dilated with 1% cyclogyl and 5% phenylephrine. After 30 min mice were anesthetized with ketamine (66.7 mg/kg) and xylazine (11.7 mg/kg) and corneas were moistened with 2% methocel (OmniVision, Puchheim, Germany). Fundi were monitored and photographed using a mouse imaging system (Micron III, Phoenix Research Laboratories, Pleasanton, CA, USA). Fluorescein solution (2% in PBS; AK-FLUOR; Lake Forest, IL, USA) was injected intraperitoneally and eyes were analyzed immediately.

5.2.6. Light and transmission electron microscopy

Eyes were enucleated and fixed in 2.5% glutaraldehyde in 0.1 M cacodylate buffer (pH 7.3) at 4˚C overnight. Cornea and lens were removed and eyecups cut dorso-ventrally through the optic nerve head. Trimmed tissue was washed in cacodylate buffer, incubated in osmium tetroxide for 1 hour at room temperature, dehydrated, and embedded in Epon 812. For light microscopy (Axioplan 2, Zeiss, Feldbach, Switzerland) semi-thin cross sections (500 nm) were cut and counterstained with toluidine blue. For transmission electron microscopy (TEM), ultra-thin sections (50 nm) were stained with uranyl acetate and lead citrate, and analyzed using a Philips CM100 transmission electron microscope.

5.2.7. RPE flat mount preparation and analysis

Unless stated otherwise, all procedures were conducted at room temperature. Eyes were enucleated and incubated in 2% paraformaldehyde (PFA) in 0.1 M phosphate buffer pH 7.4 (PB, 0.081M Na_2HPO_4, 0.019M $NaH_2PO_4 \times H_2O$) for 5 min. Cornea and lens were removed and the remaining tissue was left in PB-salt (PB containing 140 mM NaCl and 2.7 mM KCl) for 20 min to allow the retina to separate from the eyecup. The retina was gently removed and the eyecup containing the RPE cut into a "clover-leaf" shape and post-fixed in 4% PFA in PB for 1 hour. Flatmounts were blocked with blocking solution (3% normal goat serum, 0.3% Triton X-100 in PBS) for 1 hour and incubated with the primary antibody anti-β-catenin (1:300 in blocking solution; BD Biosciences, Allschwil, Switzerland) overnight at 4°C. After washing 3 x 10 min in PBS, Cy3-conjugated anti-mouse secondary antibody (1:200 in blocking solution; Jackson ImmunoResearch, Suffolk, UK) and Alexa Fluor 488-phalloidin (1.3 U/ml in blocking solution; Applied Biosystems) were applied for 2 hours. After washing, cell nuclei were stained with Hoechst (2 µg/ml in PBS; Sigma Aldrich, Buchs, Switzerland) for 30 min. Flatmounts were washed with PBS and mounted with anti-fade medium (10% Mowiol 4–88 (w/v); Calbiochem, San Diego, CA, USA; 25% glycerol (w/v); 0.1% 1,4-diazabicyclo[2.2.2]octane in 100 mM Tris, pH 8.5). RPE sheets were examined using a digitalized fluorescence microscope and an ApoTome module (Axioplan 2, Zeiss, Switzerland).

Morphometric measurements including eccentricity and form factor were performed with CellProfiler software[33]. Phalloidin-stained images (magnification: 20x) were illumination corrected and analyzed using the `Tissue Neighbours` pipeline with the background adaptive thresholding method. At least N=700 RPE cells per group were examined. RPE cells were counted in 4 quadrants of 176.8 x 235.3 µm (1040 x 1384 pixels),

approximately 800-900 µm temporal, dorsal, nasal and ventral of the optic nerve head. Three animals per genotype and condition were analyzed.

5.2.8. RNA preparation and semi-quantitative real-time PCR

Retinas were removed through a slit in the cornea and placed in an Eppendorf tube. The rest of the eye (eyecup without lens) was isolated separately. All samples were immediately frozen in liquid nitrogen and stored at -80°C. Total RNA from retina and eyecups was prepared using the High Pure RNA Isolation Kit (Roche Diagnostics, Mannheim, Germany) or the RNeasy kit (Qiagen, Hilden, Germany), respectively. RNA isolations included a DNase treatment to digest residual genomic DNA. Equal amounts of RNA were reverse transcribed using oligo(dT) primer and M-MLV reverse transcriptase (Promega, Madison, WI, USA). Real-time PCR with specific primer pairs (Table 1), a polymerase ready mix (LightCycler 480 SYBR Green I Master Mix; Roche Diagnostics, Basel, Switzerland), and a thermocycler (LightCycler, Roche Diagnostics) were used to study gene expression. Three animals per time point were analyzed in duplicates. Signals were normalized to *β-actin* and relative gene expression was calculated using the ΔΔCt method.

Table 1. Primers and conditions for real-time PCR

Gene	Forward 5`-3`	Reverse 5`-3`	Annealing temperature (°C)	Product (bp)
Pon1	GCATCTGAAAACCATCACACA	AAGCTCTCAGGTCCAATAGCA	60	72
Pon2	CAGAGGCTCTTCGTGTACCA	ATGTTCTGAATGCGGAGGAC	60	88
Pon3	TTGACCGTTGATCCAGCCAC	GAAGCACAGAGCCGTTGTTC	62	175
Sod1	GAGCAGAAGGCAAGCGGTGA	AGGTCCTGCACTGGTACAGC	62	126
Sod2	GACCTGCCTTACGACTATGG	CTGAAGAGCGACCTGAGTTG	62	168
Hmox1	CCGCCTTCCTGCTCAACATT	GACGAAGTGACGCCATCTGTG	62	99
Abca1	GCGTGAAGCCTGTCATCTAC	CATGAGAGGAGTGATCGACC	62	185
Scarb1	CGCACAGTTGGTGAGATCCT	CACCAGATGGATCCTGCTGA	62	183
Lif	AATGCCACCTGTGCCATACG	CAACTTGGTCTTCTCTGTCCCG	60	216
Edn2	AGACCTCCTCCGAAAGCTG	CTGGCTGTAGCTGGCAAAG	60	64
Fgf2	TGTGTCTATCAAGGGAGTGTGTGC	ACCAACTGGAGTATTTCCGTGACCG	62	158
Stat3	CAAAACCCTCAAGAGCCAAGG	TCACTCACAATGCTTCTCCGC	62	139
Socs3	ATTTCGCTTCGGGACTAGC	AACTTGCTGTGGGTGACCAT	58	126
Mct3	GGCTCAACCCTAAATCCAGA	CTTCGGAGTTTCCTCACCAG	58	75
Gnat1	GAGGATGCTGAGAAGGATGC	TGAATGTTGAGCGTGGTCAT	58	209
Vsx2	CCAGAAGACAGGATACAGGTG	GGCTCCATAGAGACCATACT	60	111
Opn4	CCAGCTTCACAACCAGTCCT	CAGCCTGATGTGCAGATGTC	62	111
Actb	CAACGGCTCCGGCATGTGC	CTCTTGCTCTGGGCCTCG	62	153

5.2.9. Lipid extraction

For most analyses, lipids were extracted from retinal and eyecup tissue together. We will refer to these samples as “retina/eyecup” samples from here on. In some instances retinas and eyecups were isolated separately and named accordingly. Isolated tissue samples were immediately frozen in liquid nitrogen and stored at -80°C. Retina/eyecup samples were

homogenized in lysis buffer (PBS, 0.2% Triton X-100 [v/v]) using a Precellys 24 tissue homogenizer (Bertin Technologies, Montigny-le-Bretonneux, France). The protein content was measured using the Bradford assay. Total lipids were extracted from aliquots of homogenized tissue containing 40 µg of protein. Extraction was conducted according to the procedure of Bligh and Dyer[34] in the presence of 200 ng of the internal standards PG(17:0/17:0), LPG(17:1/0:0), PA(14:0/14:0), LPA(17:0/0:0), PE(14:0/14:0), LPE(17:1/0:0), PC(14:0/14:0), PC(24:0/24:0), LPC(17:0/0:0), SM (d18:1/12:0) and Cer(d18:1/17:0) (Avanti Polar Lipids, Alabaster, AL, USA). Samples were mixed with 375 µl of methanol/chloroform (2:1, v/v) and vortexed, followed by the addition of 100 µl water and 125 µl chloroform. The mixture was shaken for 15 minutes and centrifuged at 16,100×g for 5 minutes at 25°C. The lower phase was collected, 250 µl chloroform added, shaken for 15 minutes, and centrifuged at 16,100×g for 5 minutes at 25°C. All lower phases were combined and evaporated to dryness under a stream of nitrogen. Dried material was reconstituted in 200 µl of a mixture of mobile phases A (80%) and B (20%, see below). 10 µl was injected into the liquid chromatography-mass spectrometry (LC-MS) system for phospholipid analysis.

5.2.10. Analysis of the retina/eyecup lipidome: LC-MS instrumentation and chromatographic conditions

Analyses of six different lipid classes: phosphatidylcholines (PC), sphingomyelins (SM), phosphatidylethanolamines (PE), phosphatidylglycerols (PG**)**, phosphatidic acids (PA) and ceramides/hexosylceramides (Cer/HexCer) were performed by using LC-MS. Briefly, total lipid extracts were analyzed on a LC-MS system consisting of a Rheos 2200 pump (Flux Instruments, Reinach, Switzerland), an HTC PAL autosampler (CTC Analytics, Zwingen, Switzerland) and a TSQ Quantum Access triple quadrupole mass analyzer (Thermo Fisher Scientific, Waltham, MA, USA). Separation of lipid extracts was performed on a diol silica-based column (QS Uptisphere 6 OH, 150 x 2.1 mm, 5 µm, Interchim, Montlucon, France). Mobile phase A was a mixture of hexane/isopropanol/water (70:30:2, v/v) with 15 mM ammonium formate. Mobile phase B was isopropanol/water (50:2, v/v) with 15 mM ammonium formate. The solvent-gradient was 0 to 7 minutes A/B (%) 80/20, 8 to 10 minutes A/B (%) 60/40, 11 to 23 minutes A/B (%) 40/60 and 25 to 30 minutes A/B (%) 80/20 at a flow rate of 0.35 ml/min. The column was maintained at 30°C. Mass spectrometry was performed in positive ionization mode with the following parameters: 4500 V spray voltage, skimmer voltage 2 - 14 V (depending on the scan mode), 250°C capillary temperature, and 10 and 6 (arbitrary units) sheath and auxiliary N_2 gas, respectively. Molecular masses provided

by a neutral loss and precursor scan were used to selectively detect specific phospholipids. A neutral loss of masses m/z 115 and 189 from $[M+NH_4]^+$ ions were used for analysis of PA and PG lipids, respectively. A precursor ion scan of m/z 184 specific for phosphocholine-containing lipids was used for PC, SM and LPC. A neutral loss scan of m/z 141 was used for PE and a precursor scanning of m/z 264 was applied for screening of Cer. Acquired data were analyzed using Xcalibur (version 2.0.6, Thermo Fisher Scientific). The structure of the head groups were determined from the type of MS/MS scanning. Molecular species were identified by using LIMSA software[35]. All species were assigned to the lipid classes and species with a defined total numbers of carbon atoms and double bounds in acyl and/or alkyl chains. Data were corrected for isotopic overlap. Quantification was based on calibration curves for seven lipid standards including PC(16:0/18:2), SM(d18:1/16:0), LPC(16:0), PE(18:0/18:0), Cer(d18:1/14:0), PG(16:0/16:0), and PA(14:0/14:0). The calibration curves were constructed by plotting the PL/IS peak area ratios against the nominal concentration of the standards. The concentrations for the individual lipid species were calculated from linear regressions of the calibration curves.

5.2.11. Statistical analysis

Semiquantitative real-time PCR and morphometric analysis of the RPE flat mounts. Statistical analyses were performed using Prism4 software. All data are given as means ± SD of three animals per group. Statistical differences of means were calculated using 2-way ANOVA followed by a Bonferroni post hoc test. A p value of less than 0.05 was considered significant.

Lipidomics analysis. Statistical analyses were performed using SPSS, version 19 (SPSS Switzerland, Zurich, Switzerland). Normality of the data was determined by using the Kolmogorov-Smirnov test. Since not all lipid species had normally distributed values, the nonparametric Mann-Whitney U test was used. The Mann-Whitney U test was applied for comparison between *Pon1*$^{-/-}$ and WT mice. Bonferroni correction was applied to adjust the p value for multiple comparisons (37 statistical tests). A p value of 0.001 or below was considered significant. Data are presented as median with lower and upper range values.

5.3. Results

5.3.1. *Paraoxonase 1* is highly expressed in the RPE

To evaluate the expression pattern of paraoxonases in the retina we isolated the RPE, the outer nuclear layer (ONL), the inner nuclear layer (INL) and the ganglion cell layer (GCL) by laser capture microdissection, and analyzed levels of *Pon1*, *Pon2* and *Pon3* mRNA by semiquantitative real-time PCR (Fig. 1). Expression of monocarboxylate transporter, member 3 (*Mct3*; RPE), guanine nucleotide binding protein, alpha transducing activity polypeptide (*Gnat1*; ONL), visual system homeobox 2 (*Vsx2*; INL), and melanopsin (*Opn4*; GCL) were used as layer-specific markers and showed that cross-contamination between collected layers was minimal. In WT mice, *Pon1* was highest expressed in the RPE with 267-, 590-, and 651-fold higher levels than in ONL, INL, and GCL, respectively. Similarly, *Pon3* was most abundant in the RPE (45-, 43-, 72-fold higher levels than in ONL, INL, and GCL, respectively). *Pon2* content was comparable in the RPE and the INL, approximately 25- and 9-fold higher than in ONL and GCL, respectively.

Even though *Pon1*$^{-/-}$ mice have a neomycin cassette inserted into exon 1 of *Pon1* and no paraoxonase activity[30], the RNA transcript from the disrupted gene can still be detected by real-time PCR. Interestingly, we found differential effects of the neomycin insertion on *Pon1* expression in RPE and neuronal retina. Whereas expression of the disrupted *Pon1* gene was 33-fold decreased in the RPE, it was 15-fold increased in the INL and 6-fold in the GCL, indicating differential regulation of *Pon1* expression in RPE and neuroretina. Levels of *Pon2* and *Pon3* transcripts were not significantly affected by the lack of functional PON1.

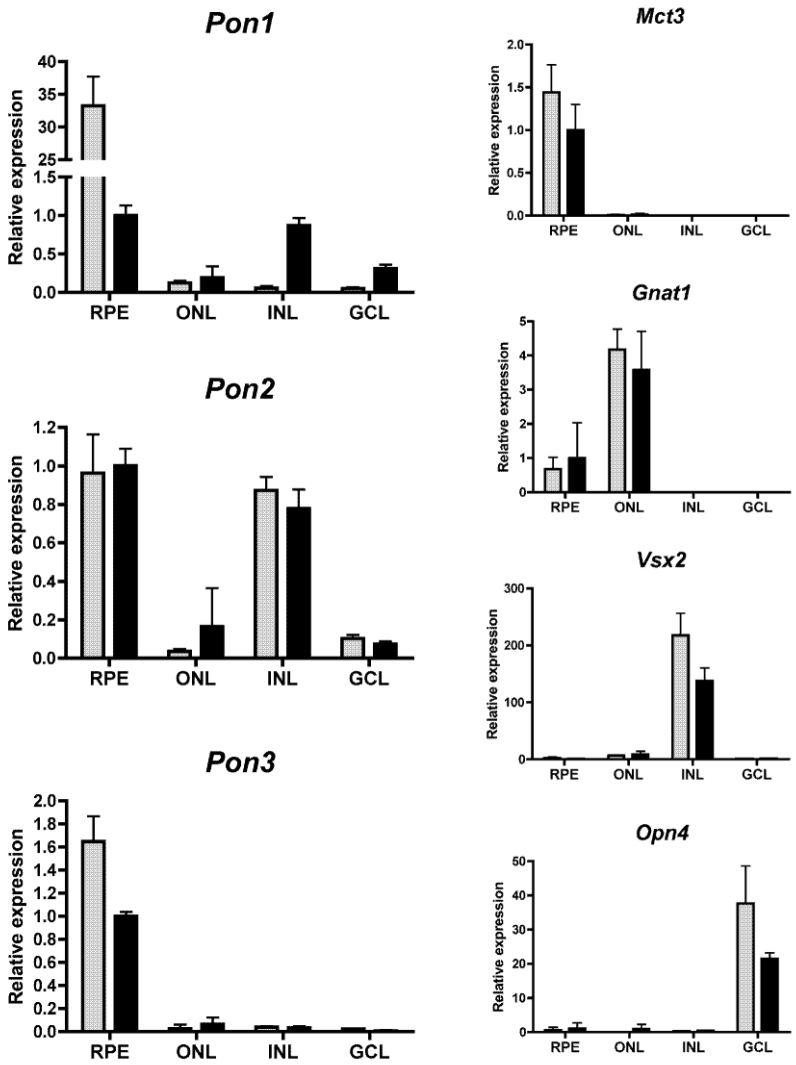

Figure 1. *Pon1* is highly expressed in the RPE.
Retinal pigment epithelium (RPE), outer nuclear layer (ONL), inner nuclear layer (INL) and ganglion cell layer (GCL) were isolated from WT (grey bars) and *Pon1*$^{-/-}$ mice (black bars) using laser capture microdissection. Relative gene expression was determined by semi-quantitative real-time PCR in each individual layer. Values were normalized to *β-actin*, and expressed relative to levels in the RPE of *Pon1*$^{-/-}$ mice, which were set to 1. Shown are mean values ± SD of N=3. Expression of *Mct3* (marker for RPE), *Gnat1* (marker for ONL), *Vsx2* (marker for INL), and *Opn4* (marker for GCL) was determined to monitor contamination between the isolated retinal layers.

5.3.2. Absence of PON1 does not compromise retinal function and architecture

To evaluate whether PON1 is important for normal retinal development, ageing and function, we analyzed 8-week and 1-year old mice. *Pon1*$^{-/-}$ mice showed regular retinal architecture and no signs of RPE or photoreceptor degeneration at either age (Fig. 2A). Similarly, funduscopy and fluorescein angiography revealed no retinal or vascular defects in *Pon1*$^{-/-}$ mice (Fig. 2B). Normal scotopic and photopic ERGs with a- and b-wave amplitudes similar to WTs (Fig. 2C) supported the conclusion that *Pon1*$^{-/-}$ mice developed a normal and functional retina.

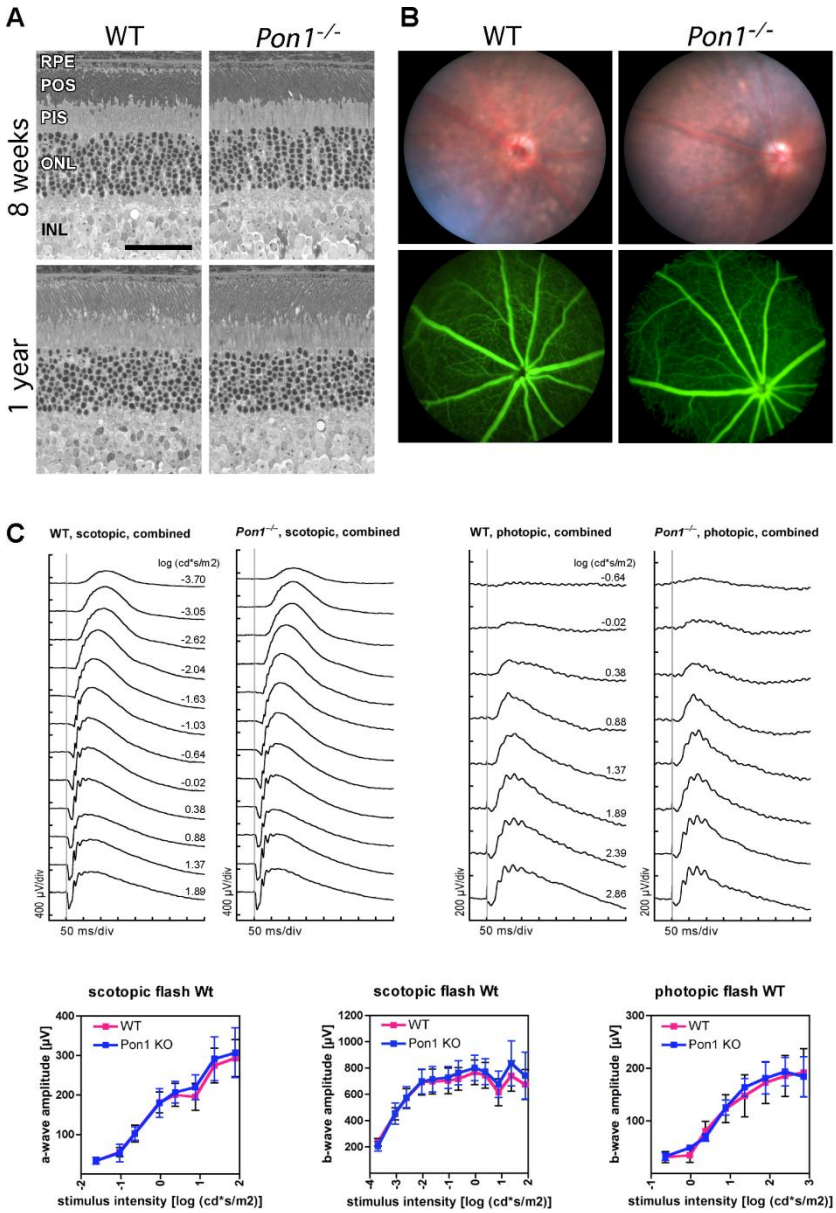

Figure 2. Lack of PON1 does not compromise retinal architecture and function

Figure 2A: Retinal morphology of *Pon1*$^{-/-}$ and control mice (WT) at 8 weeks and 1 year of age. Shown are representative sections of N=3. RPE, retinal pigment epithelium; POS, photoreceptor outer segments; PIS, photoreceptor inner segments; ONL, outer nuclear layer; INL, inner nuclear layer. Scale bar: 50 µm. Figure 2B: Funduscopy (top panels) and

fluorescein angiography (bottom panels) of WT and *Pon1*$^{-/-}$ mice at 8 weeks of age. Shown are representative images of N=3. Figure 2C: Scotopic and photopic electroretinograms from WT and *Pon1*$^{-/-}$ mice at 8 weeks of age. Top panels: representative traces from individual mice. Bottom panels: scotopic a- and b-wave amplitudes, as well as photopic b-wave amplitudes as a function of light intensity. N=3.

5.3.3. Lack of PON1 does not affect RPE morphology

Since we found high *Pon1* expression in the RPE and *PON1* was previously implicated in AMD[12-14, 27], a disease strongly affecting RPE and Bruch`s membrane, we examined these structures in young and old mice. Transmission electron microscopy did not detect any obvious differences in the ultrastructure of RPE and Bruch`s membrane between *Pon1*$^{-/-}$ and WT mice at any age (Fig. 3A). Also, RPE microvilli and basal infoldings appeared normal and no AMD-like features, such as Bruch`s membrane thickening or sub-RPE deposits[36], were present in any of the analyzed animals up to one year of age.

To analyze RPE cell morphology on a larger scale, we prepared RPE flat mounts. The RPE monolayer is normally formed by a relatively uniform array of polygonal cells containing one to two centrally positioned nuclei. The regular shape is maintained by adherens and tight junctions, as well as by the actin-myosin cytoskeleton, whose components may serve as markers of epithelial integrity. We monitored the RPE cell boundaries by immunofluorescent staining for β-catenin (adherens junctions) and phalloidin (F-actin), and did not observe any abnormalities in mice lacking PON1 up to one year of age (Fig. 3B). This was further supported by morphometric analyses, which were used to quantitatively assess RPE cell shape. The eccentricity (ECC) and form factor (FF) are two measures of distortion from a circular shape, whose values vary between 0 and 1, with ECC=0 and FF=1 for a perfect circle. These factors did not differ significantly between cells in the RPE of *Pon1*$^{-/-}$ and age-matched WT mice (Fig. 3C).

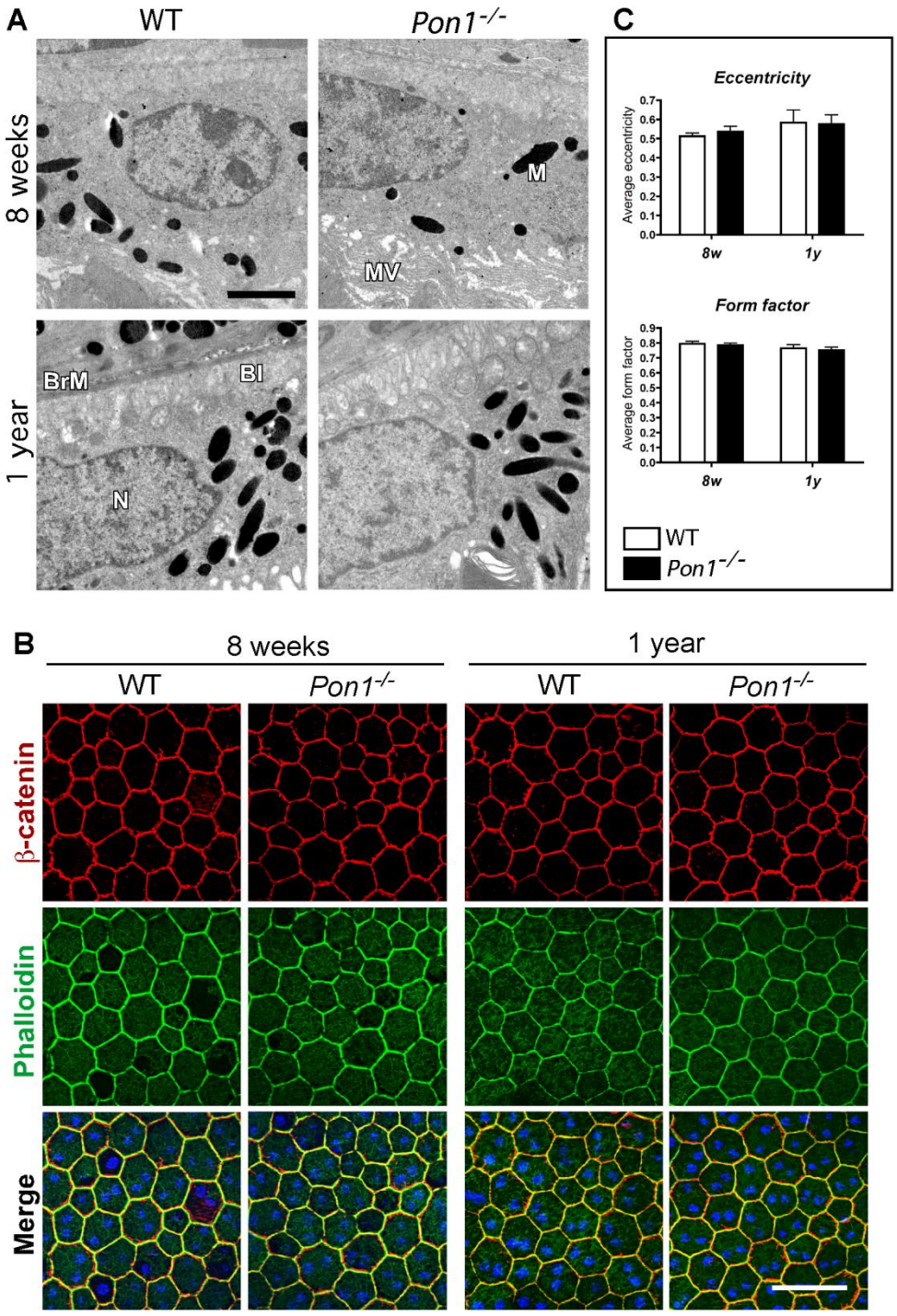

Figure 3. Lack of PON1 does not affect RPE morphology

The RPE was analyzed in *Pon1*$^{-/-}$ and control (WT) mice at 8 weeks (8w) and 1 year (1y) of age. Figure 3A: Transmission electron micrographs of the RPE and adjacent tissues. Shown are representative sections of N=3 for each panel. N, nucleus; BrM, Bruch`s membrane; BI, basal infoldings; MV, apical microvilli; M, melanosomes. Scale bar: 2 µm. Figure 3B: RPE flat mounts immunostained for β-catenin (red) and phalloidin (green). Nuclear staining (Hoechst) is visible in blue. Shown are representative microphotographs of N=3 for each panel. Scale bar: 50 µm. Figure 3C: Morphometric analysis of RPE cells. Shown are mean values ± SD of at least N=700 RPE cells examined per group. Two-way ANOVA revealed no significant differences in RPE cell shape between WT and *Pon1*$^{-/-}$ mice at 8w and 1y of age ($p>0.05$).

5.3.4. Gene expression in *Pon1*$^{-/-}$ mice

To reveal whether the lack of PON1 influences expression of related genes or of genes encoding known PON1 interaction partners, we analyzed gene expression in retina and eyecup at 8 weeks and 1 year of age. Similar to the LCM data (Fig. 1), expression of *Pon1* was lower in the neuronal retina compared to that in the eyecup (Fig. 4). Cross-contamination between RPE and neuronal retina was minimal as shown by the relative expression of *Mct3* (RPE) and *Gnat1* (retina) in both isolated compartments (Table 2).

In accordance with the LCM experiment, we found significant up-regulation of *Pon1* mRNA expression in the retina of 8 week old *Pon1*$^{-/-}$ mice and down-regulation in the eyecup. Since lack of the antioxidative PON1 protein may influence the oxidative balance in a tissue, expression of other antioxidative genes may be affected. However, both other members of the paraoxonase family (*Pon2* and *Pon3*), the two superoxide dismutases (*Sod1* and *Sod2*), as well as heme oxygenase 1 (*Hmox1*) were similarly expressed in control and *Pon1*$^{-/-}$ mice (Fig. 4). Remarkably, we detected an age-related moderate decrease in the expression of *Sod1*, *Sod2*, *Pon3* (retina and eyecup), *Pon2* (retina), *Pon1* and *Hmox1* (eyecup) independently of the *Pon1* genotype (Fig. 4 and Table 2).

Previous studies showed that the role of PON1 in HDL transport and function involves interaction with partner proteins, such as scavenger receptor class B (SCARB1, also known as SR-BI) and ATP-binding cassette transporter (ABCA1). Whereas SCARB1 facilitates acquisition of PON1 secreted from hepatocytes[37], interaction between PON1 and ABCA1 transporter enhances HDL-mediated cholesterol efflux from macrophages[38]. Both SCARB1 and ABCA1 were shown previously to be involved in lipid efflux and reverse cholesterol transport in retina and RPE[39], and this function might depend on interaction with PON1. Nevertheless, expression of *Scarb1* was similar in control and *Pon1*$^{-/-}$ mice at either age. The expression of *Abca1* was also similar in old control and knockout mice, whereas expression in young *Pon1*$^{-/-}$ mice was variable in different sets of animals (see also Fig. 5), suggesting the influence of other, yet unknown factors. Further studies are required to investigate a potential functional connection between *Pon1* and *Abca1* in the retina.

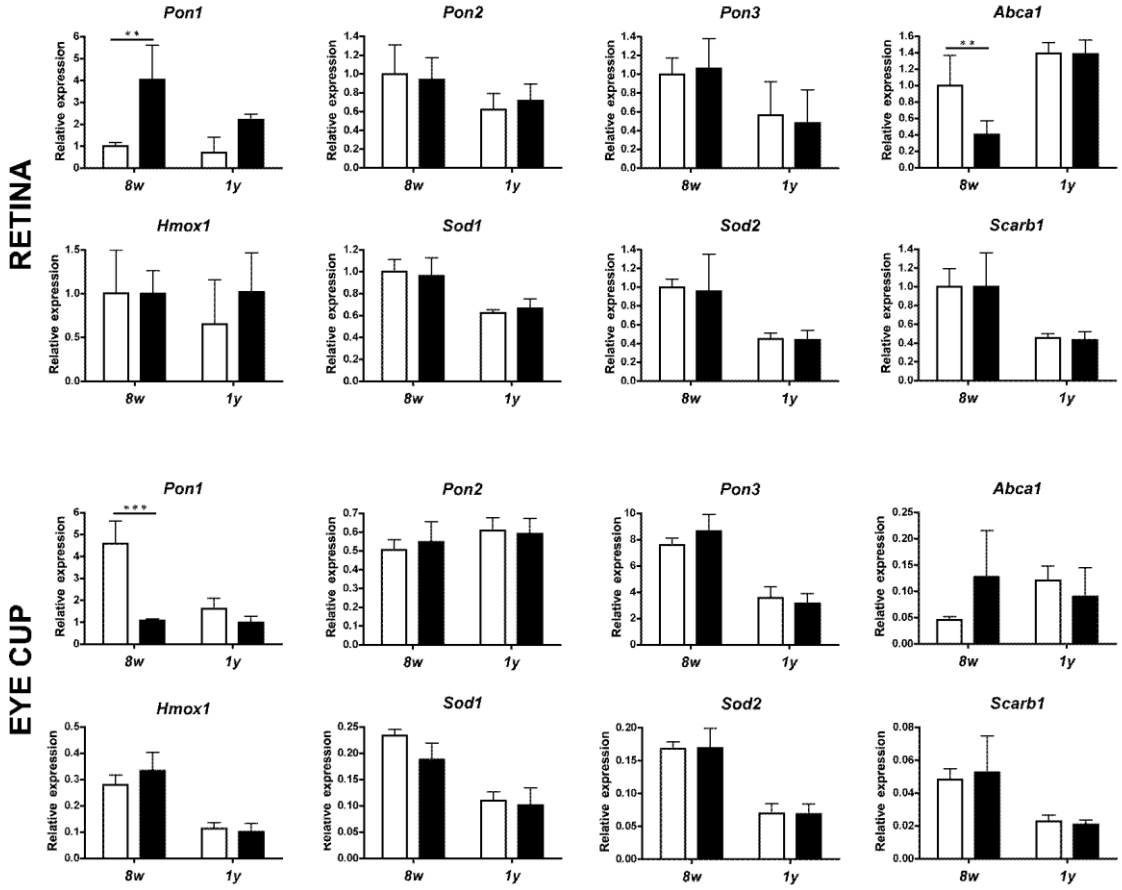

Figure 4. Expression of PON1-related genes

Expression of genes related to PON1 function was determined by semi-quantitative real-time PCR in retinas (upper panels) and eyecups (lower panels) of WT (white bars) and *Pon1*$^{-/-}$ mice (black bars) at 8 weeks (8w) and 1 year (1y) of age as indicated. Shown are mean values ± SD of N=3. Values were normalized to *β-actin*, and levels in WT mice at 8w were set to 1. Two-way ANOVA with Bonferroni post-hoc analysis was used to test statistical significance. A p-value of less than 0.05 was considered significant; **p<0.01; ***p<0.001. Shown are statistics for the comparison of expression levels in WT and *Pon1*$^{-/-}$ mice at 8w or 1y of age. See Table 2 for statistical analysis of age-dependent expression in WT and *Pon1*$^{-/-}$ mice.

Table 2. Expression of PON1-related genes in retinas and eyecups of *Pon1*$^{-/-}$ and WT mice at 8 weeks (8w) and one year (1y) of age.

		Mean ± SD				2-way ANOVA			
						WT vs. *Pon1*$^{-/-}$		8w vs. 1y	
	Gene	WT, 8w	*Pon1*$^{-/-}$, 8w	WT, 1y	*Pon1*$^{-/-}$, 1y	8w	1y	WT	*Pon1*$^{-/-}$
RETINA	***Pon1***	1 ± 0.16	4.04 ± 1.57	0.71 ± 0.7	2.21 ± 0.24	p < 0.01	ns	ns	ns
	Pon2	1 ± 0.31	0.94 ± 0.23	0.62 ± 0.17	0.72 ± 0.18	ns	ns	ns	ns
	Pon3	1 ± 0.18	1.06 ± 0.31	0.57 ± 0.36	0.48 ± 0.35	ns	ns	ns	ns
	Hmox1	1 ± 0.50	1 ± 0.26	0.65 ± 0.50	1.02 ± 0.44	ns	ns	ns	ns
	Sod1	1 ± 0.11	0.96 ± 0.16	0.62 ± 0.03	0.67 ± 0.09	ns	ns	p < 0.01	p < 0.05
	Sod2	1 ± 0.09	0.95 ± 0.40	0.45 ± 0.06	0.44 ± 0.1	ns	ns	p < 0.05	p < 0.05
	Scarb1	1 ± 0.19	1 ± 0.36	0.45 ± 0.05	0.44 ± 0.08	ns	ns	p < 0.05	p < 0.05
	Abca1	1 ± 0.18	0.4 ± 0.17	1.4 ± 0.13	1.39 ± 0.17	p < 0.01	ns	ns	p < 0.001
	Mct3	1 ± 0.75	5.1 ± 5.54	2.03 ± 2.12	0.38 ± 0.14	ns	ns	ns	ns
	Gnat1	1 ± 0.53	0.87 ± 0.32	1.74 ± 0.30	1.67 ± 0.5	ns	ns	ns	p < 0.05
EYE CUP	***Pon1***	4.58 ± 1.04	1.08 ± 0.06	1.61 ± 0.47	0.98 ± 0.28	p < 0.001	ns	p < 0.001	ns
	Pon2	0.51 ± 0.05	0.55 ± 0.11	0.61 ± 0.07	0.59 ± 0.08	ns	ns	ns	ns
	Pon3	7.59 ± 0.52	8.64 ± 1.26	3.57 ± 0.85	3.15 ± 0.74	ns	ns	p < 0.001	p < 0.001
	Hmox1	0.28 ± 0.04	0.33 ± 0.07	0.11 ± 0.02	0.1 ± 0.03	ns	ns	p < 0.01	p < 0.001
	Sod1	0.23 ± 0.01	0.19 ± 0.03	0.11 ± 0.02	0.1 ± 0.03	ns	ns	p < 0.001	p < 0.01
	Sod2	0.17 ± 0.01	0.17 ± 0.03	0.07 ± 0.01	0.07 ± 0.02	ns	ns	p < 0.001	p < 0.001
	Scarb1	0.05 ± 0.01	0.05 ± 0.02	0.02 ± 0.00	0.02 ± 0.00	ns	ns	ns	p < 0.05
	Abca1	0.05 ± 0.01	0.13 ± 0.09	0.12 ± 0.03	0.09 ± 0.05	ns	ns	ns	ns
	Mct3	48.63 ± 3.78	46.75 ± 11.48	27.28 ± 6.25	19.38 ± 12.22	ns	ns	p < 0.05	p < 0.01
	Gnat1	0.004 ± 0.01	0.01 ± 0.02	0.01 ± 0.01	0.001 ± 0.001	ns	ns	ns	ns

Expression of genes related to PON1 function was determined by semi-quantitative real-time PCR. Shown are mean values ± SD of N=3. Values were normalized to *β-actin* and expressed relative to levels in the retina of WT mice at 8 weeks of age, which were set to 1. Two-way ANOVA with Bonferroni post-hoc analysis was used to test the statistical significance. A p-value of less than 0.05 was considered significant; ns, not significant. *Pon1*, paraoxonase 1; *Pon2*, paraoxonase 2; *Pon3*, paraoxonase 3; *Abca1*, ATP-binding cassette, sub-family A (ABC1), member 1; *Scarb1*, scavenger receptor class B, member 1; *Hmox1*, heme oxygenase 1; *Sod1*, superoxide dismutase 1; *Sod2*, superoxide dismutase 2, *Mct3*, monocarboxylate transporter, member 3 (marker for RPE); *Gnat1*, guanine nucleotide binding protein, alpha transducing activity polypeptide (marker for the neuronal retina).

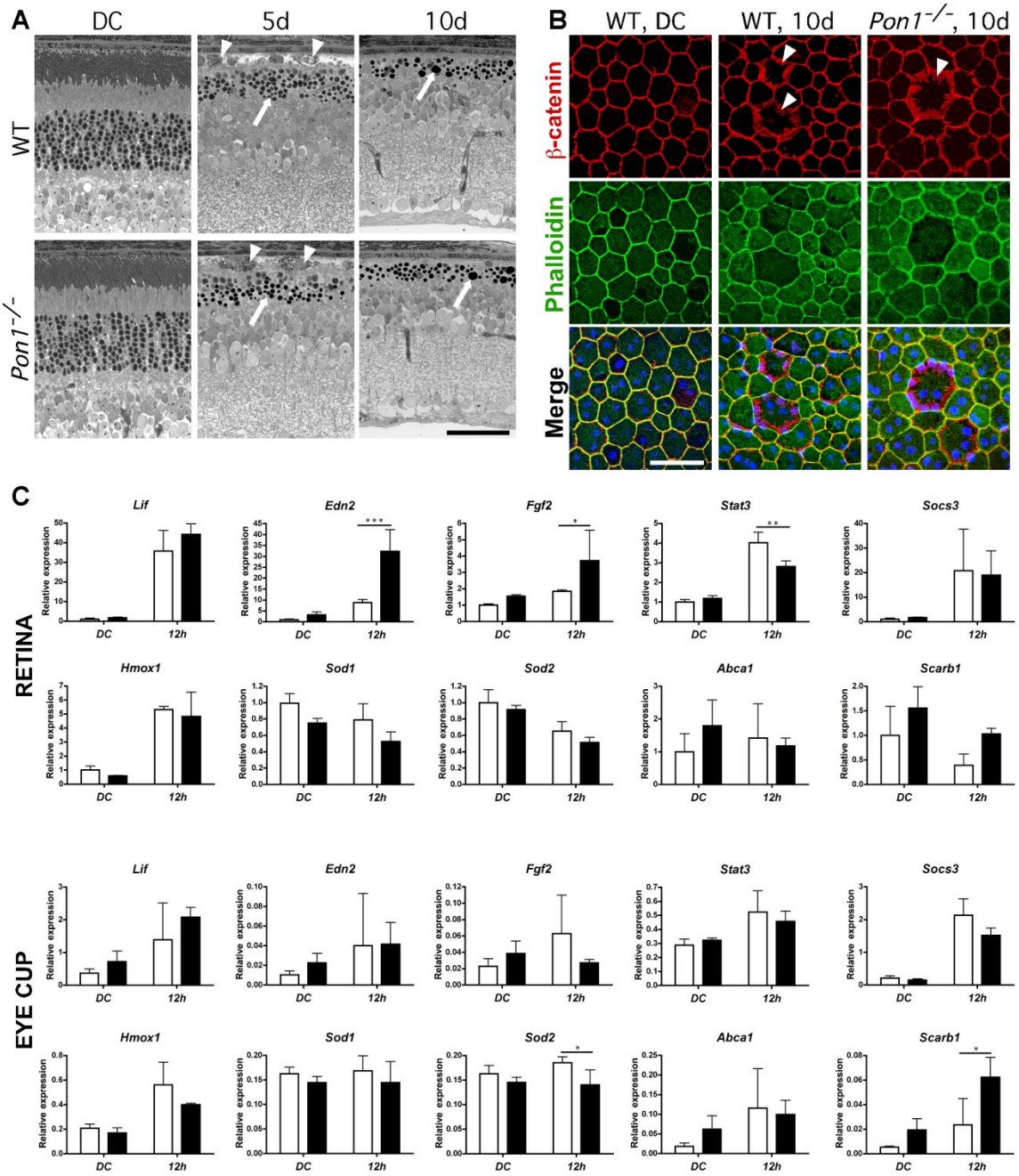

Figure 5. PON1 does not protect against damage by acute light exposure.

Figure 5A: Representative light micrographs of retinas of 8-week old control (WT) and *Pon1*$^{-/-}$ mice at 5 and 10 days after light exposure. Control mice (dark control, DC) were reared in normal cyclic light conditions (12 hours dark; 12 hours light) and not exposed to light. Arrows: pyknotic nuclei indicating photoreceptor cell death. Arrowheads: macrophages in the subretinal space. Shown are representative sections of N=3. Scale bar: 50 μm. Figure 5B: Immunostaining of RPE flat mounts from 8-week old WT and *Pon1*$^{-/-}$ dark control (DC) mice and at 10 days after light exposure (10 d). Red: β-catenin; green: phalloidin; arrowheads: diffuse β-catenin staining in RPE cells of light exposed mice. Scale bar: 50 μm. Figure C5: Gene expression in retinas (upper panels) and eyecups (lower panels) of 8-week old WT (white bars) and *Pon1*$^{-/-}$ (black bars) mice

at 12 hours after light exposure (12 h) or in dark controls (DC). Values were normalized to *b-actin* and expressed relative to the levels in the retina of unexposed WT animals, which were set to 1. Shown are mean values ± SD of N=3. Two-way ANOVA with Bonferroni post-hoc analysis was used to test significance. A p-value of less than 0.05 was considered significant; *p<0.05; **p<0.01; ***p<0.001. Shown are significantly different expression levels between WT and *Pon1*$^{-/-}$ mice in DC or light exposed mice. See Table 3 for statistical analysis of differences in gene expression between DC and light exposed WT and DC and light exposed *Pon1*$^{-/-}$ mice.

5.3.5. Alterations of phospholipid composition in retina/eyecup samples of *Pon1*$^{-/-}$ mice

The retina contains very high levels of polyunsaturated fatty acids (PUFAs). The majority of retinal PUFAs is esterified to phospholipids, which build up the membranous disks of photoreceptor outer segments[40]. Due to their molecular structure and constant exposure to a photo-oxidative environment[5, 6], retinal phospholipids are particularly prone to oxidative modifications. Based on the fact that PON1 can reduce lipid peroxidation in LDL and cell membranes[17, 19], we hypothesized that PON1 might have a similar effect on retinal phospholipids, and thus affect their composition. To test this assumption, we employed a combination of LC and MS for the identification and quantification of retina/eyecup phospholipids from WT and *Pon1*$^{-/-}$ mice.

The overall phospholipid profile was similar in the retina/eyecup samples of WT and *Pon1*$^{-/-}$ mice at the age of 8 weeks. The most abundant phospholipids were PCs and PEs (Table 4). The most abundant PE species was PE 40:6, which possibly contained polyunsaturated $C_{22:6n-3}$ docosahexaenoic (DHA) fatty acid at the *sn-1* or *sn-2* position of the glycerol backbone. The PC 40:6 was the third most abundant PC species after PC 32:0 and PC 34:1. Interestingly, highly unsaturated PC 44:12 and PE 44:12 species were identified in both mouse strains. They probably represent PC and PE lipids that were esterified with two molecules of DHA at the *sn-1* and *sn-2* position of the glycerol backbone. The third abundant lipid class was SM. Among lysophosphatidylcholines (LPC), the most abundant species contained a DHA fatty acid (LPC 22:6). Ceramides/hexosylceramides (Cer/HexCer), PGs and PAs were found at very low concentrations; therefore, we report only total concentrations of these three lipid classes.

The major difference between 8-week old *Pon1*$^{-/-}$ and WT mice was seen for total LPC (p=0.001) and in particular for LPC 22:6 species (p=0.001), which were detected at significantly reduced levels in *Pon1*$^{-/-}$ mice (Table 4). These differences remained significant after Bonferroni correction for multiple testing. Analysis of phospholipids in WT retinas and eyecups, which were isolated separately, revealed that LPC 22:6 was the most abundant LPC species in the retina,

whereas it was almost absent in the eyecup (data not shown). Some polyunsaturated and monounsaturated PCs as well as polyunsaturated PEs were also decreased in *Pon1*$^{-/-}$ mice ($p<0.05$). However, these differences missed significance after Bonferroni correction (Table 5). Other phospholipid species were not altered in *Pon1*$^{-/-}$ compared to controls. When data for retinal phospholipids were calculated as mole percent, no significant differences between *Pon1*$^{-/-}$ and WT mice were detected (Table 6). Although the relative abundance of total LPC ($p=0.0032$) and LPC 22:6 ($p=0.0015$) lipids was markedly reduced the in retina/eyecup samples of *Pon1*$^{-/-}$ mice, these differences lost significance after correcting for multiple testing.

Since aging is a major risk factor for the development of AMD, and lipid metabolism is known to be involved in the etiology of this disease, we characterized the phospholipid profiles of 1-year old WT and *Pon1*$^{-/-}$ mice. In contrast to young adults at 8 weeks of age, levels of total LPC and LPC 22:6 species in 1 year old mice did not differ between the two mice strains (Table 7). Interestingly, age-related changes in the phospholipid profiles showed different trends in WT and *Pon1*$^{-/-}$ mice. While control animals showed a trend for decreased levels of total LPC and LPC 22:6 with age, *Pon1*$^{-/-}$ mice revealed almost no age-related changes in the content of those phospholipids (Table 7).

Table 4. Phospholipids in the retina/eyecup samples from control (WT) and *Pon1*$^{-/-}$ mice at 8 weeks of age.

PLs	Content of PL in nmol per mg of retina and eyecup proteins		Mann-Whitney Test, p values WT 8w vs *Pon1*$^{-/-}$ 8w
	WT 8w Median(min;max)	*Pon1*$^{-/-}$ 8w Median(min;max)	
Total PC	143.5(92;170.5)	120.5(54.1;140.3)	0.023
Total SM	20(7.2;26.8)	17(7.2;23.7)	0.174
Total LPC	**5.2(2.1;5.9)**	**2.5(1.2;4.1)**	**0.001**
Total PE	26.5(16.2;29.8)	21.9(11.4;24.6)	0.013
Total Cer/HexCer	5.6(2.7;7.6)	6.1(2.6;9.4)	0.545
Total PG	1.2(0.2;1.9)	0.9(0.3;1.5)	0.253
Total PA	2.8(2.3;3.1)	2.9(2.5;3.2)	0.326
PC 32:0	27.3(15.5;31.5)	23.3(10.9;27.7)	0.070
PC 32:1	2.7(2.1;3.5)	2.1(1.1;2.6)	0.010
PC 34:0	6.4(3.7;8)	5.9(3;7.6)	0.257
PC 34:1	27.8(18.8;33.4)	23.4(10.9;28.9)	0.016
PC 34:2	4.7(3;5.9)	4.2(1.7;4.6)	0.096
PC 36:1	14.1(8;16.2)	11.1(5.3;13.3)	0.019
PC 36:2	5.6(4.3;7.2)	4.7(2.2;5.8)	0.023
PC 36:3	1.5(1;2)	1.3(0.4;1.7)	0.070
PC 36:4	6.4(4.1;7.2)	5.4(2.6;6.3)	0.059
PC 38:4	7.9(4.7;10.4)	6.6(2.8;8.3)	0.013
PC 38:5	2.5(1.6;2.8)	2.4(0.9;2.9)	0.450
PC 38:6	12.1(7.6;15.1)	9.5(4;12.3)	0.013
PC 40:5	1.7(0.7;2.3)	1.3(0.8;1.9)	0.023
PC 40:6	17.7(12.2;20.4)	13.7(5.7;15.6)	0.004
PC 40:7	1.4(1.2;2.4)	1.1(0.5;1.5)	0.008
PC 44:12	4.9(3.7;8.3)	3.9(1.4;5.7)	0.016
SM34:1	5.8(2.3;7.6)	5.2(2.4;7.2)	0.174
SM36:1	4.7(1.9;6.4)	3.9(1.9;5.5)	0.199
SM38:1	2.4(0.8;3.3)	2.2(0.7;2.9)	0.199
SM40:1	2.2(0.8;3.2)	2(0.8;2.9)	0.199
SM42:1	2.1(0.6;2.7)	1.7(0.5;2.6)	0.131
SM42:2	2.2(0.8;3.4)	1.8(0.7;2.7)	0.257
SM42:3	0.4(0.1;0.5)	0.3(0.1;0.4)	0.059
LPC 18:0	0.8(0.6;0.8)	0.7(0.4;0.9)	0.131
LPC 18:1	1.7(0.6;2)	0.7(0.4;1.2)	0.002
LPC 22:6	**2.8(0.9;3.1)**	**1.2(0.4;2)**	**0.001**
PE 34:1	0.8(0.6;0.9)	0.7(0.4;0.9)	0.290
PE 36:0	0.3(0.2;0.4)	0.3(0.2;0.4)	0.880
PE 36:2	0.9(0.8;1.2)	0.9(0.7;1.1)	0.151
PE 36:4	0.6(0.4;0.8)	0.6(0.4;0.8)	0.650
PE 38:4	3.3(1.8;3.7)	2.6(1.5;3.1)	0.019
PE 38:6	5(2.8;6.3)	4.2(2;5.1)	0.008
PE 40:6	12.2(7.6;13.8)	10.3(5.1;11.4)	0.013
PE 44:12	2.9(1.9;3.8)	2.3(1.1;2.7)	0.013

The phospholipid (PL) analysis was performed by LC-MS. Content of PL classes and species is shown as nmol of PL per one mg of retina and eyecup proteins. Total phospholipids represent sum of molecular species of a given class and are presented for PC, SM, LPC, PE. Species

pattern is displayed for PCs, PEs, SMs and LPCs. Data values are displayed as median with range. N=10 for both genotypes. Statistical significance was determined by the Man-Whitney U test. After Bonferroni correction a p value of 0.001 corresponds to a significance level of 0.05. Statistically significant results are indicated in bold. An assignment of PL species includes numbers of carbon atoms and double bounds in both acyl chains (for example, PC 34:1 consist of 34 carbon atoms and one double bond and can correspond to the following species PC(16:0/18:1) or PC(18:0/16:1), and so forth). SM assignment comprises the numbers of carbon atoms and double bonds in both sphingoid base and in N-linked fatty acid.

5.3.6. PON1 does not influence photoreceptor degeneration or RPE survival after light exposure

To evaluate whether the lack of the antioxidative PON1 protein influences cell survival under oxidative stress conditions, we exposed WT and *Pon1*$^{-/-}$ mice to high levels of white light[41]. At 5 days after exposure, many photoreceptors were lost and large numbers of pyknotic nuclei were detected in the ONL of WT and *Pon1*$^{-/-}$ mice (Fig. 5A). We also observed similar levels of subretinal macrophages in *Pon1*$^{-/-}$ and WT mice, although previous reports suggested inhibitory effects of PON1 on monocyte transmigration[30]. At 10 days after light exposure the photoreceptor layer was degenerated further, with only few pyknotic nuclei left in the ONL of both *Pon1*$^{-/-}$ and WT mice. Additionally, some RPE cells displayed severe morphologic changes in both mouse lines (Fig. 5B). Enlarged RPE cells with increased cytoplasmic β-catenin localization, as well as a global increase in cytoplasmic phalloidin (F-actin) staining were observed. The number of RPE cells before and after light exposure was comparable in WT and *Pon1*$^{-/-}$ mice (data not shown).

Acute LD not only induces retinal degeneration, but also activates survival pathways to protect retinal cells from cell death. Leukemia inhibitory factor (LIF) is a key cytokine regulating an endogenous rescue pathway that involves activation of the Janus kinase signal transducer and activator of transcription (Jak-STAT) signaling pathway, and expression of protective factors like endothelin-2 (*Edn2*) and fibroblast growth factor-2 (*Fgf2*)[42, 43]. In line with the comparable extent of tissue damage (Fig. 5A, 5B), light exposure caused a similar expression pattern of these genes in retinas of WT and *Pon1*$^{-/-}$ mice, even though *Edn2* and *Fgf2* were significantly stronger induced in mice lacking PON1 (Fig. 5C). No differences between the two genotypes were detected in eyecups. Remarkably, upon exposure to the light *Pon2*, *Sod1* and *Sod2* expression was reduced in the retina, but not in the eyecup, while *Hmox1* was upregulated in both tissues (Fig. 5C; Table 3). Additionally, expression of *Socs3* was strongly upregulated in the eyecup, suggesting that JAK/STAT signaling was also induced in the RPE. Whether this was a consequence of LIF signaling or whether other factors led to such activation must be established.

Untreated *Pon1*$^{-/-}$ mice had decreased levels of total LPCs and in particular of LPC 22:6 (see above). Since PON1 is an antioxidative enzyme, we tested whether its lack might impact the phospholipid composition under oxidative stress induced by light exposure. At 2 hours after light exposure, phospholipid profiles were comparable in WT and in *Pon1*$^{-/-}$ retina/eyecups and showed increased levels of PE 34:1, PE 36:0 and PE 36:4 in both strains (Table 5). Furthermore,

light exposure increased the levels of total LPC and LPC 22:6 in *Pon1*$^{-/-}$ but not in WT mice (Table 7). However, these differences did not remain statistically significant after correcting for multiple testing. In agreement with a lack of difference, concentrations of potentially DHA containing PC's (PC38:6, PC 40:6, PC:40:7 and PC 44:12) did not differ between WT and PON1 mice, neither before nor after light exposure.

On the basis of mole percent, PE 36:0 levels increased in both strains upon light exposure, while PE 34:1, PE 36:4, PE 38:6, PE 40:6 species were more abundant in WT mice, but not in *Pon1*$^{-/-}$ after the treatment. In contrary, PE 44:12 was relatively decreased in *Pon1*$^{-/-}$, but not in WT mice. Relative increases of total LPC and LPC 22:6 were observed in *Pon1*$^{-/-}$, but not in WT mice; however, without statistical significance after correction for multiple testing and without any concomitant changes in PC (Table 6).

Table 3. Gene expression in retinas and eyecups of *Pon1*$^{-/-}$ and WT mice after light damage (LD).

		Mean ± SD				2-way ANOVA			
						WT vs. *Pon1*$^{-/-}$		DC vs. LD	
	Gene	WT, DC	*Pon1*$^{-/-}$, DC	WT, 12h	*Pon1*$^{-/-}$, 12h	DC	12h after LD	WT	*Pon1*$^{-/-}$
RETINA	*Lif*	1 ± 0.47	1.73 ± 0.39	35.75 ± 10.41	44.29 ± 5.29	ns	ns	p < 0.001	p < 0.001
	Edn2	1 ± 0.23	3.18 ± 1.34	8.82 ± 1.39	32.3 ± 9.92	ns	p < 0.001	ns	p < 0.001
	Fgf2	1 ± 0.07	1.55 ± 0.09	1.85 ± 0.08	3.72 ± 1.85	ns	p < 0.05	ns	p < 0.05
	Stat3	1 ± 0.13	1.18 ± 0.14	4.02 ± 0.55	2.81 ± 0.29	ns	p < 0.01	p < 0.001	p < 0.001
	Socs3	1 ± 0.39	1.64 ± 0.17	20.71 ± 16.94	18.91 ± 9.82	ns	ns	ns	ns
	Hmox1	1 ± 0.29	0.6 ± 0.02	5.32 ± 0.22	4.83 ± 1.71	ns	ns	p < 0.001	p < 0.001
	Sod1	1 ± 0.12	0.76 ± 0.06	0.8 ± 0.20	0.53 ± 0.12	ns	ns	ns	ns
	Sod2	1 ± 0.16	0.92 ± 0.05	0.65 ± 0.12	0.51 ± 0.06	ns	ns	p < 0.01	p < 0.01
	Scarb1	1 ± 0.59	1.56 ± 0.43	0.39 ± 0.23	1.03 ± 0.11	ns	ns	ns	ns
	Abca1	1 ± 0.55	1.8 ± 0.79	1.42 ± 1.05	1.18 ± 0.24	ns	ns	ns	ns
	Mct3	1 ± 0.35	0.64 ± 0.30	0.54 ± 0.24	1.79 ± 0.69	ns	p < 0.01	ns	p < 0.05
	Gnat1	1 ± 0.11	1.14 ± 0.28	0.2 ± 0.06	0.3 ± 0.05	ns	ns	p < 0.001	p < 0.001
EYE CUP	*Lif*	0.37 ± 0.13	0.72 ± 0.32	1.39 ± 1.12	2.07 ± 0.30	ns	ns	ns	ns
	Edn2	0.01 ± 0.004	0.02 ± 0.01	0.04 ± 0.05	0.04 ± 0.02	ns	ns	ns	ns
	Fgf2	0.02 ± 0.01	0.04 ± 0.02	0.06 ± 0.05	0.03 ± 0.004	ns	ns	ns	ns
	Stat3	0.29 ± 0.04	0.32 ± 0.01	0.52 ± 0.15	0.46 ± 0.07	ns	ns	p < 0.05	ns
	Socs3	0.21 ± 0.06	0.15 ± 0.03	2.13 ± 0.50	1.52 ± 0.22	ns	ns	p < 0.001	p < 0.001
	Hmox1	0.21 ± 0.03	0.17 ± 0.04	0.56 ± 0.18	0.4 ± 0.01	ns	ns	p < 0.01	ns
	Sod1	0.16 ± 0.01	0.15 ± 0.01	0.17 ± 0.03	0.15 ± 0.04	ns	ns	ns	ns
	Sod2	0.16 ± 0.02	0.15 ± 0.01	0.19 ± 0.01	0.14 ± 0.03	ns	p < 0.05	ns	ns
	Scarb1	0.01 ± 0.001	0.02 ± 0.01	0.02 ± 0.02	0.06 ± 0.02	ns	p < 0.05	ns	p < 0.05
	Abca1	0.02 ± 0.01	0.06 ± 0.03	0.12 ± 0.10	0.1 ± 0.04	ns	ns	ns	ns
	Mct3	6 ± 3.22	8.15 ± 1.05	7.09 ± 3.38	1.5 ± 0.43	ns	p < 0.05	ns	p < 0.05
	Gnat1	< 0.001	< 0.001	0.003 ± 0.01	< 0.001	ns	ns	ns	ns

Gene expression was examined by semi-quantitative real-time PCR in retinas and eyecups of WT and *Pon1*$^{-/-}$ mice, which either were (light damage, LD) or were not (dark control, DC) exposed to damaging light. Analysis was at 12 h after light exposure (12h). Values were normalized to *β-actin* and expressed relative to levels in retinas of dark control WT mice, which were set to 1. Shown are mean values ± SD of N=3. Two-way ANOVA with Bonferroni post-hoc analysis was used to test the statistical significance. A p-value of less than 0.05 was considered significant. *Lif*, leukemia inhibitory factor; *Edn2*, endothelin 2; *Fgf2*, fibroblast growth factor 2; *Stat3*, signal transducer and activator of transcription 3; *Socs3*, suppressor of cytokine signaling 3; *Hmox1*, heme oxygenase 1; *Sod1*, superoxide dismutase 1; *Sod2*, superoxide dismutase 2; *Abca1*, ATP-binding cassette, sub-family A (ABC1), member 1; *Scarb1*, scavenger receptor class B, member 1; *Mct3*, monocarboxylate transporter, member 3 (marker for RPE); *Gnat1*, guanine nucleotide binding protein, alpha transducing activity polypeptide (marker for the neuronal retina).

Table 5. Phospholipid composition of the retina/eyecup samples from control (WT) and *Pon1*$^{-/-}$ mice at 8 weeks and 1 year of age, and from 8 weeks of age mice exposed to the light.

PLs	Median (min;max) [nmol/mg]						Mann-Whitney Test, p values						
	WT 8w	*Pon1*$^{-/-}$ 8w	WT 1y	*Pon1*$^{-/-}$ 1y	WT LD	*Pon1*$^{-/-}$ LD	WT 8w vs *Pon1*$^{-/-}$ 8w	WT 8w vs WT 1y	*Pon1*$^{-/-}$ 8w vs *Pon1*$^{-/-}$ 1y	WT 1y vs *Pon1*$^{-/-}$ 1y	WT 8w vs WT LD	*Pon1*$^{-/-}$ 8w vs *Pon1*$^{-/-}$ LD	WT LD vs *Pon1*$^{-/-}$ LD
Total PC	143.5(92;170.5)	120.5(54.1;140.3)	89.1(65.5;147.9)	109.2(39.4;147.7)	140.5(58.3;173.7)	151.9(121.7;235.6)	0.0233	0.0275	0.4477	0.8551	0.8206	0.0025	0.2265
Total SM	20(7.2;26.8)	17(7.2;23.7)	16.6(11.1;22.9)	18.6(6.1;28.9)	17.7(6.7;23.8)	19.7(13.5;30.3)	0.1736	0.5403	0.7449	1.0000	0.2899	0.1736	0.3643
Total LPC	5.2(2.1;5.9)	2.5(1.2;4.1)	1.9(1.5;6.8)	3.1(1.3;5.3)	5(2.2;6.5)	3.7(3;8.6)	**0.0013**	0.0864	0.7449	1.0000	0.9397	0.0025	0.0588
Total PE	26.5(16.2;29.8)	21.9(11.4;24.6)	16.4(11.6;22.1)	19.1(6.9;22.6)	29.4(19;51)	27.2(18;37.8)	0.0126	0.0071	0.0652	1.0000	0.0821	0.0343	0.4497
Total Cer/HexCer	5.6(2.7;7.6)	6.1(2.6;9.4)	6.9(4.5;7.3)	6.7(2.5;8.6)	6.3(1.8;10.7)	6(3.9;10.1)	0.5453	0.3272	0.7449	0.8551	0.3258	0.8206	0.8798
Total PG	1.2(0.2;1.9)	0.9(0.3;1.5)	0.5(0.2;1.7)	0.7(0.3;1.4)	1.3(0.7;1.9)	0.6(0.3;3)	0.2530	0.2703	0.6407	0.7540	0.5340	0.2885	0.0506
Total PA	2.8(2.3;3.1)	2.9(2.5;3.2)	2.8(2.6;3)	2.8(2.4;3.2)	0.9(0.6;1.1)	1.3(0.9;1.6)	0.3258	1,0000	0.5876	0.8551	**0.0004**	**0.0002**	0.0025
PC 32:0	27.3(15.5;31.5)	23.3(10.9;27.7)	15.4(12.4;21.2)	18.7(7;24.2)	25.6(10.6;30.5)	28.6(21.4;43.8)	0.0696	0.0048	0.0509	0.8551	0.5453	0.0102	0.1988
PC 32:1	2.7(2.1;3.5)	2.1(1.1;2.6)	1.4(1.2;2.2)	1.5(0.6;2.4)	2.5(0.9;3.5)	2.4(1.3;4)	0.0102	0.0048	0.1585	1.0000	0.7624	0.2899	0.7055
PC 34:0	6.4(3.7;8)	5.9(3;7.6)	5.2(3.2;6.1)	4.8(1.7;6.5)	6.6(3.2;8.8)	8.3(4.1;11.7)	0.2568	0.0864	0.1931	0.8551	0.7624	0.0082	0.0696
PC 34:1	27.8(18.8;33.4)	23.4(10.9;28.9)	16.8(13.3;27.3)	21(7.6;29.2)	28.1(11.1;34.3)	34.1(21.9;48.9)	0.0156	0.0143	0.5876	1.0000	1,0000	0.0032	0.0494
PC 34:2	4.7(3;5.9)	4.2(1.7;4.6)	3(2.1;5.6)	3.5(1.8;5.8)	4.8(1.6;6.6)	5.3(3.3;9.8)	0.0963	0.1416	0.329	0.8551	0.7055	0.0156	0.3258
PC 36:1	14.1(8;16.2)	11.1(5.3;13.3)	8.5(6;14.3)	10.5(3.7;14.8)	13.4(6.2;17.2)	14.9(9.7;23.7)	0.0191	0.0373	0.5876	0.8551	0.7624	0.0052	0.2568
PC 36:2	5.6(4.3;7.2)	4.7(2.2;5.8)	3.6(2.9;6.5)	4.8(1.6;6.4)	6(2.7;7.4)	7(5.1;11)	0.0233	0.0275	0.9136	0.8551	0.8206	**0.0015**	0.1306
PC 36:3	1.5(1;2)	1.3(0.4;1.7)	1.1(0.7;1.7)	1(0.4;1.8)	1.6(0.7;2.4)	1.7(0.7;4.8)	0.0696	0.0500	0.3855	0.8551	0.8798	0.0821	0.4057
PC 36:4	6.4(4.1;7.2)	5.4(2.6;6.3)	4.1(2.5;8.1)	4.7(1.8;7.9)	6(2.5;8.5)	5.6(3.7;10.8)	0.0587	0.1775	0.5876	0.7150	0.8205	0.2568	0.9397
PC 38:4	7.9(4.7;10.4)	6.6(2.8;8.3)	5.2(3.6;10.2)	7(2.1;9.4)	7.5(2.2;10.3)	6.8(5.9;13.3)	0.0126	0.0864	0.8283	0.8551	0.2899	0.4057	0.7055
PC 38:5	2.5(1.6;2.8)	2.4(0.9;2.9)	1.3(1;3.3)	1.7(0.9;3.3)	1.9(0.3;4.9)	2.7(0.8;5.2)	0.4497	0.0864	0.2328	1.0000	0.2265	0.3258	0.1509
PC 38:6	12.1(7.6;15.1)	9.5(4;12.3)	8(5.1;13.2)	8.6(3.4;11.3)	12.5(6.1;15.2)	12.6(9.1;19.4)	0.0126	0.0500	0.3855	0.8551	0.8798	0.0233	0.9397
PC 40:5	1.7(0.7;2.3)	1.3(0.8;1.9)	1.1(0.8;2.2)	0.9(0.3;1.6)	2(0.7;3.3)	2.5(0.4;4.1)	0.0233	0.1779	0.1037	0.3613	0.3643	0.2899	0.6501
PC 40:6	17.7(12.2;20.4)	13.7(5.7;15.6)	11.4(7.7;19.4)	13.7(4.6;17.8)	15.1(6.8;20.8)	17.2(10.2;26.5)	0.0041	0.0500	0.8283	0.8551	0.2568	0.0052	0.2265
PC 40:7	1.4(1.2;2.4)	1.1(0.5;1.5)	0.8(0.8;1.6)	1.1(0.4;1.3)	1.2(0.3;1.9)	0.9(0.5;1.8)	0.0082	0.0373	0.5505	0.8551	0.2899	0.6501	0.2568
PC 44:12	4.9(3.7;8.3)	3.9(1.4;5.7)	2.3(1.9;5.1)	3.4(1.1;4.5)	4.8(2.4;6.2)	4(2.6;13.6)	0.0156	0.0143	0.3855	0.8551	0.2899	0.4057	0.7624
SM34:1	5.8(2.3;7.6)	5.2(2.4;7.2)	5.5(3.5;6.9)	5.5(2.2;8.5)	6.4(2.8;9.5)	7.4(4.9;11.5)	0.1736	0.7133	0.8283	1.0000	0.0821	0.0191	0.5453
SM36:1	4.7(1.9;6.4)	3.9(1.9;5.5)	3.4(2.1;5)	4.1(1.1;5.8)	4.6(1.6;6.1)	4.8(3;8.6)	0.1988	0.1779	0.7449	0.8551	0.8206	0.0821	0.5453
SM38:1	2.4(0.8;3.3)	2.2(0.7;2.9)	2.4(1.1;2.9)	2.4(0.7;3.8)	1.9(0.4;2.4)	2.3(1.4;3.2)	0.1988	0.5403	0.5876	0.8551	0.0233	0.5453	0.1509
SM40:1	2.2(0.8;3.2)	2(0.8;2.9)	1.7(1.3;2.8)	2.5(0.6;3.7)	1.6(0.6;2.4)	1.7(1.2;3)	0.1988	0.4624	0.4477	0.5839	0.0102	0.5453	0.5967
SM42:1	2.1(0.6;2.7)	1.7(0.5;2.6)	1.7(1.1;2.2)	1.9(0.7;3.2)	1.1(0.5;1.9)	1.4(0.8;2.8)	0.1306	0.1779	0.8283	0.8551	0.0032	0.3258	0.1509
SM42:2	2.2(0.8;3.4)	1.8(0.7;2.7)	1.7(1.2;2.9)	1.8(0.8;3.3)	1.7(0.6;2.3)	1.6(0.7;3.5)	0.2568	0.6242	1.0000	0.8551	0.0156	0.8798	0.9397
SM42:3	0.4(0.1;0.5)	0.3(0.1;0.4)	0.3(0.2;0.6)	0.2(0.1;0.5)	0.3(0.2;0.5)	0.4(0.2;0.7)	0.0588	0.4624	0.8283	0.5839	0.1124	0.0413	0.0821
LPC 18:0	0.8(0.6;0.8)	0.7(0.4;0.9)	0.7(0.4;1.1)	0.9(0.4;1.1)	1.2(0.5;1.4)	1.2(0.6;1.9)	0.1306	0.2703	0.2328	0.5839	0.0025	0.0065	0.7055
LPC 18:1	1.7(0.6;2)	0.7(0.4;1.2)	0.6(0.5;2)	0.9(0.4;1.7)	1.3(0.5;2)	0.8(0.4;2.4)	0.0019	0.0864	0.7449	1.0000	0.1736	0.2568	0.0284
LPC 22:6	2.8(0.9;3.1)	1.2(0.4;2)	0.7(0.5;3.8)	1.3(0.4;2.5)	2.6(1.3;3.2)	1.7(1.4;4.8)	**0.0013**	0.0662	0.7449	1.0000	1.0000	0.0052	0.0494
PE 34:1	0.8(0.6;0.9)	0.7(0.4;0.9)	0.6(0.4;0.6)	0.6(0.3;0.9)	1.2(0.7;1.4)	1.1(0.9;1.4)	0.2899	0.0022	0.2781	0.7150	**0.0012**	**0.0002**	0.4963
PE 36:0	0.3(0.2;0.4)	0.3(0.2;0.4)	0.2(0.2;0.3)	0.2(0.2;0.3)	0.6(0.6;0.8)	0.6(0.6;0.7)	0.8798	0.0500	0.3290	0.7150	**0.0002**	**0.0002**	0.6501
PE 36:2	0.9(0.8;1.2)	0.9(0.7;1.1)	0.7(0.6;1.1)	0.8(0.4;1.1)	1.2(0.9;1.5)	1(0.8;1.2)	0.1509	0.1416	0.4477	0.7150	0.0065	0.0588	0.0284
PE 36:4	0.6(0.4;0.8)	0.6(0.4;0.8)	0.5(0.4;0.7)	0.5(0.3;0.7)	0.9(0.7;1.1)	0.9(0.7;1.2)	0.6501	0.1779	0.4477	1.0000	**0.0005**	**0.0004**	0.9397
PE 38:4	3.3(1.8;3.7)	2.6(1.5;3.1)	2(1.5;3)	2.7(0.9;3.1)	3.7(1.5;5.5)	3.6(1.6;5.4)	0.0191	0.0373	0.9136	0.4652	0.3643	0.0025	0.7055
PE 38:6	5(2.8;6.3)	4.2(2;5.1)	2.7(1.8;4.1)	3.4(1.3;4.1)	6(3.8;11.4)	5.2(3.9;7.5)	0.0082	0.0048	0.0170	1.0000	0.0343	0.0284	0.2265
PE 40:6	12.2(7.6;13.8)	10.3(5.1;11.4)	8.6(5.3;10.1)	9(2.7;11)	15.3(9.1;25.6)	13.7(5.8;20.3)	0.0126	0.0071	0.0652	1.0000	0.0156	0.0233	0.4057
PE 44:12	2.9(1.9;3.8)	2.3(1.1;2.7)	1.4(1.2;2.3)	1.7(0.5;2.3)	1.2(0.9;3.8)	1.1(0.9;2)	0.0126	0.0048	0.0827	0.8551	0.0025	**0.0007**	0.4497

The phospholipid (PL) analysis was performed by LC-MS. Content of PCs, PEs, SMs and LPCs, Cers/HexCers, PGs and PAs was calculated as nmol/ mg of retina and eyecup protein. Total PLs represent sum of molecular species of PC, PE, SM and LPC lipid classes. The median and ranges are given from N=10 for WT (8w), N=10 for *Pon1*$^{-/-}$ (8w), N=5 for WT (1y), N=6 for *Pon1*$^{-/-}$ (1y), N=10 for WT (LD), N=10 for *Pon1*$^{-/-}$ (LD). Man-Whitney U test was applied since data were not normally distributed. After Bonferroni correction for 37 tests a p value of 0.001 corresponds to a significance level of 0.05. Bold letters indicate statistically significant levels. An assignment of PL species includes numbers of carbon atoms and double bonds in both acyl chains (for example, PC 34:1 consist of 34 carbon atoms and one double bond and can correspond to the following species PC(16:0/18:1) or PC(18:0/16:1), and so forth). SM assignment comprises numbers of carbon atoms and double bonds in both sphingoid base and in N-linked fatty acid.

Table 6. Phospholipid composition of the retina/eyecup samples from control (WT) and *Pon1*$^{-/-}$ mice at 8 weeks and 1 year of age, and from 8 weeks of age mice exposed to the light.

PLs	Median (min;max) [mole % of total PLs]						Mann-Whitney Test, p values						
	WT 8w	*Pon1*$^{-/-}$ 8w	WT 1y	*Pon1*$^{-/-}$ 1y	WT LD	*Pon1*$^{-/-}$ LD	WT 8w vs *Pon1*$^{-/-}$ 8w	WT 8w vs WT 1y	*Pon1*$^{-/-}$ 8w vs *Pon1*$^{-/-}$ 1y	WT 1y vs *Pon1*$^{-/-}$ 1y	WT 8w vs WT LD	*Pon1*$^{-/-}$ 8w vs *Pon1*$^{-/-}$ LD	WT LD vs *Pon1*$^{-/-}$ LD
Total PC	70.2(68.1;74.47)	69.65(67.74;71.35)	67.17(66.16;70.38)	67.83(66.43;68.69)	69.45(64.02;72.21)	71.69(67.36;78.76)	0.1988	0.02	0.017	0.5839	0.1124	0.0413	0.0126
Total SM	10.21(5.69;11.03)	9.55(8.73;12.16)	11.3(10.89;12.88)	11.91(9.93;13.31)	9.19(7.59;9.64)	9.45(7.3;13.3)	0.8798	0.0048	0.017	0.8551	0.1124	0.4497	0.3643
Total LPC	2.52(1.18;3.68)	1.52(1.2;2.04)	1.51(1.34;3.25)	2.3(1.47;2.58)	2.49(1.98;2.9)	1.82(1.34;2.74)	0.0032	0.1416	0.0393	0.2733	0.7624	0.0494	0.0025
Total PE	12.84(11.52;13.65)	12.68(11.89;14.3)	11.96(10.51;12.92)	11.53(10.1;12.3)	14.71(13.26;21.44)	11.66(9.71;16.47)	0.5967	0.0662	0.0092	0.5839	**0.0004**	0.5453	0.0343
Total Cer/HexCer	2.64(1.91;3.7)	3.37(3.05;5.36)	4.54(3.26;5.39)	4.24(3.94;4.44)	3.02(2;4.24)	2.98(1.91;4.42)	0.0156	0.0048	0.017	0.4652	0.1988	0.1306	0.7624
Total PG	0.62(0.1;1.2)	0.46(0;0.85)	0.48(0.23;0.99)	0.41(0;0.69)	0.5(0;0.94)	0.28(0.13;1.29)	0.3643	0.4624	0.4805	0.8551	0.3642	0.2568	0.4055
Total PA	1.36(1.09;2.28)	1.76(1.38;3.69)	2.25(1.23;2.82)	1.75(1.4;4.58)	0.35(0;0.71)	0.59(0.4;0.99)	0.0102	0.05	0.8283	0.8551	**0.0002**	**0.0002**	0.0233
PC 32:0	13.01(11.45;14.67)	13.71(13;13.81)	11.41(3.01;12.36)	11.51(4.53;36.04)	12.03(11.73;13.72)	13.82(10.01;15.06)	0.0156	0.0101	0.2781	0.3613	0.0696	0.6501	0.0156
PC 32:1	1.3(1.2;1.61)	1.27(1.09;1.42)	1.02(0.61;1.15)	1.08(0.47;3.62)	1.27(1.01;1.51)	1.12(0.71;1.4)	0.2899	0.0022	0.5876	0.715	0.3258	0.1509	0.2899
PC 34:0	3.17(2.81;3.6)	3.54(3.22;3.77)	3.21(0.77;3.85)	3.55(1.11;7.92)	3.4(2.84;3.76)	3.64(1.91;5.34)	0.0284	0.8065	0.8283	0.2733	0.1509	0.6501	0.3643
PC 34:1	13.43(13.03;14.77)	13.59(12.86;14.41)	12.48(6.42;13.29)	13.8(4.89;43.11)	13.35(12.58;14.95)	15.29(13.18;18.14)	0.8206	0.0071	1.0000	0.4652	0.4963	0.0032	0.0032
PC 34:2	2.22(1.83;2.62)	2.35(2.04;2.63)	2.25(0.98;3.37)	2.57(1.22;7.35)	2.24(1.8;2.74)	2.49(1.66;4.58)	0.4497	0.9025	1.0000	0.715	0.5967	0.4963	0.6501
PC 36:1	6.64(6.17;7.13)	6.6(6.18;6.88)	5.95(3.31;6.76)	7.2(2.37;20.48)	6.75(5.83;7.27)	6.9(5.41;9.14)	0.4057	0.0373	1.0000	0.3613	0.7624	0.5453	0.5453
PC 36:2	2.89(2.41;3.37)	2.78(2.46;2.96)	2.66(1.37;4.42)	3.2(1.01;9.48)	2.98(2.45;3.66)	3.2(2.48;4.96)	0.2899	0.3913	0.9136	0.8551	0.8206	0.0233	0.2899
PC 36:3	0.77(0.56;0.89)	0.73(0.54;0.9)	0.71(0.36;0.8)	0.77(0.43;2.31)	0.77(0.5;1.04)	0.81(0.38;1.52)	0.4963	0.2207	0.9136	0.5839	0.8798	0.2899	0.6501
PC 36:4	2.98(2.52;3.62)	3.2(2.68;3.27)	3.06(1.25;4.03)	4.21(1.14;10.03)	3.01(2.28;3.4)	2.64(2.05;3.83)	0.5967	1.0000	0.2781	0.3613	0.9397	0.0963	0.3643
PC 38:4	3.96(3.69;4.39)	3.76(3.38;4.24)	3.62(1.98;3.86)	5.31(1.34;13.06)	3.76(2.48;4.39)	3.34(2.89;5.11)	0.1124	0.0373	0.2781	0.2733	0.1509	0.0494	0.3258
PC 38:5	1.15(1.04;1.45)	1.26(1.04;1.7)	0.99(0.54;1.15)	1.59(0.56;4.2)	0.93(0.38;1.93)	1.4(0.39;1.77)	0.3258	0.0143	0.5876	0.2012	0.0588	1.0000	0.0696
PC 38:6	6.07(5.46;6.52)	5.48(5.01;6.27)	5.23(2.43;5.97)	6.28(2.19;17.6)	6.28(5.32;6.95)	5.96(4.75;6.88)	0.0082	0.0143	1.0000	0.4652	0.2265	0.3258	0.0696
PC 40:5	0.8(0.54;0.99)	0.82(0.63;1.03)	0.79(0.39;0.83)	0.87(0.18;2.03)	1.06(0.59;1.32)	0.96(0.23;1.96)	0.9397	0.2703	1.0000	0.4652	0.0696	0.5967	0.7055
PC 40:6	8.46(7.71;9.59)	7.68(7.09;8.56)	7.65(1.25;8.5)	9.42(2.98;29.54)	7.71(6.34;8.7)	8.22(4.79;9.58)	0.0025	0.0373	0.9136	0.3613	0.0284	0.1736	0.2265
PC 40:7	0.72(0.51;1.07)	0.65(0.55;0.75)	0.56(0.31;0.78)	0.78(0.27;2.21)	0.58(0.3;0.95)	0.44(0.24;0.88)	0.0821	0.0662	0.9136	0.2733	0.3258	0.1306	0.1509
PC 44:12	2.65(2.14;3.67)	2.25(1.76;2.88)	1.55(0.24;2.26)	2.42(0.7;7.63)	2.29(1.67;2.84)	2.18(1.2;4.32)	0.0696	0.0071	0.9136	0.2012	0.1509	0.4963	0.2899
SM34:1	2.96(1.8;3.2)	2.97(2.71;3.69)	3.73(1.67;4.08)	3.92(1.42;10.82)	3.23(3.07;3.98)	3.41(2.6;5.26)	0.5967	0.0662	0.2781	0.5839	0.0015	0.1988	0.8798
SM36:1	2.42(1.49;2.62)	2.32(1.99;2.82)	2.46(1;2.75)	2.69(0.74;7.37)	2.35(1.76;2.46)	2.34(1.68;2.74)	0.9397	0.7133	0.3855	0.4652	0.1736	0.7055	0.6501
SM38:1	1.26(0.62;1.57)	1.24(0.82;1.46)	1.54(0.73;1.8)	1.65(0.42;4.87)	0.88(0.43;1.15)	1.03(0.73;1.42)	0.7624	0.3913	0.1931	0.3613	0.0233	0.0696	0.1988
SM40:1	1.14(0.59;1.32)	1.13(0.97;1.46)	1.48(0.61;2.46)	1.7(0.41;4.7)	0.81(0.65;0.93)	0.79(0.64;1.39)	0.5453	0.1416	0.0509	0.3613	0.0052	0.0041	0.7624
SM42:1	1.03(0.51;1.17)	0.99(0.66;1.28)	1.26(0.5;2.03)	1.24(0.43;4.01)	0.62(0.41;0.76)	0.6(0.36;1.3)	0.8798	0.0662	0.1585	0.8551	0.0025	0.0082	1.0000
SM42:2	1.1(0.63;1.38)	1.07(0.79;1.38)	1.24(0.69;2.51)	1.45(0.49;4.15)	0.83(0.68;1)	0.78(0.35;1.41)	0.9397	0.1416	0.329	0.715	0.0156	0.0284	0.6501
SM42:3	0.19(0.05;0.21)	0.16(0.09;0.28)	0.22(0.09;0.41)	0.21(0.05;0.65)	0.14(0.1;0.24)	0.19(0.1;0.26)	0.9397	0.1416	0.3855	0.8551	0.1124	0.4963	0.1988
LPC 18:0	0.37(0.29;0.47)	0.41(0.32;0.5)	0.42(0.24;0.55)	0.6(0.27;1.57)	0.57(0.37;0.71)	0.5(0.34;0.78)	0.2899	0.1779	0.1931	0.2012	0.0015	0.0233	0.4057
LPC 18:1	0.79(0.33;1.39)	0.42(0.35;0.61)	0.38(0.23;0.6)	0.91(0.28;2.24)	0.59(0.52;0.92)	0.39(0.18;0.78)	0.0041	0.0143	0.2781	0.2012	0.1988	0.2568	0.0065
LPC 22:6	1.32(0.52;1.83)	0.67(0.5;1.01)	0.51(0.24;0.69)	1.59(0.31;4.19)	1.27(1.09;1.55)	0.85(0.61;1.52)	0.0015	0.0033	0.329	0.1441	1.0000	0.1124	0.0082
PE 34:1	0.36(0.32;0.52)	0.39(0.33;0.56)	0.35(0.21;0.63)	0.36(0.18;1.12)	0.58(0.47;0.82)	0.52(0.33;0.66)	0.2899	0.8065	0.5152	0.8551	**0.0004**	0.1124	0.2265
PE 36:0	0.14(0.11;0.18)	0.17(0.08;0.24)	0.16(0.09;0.22)	0.14(0.11;0.42)	0.32(0.25;0.71)	0.3(0.19;0.35)	0.0413	0.3913	0.6644	1.0000	**0.0002**	**0.0005**	0.3258
PE 36:2	0.47(0.36;0.64)	0.5(0.42;0.81)	0.54(0.35;1.03)	0.56(0.37;1.44)	0.58(0.53;0.98)	0.44(0.32;0.7)	0.2899	0.7133	1.0000	0.5839	0.0019	0.1306	0.0052
PE 36:4	0.32(0.26;0.35)	0.35(0.29;0.47)	0.37(0.22;0.49)	0.39(0.2;0.86)	0.44(0.37;0.8)	0.4(0.28;0.58)	0.0284	0.0662	0.6644	0.5839	**0.0002**	0.1306	0.0821
PE 38:4	1.55(1.31;1.75)	1.54(1.27;1.94)	1.46(0.69;1.7)	1.71(0.58;5.22)	1.71(0.93;2.28)	1.72(0.84;2.17)	0.9397	0.5403	0.5876	0.3613	0.0963	0.1736	0.8206
PE 38:6	2.53(2.19;2.74)	2.48(2.29;2.8)	2.02(0.82;2.27)	2.1(0.83;6.86)	3.1(2.44;4.42)	2.37(1.75;3.27)	0.7055	0.0071	0.4477	0.3613	**0.0012**	0.5453	0.0102
PE 40:6	5.99(5.32;6.39)	6.02(5.42;6.62)	5.53(0.99;6.41)	5.47(1.76;18.55)	7.86(6.55;10.21)	5.79(3.5;8.84)	0.3643	0.5403	0.5876	0.5839	**0.0002**	0.8206	0.0233
PE 44:12	1.5(1.16;1.71)	1.35(1.26;1.45)	1.02(0.16;1.36)	1.16(0.45;3.65)	0.64(0.43;1.91)	0.52(0.43;0.86)	0.0494	0.0048	0.5152	0.4652	0.0065	**0.0002**	0.3258

Content of PCs, PEs, SMs and LPCs, Cers/HexCers, PGs and PAs was calculated as mole % of total phospholipids. The median and ranges are given from N= 10 WT (8w), N=10 *Pon1*$^{-/-}$ (8w), N = 5 WT (1y), N = 6 *Pon1*$^{-/-}$ (1y), N = 10 WT (LD), N = 10 *Pon1*$^{-/-}$ (LD). Man-Whitney U test was applied since data were not normally distributed. After Bonferroni correction for 37 tests a p-value of 0.001 corresponds to a significance level of 0.05. Bold letters indicate statistically significant levels.

Table 7. Levels of total LPCs and LPC 22:6 in the retina/eyecup samples from 8-week and 1-year old WT and *Pon1*$^{-/-}$ mice, and from 8-week old mice exposed to the light.

PLs	Median (min;max) [nmol/mg]						Mann-Whitney Test, p values					
	WT 8w	*Pon1*$^{-/-}$8w	WT 1y	*Pon1*$^{-/-}$1y	WT LD	*Pon1*$^{-/-}$LD	WT 8w vs WT 1y	*Pon1*$^{-/-}$8w vs Pon1$^{-/-}$1y	WT 1y vs Pon1$^{-/-}$1y	WT 8w vs WT LD	*Pon1*$^{-/-}$8w vs Pon1$^{-/-}$LD	WT LD vs Pon1$^{-/-}$LD
Total LPC	5.2(2.1;5.9)	2.5(1.2;4.1)	1.9(1.5;6.8)	3.1(1.3;5.3)	5(2.2;6.5)	3.7(3;8.6)	0.086	0.745	1.000	0.940	0.002	0.059
LPC 22:6	2.8(0.9;3.1)	1.2(0.4;2)	0.7(0.5;3.8)	1.3(0.4;2.5)	2.6(1.3;3.2)	1.7(1.4;4.8)	0.066	0.745	1.000	1.000	0.005	0.049

The total LPC and LPC22:6 are shown as nmol of lipid per one mg of retina and eyecup proteins. Displayed are median values with range. N=5 for WT (1y), N=6 for *Pon1*$^{-/-}$ (1y), N=10 for WT (LD), N=10 for *Pon1*$^{-/-}$ (LD). Statistical significance was determined by the Man-Whitney U test. After Bonferroni correction a p value of 0.001 corresponds to a significance level of 0.05. An assignment of LPCs includes numbers of carbon atoms and double bonds in acyl chain. Total LPC represents sum of all lysophosphatidylcholine species.

5.4. Discussion

5.4.1. PON1 in the normal retina

Since PON1 has been implicated in AMD[12-14, 27], we assessed whether lack of PON1 would alter retinal physiology in young and old *Pon1*$^{-/-}$ mice. We showed that PON1 is not essential for development and maintenance of a normal retinal structure, vasculature, or function. Similarly, RPE cells were morphologically indistinguishable between WT and *Pon1*$^{-/-}$ mice, even though the RPE has the highest level of *Pon1* expression. Although PON1 has antioxidative activity, no signs of oxidative damage were detected and no compensatory increase in the expression of other antioxidative enzymes was observed. Lack of PON1 also did not influence the susceptibility of retina and RPE to light damage.

However, retina/eyecup samples of *Pon1*$^{-/-}$ mice showed decreased levels of LPCs in general and of LPC 22:6 in particular. LPCs are molecular species produced by the hydrolysis of PCs through enzymes of the phospholipase A2 (PLA2) superfamily. Previous studies have shown that PON1 has a PLA2-like activity leading to the formation and release of LPCs from macrophages[38, 44]. Thus, in WT mice, PON1 may increase LPC production and modulate the content of phospholipids in the retina/RPE. In analogy to the stimulatory effect of PON1-generated LPCs on cholesterol efflux from macrophages[44, 45], LPCs might stimulate reverse lipid transport from RPE regulating lipid content in this cell layer[46].

Since PON1 is a secreted protein that retains its hydrophobic signal peptide[47], it may remain in the membrane of PON1-producing cells, or may reach membranes of neighboring cells. Thus, PON1 synthesized in the RPE might affect photoreceptors as well. The immunohistochemical detection of PON1 in the region of photoreceptor inner segments (and other nonnucleated areas of the retina)[48] and our observation that LPC 22:6, which was reduced in *Pon1*$^{-/-}$ mice, was very abundant in the retina but almost absent from the eyecup (data not shown) supports a role for a PLA2-like activity of PON1 in the neuronal retina.

We detected a general age-related decrease in the expression of antioxidative genes in retinas and especially eyecups of WT mice. *Pon1* was among the affected genes and down-regulated about 65%. Remarkably, also levels of total LPCs and of LPC 22:6 were decreased in 1-year old WT mice, by 63% and 75%, respectively (Table 7). This suggests a correlation between *Pon1* expression and LPC levels, and indicates that reduced expression of *Pon1* resulted in reduced PON1-related PLA2 activity and, thus, in a diminished PON1-mediated hydrolysis of PCs. Furthermore, increased lipid peroxidation and glycation in the aged eyes might have additionally compromised PON1 activity as it has been observed in metabolic syndrome and type II diabetes in humans[49-51].

5.4.2. PON1 in the light-exposed retina

Even though PON1 has antioxidative and anti-inflammatory activities, *Pon1*$^{-/-}$ and WT mice were similarly affected by light exposure: photoreceptors were equally susceptible to light induced degeneration; changes in RPE morphology after light exposure were comparable; expression of genes involved in antioxidative defense or the LIF-controlled cell survival pathway was similar; and content of PE 34:1, PE 36:0 and PE 36:4 in nmol/mg of proteins was increased to the same extent. However, levels of total LPC and LPC 22:6 increased only in *Pon1*$^{-/-}$, but not in WT mice after light exposure, suggesting that presence of PON1 prevents generation of LPC upon light exposure. Whether this is a direct effect of PON1 or whether a differential activation of phospholipases A2 in the two mouse strains influences LPC production remains to be explored.

Several possible mechanisms may explain the lack of striking differences in response to light damage between *Pon1*$^{-/-}$ and WT mice. Previous studies showed that PON1 may be inactivated by its own substrates, such as oxidized lipids[52]. Thus, generation of a large amount of oxidized molecules by light exposure may substantially reduce PON1 activity in WT mice. Alternatively, PON1 may "neutralize" only a subset of oxidized species produced in LD, such as oxidized PUFAs[53]. Other light-induced oxidation products may remain toxic and participate in the induction of cell death. It may also be of importance that PON1 is a secreted protein[47] that may not be able to detoxify intracellular molecules that have been generated by light exposure and that are involved in the degenerative process.

5.4.3. PON1 in AMD

The condition of AMD is a complex, multifactorial disease. Most existing mouse models for AMD combine advanced age, which is the major risk factor to develop AMD, with genetic defects in key genes involved in AMD pathogenesis. Considering the complex nature of the disease, it may not be surprising that some models require the combination of more than two environmental or genetic risk factors to cause a pathological phenotype. An excellent example is a murine model that combines three known AMD risk factors: advanced age, high fat, and cholesterol-rich diet, and mutations in *ApoE*[54]. Importantly, neither age nor the diet alone was sufficient to elicit changes that mimic human AMD pathology in the transgenic *ApoE4* mice.

The absence of an AMD-like phenotype in eyes of aged *Pon1*$^{-/-}$ mice suggests that even long-lasting absence of PON1 is not sufficient to cause detectable pathologic changes, like thickening of Bruch's membrane or sub-RPE deposits typical for AMD. Noteworthy,

despite the well-established antiatherogenic properties of PON1, *Pon1*$^{-/-}$ mice developed significantly larger atherosclerotic lesions than WT controls only when raised on a high-fat/high-cholesterol, but not on a regular diet[30, 55]. This suggests that additional factors/stimuli may be needed to provoke phenotypes of complex diseases, like atherosclerosis or AMD in *Pon1*$^{-/-}$ mice. This hypothesis is also supported by the observation that pathological processes in *ApoE*$^{-/-}$ mice were slowed in the presence of a human PON1 transgene[56], but accelerated by PON1 deficiency[55, 57].

These studies provide evidence that a coexisting chronic metabolic burden may be needed to reveal the role of PON1 in development and/or progression of a complex disease. A long-lasting exposure to low levels of light (in contrast to the short-term exposure to high light levels used in present study), a high-fat diet, or the inclusion of the *ApoE*-null genetic background might provide such an additional chronic stress to provoke AMD-like lesions in *Pon1*$^{-/-}$ mice.

We postulate that PON1 could be involved in AMD as a modulatory protein and that direct or indirect interactions with additional factors may influence its contribution to disease development and/or progression. Presence or absence of such factors may determine the association of PON1 with AMD in particular populations and may help to explain contradictory results regarding the implication of PON1 in AMD pathology. Nevertheless, the controversy on the role of PON1 in AMD still remains and there is a clear need for further studies to identify the precise function of PON1 in ocular tissues, such as RPE and neuronal retina. Knowledge of these functions seems a prerequisite to understand how the antioxidative and anti-inflammatory properties of PON1 may influence AMD.

Acknowledgements

The authors thank Christel Beck, Andrea Gubler, and Coni Imsand for excellent technical assistance, and Marijana Samardzija for helpful discussions.

This work was supported by a cooperative project grant by the Zurich Center for Integrative Human Physiology (ZIHP) of the University of Zurich, Zurich, Switzerland and by a matching fund of the Center for Clinical Research of the University Hospital Zurich, Zurich, Switzerland.

References

1. Guymer RH, Chong EW. Modifiable risk factors for age-related macular degeneration. *Med J Aust* 2006;184:455-458.

2. Smith W, Assink J, Klein R, et al. Risk factors for age-related macular degeneration: Pooled findings from three continents. *Ophthalmology* 2001;108:697-704.

3. Swaroop A, Branham KE, Chen W, Abecasis G. Genetic susceptibility to age-related macular degeneration: a paradigm for dissecting complex disease traits. *Hum Mol Genet* 2007;16 Spec No. 2:R174-182.

4. Ambati J, Atkinson JP, Gelfand BD. Immunology of age-related macular degeneration. *Nat Rev Immunol* 2013;13:438-451.

5. Handa JT. How does the macula protect itself from oxidative stress? *Mol Aspects Med* 2012;33:418-435.

6. Khandhadia S, Lotery A. Oxidation and age-related macular degeneration: insights from molecular biology. *Expert Rev Mol Med* 2010;12:e34.

7. Booij JC, Baas DC, Beisekeeva J, Gorgels TG, Bergen AA. The dynamic nature of Bruch's membrane. *Prog Retin Eye Res* 2010;29:1-18.

8. Curcio CA, Johnson M, Rudolf M, Huang JD. The oil spill in ageing Bruch membrane. *Br J Ophthalmol* 2011;95:1638-1645.

9. Wang L, Clark ME, Crossman DK, et al. Abundant lipid and protein components of drusen. *PLoS One* 2010;5:e10329.

10. Chen W, Stambolian D, Edwards AO, et al. Genetic variants near TIMP3 and high-density lipoprotein-associated loci influence susceptibility to age-related macular degeneration. *Proc Natl Acad Sci U S A* 2010;107:7401-7406.

11. Neale BM, Fagerness J, Reynolds R, et al. Genome-wide association study of advanced age-related macular degeneration identifies a role of the hepatic lipase gene (LIPC). *Proc Natl Acad Sci U S A* 2010;107:7395-7400.

12. Baird PN, Chu D, Guida E, Vu HT, Guymer R. Association of the M55L and Q192R paraoxonase gene polymorphisms with age-related macular degeneration. *Am J Ophthalmol* 2004;138:665-666.

13. Ikeda T, Obayashi H, Hasegawa G, et al. Paraoxonase gene polymorphisms and plasma oxidized low-density lipoprotein level as possible risk factors for exudative age-related macular degeneration. *Am J Ophthalmol* 2001;132:191-195.

14. Oczos J, Grimm C, Barthelmes D, et al. Regulatory regions of the paraoxonase 1 (PON1) gene are associated with neovascular age-related macular degeneration (AMD). *Age (Dordr)* 2013;35:1651-1662.

15. Draganov DI, La Du BN. Pharmacogenetics of paraoxonases: a brief review. *Naunyn Schmiedebergs Arch Pharmacol* 2004;369:78-88.

16. Ng CJ, Shih DM, Hama SY, Villa N, Navab M, Reddy ST. The paraoxonase gene family and atherosclerosis. *Free Radic Biol Med* 2005;38:153-163.

17. Mackness MI, Arrol S, Durrington PN. Paraoxonase prevents accumulation of lipoperoxides in low-density lipoprotein. *FEBS Lett* 1991;286:152-154.

18. Mackness MI, Durrington PN. HDL, its enzymes and its potential to influence lipid peroxidation. *Atherosclerosis* 1995;115:243-253.

19. Ahmed Z, Babaei S, Maguire GF, et al. Paraoxonase-1 reduces monocyte chemotaxis and adhesion to endothelial cells due to oxidation of palmitoyl, linoleoyl glycerophosphorylcholine. *Cardiovasc Res* 2003;57:225-231.

20. Rosenblat M, Volkova N, Ward J, Aviram M. Paraoxonase 1 (PON1) inhibits monocyte-to-macrophage differentiation. *Atherosclerosis* 2011;219:49-56.

21. Aharoni S, Aviram M, Fuhrman B. Paraoxonase 1 (PON1) reduces macrophage inflammatory responses. *Atherosclerosis* 2013;228:353-361.

22. Curcio CA, Johnson M, Huang JD, Rudolf M. Apolipoprotein B-containing lipoproteins in retinal aging and age-related macular degeneration. *J Lipid Res* 2010;51:451-467.

23. Tabas I, Williams KJ, Boren J. Subendothelial lipoprotein retention as the initiating process in atherosclerosis: update and therapeutic implications. *Circulation* 2007;116:1832-1844.

24. Altenhofer S, Witte I, Teiber JF, et al. One enzyme, two functions: PON2 prevents mitochondrial superoxide formation and apoptosis independent from its lactonase activity. *J Biol Chem* 2010;285:24398-24403.

25. Horke S, Witte I, Wilgenbus P, Kruger M, Strand D, Forstermann U. Paraoxonase-2 reduces oxidative stress in vascular cells and decreases endoplasmic reticulum stress-induced caspase activation. *Circulation* 2007;115:2055-2064.

26. Draganov DI, Stetson PL, Watson CE, Billecke SS, La Du BN. Rabbit serum paraoxonase 3 (PON3) is a high density lipoprotein-associated lactonase and protects low density lipoprotein against oxidation. *J Biol Chem* 2000;275:33435-33442.

27. Baskol G, Karakucuk S, Oner AO, et al. Serum paraoxonase 1 activity and lipid peroxidation levels in patients with age-related macular degeneration. *Ophthalmologica* 2006;220:12-16.

28. Isik B, Ceylan A, Isik R. Oxidative stress in smokers and non-smokers. *Inhal Toxicol* 2007;19:767-769.

29. Solak ZA, Kabaroglu C, Cok G, et al. Effect of different levels of cigarette smoking on lipid peroxidation, glutathione enzymes and paraoxonase 1 activity in healthy people. *Clin Exp Med* 2005;5:99-105.

30. Shih DM, Gu L, Xia YR, et al. Mice lacking serum paraoxonase are susceptible to organophosphate toxicity and atherosclerosis. *Nature* 1998;394:284-287.

31. Seeliger MW, Grimm C, Stahlberg F, et al. New views on RPE65 deficiency: the rod system is the source of vision in a mouse model of Leber congenital amaurosis. *Nat Genet* 2001;29:70-74.

32. Tanimoto N, Muehlfriedel RL, Fischer MD, et al. Vision tests in the mouse: Functional phenotyping with electroretinography. *Front Biosci (Landmark Ed)* 2009;14:2730-2737.

33. Carpenter AE, Jones TR, Lamprecht MR, et al. CellProfiler: image analysis software for identifying and quantifying cell phenotypes. *Genome Biol* 2006;7:R100.

34. Bligh EG, Dyer WJ. A rapid method of total lipid extraction and purification. *Can J Biochem Physiol* 1959;37:911-917.

35. Haimi P, Uphoff A, Hermansson M, Somerharju P. Software tools for analysis of mass spectrometric lipidome data. *Anal Chem* 2006;78:8324-8331.

36. Ramkumar HL, Zhang J, Chan CC. Retinal ultrastructure of murine models of dry age-related macular degeneration (AMD). *Prog Retin Eye Res* 2010;29:169-190.

37. James RW, Brulhart-Meynet MC, Singh AK, et al. The scavenger receptor class B, type I is a primary determinant of paraoxonase-1 association with high-density lipoproteins. *Arterioscler Thromb Vasc Biol* 2010;30:2121-2127.

38. Rosenblat M, Vaya J, Shih D, Aviram M. Paraoxonase 1 (PON1) enhances HDL-mediated macrophage cholesterol efflux via the ABCA1 transporter in association with increased HDL binding to the cells: a possible role for lysophosphatidylcholine. *Atherosclerosis* 2005;179:69-77.

39. Duncan KG, Hosseini K, Bailey KR, et al. Expression of reverse cholesterol transport proteins ATP-binding cassette A1 (ABCA1) and scavenger receptor BI (SR-BI) in the retina and retinal pigment epithelium. *Br J Ophthalmol* 2009;93:1116-1120.

40. Giusto NM, Pasquare SJ, Salvador GA, Castagnet PI, Roque ME, Ilincheta de Boschero MG. Lipid metabolism in vertebrate retinal rod outer segments. *Prog Lipid Res* 2000;39:315-391.

41. Wenzel A, Grimm C, Samardzija M, Reme CE. Molecular mechanisms of light-induced photoreceptor apoptosis and neuroprotection for retinal degeneration. *Prog Retin Eye Res* 2005;24:275-306.

42. Joly S, Lange C, Thiersch M, Samardzija M, Grimm C. Leukemia inhibitory factor extends the lifespan of injured photoreceptors in vivo. *J Neurosci* 2008;28:13765-13774.

43. Samardzija M, Wenzel A, Aufenberg S, Thiersch M, Reme C, Grimm C. Differential role of Jak-STAT signaling in retinal degenerations. *FASEB J* 2006;20:2411-2413.

44. Rosenblat M, Gaidukov L, Khersonsky O, et al. The catalytic histidine dyad of high density lipoprotein-associated serum paraoxonase-1 (PON1) is essential for PON1-mediated inhibition of low density lipoprotein oxidation and stimulation of macrophage cholesterol efflux. *J Biol Chem* 2006;281:7657-7665.

45. Hara S, Shike T, Takasu N, Mizui T. Lysophosphatidylcholine promotes cholesterol efflux from mouse macrophage foam cells. *Arterioscler Thromb Vasc Biol* 1997;17:1258-1266.

46. Ishida BY, Duncan KG, Bailey KR, Kane JP, Schwartz DM. High density lipoprotein mediated lipid efflux from retinal pigment epithelial cells in culture. *Br J Ophthalmol* 2006;90:616-620.

47. James RW, Deakin SP. The importance of high-density lipoproteins for paraoxonase-1 secretion, stability, and activity. *Free Radic Biol Med* 2004;37:1986-1994.

48. Marsillach J, Mackness B, Mackness M, et al. Immunohistochemical analysis of paraoxonases-1, 2, and 3 expression in normal mouse tissues. *Free Radic Biol Med* 2008;45:146-157.

49. Garin MC, Kalix B, Morabia A, James RW. Small, dense lipoprotein particles and reduced paraoxonase-1 in patients with the metabolic syndrome. *J Clin Endocrinol Metab* 2005;90:2264-2269.

50. Mackness B, Durrington PN, Abuashia B, Boulton AJ, Mackness MI. Low paraoxonase activity in type II diabetes mellitus complicated by retinopathy. *Clin Sci (Lond)* 2000;98:355-363.

51. Mastorikou M, Mackness B, Liu Y, Mackness M. Glycation of paraoxonase-1 inhibits its activity and impairs the ability of high-density lipoprotein to metabolize membrane lipid hydroperoxides. *Diabet Med* 2008;25:1049-1055.

52. Aviram M, Rosenblat M, Billecke S, et al. Human serum paraoxonase (PON 1) is inactivated by oxidized low density lipoprotein and preserved by antioxidants. *Free Radic Biol Med* 1999;26:892-904.

53. Draganov DI, Teiber JF, Speelman A, Osawa Y, Sunahara R, La Du BN. Human paraoxonases (PON1, PON2, and PON3) are lactonases with overlapping and distinct substrate specificities. *J Lipid Res* 2005;46:1239-1247.

54. Malek G, Johnson LV, Mace BE, et al. Apolipoprotein E allele-dependent pathogenesis: a model for age-related retinal degeneration. *Proc Natl Acad Sci U S A* 2005;102:11900-11905.

55. Rozenberg O, Shih DM, Aviram M. Human serum paraoxonase 1 decreases macrophage cholesterol biosynthesis: possible role for its phospholipase-A2-like activity and lysophosphatidylcholine formation. *Arterioscler Thromb Vasc Biol* 2003;23:461-467.

56. Tward A, Xia YR, Wang XP, et al. Decreased atherosclerotic lesion formation in human serum paraoxonase transgenic mice. *Circulation* 2002;106:484-490.

57. Shih DM, Xia YR, Wang XP, et al. Combined serum paraoxonase knockout/apolipoprotein E knockout mice exhibit increased lipoprotein oxidation and atherosclerosis. *J Biol Chem* 2000;275:17527-17535.

6. DISCUSSION

Atherosclerotic coronary artery disease (CAD) is a multifactorial disease, the progression of which is determined by many risk factors, including elevated total cholesterol and low-density lipoprotein cholesterol (LDL-C) as well as decreased high-density lipoprotein cholesterol (HDL-C) [1, 2]. However, it is now becoming clear that the odd profile of serum cholesterol cannot explain all incidence of CAD. Indeed, some individuals with high HDL-C levels and normal LDL-C levels still develop CAD [3]. In addition, our knowledge on the role of high-density lipoproteins (HDL) in the pathogenesis of atherosclerosis has changed, in the last decade. Besides their function in reverse cholesterol transport, HDL particles also exert beneficial atheroprotective effects on the cardiovascular system, which are directly linked to key bioactive protein and lipid components of HDL. Moreover, atheroprotective effects of HDL are significantly attenuated in CAD and acute coronary syndrome (ACS) patients [4, 5]. All together these findings suggest that not only the quantity, i.e. plasma content of HDL-C, but also the quality of HDL, i.e. molecular composition, are important in the pathogenesis of CAD. Furthermore, besides cholesterol, other lipids, such as glycerophospholipids and sphingolipids, are emerging as important players in the pathogenesis of CAD.

Glycerophospholipids and sphingolipids represent two primary categories of lipids with specific chemical structures and biochemical characteristics [6, 7]. All glycerophospholipids and sphingomyelins (SMs) contain a phosphate group. Therefore, they are often summarized as phospholipids. Glycerophospholipids and sphingolipids function as structural components of cell membranes and the surface lipid monolayers of lipoproteins. In addition, some glycerophospholipids and sphingolipids, such as lysophosphatidic acids (LPAs), lysophosphatidylcholines (LPCs), ceramides (Cers) and sphingosine-1-phospate (S1P), are important intracellular and extracellular signaling molecules. Among them, S1P is probably the best characterized bioactive lipid as it plays an important role in immunity, inflammation and vascular function [8, 9]. It has been suggested that HDL-bound S1P is responsible for many anti-inflammatory and cytoprotective effects of HDL [10-12]. Enrichment of HDL with S1P is explained by the presence of apolipoprotein M (apoM), a specific S1P binding protein [13]. Earlier studies showed the limiting effect of apoM on S1P transport and functions in plasma and HDL [13], but also found complex interactions between HDL, apoM and S1P in humans with monogenic disorders affecting HDL metabolism [14].

The first part of this project included the development of an analytical method for quantification of individual lipid species of glycerophospholipids and sphingolipids. To

achieve the best results, we combined normal-phase liquid chromatography with a triple quadrupole mass spectrometer. Liquid chromatography was applied for separation of lipid classes, while mass spectrometry (MS) methods, such as parent ion and neutral loss scanning, were employed for accurate identification of lipid species. After that, we developed a method for analysis of S1P lipids. This method included the acylation of the primary amine and the secondary alcohol of S1Ps in order to overcome the "carry-over" problem caused by the zwitterionic nature of these lipids. MS analysis of S1Ps was performed by multiple reaction monitoring (MRM), which provided highly selective and very specific determination of S1P species. The robustness of both methods has been evaluated by intra- and inter-day validation studies, which confirmed the precision and accuracy of the measurements.

In a case-control study, we investigated whether the plasma levels of glycerophospholipids and sphingolipids, as well as S1Ps and sphingoid bases, differ between healthy subjects and stable CAD or ACS patients. We observed statistically significant alterations in the number of lipid species in plasmas of CAD and ACS patients independent of statin therapy. Since plasma glycerophospholipids and sphingolipids are largely associated with HDL and LDL lipoproteins [15, 16], it is plausible that the massive alterations in the plasma lipidome of CAD and ACS patients are related to the changes in the structure and number of lipoprotein particles, which may affect the functionality of lipoproteins.

In the same study, four odd-chain PC species – PC33:1, PC33:2, PC33:3 and PC35:3 – indirectly identified as PC plasmalogens – were the most significantly altered in plasma of stable CAD and ACS patients. Moreover, we demonstrated that these species, similar to even-chain PCs, were prominently but not exclusively associated with HDL. This is reflected by positive correlations of PC plasmalogens with HDL-C found both by us and other studies [17]. Plasmalogens possess antioxidant properties and are able to attenuate the oxidation of cell membrane cholesterol, polyunsaturated fatty acids and LDL [18-20]. Thus, low levels of PC33:1, PC33:2, PC33:3 and PC35:3 in plasma can be explained by increased oxidative stress in CAD and ACS, which accelerates the oxidative degradation of plasmalogens.

In the same study, the analysis of plasma samples revealed the presence of different S1P species, with 18:1-S1P being the most abundant among them. Variations in the structure of S1Ps result from the promiscuous substrate use by serine:palmitoyltransferase (SPT), the enzyme responsible for the first step in the *de novo* synthesis of sphingolipids. In addition to the canonical substrates L-serine and C16:0-CoA, SPT can metabolize other acyl-CoAs, resulting in the formation of sphingoid bases with different numbers of carbon atoms in the alkyl chain [21]. The d18:1 sphingoid base is by far the most abundant in sphingolipids, since it

represents the canonical product of SPT reaction. Thus, it is not surprising that 18:1-S1P was found to be the most abundant S1P species. Most reports in the literature about S1P actually refer to the 18:1-S1P.

The plasma profile of S1P lipids was altered in CAD and ACS patients. Compared to healthy subjects, plasma levels of 18:1-S1P were lower in ACS patients, while plasma levels of 16:1-S1P were lower in CAD and ACS patients. Considering that more than half of plasma 18:1-S1P is associated with HDL and that 18:1-S1P is responsible for some of atheroprotective effects of HDL, we can deduce that the reduced plasma content of 18:1-S1P and 16:1-S1P may contribute to the loss of the atheroprotective functions of HDL in CAD and ACS patients.

We thereafter investigated the triangular relationship between HDL-associated phospholipids, anti-apoptotic activity of HDL and the presence of stable and acute CAD. The anti-apoptotic activity of HDL was evaluated by measuring endothelial cell (EC) apoptosis in the presence of HDL after cell death was induced by serum and growth factors deprivation. This case-control study showed the association of reduced HDL content of PC33:3 and PC35:2 (= PC plasmalogens) with CAD and ACS. This result is supported by previous studies that reported low levels of PE plasmalogens in acute-phase HDL, and a diminished content of some specific PC and/or PE plasmalogens in HDL of patients with low HDL-C [22, 23]. In addition, we demonstrated a significant correlation of PC33:3 and PC35:2 with the anti-apoptotic activity of HDL. Considering that a direct anti-apoptotic effect of plasmalogens has been demonstrated for the neuronal cells (line Neuro-2A) [24] and that disturbed formation of plasmalogens in the cells with peroxisomal dysfunction was found to be associated with increased apoptosis [25], the relationship between reduced content of PC plasmalogens and reduced anti-apoptotic activity of HDL may be an indication of a direct causal effect. However, it is also plausible that reduced levels of HDL-associated PC plasmalogens are the result of increased oxidative stress and, thus, elevated oxidative degradation of plasmalogens in CAD and ACS patients. At the same time, the action of pro-apoptotic derivatives of oxidased plasmalogens, such as α-chlorofatty aldehydes or acids generated by myeloperoxidase [26] may also play a role in the loss of the anti-apoptotic activity of HDL.

In addition to the two plasmalogens, HDL-associated PC34:2 showed significant association with both CAD and ACS, and inverse correlation with EC apoptosis in the presence of HDL. PC34:2, which represents the most abundant PC species in HDL, was early identified as PC(16:0/18:2) [23]. Experimental studies indicated that reconstituted HDL (rHDL) containing PC(16:0/18:2) were more effective than rHDL containing other saturated and

monounsaturated PC lipids in inhibiting the endothelial expression of vascular cell adhesion molecule 1 [27, 28] and inhibiting the activation of NADPH oxidase in neutrophils [29]. Moreover, rHDL containing PC(16:0/18:2) but not PC(16:0/18:1) induced CETP-mediated release of prebeta1-HDL, a promoter of cholesterol efflux [30]. In addition, NMR-based lipidomic analysis of HDL revealed significant associations of diminished contents of total PC with coronary heart disease in a case-control study [31]. However, it remains unknown whether the association of PC34:2 with CAD and its correlation with the anti-apoptotic activity of HDL directly reflect anti-atherogenic properties of PC34:2 or whether low levels of PC34:2 in HDL may be an indicator of oxidative processes or enzyme activity affecting HDL functionality.

We also found that HDL-associated 18:1-S1P and 18:2-S1P, but not 16:1-S1P, exhibited a significant correlation with the anti-apoptotic activity of HDL. However, none of the S1P species was associated with CAD or ACS. This may initially seem contrary to the previous reports on reduced amounts of HDL-bound S1P in CAD patients [32], however, variations in methodology of S1P quantification and HDL isolation may account for the different findings. First, that analysis of S1P was performed by HPLC coupled with a fluorescence detector, which did not provide information about the molecular structure of S1P and how many different S1P species were detected. Second, we as well as others showed that only 60% of plasma S1P is associated with HDL [12-14, 33], while Sattler and colleagues reported an almost 100% recovery of S1P in HDL of the healthy controls [32].

In the next study, we investigated whether apoM can influence the plasma levels of the 18:1-S1P, termed S1P hereafter. We showed that human HDL as well as HDL of wild type (wt) mice, induce time-dependent and saturable S1P efflux, which results in doubling the endogenous concentration of S1P. The fact that the doubled S1P concentration is still below the particle number of HDL may indicate the presence of a specific binding site that is not saturated after isolation of HDL from plasma, such as apoM. In agreement with this explanation, we found that HDL from *Apom*^{tg} mice overexpressing apoM significantly increase S1P efflux. However, compared to HDL from wt mice, S1P efflux was not diminished in the presence of HDL from *Apom*$^{-/-}$ mice lacking apoM. This indicates the presence of additional apoM-independent mechanisms by which HDL facilitates S1P efflux from erythrocytes. Given that S1P efflux induced by HDL of *Apom*$^{-/-}$ mice reaches a saturation point much below the number of HDL particles, it is unlikely that the apoM-independent mechanism of S1P efflux is unspecific. Moreover, rHDL consisting only of apoA1 and PC(16:0/18:1) also induced S1P efflux, further confirming the existence of apoM-independent mechanisms, with apoA1 as a possible inducer of S1P efflux. However, further

experiments indicated that delipidated apoA1 did not induce S1P efflux from erythrocytes, so it can be inferred that additional and yet unknown factors contribute to S1P efflux [34].

In addition, we investigated whether apoM regulates the plasma content of S1P beyond mediating S1P transport in HDL. We showed that, in contrast to wt mice, the urine of *Apom*$^{-/-}$ mice contained quantifiable amounts of S1P, indicating that apoM may play a role in preventing the urinary loss of S1P. Then we investigated the urinary excretion of apoM and S1P by mice with defective tubular endocytosis, including megalin knock-out mice (*Lrp2*$^{-/-}$), mice lacking the chloride-proton exchanger CIC-5 (*Clcn5*$^{-/-}$) or the lysosomal cystine transporter cystinosin (*Ctns*$^{-/-}$). We detected apoM in the urine samples of *Lrp2*$^{-/-}$, *Clcn5*$^{-/-}$ and *Ctns*$^{-/-}$ mice but not in their corresponding wt littermates. At the same time, increased urinary excretion of S1P was found in *Lrp2*$^{-/-}$ and *Clcn5*$^{-/-}$ mice, indicating that tubular reabsorption of apoM interferes with the urinary loss of S1P. However, the urinary loss of apoM and S1P in the mice with defective tubular endocytosis was too low to considerably decrease plasma levels of apoM and S1P [34].

The anti-oxidant enzyme paraoxonase 1 (PON1), which is involved in the atheroprotective functions of HDL, was found to be associated with age-related macular degeneration (AMD). We investigated whether the lack of PON1 has any impact on the phospholipid profile of retina/eyecup tissues, indicating some role in AMD. Assessment of retinal physiology of *Pon1*$^{-/-}$ mice revealed that PON1 is not essential for the development and maintenance of normal retinal structure or function. However, retina/eyecup samples of *Pon1*$^{-/-}$ mice had decreased levels of LPCs in general, and of LPC22:6 in particular. Considering that PON1 has a phospholipase A2 (PLA2)-like activity leading to the formation of LPCs in macrophages [35], PON1 in wt mice may regulate the production of LPC lipids in the retina/eyecup. A large amount of LPC22:6 in the retina but not in the eyecup indicates that the PLA2-like activity of PON1 affects photoreceptors and neuronal retina. Furthermore, our study showed a decrease in the content of total LPCs and LPC22:6 in one year old wt mice, by 63% and 75%, respectively. This, and the fact that ageing decreases the expression of *Pon1* gene, indicates that a reduced amount of PON1 resulted in a diminished content of LPCs. However, the absence of an AMD-like phenotype in the eyes of aged *Pon1*$^{-/-}$ mice suggests that even a long-lasting absence of PON1 is not sufficient to cause detectable pathological changes, and indicates that additional factors or stimuli may be needed to provoke the phenotype of AMD in *Pon1*$^{-/-}$ mice [36].

Future research should focus on the development of LC-MS methods for the structural characterization and quantification of PC and PE plasmalogens. Our results of

glycerophospholipid and sphingolipid screening of the plasma and HDL samples from healthy subjects, CAD and ACS patients should be further verified in larger case-control and prospective studies. Moreover, further *in vitro* experiments with native HDL enriched with PC plasmalogens are required in order to directly evaluate the role of PC plasmalogens in the anti-apoptotic activity of HDL. Additional experiments are also needed for a better understanding of the apoM-independent mechanism by which HDL mediate S1P efflux from erythrocytes. Finally, there is a great need for the detailed characterization of PON1 functions in retinal tissue in order to clarify the so-far controversial role of PON1 in AMD.

References

1. Prospective Studies Collaboration, Lewington S, Whitlock G, et al. Blood cholesterol and vascular mortality by age, sex, and blood pressure: a meta-analysis of individual data from 61 prospective studies with 55,000 vascular deaths. *Lancet* 2007;370:1829-1839.
2. Emerging Risk Factors Collaboration, Di Angelantonio E, Gao P, et al. Lipid-related markers and cardiovascular disease prediction. *JAMA : the journal of the American Medical Association* 2012;307:2499-2506.
3. Ansell BJ, Navab M, Hama S, et al. Inflammatory/antiinflammatory properties of high-density lipoprotein distinguish patients from control subjects better than high-density lipoprotein cholesterol levels and are favorably affected by simvastatin treatment. *Circulation* 2003;108:2751-2756.
4. Luscher TF, Landmesser U, von Eckardstein A, Fogelman AM. High-density lipoprotein: vascular protective effects, dysfunction, and potential as therapeutic target. *Circulation research* 2014;114:171-182.
5. Riwanto M, Landmesser U. High density lipoproteins and endothelial functions: mechanistic insights and alterations in cardiovascular disease. *Journal of lipid research* 2013;54:3227-3243.
6. Fahy E, Subramaniam S, Brown HA, et al. A comprehensive classification system for lipids. *Journal of lipid research* 2005;46:839-861.
7. Fahy E, Subramaniam S, Murphy RC, et al. Update of the LIPID MAPS comprehensive classification system for lipids. *Journal of lipid research* 2009;50 Suppl:S9-14.
8. Lucke S, Levkau B. Endothelial functions of sphingosine-1-phosphate. *Cellular physiology and biochemistry : international journal of experimental cellular physiology, biochemistry, and pharmacology* 2010;26:87-96.
9. Kim RH, Takabe K, Milstien S, Spiegel S. Export and functions of sphingosine-1-phosphate. *Biochimica et biophysica acta* 2009;1791:692-696.
10. Nofer JR, Assmann G. Atheroprotective effects of high-density lipoprotein-associated lysosphingolipids. *Trends in cardiovascular medicine* 2005;15:265-271.
11. Sattler K, Levkau B. Sphingosine-1-phosphate as a mediator of high-density lipoprotein effects in cardiovascular protection. *Cardiovascular research* 2009;82:201-211.
12. Rodriguez C, Gonzalez-Diez M, Badimon L, Martinez-Gonzalez J. Sphingosine-1-phosphate: A bioactive lipid that confers high-density lipoprotein with vasculoprotection mediated by nitric oxide and prostacyclin. *Thrombosis and haemostasis* 2009;101:665-673.

13. Christoffersen C, Obinata H, Kumaraswamy SB, et al. Endothelium-protective sphingosine-1-phosphate provided by HDL-associated apolipoprotein M. *Proceedings of the National Academy of Sciences of the United States of America* 2011;108:9613-9618.

14. Karuna R, Park R, Othman A, et al. Plasma levels of sphingosine-1-phosphate and apolipoprotein M in patients with monogenic disorders of HDL metabolism. *Atherosclerosis* 2011;219:855-863.

15. Wiesner P, Leidl K, Boettcher A, Schmitz G, Liebisch G. Lipid profiling of FPLC-separated lipoprotein fractions by electrospray ionization tandem mass spectrometry. *Journal of lipid research* 2009;50:574-585.

16. Dashti M, Kulik W, Hoek F, Veerman EC, Peppelenbosch MP, Rezaee F. A phospholipidomic analysis of all defined human plasma lipoproteins. *Scientific reports* 2011;1:139.

17. Maeba R, Maeda T, Kinoshita M, et al. Plasmalogens in human serum positively correlate with high- density lipoprotein and decrease with aging. *Journal of atherosclerosis and thrombosis* 2007;14:12-18.

18. Wallner S, Schmitz G. Plasmalogens the neglected regulatory and scavenging lipid species. *Chemistry and physics of lipids* 2011;164:573-589.

19. Reiss D, Beyer K, Engelmann B. Delayed oxidative degradation of polyunsaturated diacyl phospholipids in the presence of plasmalogen phospholipids in vitro. *The Biochemical journal* 1997;323 (Pt 3):807-814.

20. Jurgens G, Fell A, Ledinski G, Chen Q, Paltauf F. Delay of copper-catalyzed oxidation of low density lipoprotein by in vitro enrichment with choline or ethanolamine plasmalogens. *Chemistry and physics of lipids* 1995;77:25-31.

21. Hornemann T, Penno A, Rutti MF, et al. The SPTLC3 subunit of serine palmitoyltransferase generates short chain sphingoid bases. *The Journal of biological chemistry* 2009;284:26322-26330.

22. Pruzanski W, Stefanski E, de Beer FC, de Beer MC, Ravandi A, Kuksis A. Comparative analysis of lipid composition of normal and acute-phase high density lipoproteins. *Journal of lipid research* 2000;41:1035-1047.

23. Yetukuri L, Soderlund S, Koivuniemi A, et al. Composition and lipid spatial distribution of HDL particles in subjects with low and high HDL-cholesterol. *Journal of lipid research* 2010;51:2341-2351.

24. Hossain MS, Ifuku M, Take S, Kawamura J, Miake K, Katafuchi T. Plasmalogens rescue neuronal cell death through an activation of AKT and ERK survival signaling. *PloS one* 2013;8:e83508.

25. Brites P, Mooyer PA, El Mrabet L, Waterham HR, Wanders RJ. Plasmalogens participate in very-long-chain fatty acid-induced pathology. *Brain : a journal of neurology* 2009;132:482-492.

26. Wang WY, Albert CJ, Ford DA. Alpha-chlorofatty acid accumulates in activated monocytes and causes apoptosis through reactive oxygen species production and endoplasmic reticulum stress. *Arteriosclerosis, thrombosis, and vascular biology* 2014;34:526-532.

27. Baker PW, Rye KA, Gamble JR, Vadas MA, Barter PJ. Phospholipid composition of reconstituted high density lipoproteins influences their ability to inhibit endothelial cell adhesion molecule expression. *Journal of lipid research* 2000;41:1261-1267.

28. Zhang WJ, Stocker R, McCall MR, Forte TM, Frei B. Lack of inhibitory effect of HDL on TNFalpha-induced adhesion molecule expression in human aortic endothelial cells. *Atherosclerosis* 2002;165:241-249.

29. Peshavariya H, Dusting GJ, Di Bartolo B, Rye KA, Barter PJ, Jiang F. Reconstituted high-density lipoprotein suppresses leukocyte NADPH oxidase activation by disrupting lipid rafts. *Free radical research* 2009;43:772-782.

30. Rye KA, Duong M, Psaltis MK, et al. Evidence that phospholipids play a key role in pre-beta apoA-I formation and high-density lipoprotein remodeling. *Biochemistry* 2002;41:12538-12545.

31. Kostara CE, Papathanasiou A, Psychogios N, et al. NMR-Based Lipidomic Analysis of Blood Lipoproteins Differentiates the Progression of Coronary Heart Disease. *Journal of proteome research* 2014.

32. Sattler KJ, Elbasan S, Keul P, et al. Sphingosine 1-phosphate levels in plasma and HDL are altered in coronary artery disease. *Basic research in cardiology* 2010;105:821-832.

33. Murata N, Sato K, Kon J, et al. Interaction of sphingosine 1-phosphate with plasma components, including lipoproteins, regulates the lipid receptor-mediated actions. *The Biochemical journal* 2000;352 Pt 3:809-815.

34. Sutter I, Park R, Othman A, et al. Apolipoprotein M modulates erythrocyte efflux and tubular reabsorption of sphingosine-1-phosphate. *Journal of lipid research* 2014;55:1730-1737.

35. Rosenblat M, Vaya J, Shih D, Aviram M. Paraoxonase 1 (PON1) enhances HDL-mediated macrophage cholesterol efflux via the ABCA1 transporter in association with

increased HDL binding to the cells: a possible role for lysophosphatidylcholine. *Atherosclerosis* 2005;179:69-77.

36. Oczos J, Sutter I, Kloeckener-Gruissem B, et al. Lack of paraoxonase 1 alters phospholipid composition, but not morphology and function of the mouse retina. *Investigative ophthalmology & visual science* 2014;55:4714-4727.

ACKNOWLEDGEMENTS

Foremost, I would like to express my sincere gratitude and appreciation to my supervisor, Prof. Arnold von Eckardstein, head of the Institute of Clinical Chemistry at the University Hospital Zurich, for giving me the opportunity to work on diverse exciting projects, and for his encouragement, support and thoughtful guidance throughout my PhD study. I would also like to thank Prof. Arnold von Eckardstein for his patience, for sharing his immense knowledge in cardiovascular disease, and for his detailed review of this thesis during the writing process and its preparation.

Furthermore, I would like to thank my supervisor, Dr. Thorsten Hornemann of the Institute of Clinical Chemistry at the University Hospital Zurich, for accepting me as a PhD student in his research group and for the valuable advice and continuous support throughout my PhD thesis, and also for creating a good work environment and friendly atmosphere.

I would also like to thank to my former supervisor, Prof. Katharina Rentsch, head of the Laboratory Medicine at the University Hospital Basel (present address), for giving me the opportunity to start my PhD study at the Institute of Clinical Chemistry at the University Hospital Zurich and for introducing me to the various mass spectrometry techniques.

I am sincerely grateful to my thesis committee members, Prof. Oliver Devuyst and Prof. Ulf Landmesser of the Institute of Physiology at the University of Zurich, for their insightful comments, remarks and suggestions during the thesis committee meetings. I further want to thank Prof. Oliver Devuyst for his interest and support in the preparation of the sphingosine-1-phosphate paper.

My special thanks go to my research colleagues, Jadwiga Oczos, Rebekka Park and Meliana Riwanto, for their excellent work and fruitful collaboration, which greatly contributed to the work presented in this thesis.

I am very grateful to all the members of Dr. Thorsten Hornemann`s group, who all contributed to the friendly working environment. In particular, I would like to thank Alaa Othman for his kind help with the statistical analysis and fruitful scientific discussions which have been of a great value to this project. My special thanks also go to Heiko Bode for his

excellent technical assistance with the mass spectrometers. I want to express my deep thanks to Irina Alecu, Assem Zhakupova, Regula Steiner, Saranya Suriyanarayanan and Yu Wei for being willing to help me whenever it was needed and for their answers to my general questions.

I would also like to acknowledge some former members of the Institute of Clinical Chemistry, namely Carine Steiner and Ratna Karuna, for their help at the beginning of my PhD project and for helping to create a positive collaborative working atmosphere. Furthermore, I want to express my gratitude to Dr. Lucia Rohrer and Silvija Radosavljevic for their work on the isolation of the lipoproteins and their help with the erythrocyte`s experiment to enable me to complete the revision of the sphingosine-1-phosphate paper. I would also like to thank the secretaries, Sonja Bernhard and Christine Genné, for efficient handling of all the paperwork and for their administrative support.

Finally, my biggest thanks go to my husband, Thomas Sutter, who always understands, supports and assists me in many different ways.

CURRICULUM VITAE

Personal Data

Name	Iryna SUTTER
Date of birth	06.05.1986
Place of birth	Lviv, Ukraine
Nationality	Ukraine

Education

03.2010 – 2015 **PhD thesis**
Institute of Clinical Chemistry, University Hospital Zurich, University of Zurich, Zurich, Switzerland

09.2007 – 06.2008 **Master of Analytical Chemistry**
Ivan Franko National University of Lviv, Lviv, Ukraine
"The X-ray phase analysis of the interaction of vanadium and phosphorus with iron or manganese"

09.2003 – 06.2007 **Bachelor of Analytical Chemistry**
Ivan Franko National University of Lviv, Lviv, Ukraine

09.2000 – 06.2003 **Physical-Mathematical Lyceum, Lviv, Ukraine**

Work experience

03.2010 – 06.2014 PhD student in the Institute of Clinical Chemistry at the University Hospital Zurich, Zurich, Switzerland

05.2008 – 06.2009 Chemist in the Food Control Laboratory at the Lviv Cholod, Lviv, Ukraine

PUBLICATIONS AND PRESENTATIONS

Publications:

R. Karuna, R. Park, A. Othman, A. G. Holleboom, M. M. Motazacker, **I. Sutter**, J. A. Kuivenhoven, L. Rohrer, H. Matile, T. Hornemann, M. Stoffel, K. M. Rentsch, and A. von Eckardstein. 2011. **Plasma levels of sphingosine-1-phosphate and apolipoprotein M in patients with monogenic disorders of HDL metabolism.** *Atherosclerosis* 219: 855-863.

I. Sutter, R. Park, A. Othman, L. Rohrer, T. Hornemann, M. Stoffel, O. Devuyst, and A. von Eckardstein. 2014. **Apolipoprotein M modulates erythrocyte efflux and tubular reabsorption of sphingosine-1-phosphate.** *Journal of lipid research* 55: 1730-1737.

J. Oczos, **I. Sutter**, B. Kloeckener-Gruissem, W. Berger, M. Riwanto, K. Rentsch, T. Hornemann, A. von Eckardstein, and C. Grimm. 2014. **Lack of paraoxonase 1 alters phospholipid composition, but not morphology and function of the mouse retina.** *Investigative ophthalmology & visual science* 55: 4714-4727.

I. Sutter, A. Othman, M. Riwanto, J. Manz , L. Rohrer, K. Rentsch, T. Hornemann, U. Landmesser, and A. von Eckardstein. **Plasmalogens of high-density lipoproteins (HDL) are associated with coronary artery disease and anti-apoptotic activity of HDL**. (*Atherosclerosis*, submitted).

I. Sutter, A. Othman, L. Rohrer, R. Klingenberg, A. von Eckardstein, and T. Hornemann **Association with coronary artery disease and lipoprotein distribution of plasma glycerophospholipids and sphingolipids.** (in preparation).

External oral presentations:

I. Sutter, A. von Eckardstein, T. Hornemann: Analysis of different phospholid classes with LC-MS. Fall Meeting of Swiss Chemical Society 2012, ETH Zurich, September 13th 2012.

External poster presentations:

I. Sutter, K. M. Rentsch: Quantification of long-chain fatty acids with GC-MS. 10th Day of Clinical Research, University Hospital Zurich, June 9th 2011.

I. Sutter, C. Grimm, J. Oczos, K. Rentsch: Quantification of long-chain fatty acids with GC-MS and application of the method in retina samples of PON1 knockout mice. 7th Symposium of the Zurich Center for Integrative Human Physiology, Zurich, August 2011.

I. Sutter, K. M. Rentsch: Quantification of long-chain fatty acids with GC-MS. Fall Meeting of Swiss Chemical Society 2011, EPF Lausanne, September 9th 2011.

I. Sutter, K. M. Rentsch: Quantification of long-chain fatty acids with GC-MS. Annual Congress of the Swiss Society of Clinical Chemistry& Tri-National Congress of Laboratory Medicine, Kongresshaus Zurich, November 2nd-4th 2011.

I. Sutter, A. von Eckardstein, T. Hornemann: Analysis of different phospholid classes with LC-MS. 11th Day of Clinical Research, University Hospital Zurich, April 19th 2012.

I. Sutter, R. Karuna, R. Park, M. Stoffel, A. von Eckardstein, T. Hornemann: ApoM mediates binding of sphingosine-1-phosphate to HDL. Gordon Research Conference on Glycolipids & Sphingolipid Biology, Lucca (Barga), 22nd-27th of April 2012.

I. Sutter, A. von Eckardstein, T. Hornemann: Analysis of six major phospholipid classes in human plasma and the application in atherosclerosis. ALGA & Cardiovascular Biology Meeting 2013, Bern, 10th-11th January 2013.

I. Sutter, A. von Eckardstein, T. Hornemann: Analysis of six major phospholipid classes in human plasma and the application in atherosclerosis. 12th Day of Clinical Research, University Hospital Zurich, April 2013.

I. Sutter, T. Hornemann, A von Eckardstein: Analysis of different phospholipid classes with LC-MS/MS. 9th Symposium of the Zurich Center for Integrative Human Physiology, Zurich, August 2013.

I. Sutter, U. Landmesser, T. Hornemann, A. von Eckardstein : Low concentrations of sphingosine-1-phosphates and plasmalogens in HDL are associated with coronary artery disease and reduced anti-apoptotic activity of high density lipoproteins. 7th IAS Workshop on HDL, Rome, Italy, 24th – 26th March 2014.

I. Sutter, R. Park, A. Othman, L. Rohrer, T. Hornemann, M. Stoffel, O. Devuyst, A. von Eckardstein: Apolipoprotein M modulates erythrocyte efflux and urinary excretion of sphingosine-1-phosphate. 7th IAS Workshop on HDL, Rome, Italy, 24th – 26th March 2014.

I. Sutter, U. Landmesser, T. Hornemann, A. von Eckardstein: Low concentrations of sphingosine-1-phosphates and plasmalogens in HDL are associated with coronary artery disease and reduced anti-apoptotic activity of high density lipoproteins. 82nd Congress of the European Atherosclerosis Society, Madrid, Spain, May31st – June 3rd 2014.

I. Sutter, R. Park, A. Othman, L. Rohrer, T. Hornemann, M. Stoffel, O. Devuyst, A. von Eckardstein: Apolipoprotein M modulates erythrocyte efflux and urinary excretion of sphingosine-1-phosphate. 82nd Congress of the European Atherosclerosis Society, Madrid, Spain, May31st – June 3rd 2014.